

# Quantum Transport Through Open Systems

by

Jinshan Wu

B.Sc., The Beijing Normal University, 1999  
M.Sc., The Beijing Normal University, 2002  
M.Sc., The University Of British Columbia, 2006

A THESIS SUBMITTED IN PARTIAL FULFILLMENT OF  
THE REQUIREMENTS FOR THE DEGREE OF

DOCTOR OF PHILOSOPHY

in

The Faculty of Graduate Studies

(Physics)

THE UNIVERSITY OF BRITISH COLUMBIA

(Vancouver)

April, 2011

© Jinshan Wu 2011

# Abstract

To study transport properties, one needs to investigate the system of interest when coupled to biased external baths. This requires solving a master equation for this open quantum system. Obtaining this solution is very challenging, especially for large systems. This limits applications of the theories of open quantum systems, especially insofar as studies of transport in large quantum systems, of interest in condensed matter, is concerned.

In this thesis, I propose three efficient methods to solve the Redfield equation — an example of such a master equation. The first is an open-system Kubo formula, valid in the limit of weak bias. The second is a solution in terms of Green's functions, based on a BBGKY (Bogoliubov–Born–Green–Kirkwood–Yvon)-like hierarchy. In the third, the Redfield equation is mapped to a generalized Fokker-Planck equation using the coherent-state representation. All three methods, but especially the latter two, have much better efficiency than direct methods such as numerical integration of the Redfield equation via the Runge-Kutta method. For a central system with a  $d$ -dimensional Hilbert space, the direct methods have complexity of  $d^3$ , while that of the latter two methods is on the order of polynomials of  $\log d$ . The first method, besides converting the task of solving the Redfield equation to solving the much easier Schrödinger's equation, also provides an even more important conceptual lesson: the standard Kubo formula is not applicable to open systems.

Besides these general methodologies, I also investigate transport properties of spin systems using the framework of the Redfield equation and with direct methods. Normal energy and spin transport is found for integrable but interacting systems. This conflicts with the well-known conjecture linking anomalous conductivity to integrability, and it also contradicts the relationship, suggested by some, between gapped systems ( $J_z > J_{xy}$ ) and normal spin conductivity. I propose a new conjecture, linking anomalous transport to the existence of a mapping of the problem to one for non-interacting particles.

# Preface

The work presented in Chapters 2 and 6 are a continuation of the work done for my M.Sc. thesis. This work is reported in the manuscript:

“Heat transport in quantum spin chains: the relevance of integrability”, Jinshan Wu and Mona Berciu, submitted to Physical Review B and posted as arXiv:1003.1559.

The work presented in Chapter 3 is reported in Jinshan Wu and Mona Berciu 2010 Europhysics Letters **92** 30003.

The first part of the work presented in Chapter 4 is reported in Jinshan Wu 2010 New J. Phys. **12** 083042. The second part, which is on the second-order BBGKY-like method, is currently under preparation for publication.

Original work reported in other chapters will be prepared for publication in the near future.

All the original work in this thesis was carried out by JW who also developed the conception, scope and methods of this research, with various degrees of consultation and editing support from MB.

# Table of Contents

<b>Abstract</b> . . . . .	ii
<b>Preface</b> . . . . .	iii
<b>Table of Contents</b> . . . . .	iv
<b>List of Figures</b> . . . . .	vii
<b>Acknowledgements</b> . . . . .	ix
<b>Dedication</b> . . . . .	x
<b>Chapter 1 Introduction</b> . . . . .	1
1.1 Two major theoretical approaches . . . . .	2
1.2 A big challenge for the system-baths scenario . . . . .	5
1.3 Our methods and their applications . . . . .	7
1.3.1 Linear response theory . . . . .	7
1.3.2 The BBGKY-like hierarchy . . . . .	8
1.3.3 The GFPE in the coherent-state representation . . . . .	9
1.3.4 Thermal conductance of spin chains . . . . .	9
1.4 Summary . . . . .	11
<b>Chapter 2 The projector technique and the Redfield equation</b> . . . . .	12
2.1 Outline . . . . .	12
2.2 The effective equation of motion for open systems . . . . .	12
2.2.1 The projector operator technique . . . . .	14
2.2.2 An alternative derivation . . . . .	19
2.2.3 QME in terms of creation and annihilation operators . . . . .	20
2.3 Relaxation towards thermal equilibrium . . . . .	22
2.3.1 One-site open system . . . . .	22
2.3.2 Two-site open system . . . . .	24
2.4 Various other extensions . . . . .	28

*Table of Contents*

---

2.5	Evolution towards a NESS . . . . .	30
2.5.1	NESSs from the RE . . . . .	31
2.5.2	NESSs from the LOLE and the MQME . . . . .	34
2.5.3	The general Lindblad form . . . . .	37
2.6	Major challenge for large systems . . . . .	38
<b>Chapter 3 Linear Response Theory: Kubo formula for open systems</b> . . . . .		40
3.1	Introduction . . . . .	40
3.2	General Linear Response Theory . . . . .	41
3.3	Limitations of the standard Kubo formula . . . . .	43
3.4	OKF: the Kubo formula for open finite-size systems . . . . .	47
3.5	Comparison of the two OKFs . . . . .	50
3.6	Summary and discussion . . . . .	53
<b>Chapter 4 BBGKY-like hierarchy for the Redfield equation</b> . . . . .		55
4.1	Introduction . . . . .	55
4.2	Derivation of the BBGKY-like hierarchy . . . . .	56
4.3	Non-equilibrium Wick's theorem . . . . .	59
4.4	Truncation of the hierarchy . . . . .	62
4.4.1	Method 1: equilibrium substitution . . . . .	62
4.4.2	Method 2: first-level cluster expansion . . . . .	67
4.4.3	Method 2: second-level cluster expansion . . . . .	72
4.5	Conclusion and discussion . . . . .	78
<b>Chapter 5 Solving the Redfield equation using coherent-state representations</b> . . . . .		79
5.1	Introduction . . . . .	79
5.2	The model and its effective equation of motion . . . . .	81
5.3	Exact solution for non-interacting systems . . . . .	85
5.4	Interacting systems: BBGKY-like hierarchy derived from the GFPE . . . . .	87
5.5	Approximate numerical solution for interacting systems . . . . .	90
5.6	Solving the LOLE via the GFPE method . . . . .	94
5.7	Conclusions . . . . .	96
<b>Chapter 6 Application: heat transport in spin chains</b> . . . . .		97
6.1	Introduction . . . . .	97
6.2	The model and its Redfield equation . . . . .	99
6.3	Numerical methods . . . . .	100

*Table of Contents*

---

6.4	Definitions of the thermal current and local temperatures . .	101
6.5	Results . . . . .	103
6.6	Conclusions . . . . .	111
<b>Chapter 7 Conclusions and discussions . . . . .</b>		<b>112</b>
<b>Bibliography . . . . .</b>		<b>117</b>
<b>Appendix A Perturbational decomposition of the operators <math>\hat{m}</math></b>		<b>128</b>
A.1	Expanded in eigenbasis of $H_S$ . . . . .	128
A.2	Perturbational expansion starting from non-interacting systems . . . . .	129
<b>Appendix B Second-order cluster expansion: <math>G_1, \mathfrak{G}_2</math> . . . . .</b>		<b>134</b>
B.1	Second-order cluster expansion . . . . .	134
B.2	Second-order equations of $G_1$ and $\mathfrak{G}_2$ . . . . .	135
<b>Appendix C Estimation of convergence of the BBGKY-like methods . . . . .</b>		<b>141</b>
C.1	$\Delta_1^{E,(1)}$ from method 1 . . . . .	141
C.2	$\Delta_1^{C,(1)}$ from method 2 . . . . .	145
<b>Appendix D Coherent states and coherent-state representation . . . . .</b>		<b>148</b>
D.1	Coherent states for systems with a single mode . . . . .	148
D.2	Coherent states for multi-mode systems . . . . .	151
<b>Appendix E FPE and Langevin equation . . . . .</b>		<b>153</b>
E.1	Langevin equation for standard FPEs . . . . .	153
E.2	Analytical solution for the Ornstein-Uhlenbeck process . . .	155
E.3	Stochastic difference equation for truncated GFPEs . . . . .	155
<b>Appendix F Solving the RE and LOLE of bosonic systems with BBGKY-like hierarchy . . . . .</b>		<b>157</b>
F.1	Exact solution on non-interacting systems . . . . .	158
F.2	Approximate solution on interacting systems . . . . .	159

# List of Figures

1.1	Sketch of a typical setup of heat conduction. . . . .	10
2.1	Sketch of a one-site system coupled to a heat bath. . . . .	23
2.2	Sketch of a two-site system coupled to a heat bath. . . . .	24
2.3	Sketch of a two-site system coupled to two heat baths. . . . .	27
2.4	Difference between non-equilibrium and equilibrium states . .	33
2.5	Stationary states from the local-operator Lindblad equation and the multi-mode quantum master equation compared against those from the Redfield equation . . . . .	36
3.1	Difference between $\rho^{(1)}(\infty)$ and $\rho^{(2)}(\infty)$ for different values of $\delta$ . . . . .	51
3.2	Difference between $\rho^{(1)}(\infty)$ and $\rho^{(2)}(\infty)$ for different values of $\lambda$ . . . . .	52
3.3	Difference between $\rho^{(1)}(\infty)$ and $\rho^{(2)}(\infty)$ for different values of $V_0$ . . . . .	53
4.1	$g_1^{E,(1)}$ compared with $g_1^{Ex}$ for interacting systems at non- equilibrium . . . . .	66
4.2	$g_1^{C,(1)}$ compared with $g_1^{Ex}$ for non-equilibrium interacting sys- tems . . . . .	71
4.3	$g_1^{C,(2)}$ compared with $g_1^{Ex}$ for non-equilibrium interacting sys- tems . . . . .	74
4.4	$g_2^{C,(2)}$ is compared with $g_2^{Ex}$ for non-equilibrium interacting systems . . . . .	75
4.5	Particle currents calculated from the second-, first- and the zeroth-order forms are compared . . . . .	76
4.6	Heat currents calculated from the second-, first- and the zeroth- order forms are compared . . . . .	77
5.1	Analytical solution compared against the BBGKY numerical solution . . . . .	88

*List of Figures*

---

5.2	The numerical simulation of the generalized Fokker-Planck equation for interacting systems . . . . .	93
5.3	A similar application to the local-operator Lindblad equation	96
6.1	Typical temperature profiles for $N = 10$ spin chains . . . . .	104
6.2	Current v.s. system size . . . . .	105
6.3	Normalized profiles . . . . .	106
6.4	Typical temperature profile for the cases of small $J_z$ and small $B_z$ . . . . .	107
6.5	Temperature profiles on Ising spin chains and fermionic chains	109
7.1	A sketch of an exactly solvable decoherence model and its variation . . . . .	114

# Acknowledgements

It is a pleasure to thank those who made this thesis possible.

I owe my deepest gratitude to my supervisor, Dr. Mona Berciu. This thesis would not have been possible without her great efforts to educate and to help me in so many ways. She taught me not only physics, but also more importantly how to appreciate physics, and how to write up and explain things clearly and simply. She also encouraged and protected my interest in fundamental physical questions. Throughout my years of graduate study at UBC, she has always been a good advisor and a good friend to me.

It is an honor for me to thank the many people with whom I discussed the related work and have been benefited greatly from such discussion: Ian Affleck, Keiji Saito, Philip Stamp, Tomaz Prosen, Peter Drummond, Hong Guo and Shouyong Pei.

I would like to thank the many great teachers I ever had especially: Yue'e Yi, Jianjiang Zhang, Anshen Qi, Jiaruan Wang, Yongcheng Wang, Zhanru Yang, Shouyong Pei, Canbing Liang, Jingdong Bao, Zengru Di, Qiang Yuan, Andrew DeBenedictis, Leslie Ballentine, Ariel Zhitnitsky, Mark Van Raamsdonk and Ian Affleck.

I am indebted to my many colleagues for the stimulating discussion and sometimes even excited and heated argument: Yong Sun, Mandy Wang, Kelly Cheung, Bayo Lau, Arthur James Charbonneau, Jennell Van Dongen, Kory Stevens, Si Chen, Junliang Song, Menghui Li, Liang Gao, Ying Fan, Dahui Wang, Limei Xu, Yougui Wang, Zhangang Han, Honggang Li.

Lastly but most importantly, I wish to thank my wife, Qian Feng, for her unconditional love and support; and my daughters, Lindsay Wu and Elysia Wu for the happiness that they have already brought to this family. To them I dedicate this thesis.

To Qian Feng, Lindsay Wu and Elysia Wu

# Chapter 1

## Introduction

Theories of open quantum systems [1–3] usually start from an effective equation of motion of the central systems of interest, which is usually derived from the exact equation of motion for the composite system — the central system plus the bath(s). Although various approximations are involved in deriving such effective equations of motion, which are sometimes called quantum master equations, they are believed to be reasonably reliable since they are built on relatively firm grounds, i.e. an equation of motion derived from first-principles.

Theories of transport [4, 5] in solid state physics deal with a specific type of open system, where the central system is coupled to multiple baths held at different temperatures, chemical potentials, etc. As a result, study of transport should be a branch of the theories of open quantum systems. In practice, different theories based on other approaches have been developed for transport studies, such as the Kubo formula [6, 7], the Landauer-Buttiker formula [8–11] and the non-equilibrium Green’s function method [4, 12–16]. One important reason why theories of open quantum systems are not widely used when studying transport is the computational difficulty in applying them to large systems. In studies of relaxation times in nuclear magnetic resonance [17], where the theories of open quantum systems provide the standard tools, a typical central system has usually only a few degrees of freedom. In contrast, in discussions of transport, one studies quite often mesoscopic systems whose Hilbert space’s dimension easily exceeds  $2^{20}$ .

It is the primary goal of this thesis to find new ways of making the theories of open quantum systems amenable for the study of transport in large(r) systems, by finding efficient calculation schemes. For non-interacting systems there are straightforward methods to calculate stationary states and therefore physical quantities, even if the system is large. Thus, the real challenge is for systems with interactions, just as is the case in the study of equilibrium properties and dynamical processes [18]. We will propose various efficient and accurate approximations, and test them.

This chapter serves as an introduction to the subject and also an overview of this thesis. Sections §1.1 and §1.2 briefly review the theories of open sys-

tems while focusing on their applications to the study of transport. Section §1.3 lists our contributions, including the development of new methodologies and discovery of new physics from application of these methodologies to certain specific systems.

The rest of this thesis follows the same line of logic as this overview, but in more details. Chapter 2 reviews the projector technique used in theories of open quantum systems. Examples are given to illustrate the basic procedure. The resulting effective equations of motion are solved via direct methods, which have very poor efficiency. Then we present an approximate solution based on linear response theory in Chapter 3. This approximation has better efficiency than the direct methods but not good enough to be comparable to the non-equilibrium Green's function method. Chapters 4 and 5 introduce two very efficient and accurate approximations. One is based on a Bogoliubov–Born–Green–Kirkwood–Yvon (BBGKY)-like equation hierarchy and the other is based on the coherent-state representation of density matrices. In Chapter 6 we apply the direct methods to discuss thermal transport of spin systems and the validity of Fourier's Law.

At last, in Chapter 7 we summarize these results and list some of the potentially valuable questions to be investigated in future, with our newly developed methods. We also comment on the value and implications of the work presented in this thesis.

## 1.1 Two major theoretical approaches

A rough picture of a typical experimental setup for measuring transport properties is that of a quasi 1-d system coupled to multiple biased baths. We want to calculate currents flowing through the system given the parameters of the baths such as their temperatures, chemical potentials, etc. Such calculations are relevant for comparison against experimental measurements of charge, energy and spin transport, for example through quasi 1-d spin systems [19], quantum wires including nanotubes [20], molecular devices [21–24] and quantum dots [25, 26].

In particular, in recent years there have been many experiments looking at heat transport of spin systems. The heat conductance  $\kappa = \frac{J_h}{\Delta T}$ , where  $J_h$  is the heat current and  $\Delta T$  the applied temperature bias, is measured for a crystal with spin-chain structures. Typical crystals sizes are of roughly a few  $mm$ . In order to measure the heat conductance contributed by the spin chains, one has to subtract the conductance due to phonons and charge carriers. Usually this is achieved by using anisotropic spin-chain compounds

### 1.1. Two major theoretical approaches

---

such as  $(\text{Ca,Sr})_{14}\text{Cu}_{24}\text{O}_{41}$  [27], which contain  $S = \frac{1}{2}$  two-leg ladders with an intra-chain coupling much stronger than the inter-chain coupling. By measuring the difference between the conductance parallel to the chain and that perpendicular to the chain, one finds the pure spin conductance. The idea is that the parallel conductance is due to both the spin-chain and other sources, while the perpendicular one only has the contributions from other sources. Experimental results on spin chains in strong magnetic fields have also been reported [28, 29]. However, at present, for spin chains, there is no available data regarding temperature profiles and finite size-scaling for the heat currents. This makes comparison with our theoretical results, discussed in Chapter 6, impossible at this time.

In a recent measurement of thermal conductance of nanotubes [30], Wang et al. reported the size dependence of heat currents and concluded that it violates Fourier's law.

For small, and especially also quantum, systems, it is not reliable to use phenomenological laws such as Fourier's law and Ohm's law to characterize their transport. To understand and model such systems, a theoretical framework based on first principle is necessary. Developing such a framework is not just a matter of theoretical interest, but also has obvious practical value.

Various theoretical models have been used so far. Some studies are based on the phenomenological balance equation [31] or rate equation [32, 33], but the most common and systematic approaches are the Kubo formula [6, 34, 35], the non-equilibrium Green's function method [13–15], and the open quantum system approach [1–3] with the system-bath scenario [36–38]. In the approach based on the standard Kubo formula, the system itself is assumed to be infinite and homogeneous. There is no explicit use of the baths but instead the system is treated as being isolated. The current is calculated as a response to a presumed applied electrical potential [6] or temperature gradient drop [39], or uneven mass gradient distribution [40]. In the approach of non-equilibrium Green's function and Landauer formula, the system is modeled by three pieces: the left lead, the central system and the right lead. The leads are taken as half-infinite non-interacting systems and the central system is usually finite. There are no explicit baths included in this picture. The parameters of the baths, such as temperatures and chemical potentials, are attached to the corresponding leads. Finally, the theories of open quantum systems deal with a finite-size central system coupled explicitly to baths, whose degrees of freedom are then integrated out. There are no infinite leads in this picture.

These three different physical pictures are supposed to describe the same problem. Fisher and Lee [41] showed that for non-interacting systems the

### 1.1. Two major theoretical approaches

---

first two are somewhat equivalent if the same three-piece system is used when applying the Kubo formula. We should note, however, that the majority of studies of conductance via the Kubo formula are using an infinite homogeneous system [35, 42], or extrapolate from results on finite-size systems [43, 44]. With that being said, let us ignore the question of whether these methods are equivalent, and focus only on the latter two approaches. Comparisons between them, or even settling how to make them directly comparable, has not been extensively studied.

Non-equilibrium Green's functions is a perturbational theory starting from a well-defined piece-wise equilibrium state of the disconnected three-piece system. The left/right lead is assumed to be in its own equilibrium state correspondingly defined by the left/right temperature and chemical potential, while the central system is in an arbitrary equilibrium state [14]. From this, the Green's function of the disconnected system is calculated and later used to construct the full Green's function of the connected system, with the connection between the central system and the leads treated as perturbation. The standard diagrammatic perturbation theory does not apply here since the initial and final states are qualitatively different. It is an essential assumption of the standard diagrammatic perturbation theory that the states at both  $\pm\infty$  in time are the same equilibrium state (or the ground state if  $T = 0$ ) of the unperturbed system. At this point a non-equilibrium Keldysh formalism [12, 18] is used instead. Conceptually, the condition that the two leads are half-infinite is essential. With any finite-size leads, an equilibrium state – instead of the desired non-equilibrium stationary state – will be reached ultimately since the unbalanced energies or chemical potentials will be eventually dissipated over the whole system. However, even for infinite leads, theoretically there is still no guarantee that the proper stationary state can be calculated perturbationally [13]. In practice, for interacting systems, the non-equilibrium Green's function method is often used together with the density functional theory [13, 16]. Additional approximations, thus possibly additional errors [45, 46], are involved in dealing with the interactions.

Theories of open quantum systems, on the other hand, are based on relatively firmer grounds. They start from the first-principle equation of motion of the composite system, and arrive at an effective equation of motion of the central system. Various equations can be derived depending on the level of approximations. Using the influence functional theory [47, 48], exact time-dependent master equations have been derived for simple central systems [49]. Examples include a two-level system, one harmonic oscillator and two coupled harmonic oscillators, which is the current limit of

such exact approaches [50]. When the Markovian approximation is used, time-independent master equations have also been derived from the exact ones [51]. For more general central systems, some direct brute-force generalization of the master equation of a simple two-site system have also been used in the literature. We will call one kind of such equations the local-operator Lindblad equation for reasons that will be clear later. It is in fact very hard to derive exact master equations from influence functional theory for general central systems. Instead, approximate equations can be derived from the projector technique [51] or other similar techniques. Such a master equation is sometimes called the Redfield equation [52–54]. Applications of the Redfield equation to transport studies are in an early but fast developing stage [36–38, 55–57]. Others prefer to use the local-operator Lindblad equation [58, 59], which turns out to be relatively easier to solve numerically.

It is usually easier to deal with large systems using non-equilibrium Green’s functions, than it is with theories of open quantum systems. In practice, quite often a set of few-particle Green’s functions are enough for calculating the physical quantities of interest. The number of single-particle Green’s functions, for instance, is much smaller than the number of matrix elements of the density matrix, which appears in the Redfield equation. Consider for example an  $N$ -site 1-d spinless fermionic system. The set of all single-particle Green’s functions has  $N^2$  unknowns while a density matrix has  $2^{2N}$  unknowns. Therefore, unless an efficient calculation scheme whose complexity scales as  $N^2$  can be found, numerically the two approaches are not comparable at all. This explains why the non-equilibrium Green’s function method is much more widely used than other methods to study transport in solid state systems. To many, it does not even seem necessary and urgent to compare results from the two methods and determine which is more accurate or even which one is correct.

This situation may change if efficient methods to solve the Redfield equation are found, as is the goal of this thesis.

## 1.2 A big challenge for the system-baths scenario

Both the general Redfield equation and the general local-operator Lindblad equation can be cast into the form of a generalized Liouville equation,

$$\frac{d}{dt}\rho(t) = \mathcal{L}\rho(t), \quad (1.1)$$

where  $\rho(t)$  is the density matrix of the central system and  $\mathcal{L}$  is a linear superoperator acting on the density matrix. We are only interested in the

long-term stationary state and the steady current associated with it. The stationary state is defined by

$$\mathcal{L}\rho(\infty) = 0, \quad (1.2)$$

where  $\rho(\infty)$  is the long-term non-equilibrium stationary state. If the Hilbert space of the central system is  $d$ -dimensional, then the density matrix has  $d^2$  elements. If we represent the density matrix as a vector, for example,

$$P = [\rho_{11}, \rho_{12}, \dots, \rho_{dd}]^T, \quad (1.3)$$

then the linear superoperator  $L$  is a  $d^2 \times d^2$  matrix. The task of finding  $\rho(\infty)$  thus implies finding the zeroth mode of  $\mathcal{L}$  — the eigenvector corresponding to the zero eigenvalue. One can imagine that this becomes nontrivial when  $d > 2^{10}$ , as in the example of a fermionic chain with  $N > 10$  mentioned earlier.

The central task of this thesis is to find efficient methods to solve this equation. Before we present our work, we briefly review the currently available methods.

Instead of solving directly for the zero mode of  $\mathcal{L}$ , we may instead let the system evolve from an arbitrary initial state long enough to arrive at  $\rho(\infty)$ . Thus, the first class of solutions are based on propagators — this includes the direct Runge-Kutta method [37, 60], the Newtonian polynomial propagator [61], the short-iterative-Arnoldi propagator [62] and the short-time Chebyshev polynomial propagator [63]. All these methods have been compared in Ref. [64]. As for their efficiency, they are all roughly on the same scale — their complexities scale roughly as  $d^3$ .

A more efficient approach is the stochastic wave-function method [2, 65, 66]. The basic idea is to replace the effective equation of motion by a stochastic Schrödinger equation for wave functions. The method has a complexity scaling as  $d^2$ . On the local-operator Lindblad equation it has been shown that the stochastic wave-function method leads to accurate results [67]. Breuer et al. showed that it can also be applied to the Redfield equation [65], but its efficiency is still not comparable with that of the non-equilibrium Green's functions method.

For the local-operator Lindblad equation, in fact, there is another quite efficient method developed recently by Prosen et al. [59]. It is based on the time-dependent density matrix renormalization technique. This method makes it possible to analyze systems roughly of the same size as those that can be studied with the non-equilibrium Green's functions method. It is still

an open problem to extend this approach to the Redfield equation. However, we should note that the same central system might behave differently under evolution described by the local-operator Lindblad equation versus the Redfield equation. In fact, this issue has not been settled because of the lack of comparison between the results of the two approaches. The lack of efficient methods for the Redfield equation has certainly contributed to this state of affairs. With our newly developed methods, such a comparison can finally be undertaken.

## 1.3 Our methods and their applications

In this section, we roughly summarize the ideas, performances and applications of our newly developed methods. Their details will be discussed in the rest of this thesis. We have developed three different methods, with different strengths and weaknesses.

### 1.3.1 Linear response theory

The first method is a linear response theory based on the Redfield equation. The basic idea is very simple. The equilibrium state of the central system (when unbiased) is known to be the Boltzmann distribution. The stationary state of the Redfield equation under appropriate conditions, i.e. all baths at the same temperature and chemical potential, is indeed the Boltzmann distribution. This makes it possible to separate the operator  $\mathcal{L}$  into a large part  $\mathcal{L}_0$  and a small part  $\Delta\mathcal{L}$ , where the former part is the operator describing the equilibrium conditions. Then, the non-equilibrium distribution can be treated as a perturbational response to the small part  $\Delta\mathcal{L}$ . This method has efficiency comparable to the stochastic wave-function method.

Besides the gain in efficiency, which is not that remarkable, an important conceptual conclusion is drawn from this work. The standard Kubo formula [6], as we already knew, does produce a proper first-order correction to equilibrium states when an additional potential is included into the Hamiltonian. However, our work shows that it fails to describe the non-equilibrium stationary states. If infinite-size systems are used as the central system, there are ways to get around this conceptual problem. For non-equilibrium stationary states in finite-size systems, the standard Kubo formula must be replaced by a Kubo-like formula based on the Redfield equation – the standard Kubo formula is no longer valid. The key difference is that the standard Kubo formula uses Schrödinger’s equation and the system is treated as isolated while in the new Kubo-like formula, the Redfield

equation of an open system is used. Given that there are still many studies of transport based on various forms of the standard Kubo formula, this is a very important conclusion.

### 1.3.2 The BBGKY-like hierarchy

The second method mirrors the ideas of the well-known BBGKY hierarchy. The original BBGKY hierarchy [68] is a set of coupled equations for equilibrium correlation functions (Green's functions). For non-interacting systems, the hierarchy is decoupled, meaning that the equation of a single-particle Green's function only depends on other single-particle Green's functions, leading to a closed system of equations. Using Wick's theorem, which holds for correlation functions of non-interacting systems, higher order  $n$ -particle Green's functions can then be constructed from the single-particle Green's functions. However, when there are interactions in the system, equations for all orders of Green's functions are coupled together. Fortunately, other approximations can be used to truncate the hierarchy and then one solves the truncated hierarchy. These approximations can be performed in such a way that they are equivalent to the diagrammatic perturbation theory [18, 69].

Here, we extend the same approach to non-equilibrium stationary states. A BBGKY-like hierarchy is derived from the Redfield equation. We find again that for non-interacting systems, the equations decouple and a similar Wick's theorem can be proved. All equations are coupled together for interacting systems. Two further approximations are introduced to truncate the hierarchy. The first one is based on the known equilibrium distribution of the interacting system. The second one is based on the cluster expansion [69]: the observation that higher-order Green's functions can be constructed from the lower-order ones through Wick's Theorem and an additional correlation term. Ignoring these correlation terms at a certain order leads to a truncation of the hierarchy at the corresponding order.

Our tests of the two approximations for small systems, where exact solutions needed for comparisons are also possible, indicate that they have very good accuracy. Moreover, they can be systematically improved by going to higher orders in the truncation schemes. The complexity of this approach scales only like polynomials of  $N$ , not  $d$ , therefore this is a huge improvement of the efficiency.

### 1.3.3 The general Fokker-Planck equation in the coherent-state representation

The third method we propose is to map and solve the Redfield equation in the coherent-state representation of quantum states [70, 71]. Consider a simple harmonic oscillator for example. The set of all coherent states  $|\xi\rangle$ , which are eigenvectors of the annihilation operator  $a|\xi\rangle = \xi|\xi\rangle$ , provides an overcomplete basis for quantum states. Expanding a density matrix in such a basis results in a “distribution” function  $P(\xi)$  over the complex plane  $\mathbb{C}$ . Here we use quotation marks because of the possibility that  $P(\xi)$  could be a negative or even complex number. In this way, creation and annihilation operators become differential operators, and the Redfield equation becomes a stochastic differential equation of the distribution function over  $\mathbb{C}^N$  for a general coupled interacting system of  $N$  harmonic oscillators. Instead of dealing with the huge size of the linear system, like with the direct methods, now we need to solve an  $N$ -dimension stochastic differential equation, which generally can be simulated classically. For non-interacting systems, in fact, the equation can be solved analytically. We have obtained analytical expressions of non-equilibrium stationary states and compared them to the exact solutions. We find perfect agreement, as expected.

For interacting systems, once the classical simulations are performed, the same comparisons can be done. The number of variables increases linearly with the system size so this method is capable of looking at very large systems. A similar procedure [72–74] has been proposed and implemented for the study of equilibrium and pure dynamical systems. There the method is applied successfully for bosonic systems with roughly  $N = 10^6$  modes [75]. In a way, our method can be regarded as an extension of that method to the study of non-equilibrium stationary states. Although this extension involves additional technical difficulties, its efficiency remains comparable to that of its counterpart for the study of equilibrium states and pure dynamical processes.

### 1.3.4 Thermal conductance of spin chains

The physical question we discuss using this open-system approach is the validity of Fourier’s Law of heat conduction,

$$j_h = -\kappa\nabla T, \tag{1.4}$$

where  $j_h$  is the heat current density,  $T$  is the local temperature and  $\kappa$  is the heat conductivity. This phenomenological law is found to be obeyed by

### 1.3. Our methods and their applications

---

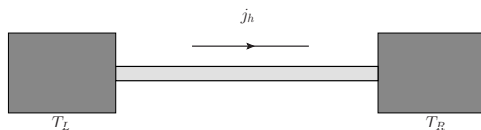


Figure 1.1: Sketch of a typical setup of heat conduction: left and right baths have different temperatures and the conductor is a quasi 1D system.  $j_h$  is the current density on the conductor. It is usually assumed that there is a linearly decreasing temperature profile on the conductor.

macroscopic systems, when measured experimentally in set-ups such as the one sketched in Fig. 1.1.

The derivation of the law from the microscopic equation has been an open question for many decades [34, 76]. The question has been investigated in both classical [76] and quantum systems [34]. For classical systems, a plausible relation between chaotic behavior and the validity of Fourier's Law (also referred to as normal transport), has been observed. But there is still no consensus on the criteria required for a system to exhibit normal transport. The situation is even less clear-cut for quantum systems. Most experimental [19] and theoretical work [34] have focused on spin and energy transport of spin chains or spin ladders. It has been conjectured, based on investigations using the standard Kubo formula [34, 35], that integrability is the criterion for anomalous conductivity. Other studies based on different approaches, however, reach different conclusions. For example, it has been suggested that the existence of gap leads to anomalous transport [77] and also that spin transport could be qualitatively different from energy transport [59]. Experimental results on integrable systems range too from anomalous conductance [78–80] to normal conductance [81].

Most of the previous studies use the standard Kubo formula [34, 44, 82]. Some are based on the local-operator Lindblad equation [56, 59] and some are based on the Redfield equation [36, 37, 83]. However, the spin systems studied via the Redfield equation are either non-interacting (and thus trivially integrable) or non-integrable. We denote, for example, the XY chains as non-interacting since via Jordan-Wigner transformation [84] they can be mapped to systems of free fermions. In the same sense we regard the integrable Heisenberg chains to be interacting since by the same transformation the resulting fermionic systems are interacting. Anomalous transport was found for (trivially) integrable systems and normal transport for non-integrable systems. Disordered spin systems, which are non-integrable,

have also been investigated and found to have normal transport [37]. Prior to our work, there were no integrable interacting systems investigated via the Redfield equation. We apply the Redfield equation to investigate the energy transport of spin 1/2 chains. We also find anomalous transport for XY chains, but normal transport for XXZ chains, which are integrable but interacting. Therefore, we conclude that integrability does not necessarily imply anomalous transport. We then investigate a wider class of systems and conjecture another criterion: interacting systems have normal transport. The reliability of this conjecture needs to be checked further.

## 1.4 Summary

In summary, this chapter has presented a brief synopsis of the challenges that we are trying to address in this thesis, and the directions we have used to achieve these goals. The rest of the thesis will now discuss each of these issues in detail.

## Chapter 2

# The projector technique and the Redfield equation

### 2.1 Outline

In this chapter we review the projector technique for central systems coupled to single or multiple baths, and illustrate its application to small systems with only a few degrees of freedom, where the equations can be solved directly. The challenge it faces when applied to large systems, and our solution to this challenge, will be the topics of other chapters.

This chapter is organized as follows. Section §2.2 contains a brief review of an open system's dynamics based on the system-bath scenario, as a preparation for our method. In Section §2.3, we discuss how systems coupled to a single bath, or to multiple baths held at the same temperature and the same chemical potential, arrive at thermal equilibrium. As examples, the Redfield equations of both a single-mode central system and a two-site central system are solved to illustrate the general procedure. Besides the Redfield equation, there are other various forms of open-system quantum master equations. Usually they can be regarded as generalizations of the Redfield equation of a single-mode central system. Two such equations, which are widely used in literature, are presented in Section §2.4. Then, in Section §2.5 we generalize the Redfield equation to systems coupled to two or more baths of different temperatures but with the same chemical potential, and discuss their heat conductance. The method is also valid for electrical and spin transport, where the chemical potentials of baths could also be different.

### 2.2 The effective equation of motion for open systems

In this section we derive a general effective equation of motion for a central system coupled to a single bath, starting from the Schrödinger's equation for

## 2.2. The effective equation of motion for open systems

---

the total composite system. A similar derivation can be found in Refs. [1, 2, 51, 85]. Unless otherwise stated, in this thesis we use  $\hbar = 1, k_B = 1, c = 1$ .

Consider a system  $S$  interacting with a single bath/reservoir  $B$ . In the Schrödinger picture, the Liouville equation for the evolution of the density matrix of the total closed quantum system  $S + B$  is:

$$i \frac{\partial \hat{\rho}_T(t)}{\partial t} = [\hat{H}, \hat{\rho}_T(t)] \equiv \hat{\mathcal{L}} \hat{\rho}_T(t). \quad (2.1)$$

Here we denote the density matrix of the total composite system as  $\hat{\rho}_T$  and the reduced density matrix of the central system (the bath) as  $\hat{\rho}$  ( $\hat{\rho}_B$ ),

$$\hat{\rho}(t) = tr^B(\hat{\rho}_T(t)), \quad (2.2)$$

$$\hat{\rho}_B(t) = tr^S(\hat{\rho}_T(t)), \quad (2.3)$$

where  $tr^B$  ( $tr^S$ ) stands for the operation of partial trace over the bath (the central system) degrees of freedom.

The total Hamiltonian has the generic form:

$$\hat{H} = \hat{H}_0(S, B) + \hat{V}(S, B), \quad (2.4)$$

where

$$\hat{H}_0(S, B) = \hat{H}_S(S) \otimes \hat{I}(B) + \hat{I}(S) \otimes \hat{H}_B(B) \quad (2.5)$$

describes the system, respectively the bath, and

$$\hat{V}(S, B) = \sum_i \hat{L}_i(S) \otimes \hat{F}_i(B) \quad (2.6)$$

describes their interactions, with  $\hat{L}_i(S)$  and  $\hat{F}_i(B)$  being system, respectively bath operators.  $\hat{I}(B)$  and  $\hat{I}(S)$  are the identity operators in the Hilbert space of the bath and the central system, respectively.

If we are interested only in the properties of  $S$ , we call it an open quantum system. Typically, we need to calculate the ensemble average of physical quantities depending on operators acting on  $S$  only,

$$\langle A \rangle = tr([\hat{A}_S \otimes \hat{I}(B)] \hat{\rho}_T). \quad (2.7)$$

This can be trivially rewritten as:

$$\langle A \rangle = tr^S(\hat{A}_S \hat{\rho}). \quad (2.8)$$

Therefore, it is convenient to try to find  $\hat{\rho}(t)$  directly, and avoid solving for the total density matrix  $\hat{\rho}_T(t)$ , which is a much more complicated problem

## 2.2. The effective equation of motion for open systems

---

due to the significant increase in the number of degrees of freedom. Instead we are looking for the evolution equation of the reduced matrix density in a form similar to Eq. (2.1):

$$\frac{\partial \hat{\rho}(t)}{\partial t} = \hat{\mathcal{L}} \hat{\rho}(t), \quad (2.9)$$

but now  $\hat{\mathcal{L}}$  is obviously neither  $[\hat{H}, \cdot]$  of the whole system nor  $[\hat{H}_S, \cdot]$  of the central system only. The task of this section is to derive the proper Liouville operator starting from knowledge of the total Hamiltonian  $\hat{H}$ .

There are two main types of approaches to discuss the dynamics of an open system: based on dynamic variables or based on density matrices. The first approach uses equations of motion for dynamic variables such as  $\hat{X}, \hat{P}$  etc. The dynamic variables of the bath are integrated out, resulting in noise-sources terms in the Langevin-type equations for the dynamic variables of the system. If one can solve these Langevin equations, the full time dependence of the central system is known. From a quantum mechanics point of view, this approach is similar to the Heisenberg picture.

The second approach focuses on distribution functions in the phase space of the system, such as  $\rho(x, p)$  for classical systems and the density matrix  $\hat{\rho}$  for quantum systems. Equations of motion are generated for them, the bath is projected out, and then the equation for the reduced density matrix is solved. From a quantum mechanics point of view, this approach is more similar to the Schrödinger picture.

We will use the latter approach. In this section we summarize the general formalism of this method. There are two well-known techniques to derive the equation of motion of the reduced density matrix, namely the projector operator technique and the non-correlation approximation. We discuss the first one in reasonable detail and then shortly review the second one.

### 2.2.1 The projector operator technique and the reduced Liouville equation

One way to derive the unknown  $\hat{\mathcal{L}}$  in Eq. (2.9) is through the technique of projection. We define the projector operator on the Hilbert space of the total system  $S + B$ ,  $\mathcal{P} : \mathcal{H} \rightarrow \mathcal{H}$ , such that

$$\mathcal{P}(\hat{\rho}_T) \triangleq \text{tr}^B(\hat{\rho}_T) \otimes \hat{\rho}_B^{eq} = \hat{\rho} \otimes \hat{\rho}_B^{eq} \quad (2.10)$$

where  $\hat{\rho}_B^{eq}$  is the density matrix of the isolated bath in equilibrium, although this requirement could be relaxed. It is easy to verify that  $\mathcal{P}$  is a projector,

## 2.2. The effective equation of motion for open systems

---

i.e. that  $\mathcal{P}\mathcal{P} = \mathcal{P}$ . We denote  $\mathcal{Q} = I - \mathcal{P}$ , and rewrite the equation of motion for the total system, Eq. (2.1), as:

$$\begin{cases} \frac{\partial}{\partial t} \mathcal{P} \hat{\rho}_T(t) = \mathcal{P} \hat{\mathcal{L}} \mathcal{P} \hat{\rho}_T(t) + \mathcal{P} \hat{\mathcal{L}} \mathcal{Q} \hat{\rho}_T(t) \\ \frac{\partial}{\partial t} \mathcal{Q} \hat{\rho}_T(t) = \mathcal{Q} \hat{\mathcal{L}} \mathcal{P} \hat{\rho}_T(t) + \mathcal{Q} \hat{\mathcal{L}} \mathcal{Q} \hat{\rho}_T(t) \end{cases} \quad (2.11)$$

The second equation is integrated formally and its solution is substituted into the first equation, to obtain:

$$\frac{\partial}{\partial t} \mathcal{P} \hat{\rho}_T(t) = \mathcal{P} \hat{\mathcal{L}} \mathcal{P} \hat{\rho}_T(t) + \mathcal{P} \hat{\mathcal{L}} \int_0^t d\tau e^{(t-\tau)\mathcal{Q}\hat{\mathcal{L}}} \mathcal{Q} \hat{\mathcal{L}} \mathcal{P} \hat{\rho}_T(\tau) + \mathcal{P} \hat{\mathcal{L}} e^{t\mathcal{Q}\hat{\mathcal{L}}} \mathcal{Q} \hat{\rho}_T(0). \quad (2.12)$$

If we start from the reasonable initial condition

$$\hat{\rho}_T(0) = \hat{\rho}(0) \otimes \hat{\rho}_B^{eq}, \quad (2.13)$$

then

$$\mathcal{Q} \hat{\rho}_T(0) = 0 \quad (2.14)$$

and the last term vanishes identically. Let  $\mathcal{L}_S, \mathcal{L}_B, \mathcal{L}_V$  be the Liouville operators corresponding respectively to  $\hat{H}_S(S), \hat{H}_B(B)$  and  $\hat{V}(S, B)$ . Then,

$$\hat{\mathcal{L}} = \hat{\mathcal{L}}_S + \hat{\mathcal{L}}_B + \hat{\mathcal{L}}_V \triangleq \hat{\mathcal{L}}_0 + \hat{\mathcal{L}}_V. \quad (2.15)$$

Since  $\hat{\mathcal{L}}_B \hat{\rho}_B^{eq} = 0$ , we can rewrite the dynamic equation as

$$\frac{\partial}{\partial t} \hat{\rho}(t) \otimes \hat{\rho}_B^{eq} = \mathcal{P} \hat{\mathcal{L}}_S [\hat{\rho}(t) \otimes \hat{\rho}_B^{eq}] + \mathcal{P} \hat{\mathcal{L}}_1 [\hat{\rho}(t) \otimes \hat{\rho}_B^{eq}] \quad (2.16)$$

$$+ \mathcal{P} \hat{\mathcal{L}} \int_0^t d\tau e^{(t-\tau)\mathcal{Q}\hat{\mathcal{L}}} \mathcal{Q} \hat{\mathcal{L}} [\hat{\rho}(t) \otimes \hat{\rho}_B^{eq}]. \quad (2.17)$$

The second term is identically zero if we require that for any eigenstate in the bath's Hilbert space, the expectation value of the bath operators involved in the bath-system coupling [see Eq. (2.6)] vanishes:

$$\langle b | \hat{F}_i(B) | b \rangle = 0. \quad (2.18)$$

In this case, we have:

$$\begin{aligned} i \langle b | \hat{\mathcal{L}}_1 [\hat{\rho}(t) \otimes \hat{\rho}_B^{eq}] | b \rangle &= \sum_i \langle b | \left[ \hat{L}_i(S) \otimes \hat{F}_i(B), \hat{\rho}(t) \otimes \hat{\rho}_B^{eq} \right] | b \rangle \\ &= \sum_i \left( \hat{L}_i(S) \hat{\rho}(t) \langle b | \hat{F}_i(B) \hat{\rho}_B^{eq} | b \rangle - \hat{\rho}(t) \hat{L}_i(S) \langle b | \hat{\rho}_B^{eq} \hat{F}_i(B) | b \rangle \right) \\ &= 0 \end{aligned}$$

## 2.2. The effective equation of motion for open systems

---

showing that indeed,  $\mathcal{P}\hat{\mathcal{L}}_V\mathcal{P} = 0$ . This condition, which is satisfied for most types of couplings, is not however necessary. If it is not obeyed, there will be a term of the form  $\sum_{i,b} \frac{e^{-\beta E_b}}{\mathcal{Z}} \langle b | \hat{F}_i | b \rangle [\hat{L}_i, \cdot]$ , which can be added to  $\hat{\mathcal{L}}_S$ . It follows that this assumption is not essential, although all the coupling Hamiltonians we study satisfy it. With these assumptions and after tracing out the bath degrees of freedom, we find that:

$$\frac{\partial}{\partial t} \hat{\rho}(t) = \hat{\mathcal{L}}_S \hat{\rho}(t) + tr^B \left\{ \mathcal{P} \hat{\mathcal{L}} \int_0^t d\tau e^{(t-\tau)\mathcal{Q}\hat{\mathcal{L}}} \mathcal{Q} \hat{\mathcal{L}} \mathcal{P} \hat{\rho}_T(\tau) \right\}. \quad (2.19)$$

Subject to the two assumptions mentioned above, this equation is exact. Clearly, all the effects of the bath on the system's dynamics are contained in the second term on the right-hand side.

This term can be further simplified. One can verify that

$$\mathcal{Q} \hat{\mathcal{L}} \mathcal{P} = \mathcal{Q} \hat{\mathcal{L}}_0 \mathcal{P} + \mathcal{Q} \hat{\mathcal{L}}_V \mathcal{P} = \mathcal{Q} \hat{\mathcal{L}}_V \mathcal{P} = -\mathcal{P} \hat{\mathcal{L}}_V \mathcal{P} + \hat{\mathcal{L}}_V \mathcal{P} = \hat{\mathcal{L}}_V \mathcal{P} \quad (2.20)$$

where the second assumption has been invoked again. Now we use the first essential assumption, replacing:

$$e^{(t-\tau)\mathcal{Q}\hat{\mathcal{L}}} \rightarrow e^{(t-\tau)\mathcal{Q}\hat{\mathcal{L}}_0}. \quad (2.21)$$

This is valid when the system-bath interaction is weak, since, as shown in the following, it is equivalent to second order perturbation in the ‘‘coupling strength’’ between system and bath. This follows because we can then simplify:

$$e^{(t-\tau)\mathcal{Q}\hat{\mathcal{L}}_0} = e^{(t-\tau)(\mathcal{I}-\mathcal{P})\hat{\mathcal{L}}_0} = e^{(t-\tau)(\hat{\mathcal{L}}_0 - \mathcal{P}\hat{\mathcal{L}}_0)} = e^{(t-\tau)\hat{\mathcal{L}}_0}, \quad (2.22)$$

where we make use of  $\mathcal{P}\hat{\mathcal{L}}_0 = \mathcal{P}\hat{\mathcal{L}}_0\mathcal{P} + \mathcal{P}\hat{\mathcal{L}}_0\mathcal{Q} = 0$ . Therefore we obtain:

$$\frac{\partial}{\partial t} \hat{\rho}(t) = \hat{\mathcal{L}}_S \hat{\rho}(t) + tr^B \left\{ \hat{\mathcal{L}}_V \int_0^t d\tau e^{(t-\tau)\hat{\mathcal{L}}_0} \hat{\mathcal{L}}_V \hat{\rho}(\tau) \otimes \hat{\rho}_B^{eq} \right\}, \quad (2.23)$$

where indeed the second term is of second order in the interaction  $\hat{V}$ . This can be further simplified in the interaction picture, where we define

$$\hat{\rho}^I(t) = e^{i\hat{H}_S t} \hat{\rho}(t) e^{-i\hat{H}_S t}, \quad (2.24a)$$

$$\hat{L}_j^I(t) = e^{i\hat{H}_S t} \hat{L}_j e^{-i\hat{H}_S t}, \quad (2.24b)$$

$$\hat{F}_j^I(t) = e^{i\hat{H}_B t} \hat{F}_j e^{-i\hat{H}_B t}. \quad (2.24c)$$

## 2.2. The effective equation of motion for open systems

---

In this case, the first term cancels out, and the dynamic equation becomes:

$$\begin{aligned} \frac{\partial \hat{\rho}^I(t)}{\partial t} = & - \sum_{jl} \int_0^t d\tau \left\{ \left[ \hat{L}_j^I(t), \hat{L}_l^I(t-\tau) \hat{\rho}^I(t-\tau) \right] G_{jl}(\tau) \right. \\ & \left. - \left[ \hat{L}_j^I(t), \hat{\rho}^I(t-\tau) \hat{L}_l^I(t-\tau) \right] G_{lj}(-\tau) \right\} \end{aligned} \quad (2.25)$$

where

$$G_{jl}(\tau) = \text{tr}^B \left( \hat{F}_j^I(\tau) \hat{F}_l^I(0) \hat{\rho}_B^{eq} \right). \quad (2.26)$$

are Green's functions which depend only on the bath characteristics and can be calculated directly.

Depending on the specific form of the Hamiltonian, Eq. (2.25) may or may not have a unique long-term stationary solution. For example, it may oscillate between several metastable states. The exact criteria guaranteeing the existence of such a steady-state are not known. Finding such criteria would be an interesting topic for further research. In the following, we take the pragmatic approach and assume that if a stationary steady-state solution has been found, then it is unique.

Now comes our second essential assumption, the Markov approximation:

$$\hat{\rho}^I(t-\tau) \approx \hat{\rho}^I(t) \text{ for } t \gg \tau_c, \quad (2.27)$$

where  $\tau_c$  is the characteristic relaxation time of  $G_{jl}(\tau)$  (i.e., of the bath). Since in this thesis we investigate the steady-state solution when  $t \rightarrow \infty$ , the Markov approximation is likely justified. Using the influence functional technique, similar but more complicated equations can be derived if the Markov approximation is relaxed [47–50, 86]. These more complicated equations are necessary in the study of transient process. We believe that for the purpose of study of stationary states, the Markov approximation is accurate enough.

With this final approximation, we find the desired equation of motion for the reduced density matrix:

$$\begin{aligned} \frac{\partial \hat{\rho}^I(t)}{\partial t} = & - \sum_{jl} \int_0^t d\tau \left\{ \left[ \hat{L}_j^I(t), \hat{L}_l^I(t-\tau) \hat{\rho}^I(t) \right] G_{jl}(\tau) \right. \\ & \left. - \left[ \hat{L}_j^I(t), \hat{\rho}^I(t) \hat{L}_l^I(t-\tau) \right] G_{lj}(-\tau) \right\}. \end{aligned} \quad (2.28)$$

It can be transformed back to the Schrödinger picture,

$$\begin{aligned} \frac{\partial \hat{\rho}(t)}{\partial t} = & -i[H_S, \hat{\rho}(t)] - \sum_{jl} \int_0^t d\tau \left\{ \left[ \hat{L}_j, \hat{L}_l^I(-\tau) \hat{\rho}(t) \right] G_{jl}(\tau) \right. \\ & \left. - \left[ \hat{L}_j, \hat{\rho}(t) \hat{L}_l^I(-\tau) \right] G_{lj}(-\tau) \right\}. \end{aligned} \quad (2.29)$$

## 2.2. The effective equation of motion for open systems

---

This equation can also be projected in the eigenbasis of  $H_S$ , denoted as  $\{|s\rangle\}$  such that  $H_S |s\rangle = E_s |s\rangle$ . In this case, the effective equation of motion becomes

$$\frac{d}{dt} \rho_{s's}^I(t) = \sum_{m,n} R_{s'smn}(t) \rho_{mn}^I(t), \quad (2.30)$$

with

$$R_{s'smn} = -e^{i\Delta E_{s'smn}t} \cdot \left[ \sum_k \delta_{sn} \Gamma_{s'kkm}^+ - \Gamma_{nss'm}^+ - \Gamma_{nss'm}^- + \sum_k \delta_{s'm} \Gamma_{nkks}^- \right], \quad (2.31)$$

where

$$\Delta E_{s'smn} = E_{s'}^S - E_s^S + E_n^S - E_m^S \quad (2.32)$$

and

$$\Gamma_{mklm}^+(t) = \sum_{ij} \langle m | \hat{L}_i | k \rangle \langle l | \hat{L}_j | n \rangle \int_0^t e^{-i(E_i^S - E_n^S)\tau} G_{ij}(\tau) d\tau \quad (2.33)$$

and  $\Gamma_{mklm}^-(t) = (\Gamma_{nlkm}^+(t))^*$ . The above effective equation of motion is sometimes called a quantum master equation. If we focus only on the diagonal terms for  $\rho_{ss}^I(t)$ , then we obtain the secular quantum master equation, which requires the so-called secular approximation [1] in order to be consistent with Fermi's Golden Rule. The secular approximation is to ask that

$$E_{s'}^S - E_s^S + E_n^S - E_m^S = 0, \quad (2.34)$$

so as to eliminate the explicit time dependence of the right hand side of Eq. (2.31). Then, finally,

$$\frac{d}{dt} \rho_{ss}^I(t) = \sum_m W_{sm} \rho_{mm}^I(t) - \sum_m W_{ms} \rho_{ss}^I(t), \quad (2.35)$$

where  $W_{sm} = \Gamma_{mssm}^+ + \Gamma_{mssm}^-$ . This is now consistent with Fermi's Golden Rule. While there is a considerable body of work based on such secular quantum master equations, we choose to work directly with the full effective equation of motion Eq. (2.28).

### 2.2.2 An alternative derivation: the non-correlation approximation

This is a different way to derive the above equation of motion for the reduced density matrix, using the so-called non-correlation approximation. Suppose that both  $\hat{H}_S$  and  $\hat{H}_B$  are solvable, and their eigenstates are respectively  $\{|s\rangle\}$  for  $E_s^S$  and  $\{|b\rangle\}$  for  $E_b^B$ . Then, a complete basis for the total Hilbert space can be chosen as  $\{|s\rangle|b\rangle\}$ .

In the interaction picture  $|\psi^I(t)\rangle = e^{i(\hat{H}_S + \hat{H}_B)t} |\psi(t)\rangle$ , the time evolution of the operators describing the coupling is

$$\hat{L}_i^I(t) = e^{i\hat{H}_S t} \hat{L}_i(t) e^{-i\hat{H}_S t} \quad (2.36)$$

and

$$\hat{F}_i^I(t) = e^{i\hat{H}_B t} \hat{F}_i(t) e^{-i\hat{H}_B t}. \quad (2.37)$$

The dynamical equation of the whole system is:

$$i \frac{\partial \hat{\rho}_T^I(t)}{\partial t} = [\hat{V}^I(t), \hat{\rho}_T^I(t)]. \quad (2.38)$$

Integrating this formally and substituting the resulting expression for  $\hat{\rho}^I$  in the right-hand side of Eq. (2.38), we obtain:

$$\frac{\partial \hat{\rho}_T^I(t)}{\partial t} = -i [\hat{V}^I(t), \hat{\rho}_T^I(0)] - \int_0^t d\tau [\hat{V}^I(t), [\hat{V}^I(\tau), \hat{\rho}_T^I(\tau)]]. \quad (2.39)$$

Integrating out the bath, this becomes:

$$\begin{aligned} \frac{\partial \hat{\rho}^I(t)}{\partial t} &= -i \text{tr}^B \left( [\hat{V}^I(t), \hat{\rho}_T^I(0)] \right) \\ &\quad - \int_0^t d\tau \text{tr}^B \left( [\hat{V}^I(t), [\hat{V}^I(\tau), \hat{\rho}_T^I(\tau)]] \right), \end{aligned} \quad (2.40)$$

which is still exact. Now we begin to introduce several approximations. First, we again assume

$$\langle b | \hat{F}_i(B) | b \rangle = 0, \quad (2.41)$$

so that the first term in Eq. (2.40) vanishes. As before, this is not an essential assumption. Second, we also assume,

$$\hat{\rho}_T^I(\tau) = \hat{\rho}^I(\tau) \otimes \hat{\rho}_B^I(\tau), \quad (2.42)$$

such that the second term in Eq. (2.40) can be separated and simplified. This is the essential approximation. In fact this is stronger than the corresponding approximation, Eq. (2.13), used in the previous section, where this factorization is assumed to be true only for the initial state. Third, we take,

$$\hat{\rho}_B^I(\tau) = \hat{\rho}_B^{eq} = \frac{1}{Z_B} e^{-\beta \hat{H}_B}. \quad (2.43)$$

With these assumptions, we get a simplified dynamic equation for the reduced density matrix identical to Eq. (2.25). If we further apply the Markov condition, we arrive at the same effective equation of motion as in Eq. (2.28).

### 2.2.3 The quantum master equation in terms of creation and annihilation operators

From now on, we will work in the Schrödinger picture and directly deal with the reduced density matrix of the central system. In this thesis, we will mostly use the second quantization language. In terms of creation and annihilation operators, Eq. (2.28) can be simplified further. Let us now derive such a simplified version for a general central system, whose  $\nu$ th site is coupled to the  $\nu$ th bath with bath parameters  $T_\nu, \mu_\nu$  and coupling constant  $V_{k,\nu}$  and  $\lambda$ ,

$$H_S = \mathcal{H}(a_j, a_j^\dagger), \quad (2.44a)$$

$$H_{B\nu} = \sum_k \omega^\nu(k) b_{k,\nu}^\dagger b_{k,\nu}, \quad (2.44b)$$

$$H_{SB} = \lambda \sum_{k,\nu} \left( V_{k,\nu} a_\nu^\dagger b_{k,\nu} + h.c. \right). \quad (2.44c)$$

Here  $\mathcal{H}(a_j, a_j^\dagger)$  can be any function of  $a_j$  and  $a_j^\dagger$ .  $\lambda$  refers to the strength of the coupling between the central system and the baths. It could be absorbed into the coupling coefficients  $V_{k,\nu}$  but we separate it and use it as a relatively small dimensionless number for bookkeeping purpose. Here we assume that every site connected to a bath, is connected to its own bath. If two sites happen to share a bath, then the formula we derive below needs to be adjusted. First we identify

$$L_{k,\nu}^{(1)} = \lambda V_{k,\nu} a_\nu, F_{k,\nu}^{(1)} = b_{k,\nu}^\dagger; L_{k,\nu}^{(2)} = \lambda V_{k,\nu}^* a_\nu^\dagger, F_{k,\nu}^{(2)} = b_{k,\nu} \quad (2.45)$$

## 2.2. The effective equation of motion for open systems

---

and note that the only non-vanishing bath Green's functions are:

$$G_{k,\nu,k,\nu'}^{1,2}(\tau) = \text{tr}_B \left( F_{k,\nu}^{(1)}(\tau) F_{k,\nu'}^{(2)}(0) \rho_B \right) = \langle n_{k,\nu} \rangle e^{i\omega_\nu(k)\tau} \delta_{\nu,\nu'}, \quad (2.46a)$$

$$G_{k,\nu,k,\nu'}^{2,1}(\tau) = \text{tr}_B \left( F_{k,\nu}^{(2)}(\tau) F_{k,\nu'}^{(1)}(0) \rho_B \right) = \langle 1 - n_{k,\nu} \rangle e^{-i\omega_\nu(k)\tau} \delta_{\nu,\nu'}. \quad (2.46b)$$

The  $\delta_{\nu,\nu'}$  comes from the assumption of independent baths for each site, which means that Green's functions among operators belonging to baths coupled to different sites are zero. By definition,

$$\langle n_{k,\nu} \rangle \equiv \langle n(\omega_\nu(k), T_\nu, \mu_\nu) \rangle = \left( e^{\frac{\omega_\nu(k) - \mu_\nu}{T_\nu}} - 1 \right)^{-1} \quad (2.47)$$

is the average particle number in state  $k$  in bath  $\nu$ . For simplicity of notation,  $\langle n_{k,\nu} \rangle$  will be denoted as  $n_{k,\nu}$  whenever it is safe to do so.

After plugging these Green's functions into Eq. (2.28), we arrive at a quantum master equation

$$\begin{aligned} \frac{\partial \rho(t)}{\partial t} &= -i[\mathcal{H}_S, \rho(t)] \\ &- \lambda^2 \sum_\nu \left\{ [a_\nu^\dagger, \hat{m}_\nu \rho(t)] + [a_\nu, \hat{m}_\nu \rho(t)] + h.c. \right\}, \end{aligned} \quad (2.48)$$

with operators  $\hat{m}$  and  $\hat{m}_\nu$  defined as follows:

$$\hat{m}_\nu = \sum_k |V_k|^2 \int_0^\infty d\tau a_\nu(-\tau) e^{-i\omega_\nu(k)\tau} \langle 1 - n_{k,\nu} \rangle, \quad (2.49a)$$

$$\hat{m}_\nu = \sum_k |V_k|^2 \int_0^\infty d\tau a_\nu^\dagger(-\tau) e^{i\omega_\nu(k)\tau} \langle n_{k,\nu} \rangle. \quad (2.49b)$$

Here  $a_\nu(\tau) = e^{iH_S \tau} a_\nu e^{-iH_S \tau}$  is expressed in the Heisenberg picture. Note that we have also changed the integral limit from  $t$  to  $\infty$ . Again this is reasonable only if the stationary solution itself is of interest, not the whole evolution process. *This quantum master equation in creation and annihilation operators is the central equation of this chapter and will be used later throughout the whole thesis. Eq. (2.48) is sometimes called the Redfield equation [52, 53, 87].*

In some cases, it is convenient to use the eigenstates of  $H_S$  as a basis,  $\{|E_n\rangle\}$ . In that case, using element-wise products in this basis, the expressions of the operators  $\hat{m}$  and  $\hat{m}_\nu$  can be rewritten as

$$\hat{m}_\nu = a_\nu \cdot \Sigma_\nu, \hat{m}_\nu = a_\nu^\dagger \cdot \bar{\Sigma}_\nu, \quad (2.50)$$

where

$$\Sigma_\nu = \pi \sum_{m,n} |m\rangle \langle n| [1 - n(E_n - E_m, T_\nu, \mu_\nu)] J_\nu(E_n - E_m), \quad (2.51a)$$

$$\bar{\Sigma}_\nu = \pi \sum_{m,n} |m\rangle \langle n| n_\nu(E_m - E_n, T_\nu, \mu_\nu) J_\nu(E_m - E_n), \quad (2.51b)$$

and

$$J_\nu(\epsilon) = \sum_k |V_k|^2 \delta(\epsilon - \omega_\nu(k)) \quad (2.52)$$

is usually called the spectrum density function [36, 48] of the bath  $\nu$ .

## 2.3 Relaxation towards thermal equilibrium

We first apply this general procedure to the simplest example — a single-site fermionic system coupled to a bath — and show that the system evolves to the correct thermal equilibrium as  $t \rightarrow \infty$ . We then briefly investigate a corresponding two-site system.

### 2.3.1 One-site open system

Consider a one-state fermionic system in a strong magnetic field, describing for instance a single quantum dot, defined by a Hamiltonian:

$$H_S = \epsilon a^\dagger a \quad (2.53)$$

where  $a, a^\dagger$  are fermionic operators. The system is coupled to a single bath ( $\nu = 1$  only), which is regarded as an ensemble of fermions with fixed  $T$  and  $\mu$ , so that both particles and energy are exchanged. Using the general quantum master equation Eq. (2.48), we have

$$\frac{\partial}{\partial t} \rho = -i [\epsilon a^\dagger a, \rho] - \lambda^2 \left\{ [a^\dagger, \hat{m} \rho] + [a, \hat{m} \rho] + h.c. \right\}, \quad (2.54)$$

where

$$\hat{m} = \pi J(\epsilon) [1 - n(\epsilon)] a, \quad (2.55a)$$

$$\hat{m} = \pi J(\epsilon) n(\epsilon) a^\dagger, \quad (2.55b)$$

and  $n(\epsilon)$  is shorthand for  $n(\epsilon, T, \mu) = \left( e^{\frac{\epsilon - \mu}{T}} - 1 \right)^{-1}$ , the average number of particles with energy  $\epsilon$  in the bath (since there is a single bath, there is no

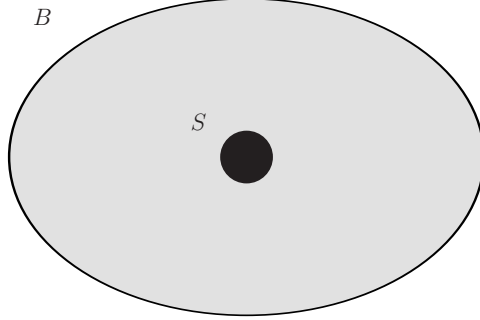


Figure 2.1: Sketch of a one-site system coupled to a heat bath.

need to explicitly write down  $T_\nu$  and  $\mu_\nu$  everywhere).  $J(\epsilon)$  can be defined accordingly for this specific system using Eq. (2.52).

Now we can solve the dynamical equation and check the stationary solution. The density matrix of the above system can be written in the general form:

$$\rho(t) = \frac{1+p(t)}{2} |0\rangle\langle 0| + \frac{1-p(t)}{2} |1\rangle\langle 1| + q(t) |0\rangle\langle 1| + q^*(t) |1\rangle\langle 0|, \quad (2.56)$$

so that the trace is preserved. Then we get evolution equations for these parameters from the Redfield equation:

$$\frac{d}{dt}p(t) = 2(1 - 2n(\epsilon)) - 2p(t), \quad (2.57a)$$

$$\frac{d}{dt}q(t) = -q(t). \quad (2.57b)$$

This has a stationary solution, independent of the initial state:

$$p(\infty) = 1 - 2n(\epsilon) = \frac{e^{\beta(\epsilon-\mu)} - 1}{e^{\beta(\epsilon-\mu)} + 1}, \quad (2.58a)$$

$$q(\infty) = 0, \quad (2.58b)$$

which leads indeed to the expected equilibrium grand-canonical distribution

$$\rho(\infty) = \frac{1}{e^{-\beta(\epsilon-\mu)} + 1} |0\rangle\langle 0| + \frac{e^{-\beta(\epsilon-\mu)}}{e^{-\beta(\epsilon-\mu)} + 1} |1\rangle\langle 1| \quad (2.59)$$

for the two-level system. Note that in this example, the value of  $\lambda$  itself is irrelevant: this equilibrium state will be reached irrespective of the strength of the coupling to the bath. As we show later, this is not true for non-equilibrium stationary states, which depend on the details of the coupling between the central system and the baths.

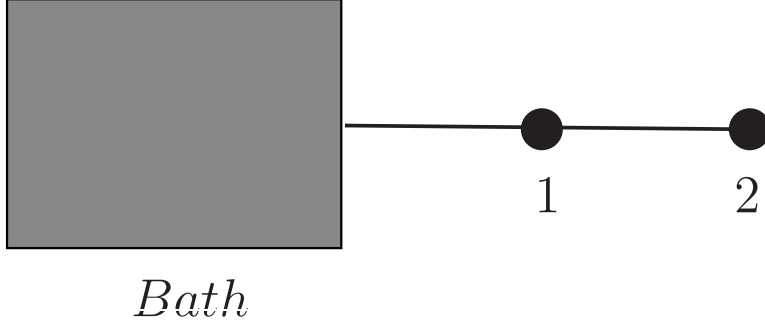


Figure 2.2: Sketch of a two-site system coupled to a heat bath.

### 2.3.2 Two-site open system

Let us now consider a two-site fermionic system coupled to one heat bath, see Fig. 2.2. The system's Hamiltonian is taken to be a simple hopping Hamiltonian:

$$H_S = -\epsilon \left( a_1^\dagger a_2 + a_2^\dagger a_1 \right), \quad (2.60)$$

and we assume that only site 1 is coupled to the bath, so that:

$$V = \sum_k \left( \lambda V_k a_1 b_k^\dagger + \lambda V_k^* a_1^\dagger b_k \right). \quad (2.61)$$

Using the general effective equation of motion Eq. (2.48), we arrive at

$$\frac{d}{dt} \rho = -i [H_S, \rho] - \lambda^2 \left\{ [a_1^\dagger, \hat{m}_1 \rho] + [a_1, \hat{m}_1 \rho] + h.c. \right\}, \quad (2.62)$$

where

$$\hat{m}_1 = \frac{\pi J(-\epsilon) [1 - n(-\epsilon)]}{2} (a_1 + a_2) + \frac{\pi J(\epsilon) [1 - n(\epsilon)]}{2} (a_1 - a_2), \quad (2.63a)$$

$$\hat{\hat{m}}_1 = \frac{\pi J(-\epsilon) n(-\epsilon)}{2} (a_1^\dagger + a_2^\dagger) + \frac{\pi J(\epsilon) n(\epsilon)}{2} (a_1^\dagger - a_2^\dagger), \quad (2.63b)$$

and  $J(\pm\epsilon)$  can be calculated similarly as in Eq. (2.52) but now for the eigenenergies  $\pm\epsilon$ . Again, for simplicity we assume  $J(\pm\epsilon) = 1$ . Note that when  $\epsilon = 0$ , the operators  $\hat{m}_1$  and  $\hat{\hat{m}}_1$  become

$$\hat{m}_1 = J(0) [1 + n(0)] a_1, \quad (2.64a)$$

$$\hat{\hat{m}}_1 = J(0) n(0) a_1^\dagger, \quad (2.64b)$$

### 2.3. Relaxation towards thermal equilibrium

---

in agreement with results in the previous section. This shows that only if  $\epsilon$  is zero, then the operators  $\hat{m}_1$  and  $\hat{\hat{m}}_1$  depend only on  $a_1$  and  $a_1^\dagger$ . Otherwise, they also involve the creation and annihilation operators for other sites in the system (here, site 2). In fact, unless  $a_\nu^\dagger$  happens to be the creation operator of an eigenmode of  $H_S$ , which is generally not the case,  $\hat{\hat{m}}_\nu$  involves other operators than  $a_\nu, a_\nu^\dagger$ . We will revisit this issue in Section §2.4.

The eigenmodes of this Hamiltonian are,

$$H_S = -\epsilon a_+^\dagger a_+ + \epsilon a_-^\dagger a_-, \quad (2.65)$$

where

$$a_\pm = \frac{a_1 \pm a_2}{\sqrt{2}}. \quad (2.66)$$

In terms of occupation states of these eigenmodes  $|n_+ n_- \rangle$ , eigenstates are  $|00\rangle, |10\rangle, |01\rangle, |11\rangle$  with eigenvalues respectively  $\epsilon_1 = 0, \epsilon_2 = -\epsilon, \epsilon_3 = \epsilon, \epsilon_4 = 0$ . A density matrix in this basis

$$\rho = \begin{bmatrix} p_{11} & p_{12} & p_{13} & p_{14} \\ p_{21} & p_{22} & p_{23} & p_{24} \\ p_{31} & p_{32} & p_{33} & p_{34} \\ p_{41} & p_{42} & p_{43} & p_{44} \end{bmatrix} \quad (2.67)$$

can be cast into a 16-dimensional vector,

$$P = [p_{11}, p_{12}, \dots, p_{44}]^T. \quad (2.68)$$

### 2.3. Relaxation towards thermal equilibrium

---

In this basis, operators are represented by:

$$a_1 = \frac{1}{\sqrt{2}} \begin{bmatrix} 0 & 1 & 1 & 0 \\ 0 & 0 & 0 & 1 \\ 0 & 0 & 0 & -1 \\ 0 & 0 & 0 & 0 \end{bmatrix}, \quad (2.69)$$

$$a_2 = \frac{1}{\sqrt{2}} \begin{bmatrix} 0 & 1 & -1 & 0 \\ 0 & 0 & 0 & -1 \\ 0 & 0 & 0 & -1 \\ 0 & 0 & 0 & 0 \end{bmatrix}, \quad (2.70)$$

$$\hat{m}_1 = \frac{\pi}{\sqrt{2}} \begin{bmatrix} 0 & 1 - n(-\epsilon) & 1 - n(\epsilon) & 0 \\ 0 & 0 & 0 & 1 - n(\epsilon) \\ 0 & 0 & 0 & -1 + n(-\epsilon) \\ 0 & 0 & 0 & 0 \end{bmatrix}, \quad (2.71)$$

$$\hat{\hat{m}}_1 = \frac{\pi}{\sqrt{2}} \begin{bmatrix} 0 & 0 & 0 & 0 \\ n(-\epsilon) & 0 & 0 & 0 \\ n(\epsilon) & 0 & 0 & 0 \\ 0 & n(\epsilon) & -n(-\epsilon) & 0 \end{bmatrix}. \quad (2.72)$$

Plugging the above operators and density matrix into Eq. (2.62), we can derive the explicit form of matrix  $\Gamma$  and rewrite Eq. (2.62) in the following form,

$$\frac{d}{d\tau} P = \Gamma P, \quad (2.73)$$

where the matrix  $\Gamma$  has dimension  $16 \times 16$ , or generally  $4^N \times 4^N$  for an  $N$ -site spinless fermionic system.

Fortunately, since we are only interested in equilibrium states in this section, we know that the off-diagonal elements of the equilibrium density matrices will vanish. Therefore, we work with  $P^{dia} = [p_{11}, p_{22}, p_{44}, p_{44}]^T$  in this section and derive and solve only its evolution equation. In this case, the matrix  $\Gamma$  can also be reduced to a matrix  $\Gamma^{dia}$ . Using the above operators  $a_1$ ,  $a_1^\dagger$ ,  $\hat{m}_1$ , and  $\hat{\hat{m}}_1$ , we find

$$\Gamma^{dia} = \lambda^2 \pi \begin{bmatrix} -n(-\epsilon) - n(\epsilon) & 1 - n(-\epsilon) & 1 - n(\epsilon) & 0 \\ n(-\epsilon) & n(-\epsilon) - n(\epsilon) - 1 & 0 & 1 - n(\epsilon) \\ n(\epsilon) & 0 & n(\epsilon) - n(-\epsilon) - 1 & 1 - n(-\epsilon) \\ 0 & n(\epsilon) & n(-\epsilon) & n(\epsilon) + n(-\epsilon) - 2 \end{bmatrix}, \quad (2.74)$$

### 2.3. Relaxation towards thermal equilibrium

---

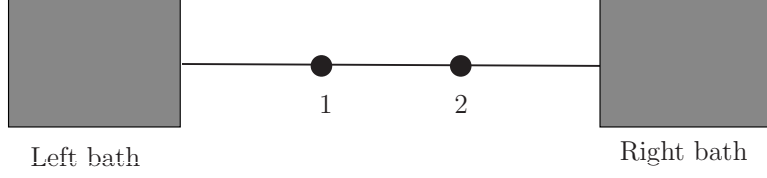


Figure 2.3: Sketch of a two-site system coupled to two heat baths.

and the reduced equation becomes

$$\frac{d}{d\tau} P^{dia} = \Gamma^{dia} P^{dia}. \quad (2.75)$$

A general time-dependent solution of Eq. (2.75) with initial condition  $P_0^{dia}$  is

$$P^{dia}(\tau) = e^{\Gamma^{dia}\tau} P_0^{dia}. \quad (2.76)$$

It converges to a long term stationary state only when all eigenvalues of  $\Gamma^{dia}$  are non-positive. Its stationary state is the eigenvector of  $\Gamma^{dia}$  with eigenvalue equal to zero,

$$\Gamma^{dia} P^{dia}(\infty) = 0. \quad (2.77)$$

We verified that  $\Gamma^{dia}$  indeed only has one zero eigenvalue, and that its corresponding eigenvector  $P^{dia}(\infty)$  leads to the proper thermal equilibrium state,

$$P^{dia}(\infty) = \frac{1}{Z} \left[ 1, e^{\beta(\mu+\epsilon)}, e^{\beta(\mu-\epsilon)}, e^{\beta 2\mu} \right]^T, \quad (2.78)$$

where  $Z = 1 + e^{\beta(\mu+\epsilon)} + e^{\beta(\mu-\epsilon)} + e^{\beta 2\mu}$ .

Up to this point, we have illustrated the general procedure for a system coupled to one bath and confirmed that its stationary state is the expected thermal equilibrium. A straightforward extension is to consider a system coupled to multiple baths, for example different sites in the system are locally coupled to different baths. In fact, our general formula Eq. (2.48) has already been derived to be applicable for such situations. The only change to be made is to allow every bath to have its own operators  $\hat{m}_\nu$  and  $\hat{\hat{m}}_\nu$ .

Specifically, if as sketched in Fig.2.3, we couple site 2 to a bath 2 with the same bath parameters, then our effective equation of motion reads:

$$\begin{aligned} \frac{d}{dt}\rho = & -i[H_S, \rho] - \lambda^2 \left\{ [a_1^\dagger, \hat{m}_1\rho] + [a_1, \hat{m}_1\rho] + h.c. \right\} \\ & - \lambda^2 \left\{ [a_2^\dagger, \hat{m}_2\rho] + [a_2, \hat{m}_2\rho] + h.c. \right\}, \end{aligned} \quad (2.79)$$

where the additional operators are defined as

$$\hat{m}_2 = \frac{\pi [1 - n_2(-\epsilon)]}{2} (a_1 + a_2) - \frac{\pi [1 - n_2(\epsilon)]}{2} (a_1 - a_2), \quad (2.80a)$$

$$\hat{m}_2 = \frac{\pi n_2(-\epsilon)}{2} (a_1^\dagger + a_2^\dagger) - \frac{\pi n_2(\epsilon)}{2} (a_1^\dagger - a_2^\dagger). \quad (2.80b)$$

Repeating the above calculation, we find the same stationary state.

It is now natural to ask what kind of stationary state will emerge if the two baths have different parameters, for example different temperatures and/or chemical potentials. Ideally this should be the non-equilibrium stationary state which can be used to calculate transport properties.<sup>1</sup> We will use examples of simple systems to investigate this question in §2.5. Before that, however, we have a subtle issue to settle, in the next section.

## 2.4 Various other extensions of the single-site quantum master equation

There are several forms of the effective equation of motion used in the literature. Besides the multi-bath Redfield equation derived above, a local-operator Lindblad equation and a multi-mode quantum master equation are also used quite often to study transport or relaxation processes. In this section, we will introduce the latter two and discuss their limitations.

Another way to write Eq. (2.54) for a single-site system is:

$$\begin{aligned} \frac{\partial}{\partial t}\rho = & -i[H_S, \rho] - J(\epsilon) \left\{ (1 - n(\epsilon)) \left( a^\dagger a \rho + \rho a^\dagger a - 2a \rho a^\dagger \right) \right. \\ & \left. + n(\epsilon) \left( a a^\dagger \rho + \rho a a^\dagger - 2a^\dagger \rho a \right) \right\}. \end{aligned} \quad (2.81)$$

---

<sup>1</sup>What we have argued above shows only that it is natural to link this state to the non-equilibrium stationary state, since the proper equilibrium states are reached when the system is coupled to unbiased baths. However, we note that this is not a real first-principle derivation: thermal equilibrium of the baths has been explicitly assumed. The question of establishing thermal equilibrium from only first principles is not the scope of this thesis although many mathematicians and physicists are very much interested in this issue.

## 2.4. Various other extensions

---

It is very tempting to generalize the above form directly to multi-site systems coupled to multiple local baths as follow,

$$\begin{aligned} \frac{\partial}{\partial t} \rho = & -i [H_S, \rho] \\ - \sum_{\nu} J_{\nu}(\epsilon_{\nu}) \left\{ (1 - n_{\nu}(\epsilon_{\nu})) \left( a_{\nu}^{\dagger} a_{\nu} \rho + \rho a_{\nu}^{\dagger} a_{\nu} - 2a_{\nu} \rho a_{\nu}^{\dagger} \right) \right. \\ & \left. + n_{\nu}(\epsilon_{\nu}) \left( a_{\nu} a_{\nu}^{\dagger} \rho + \rho a_{\nu} a_{\nu}^{\dagger} - 2a_{\nu}^{\dagger} \rho a_{\nu} \right) \right\}, \end{aligned} \quad (2.82)$$

i.e. as if each new bath adds the contribution it would if the site it is coupled to was *isolated* from the rest of the central system. Here,  $\epsilon_{\nu}$  is the on-site energy of site  $\nu$  and  $n_{\nu}(\epsilon_{\nu})$  is the occupation number for a mode of energy  $\epsilon_{\nu}$  given the parameters of bath  $\nu$ .

We call this simplified equation the local-operator Lindblad equation. Because of its simplicity, it has been used often for the study of transport properties [58, 59, 88, 89]. We have seen, however, that Eq. (2.48) or more specifically Eq. (2.79) can not be cast into this form because the operator  $\hat{m}_{\nu}$  usually involves not only  $a_{\nu}$ , but also the operators for all other sites  $a_{\nu'}$  through formulas that depend on the particular  $H_s$  of the system. Therefore, the two equations are different. The question, then, is whether the stationary states of the two equations are qualitatively different, and if yes, whether the solution of the local-operator Lindblad equation still captures most features of the non-equilibrium stationary states properly? These questions have not been answered yet. In this section, we will provide some preliminary results.

Before that, we also introduce the multi-mode quantum master equation that arises from another extension of the Redfield equation for a single-site system [70]. For multi-site systems, let us assume we can rewrite the Hamiltonian as follows:

$$H_S = \sum_q \epsilon(q) a_q^{\dagger} a_q, \quad (2.83)$$

We further assume that each eigenmode of the system is coupled to its own individual bath with temperature  $T_q$ :

$$\hat{V} = \lambda \sum_{k,q} \left[ V_{qk} a_q \otimes b_{q,k}^{\dagger} + h.c. \right] \quad (2.84)$$

where creation and annihilation operators of bath  $q$  satisfy the fermionic commutation relation,  $\{b_{q,k}, b_{q',k'}^{\dagger}\} = \delta_{k,k'} \delta_{q,q'}$ . Note that this is different from our setup of Redfield equation, where some of the sites, not eigenmodes, are coupled each to its own individual bath.

For this new setup, every eigenmode is independent so that the operators  $\hat{m}_q$  and  $\hat{n}_q$  involve only  $a_q$  and  $a_q^\dagger$ . Therefore, from Eq. (2.48) the effective equation of motion reads

$$\begin{aligned} \frac{d}{dt}\rho = & -i \sum_q \epsilon(q) [a_q^\dagger a_q, \rho] \\ & - \sum_q J_q(\epsilon(q)) \left\{ (1 - n_q(\epsilon(q))) \left( a_q^\dagger a_q \rho + \rho a_q^\dagger a_q - 2a_q \rho a_q^\dagger \right) \right. \\ & \left. + n_q(\epsilon(q)) \left( a_q a_q^\dagger \rho + \rho a_q a_q^\dagger - 2a_q^\dagger \rho a_q \right) \right\}, \end{aligned} \quad (2.85)$$

i.e. it is simply a sum over all eigenmodes, consisting of contributions similar to those in Eq. (2.54). We call this equation the multi-mode quantum master equation. It has been used in quantum optics to study relaxation processes.

We should emphasize that the two equations Eq. (2.82) and Eq. (2.85) are different from each other, except for a single-site system in which case all three equations are the same. For example, for our two-site system,  $a_\nu$  in Eq. (2.82) refers to  $a_1, a_2$  while  $a_q$  in Eq. (2.85) refers to  $a_\pm = \frac{a_1 \pm a_2}{\sqrt{2}}$ . In the local-operator Lindblad equation  $a_1, a_1^\dagger$  does not mix with  $a_2, a_2^\dagger$ , while in the Redfield equation there are terms mixing them.

Next, we investigate the difference between these three equations: the Redfield equation, the local-operator Lindblad equation and the multi-mode quantum master equation. We will argue firstly that while the local-operator Lindblad equation gives both wrong equilibrium states and wrong non-equilibrium stationary states, it may lead to qualitatively correct results for some physical quantities such as certain currents; and secondly that while the proper equilibrium states can be found from the multi-mode quantum master equation, it does not describe any proper non-equilibrium stationary states. In order to do this, we begin by finding the “proper” non-equilibrium stationary state from the Redfield equation of a two-site system coupled to two baths. This solution is discussed in the next section.

## 2.5 Evolution towards a non-equilibrium stationary state

In this section, we first solve the Redfield equation for a two-site system locally coupled to two baths, and then compare it with solutions from the local-operator Lindblad equation and the multi-mode quantum master equation. The general procedure presented in this section is the general method

underlying all the later work in this thesis. In a sense, all the later work focuses either on the technical side of this procedure or on applications of this procedure. Of course, these are non-trivial because solving the Redfield equation directly for large systems is a difficult task.

### 2.5.1 Non-equilibrium stationary states from the Redfield equation

We begin from Eq. (2.79). Note that when the bath parameters are different:  $T_1 \neq T_2$  and/or  $\mu_1 \neq \mu_2$ , unlike in the case of thermal equilibrium states, the off-diagonal elements of the density matrix are no longer necessarily zero. As a result, we need to find all the elements of the density matrix. Correspondingly the matrix  $\Gamma$  has  $d^4 = 2^8$  elements. For such a large linear system we have to solve the problem numerically. We are interested in its stationary solution, i.e.

$$\Gamma P(\infty) = 0. \quad (2.86)$$

This can be solved by finding the eigenvector of  $L$  corresponding to the zero eigenvalue. Or, it can also be solved as the solution of the following linear system of equations,

$$\bar{\Gamma} P(\infty) = \mathcal{V}, \quad (2.87)$$

where  $\mathcal{V} = [1, 0, \dots]^T$  and  $\bar{\Gamma}$  is defined by replacing the first row of  $\Gamma$  by the normalization condition  $tr(\rho) = 1$ , i.e.  $\sum_j P_{j*d+j} = 1$  with our notation. The advantage of this is that  $\Gamma$  is a singular matrix but  $\bar{\Gamma}$  is not. Therefore, while Eq. (2.86) has to be treated as a computationally costly eigenvalue problem, Eq. (2.87) is a non-singular system of linear equations that can be solved more efficiently.

For simplicity of notation in later chapters, the above two equations defining the non-equilibrium stationary states are also written as

$$L\rho(\infty) = 0. \quad (2.88)$$

and

$$\bar{L}\rho(\infty) = \nu. \quad (2.89)$$

Here instead of superoperator  $\Gamma, \bar{\Gamma}$  and supervector  $P, \mathcal{V}$ , we use directly the Liouvillian  $L, \bar{L}$  and matrix  $\rho, \nu$ , which are defined from mapping the supervector  $P, \mathcal{V}$  in the above supervector representation back into the usual

density matrix representation. These two sets of equations are equivalent, but the later has simpler notation since it is still formulated in terms of the Liouvillian and density matrices.

Let us summarize the general algorithm for this direct method:

1. Find all eigenvalues and eigenstates of  $H_S$ , and express all the original operators  $a_\nu$  and  $a_\nu^\dagger$  in this basis of eigenstates;
2. Evaluate the correlation functions for every bath to calculate the matrices  $\Sigma_\nu$  and  $\bar{\Sigma}_\nu$  defined in Eq. (2.51);
3. From these, derive the expressions of the operators  $\hat{m}_\nu$  and  $\hat{\bar{m}}_\nu$  as in Eq. (2.50);
4. Construct  $\Gamma$  or  $\bar{\Gamma}$  using Eq. (2.48) and the previous results;
5. Solve for the zero eigenvectors of  $\Gamma$  or the linear system defined by  $\bar{\Gamma}$  in Eq. (2.89).

Using this procedure we solve Eq. (2.79). Typical results are shown in the Fig. 2.4 for the specific parameters  $\epsilon = 1, \lambda = 0.1, \mu_1 = 0 = \mu_2, T_1 = T(1 + \frac{\delta}{2}), T_2 = T(1 - \frac{\delta}{2})$ , and  $T = 2.0$ . We have calculated the difference between the general non-equilibrium stationary state  $\rho(\infty)$  and the thermal equilibrium  $\rho^{Eq}(T)$  at temperature  $T$ . The results are presented separately for off-diagonal elements and diagonal elements,

$$d^{diag} = \sqrt{\frac{\sum_j (\rho_{jj} - \rho_{jj}^{Eq})^2}{\sum_{ij} (\rho_{ij})^2}}, d^{off} = \sqrt{\frac{\sum_{i \neq j} (\rho_{ij} - \rho_{ij}^{Eq})^2}{\sum_{ij} (\rho_{ij})^2}}. \quad (2.90)$$

The charge current operator is defined as

$$J = -ie\epsilon (a_1^\dagger a_2 - a_2^\dagger a_1), \quad (2.91)$$

and we also separate its expectation value into contributions from the diagonal and off-diagonal parts,

$$J^{diag} = \sum_j J_{jj} \rho_{jj}, J^{off} = \sum_{i \neq j} J_{ji} \rho_{ij}. \quad (2.92)$$

From Fig. 2.4(a) we see that compared to the diagonal part, the off-diagonal elements of the non-equilibrium stationary states are relatively small but

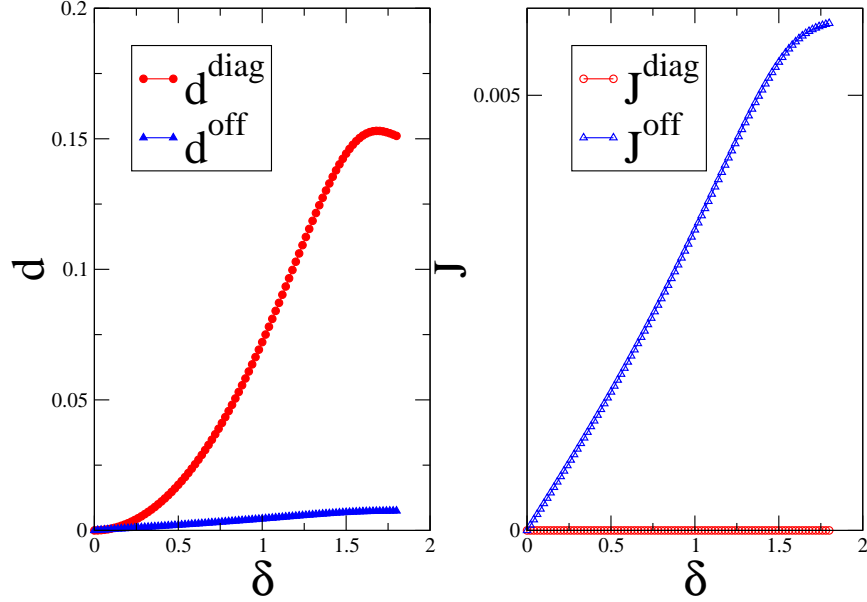


Figure 2.4: Density matrices for non-equilibrium stationary states are compared to those of equilibrium states. In (a)  $d^{diag}$  and  $d^{off}$  are plotted vs. the temperature bias  $\delta$ . Diagonal elements of the density matrices for non-equilibrium stationary states are found to be quite different from those of equilibrium states. The difference between off-diagonal elements of non-equilibrium stationary states and equilibrium density matrices are much smaller. Note that the off-diagonal elements of equilibrium density matrices are zero always. (b) Charge currents,  $J^{diag}$  and  $J^{off}$ , for the non-equilibrium stationary states, are plotted vs.  $\delta$ . We see that only the off-diagonal terms of the density matrix contribute to the current.

non-zero. However, Fig. 2.4(b) shows that the diagonal part does not contribute at all to the current,  $J^{diag} = 0$ ; the current comes entirely from the off-diagonal part. So the seemingly small change in the off-diagonal part makes a big qualitative difference: off-diagonal elements are essential to describe transport properties. This is not surprising since we know that if the time-reversal symmetry is not broken, the eigenstates of  $H_S$  do not support currents,  $J_{jj} = 0$ .

Next, we will perform a comparison between stationary states from the local-operator Lindblad equation/multi-mode quantum master equation and these non-equilibrium stationary states obtained from the Redfield equation, to see whether they agree or not.

### 2.5.2 Non-equilibrium stationary states from the local-operator Lindblad equation and the multi-mode quantum master equation

We have claimed before that the local-operator Lindblad equation leads to wrong equilibrium states but possibly qualitatively correct non-equilibrium stationary states, while the multi-mode quantum master equation gives proper equilibrium states but not non-equilibrium stationary states. In this section, we will confirm these statements by presenting results for the simple example of a two-site fermionic system coupled to two baths held at different temperatures but the same chemical potential.

The Redfield equation for this system has been written down in Eq. (2.79). Following the general form in Eq. (2.85) and Eq. (2.82), the local-operator Lindblad equation and the multi-mode quantum master equation for this specific system are, respectively,

$$\begin{aligned} \frac{\partial \rho^L}{\partial t} = & -i[\mathcal{H}_S, \rho^L] - \lambda^2 \pi \left\{ \langle 1 + n(0, T_1, \mu_1) \rangle \left[ a_1^\dagger, a_1 \rho^L \right] \right. \\ & + \langle n(0, T_1, \mu_1) \rangle \left[ a_1, a_1^\dagger \rho^L \right] \\ & + \langle 1 + n(0, T_2, \mu_2) \rangle \left[ a_2^\dagger, a_2 \rho^L \right] \\ & \left. + \langle n(0, T_2, \mu_2) \rangle \left[ a_2, a_2^\dagger \rho^L \right] + h.c. \right\}. \end{aligned} \quad (2.93)$$

and

$$\begin{aligned} \frac{\partial \rho^M}{\partial t} = & -i[\mathcal{H}_S, \rho^M] - \lambda^2 \pi \left\{ \langle 1 + n(-\epsilon, T, \mu) \rangle [a_+^\dagger, a_+ \rho^M] \right. \\ & + \langle n(-\epsilon, T, \mu) \rangle [a_+, a_+^\dagger \rho^M] \\ & + \langle 1 + n(\epsilon, T, \mu) \rangle [a_-^\dagger, a_- \rho^M] \\ & \left. + \langle n(\epsilon, T, \mu) \rangle [a_-, a_-^\dagger \rho^M] + h.c. \right\}, \end{aligned} \quad (2.94)$$

where  $n(\epsilon, T, \mu)$  is the average particle number in state with energy  $\epsilon$  in a bath with temperature  $T$  and chemical potential  $\mu$ . For the multi-mode quantum master equation, in which every eigenmode — not every site — is treated independently, it is impossible to incorporate the local coupling (the fact that only certain local sites couple to their own individual local baths), so we have just set all  $T_q = T$ . This makes the multi-mode quantum master equation not applicable to calculation of non-equilibrium stationary states. We will find so in the following numerical study.

Following a similar procedure like in the last section, we solve for the stationary states,  $\rho^L(\infty)$  and  $\rho^M(\infty)$ . We compare them against the non-equilibrium stationary states of the Redfield equation,  $\rho^R(\infty)$  using the following measure for distances:

$$d_B^A = \sqrt{\frac{\sum_{i,j} (\rho_{ij}^A - \rho_{ij}^B)^2}{\sum_{ij} (\rho_{jj}^B)^2}}. \quad (2.95)$$

Typical results are shown in Fig. 2.5. We see that the difference between the multi-mode quantum master equation and the Redfield equation is relatively small compared to the difference between the local-operator Lindblad equation and the Redfield equation. At equilibrium ( $\delta = 0$ ), the multi-mode quantum master equation and the Redfield equation lead to the same stationary state, which is of course the thermal equilibrium. The local-operator Lindblad equation is quite different from the Redfield equation for all values of  $\delta$ , and in particular it fails to predict the proper thermal equilibrium for unbiased baths. It can be shown that this is always the case, even for more general systems.

However, we cannot discard the local-operator Lindblad equation on this basis, when analyzing transport, since we just argued that transport is related only to off-diagonal matrix elements. Fig. 2.5(b) shows that while

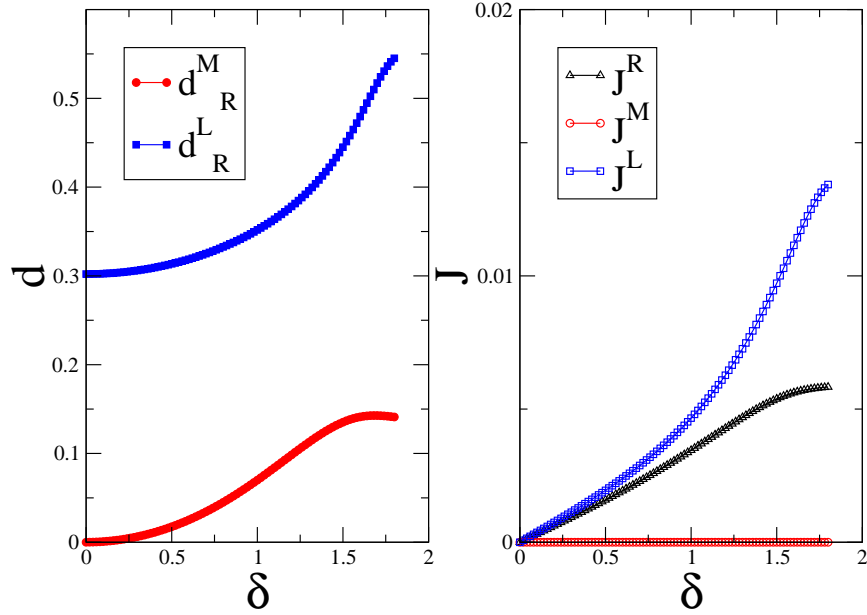


Figure 2.5:  $\rho^L(\infty)$  and  $\rho^M(\infty)$  are compared with  $\rho^R(\infty)$ . In (a) we plot  $d_R^L$  and  $d_R^M$  vs. the temperature bias  $\delta$ . We see that at equilibrium ( $\delta = 0$ ), the difference between  $\rho^M(\infty)$  and  $\rho^R(\infty)$  is zero but the difference between  $\rho^L(\infty)$  and  $\rho^R(\infty)$  is not. For all other cases, the differences are finite. However, as shown in (b), the steady-state charge current  $J^L$  and  $J^R$ , respectively calculated from  $\rho^L(\infty)$  and  $\rho^R(\infty)$ , show qualitatively similar behavior. On the other hand,  $J^M = 0$  shows that the multi-mode quantum master equation does not capture non-equilibrium stationary states at all.

the charge current from the multi-mode quantum master equation is always zero, the currents from the local-operator Lindblad equation and the Redfield equation are qualitatively similar. The first fact confirms that the multi-mode quantum master equation captures properly only the equilibrium distribution, but cannot describe transport through the system, as should be obvious from its structure. The second fact suggests that the local-operator Lindblad equation may be used to study, qualitatively, transport properties. However, since the ratio between the two currents changes for different parameters, it is impossible to link  $J^R$  quantitatively to  $J^L$ .

This qualitative similarity, if confirmed for more complicated problems, could still be valuable for qualitative studies, for example in the question of normal v.s. anomalous conductance. More investigation are needed to check how universal this similarity is, but they are hampered by the lack of efficient solutions for the Redfield equation. If confirmed, this similarity would be useful since it is much easier to solve the local-operator Lindblad equation than the Redfield equation [59]. While not a proof, the results shown here for a 2-site system coupled to 2 baths clearly illustrate why the local-operator Lindblad equation and the multi-mode quantum master equation approaches are questionable when studying transport through open systems. This is why we focus on the Redfield equation from now on.

To summarize, up to this point we have derived the general effective equation of motion and the more specific Redfield equation, and we have also illustrated the general procedure of solving the Redfield equation by brute force direct methods. Before we develop more efficient approaches in the next chapters, we would also like to discuss its relation to the most general evolution equation, the semigroup Lindblad form. This is the topic of the next section.

### 2.5.3 The general Lindblad form

The evolution operators of a closed quantum system  $H$ ,  $U(t) = e^{-iHt}$ , form a group. In general, however, the evolution operators of an open system form a semigroup so as to keep the density matrix always positive and normalized, but not necessary reversible,

$$\rho(t) = \mathcal{U}(t) \rho(0) \tag{2.96}$$

such that

$$\mathcal{U}(t_1 + t_2) = \mathcal{U}(t_1) \mathcal{U}(t_2). \tag{2.97}$$

For a closed system, we have the additional condition:

$$U(-t) = U^{-1}(t) \tag{2.98}$$

which insures reversibility.

Lindblad discussed the generators of such trace-preserving positive semi-groups [90]. As shown in a theorem by Gorini, Kossakowski and Sudarshan [91], a completely positive semigroup evolution of a quantum system in a  $n$ -dimensional Hilbert space can be characterized by a Lindblad operator that governs its evolution

$$\frac{d}{dt}\rho(t) = \mathcal{L}\rho(t), \quad (2.99)$$

where generally:

$$\mathcal{L}\rho(t) = -i[\hat{H}, \rho] + \frac{1}{2} \sum_{ij}^{n^2-1} A_{ij} \left( [L_i, \rho L_j^\dagger] + [L_i \rho, L_j^\dagger] \right), \quad (2.100)$$

where the operators  $\{L_i\}$  form an orthonormal basis of the operators on the system's Hilbert space, and the constants coefficient matrix  $A$  must be positive. Note that the local-operator Lindblad equation is of the Lindblad form, where  $L_i = a_\alpha$  and  $A_{ij} = A_i \delta_{ij}$ , and  $\alpha = L, R$  stands for the left and the right baths respectively. This is why, especially in practical usage, some [59, 75] refer to the local-operator Lindblad equation as the Lindblad equation.

More importantly, the Redfield equation of Eq. (2.48) is not of the Lindblad form. In principle, this means that it may lead to non-physical results such as non-positive density matrices, however we have never encountered such problems in any of our simulations.

## 2.6 Major challenge for large systems

As it is clear from the examples presented above, the major challenge in solving the Redfield equation has to do with the dimension of the vector  $P$ . This is  $2^{2N}$  for a  $N$ -site system of spinless fermions,  $(2S + 1)^{2N}$  for an  $N$ -site chain of spins- $S$ , and infinity for bosonic systems. With such exponential growth, it is impossible to deal with large systems by direct methods, including the Runge-Kutta method, the eigenvector corresponding to the zero eigenvalue, the solution of the linear system and other propagator-based methods [64]. Using these methods, current computational power allows us to deal with systems with up to  $N = 10$  [37, 38]. There are interesting physical systems well within this size which already show rich behavior. However, such limitations on the system's size does not give us a lot of freedom to

separate reliably bulk behavior from boundary effects, for larger systems. In contrast, quite often the non-equilibrium Green's function methods [4, 13] are capable of dealing with system sizes of up to  $N \sim 200$ .

The various methods mentioned in the introduction are either not efficient enough, or involve additional approximations. As we mentioned earlier, efficient stochastic wave-function methods [65] have been developed for both the local-operator Lindblad equation and the Redfield equation. This has better efficiency than the direct methods and it is capable of dealing with roughly  $N \sim 20$ . For the local-operator Lindblad equation only, an efficient method has been developed based on the time-dependent density matrix renormalization [59], capable of dealing with  $N \sim 100$ . However, we have argued that the local-operator Lindblad equation's predictions are quantitatively different from those of the Redfield equation. In the rest of this thesis, we will search for more efficient methods to calculate non-equilibrium stationary states of large systems for the Redfield equation, and discuss some preliminary applications.

This chapter served as a foundation for our theory. None of it, except for the comparison between the Redfield equation, the local-operator Lindblad equation and the multi-mode quantum master equation, is our original contribution. These start in the next chapter.

## Chapter 3

# Linear Response Theory: Kubo formula for open systems

### 3.1 Introduction

Consider a finite size one-dimensional system whose ends are coupled to two baths held at different temperatures and/or different chemical potentials, leading to flow of energy or charge through the system. The question of interest to us is to find the stationary state and thus physical quantities, in particular the steady-state charge and heat currents. Since it is hard to solve exactly for the non-equilibrium stationary states of large systems, in this chapter we introduce an approximate solution for the Redfield equation valid for small biases. We call this approach the open Kubo formula as it is somewhat similar to the standard Kubo formula for isolated systems. While the size limitation of direct methods is around  $N = 10$  (measured in qubit), in certain circumstances detailed below the open Kubo formula is capable of dealing with systems of up to  $N = 20$  sites, the same size limitation as with exact diagonalization of Hamiltonians.

The open Kubo formula gives the first-order corrections towards non-equilibrium stationary states for finite-size systems, starting from the corresponding equilibrium states. Two forms of such Kubo-like formulae are proposed. The first, while computationally less efficient, gives proper general density matrices. The more efficient second form produces correct average values only for certain special physical quantities. Conditions for these special cases will also be discussed.

Besides efficiency, this work is also motivated by considerations of the applicability of the standard Kubo formula to finite-size open systems. The standard Kubo formula has been widely used for both infinite [42] and finite-size systems [82], usually with periodic boundary conditions. Open boundary conditions have also been considered, leading to qualitatively different

results [44]. For finite-size systems, the standard Kubo formula leads to a summation of many Dirac  $\delta$ -function peaks at different energies. Various ways to get around or to smooth out such  $\delta$  peaks have been proposed [92, 93]. However, there is no guarantee that correct physical quantities can be extracted via such procedures.

More importantly, we show that the standard Kubo formula gives the first-order corrections towards equilibrium states of the perturbed systems, instead of the desired non-equilibrium stationary states. We also prove that the standard formulas for Drude weight and *dc* conductance only work for infinite-size systems, not for finite-size ones. One way to solve these issues is to explicitly take into consideration the coupling to baths. This is why we are interested in linear response theory based on the Redfield equation.

This chapter is organized as follows. In Section §3.2 we briefly review the general linear response theory, and in Section §3.3 we discuss the applicability of the standard Kubo formula. In Section §3.4 we present the open Kubo formula based on the Redfield equation, and finally, in Section §3.5, for small systems, we compare the approximate solution from this open Kubo formula with the direct numerical solution of the Redfield equation, in order to gauge its validity.

## 3.2 General Linear Response Theory

Consider a general linear equation of motion,

$$\frac{\partial \rho(t)}{\partial t} = (L_0 + \Delta L) \rho, \quad (3.1)$$

where  $L_0$  is the “large” term and  $\Delta L$  is the “perturbation”. Explicit forms for  $L_0$  and  $\Delta L$  will be given later. We are particularly interested in stationary states of the above equation,  $\rho(\infty)$ , given by:

$$(L_0 + \Delta L) \rho(\infty) = 0. \quad (3.2)$$

Let us assume that  $\rho_0$  is known and it satisfies

$$L_0 \rho_0 = 0. \quad (3.3)$$

Then, to first order,  $\delta\rho = \rho - \rho_0$  is the solution of

$$\frac{\partial \delta\rho(t)}{\partial t} = L_0 \delta\rho + \Delta L \rho_0, \quad (3.4)$$

### 3.2. General Linear Response Theory

---

where we have neglected the second order term  $\Delta L \delta \rho$ . A general solution of the above equation is

$$\delta \rho(t) = \int_{t_0}^t d\tau e^{L_0(t-\tau)} \Delta L \rho_0 + \delta \rho(t_0), \quad (3.5)$$

Assuming that  $\Delta L$  was turned on at  $t_0 = -\infty$  when the initial state was  $\rho_0$  so that  $\delta \rho(t_0) = 0$ , we have the steady-state solution at  $t = 0$  to be,

$$\delta \rho(t=0) = \int_{-\infty}^0 dt e^{-L_0 t} \Delta L \rho_0. \quad (3.6)$$

Changing the variable  $t$  to  $-t$ , we then arrive at

$$\delta \rho(\infty) = \int_0^{\infty} dt e^{L_0 t - \eta t} \Delta L \rho_0. \quad (3.7)$$

Here we have inserted an infinitesimal positive number  $\eta$  ( $\eta \rightarrow 0^+$ ) to make sure that the expression converges. This  $\eta$  is necessary if the real part of any eigenvalues of  $L_0$  are zero. The stationary state is  $\rho(\infty) = \delta \rho(\infty) + \rho_0$ . This is the basic formulation of linear response theory.

It is required that every eigenvalue of  $L_0$  must have a negative or zero real part, so that the unperturbed system described by  $L_0$  eventually reaches a stationary state. If every eigenvalue of  $L_0$  happens to have a negative real part, as will be the case in one of the methods described below, then  $L_0$  is invertible and

$$\delta \rho(\infty) = -(L_0 - \eta)^{-1} \Delta L \rho_0. \quad (3.8)$$

This can also be derived from Eq. (3.2) since  $L_0$  is non-singular,

$$0 = (L_0 + \Delta L) (\rho_0 + \delta \rho(\infty)) \Rightarrow \delta \rho(\infty) = -L_0^{-1} \Delta L \rho_0. \quad (3.9)$$

This is a straightforward formula if  $L_0$  is indeed invertible but it becomes tricky if  $L_0$  has zero eigenvalues. In this latter case, we can still use Eq. (3.7), but not Eq. (3.8). We may transform  $L_0$  to a non-singular  $\bar{L}_0$  using the fact that  $\rho$  is normalized,  $tr(\rho) = 1$  as we have done in rewriting Eq. (2.88) as Eq. (2.89). Following that we find a corresponding expression similar to Eq. (3.8), more specifically

$$\delta \rho(\infty) = -\bar{L}_0^{-1} \Delta \bar{L} \rho_0. \quad (3.10)$$

### 3.3 Limitations of the standard Kubo formula

The Liouville-von Neumann equation of motion for the density matrix  $\rho(t)$  of a closed system is:

$$\frac{\partial \rho(t)}{\partial t} = L_H \rho(t) = -i[H, \rho], \quad (3.11)$$

where  $H$  is its Hamiltonian. Long-term stationary solutions of this equation are not unique. A special class of such states are the Boltzmann equilibrium distributions:

$$\rho_{eq}(H) = \frac{1}{Z} e^{-\beta H}, \quad (3.12)$$

where  $Z = \text{tr}(e^{-\beta H})$ ,  $\beta = 1/T$ .

If  $H = H_S + V_{ext}$ , where  $H_S$  is the isolated system and  $V_{ext}$  is a static weak coupling to an external field, one can formally use the above general linear response theory to find a stationary solution  $\rho(\infty) = \rho_0 + \delta\rho(\infty)$  near a state  $\rho_0$  of the unperturbed system,  $L_{H_S}\rho_0 = 0$ :

$$\delta\rho(\infty) = \int_0^\infty dt e^{L_0 t - \eta t} L_{V_{ext}} \rho_0. \quad (3.13)$$

If  $\rho_0 = \rho_{eq}(H_S)$  describes the unperturbed system in equilibrium, then this leads to the standard Kubo formula [6, 40]:

$$\delta\rho(\infty) = -i \int_0^\infty dt e^{-\eta t} \left[ V_{ext}(-t), \frac{e^{-\beta H_S}}{Z} \right], \quad (3.14)$$

where  $V_{ext}(t) = e^{iH_S t} V_{ext} e^{-iH_S t}$ . We can use the identity  $[V_{ext}(-t), e^{-\beta H_S}] = -i e^{-\beta H_S} \int_0^\beta d\tau \dot{V}_{ext}(-t - i\tau)$ , where  $\dot{V}_{ext}(-t - i\tau) = \frac{d}{dt} V_{ext}(t)|_{t=-t-i\tau}$ , to rewrite:

$$\delta\rho(\infty) = - \int_0^\infty dt e^{-\eta t} \int_0^\beta d\tau \rho_0 \dot{V}_{ext}(-t - i\tau). \quad (3.15)$$

In terms of the eigenvectors of  $H_S$ ,  $H_S|n\rangle = \epsilon_n|n\rangle$ ,

$$\langle m | \dot{V}_{ext}(t) | n \rangle = i(\epsilon_m - \epsilon_n) \langle m | V_{ext} | n \rangle e^{i(\epsilon_m - \epsilon_n)t}, \quad (3.16)$$

leading to:

$$\delta\rho(\infty) = \sum_{\substack{m,n \\ \epsilon_m \neq \epsilon_n}} \frac{e^{-\beta\epsilon_m} - e^{-\beta\epsilon_n}}{Z} \frac{\langle m | V_{ext} | n \rangle}{\epsilon_m - \epsilon_n - i\eta} |m\rangle \langle n|. \quad (3.17)$$

### 3.3. Limitations of the standard Kubo formula

---

Incidentally, note that there is no contribution from states with  $\epsilon_n = \epsilon_m$ , for which  $\langle m | \dot{V}_{ext}(t) | n \rangle = 0$ . This also follows directly from Eq. (3.14); if we write  $V_{ext} = V_{ext}^0 + V_{ext}^\perp$ , where  $V_{ext}^0 = \sum_{\epsilon_m = \epsilon_n} \langle m | V_{ext} | n \rangle | m \rangle \langle n |$  commutes with  $H_S$ , then  $[V_{ext}(-t), \rho_0] = [V_{ext}^\perp(-t), \rho_0]$ . The ‘‘diagonal’’ part  $V_{ext}^0$  of  $V_{ext}$  does not contribute to  $\delta\rho(\infty)$ , and consequently has no influence on the static response functions.

The lack of diagonal contribution is, however, very puzzling. The well-known Drude weight, which is derived from the standard Kubo formula and is used quite often when discussing charge or thermal transport [42, 44, 82] reads

$$D = \frac{\pi\beta}{L} \sum_{\substack{m,n \\ \epsilon_m = \epsilon_n}} \frac{e^{-\beta\epsilon_m}}{Z} |\langle m | \hat{J} | n \rangle|^2. \quad (3.18)$$

It has contributions only from states with  $\epsilon_m = \epsilon_n$ .

To understand the reason for this difference, consider the derivation of Eq. (3.18) from Eq. (3.15), *e.g.* for spinless fermions in a one-dimensional chain (lattice constant  $a = 1$ ), described by

$$H_S = -t \sum_l \left( c_l^\dagger c_{l+1} + h.c. \right) + V_0 \sum_l n_l n_{l+1}, \quad (3.19)$$

where  $n_l = c_l^\dagger c_l$ , plus a static electric potential

$$V_{ext} = \sum_l V_l n_l \quad (3.20)$$

induced by a homogeneous electric field  $E = -\nabla V$ . From the continuity equation:

$$\dot{V}_{ext}(t) = \sum_l V_l \frac{d}{dt} n_l(t) = - \sum_l V_l [J_{l+1}(t) - J_l(t)], \quad (3.21)$$

where  $J_l = it (c_{l+1}^\dagger c_l - c_l^\dagger c_{l+1})$  is the local current operator. The sum can be changed to

$$- \sum_l [V_{l-1} J_l(t) - V_l J_l(t)] = -E J(t), \quad (3.22)$$

where  $J(t) = \sum_l J_l(t)$  is the total current operator. Using  $\dot{V}_{ext}(t) = -E J(t)$  (or, on a lattice,  $E = V_{l-1} - V_l$ ) in Eq. (3.15) gives

$$\delta\rho(\infty) = E \int_0^\infty dt e^{-\eta t} \int_0^\beta d\tau \rho_0 J(-t - i\tau). \quad (3.23)$$

### 3.3. Limitations of the standard Kubo formula

---

The *dc* conductivity is then

$$\sigma = \int_0^\infty dt e^{-\eta t} \int_0^\beta d\tau \langle J(-t - i\tau) J \rangle, \quad (3.24)$$

where  $\langle O \rangle = \text{Tr}[\rho_{eq}(H_S)O]$ . This expression can be further simplified to arrive at Eq. (3.18).

The only questionable step in this derivation, and the one responsible for going from a result with no contributions from states with  $\epsilon_n = \epsilon_m$ , to one with contributions only from these states, is the change

$$\sum_l V_l J_{l+1}(t) \rightarrow \sum_l V_{l-1} J_l(t). \quad (3.25)$$

This is only justified for an infinite system (where boundary terms are presumed to be negligible), or a system with periodic boundary conditions and *an external field with the same periodicity*. This latter condition can only be achieved for a charge current in a finite system with periodic boundary conditions driven by a varying magnetic flux through the area enclosed by the system. For a finite-size system (even one with periodic boundary conditions) in a static applied electric field this approach is not valid. The same is true for thermal transport, which cannot experimentally be induced in a system with periodic boundary conditions. In both cases, the physical relevance of the results of Eq. (3.18) are hard to fathom.

There is an even more serious conceptual problem with the standard Kubo formula: the resulting distribution  $\tilde{\rho} = \rho_{eq}(H_S) + \delta\rho(\infty)$  is the first order perturbational expansion of  $\rho_{eq}(H)$ , not the expected non-equilibrium stationary state. This statement is proved below, where for convenience, we assume that the diagonal part  $V_{ext}^0 = 0$ . If it is not, we simply remove the “diagonal” part  $V_{ext}^0$  from  $V_{ext}$  and add it to  $H_S$ .

Consider then the eigenstates of the full Hamiltonian,  $H|\tilde{n}\rangle = \tilde{\epsilon}_n|\tilde{n}\rangle$ , to first order perturbation in  $V_{ext}$ . Since  $\langle m|V_{ext}|n\rangle = 0$  for all  $\epsilon_m = \epsilon_n$ , we can apply the first order perturbation theory for non-degenerate states to all the states, whether degenerate or not, to find

$$\tilde{\epsilon}_n = \epsilon_n + \mathcal{O}(V_{ext}^2) \quad (3.26)$$

and

$$|\tilde{n}\rangle = |n\rangle + \sum_{m, \epsilon_m \neq \epsilon_n} \frac{\langle m|V_{ext}|n\rangle}{\epsilon_n - \epsilon_m} |m\rangle + \mathcal{O}(V_{ext}^2). \quad (3.27)$$

### 3.3. Limitations of the standard Kubo formula

---

This immediately leads to

$$\rho_{eq}(H) = \sum_n \frac{1}{\tilde{Z}} e^{-\beta \tilde{\epsilon}_n} |\tilde{n}\rangle \langle \tilde{n}| = \rho_{eq}(H_S) + \delta\rho(\infty) + \mathcal{O}(V_{ext}^2), \quad (3.28)$$

where  $\delta\rho(\infty)$  is indeed given by Eq. (3.17). Intuitively this is easy to understand. In a sense, we found the original thermal equilibrium distribution  $\rho_{eq}(H_S)$  from the Liouville equation with  $H = H_S$ . Then, it is not so surprising that a perturbation based on the same Liouville equation for the full  $H = H_S + V_{ext}$  leads to  $\rho_{eq}(H)$ .

This verifies our previous statement that the standard Kubo formula implies  $\rho(\infty) \rightarrow \rho_{eq}(H)$ . This is rather problematic because normally – for example if invariance to time reversal symmetry is not broken – no currents are generated in a thermal equilibrium state and therefore no steady-state transport through the closed finite system can be described by this approach. However, because we only keep the first-order perturbational correction, the situation is less clear-cut. In principle, it is not impossible for  $\delta\rho$  of Eq. (3.17) to also be a first order approximation to the true non-equilibrium stationary state, or at least to capture a sizable part from it. This needs to be investigated in more detail, and we do so below.

Before that, let us also note that the fact that the use of Eq. (3.18) and its equivalents for finite size systems is problematic can also be seen from the following technical considerations. The spectrum of a finite-size system is always discrete. As a result, any pair of degenerate eigenstates  $\epsilon_m = \epsilon_n$  gives a  $\delta$ -function contribution to the response functions. Such a singular response is unphysical for finite-size systems (for an infinite system, the integration over the continuous spectrum removes these singularities). Various techniques have been proposed to smooth out these singular contributions in order to extract some finite values, such as use of imaginary frequencies [93] or averaging  $\sigma(\omega)$  over a small range of frequencies  $\delta\omega$  and then taking  $\delta\omega \rightarrow 0$  [92]. These different approaches may lead to different results. Moreover, the order in which the various limits are approached, *e.g.*, taking  $\eta \rightarrow 0$  before  $L \rightarrow \infty$  or vice versa, also make a difference [92]. All of these subtleties of the standard Kubo formula are related to the potential divergence whenever  $\epsilon_m = \epsilon_n$  in Eq. (3.18).

To summarize, using the standard Kubo formula blindly for finite-size systems is fraught with both conceptual and technical problems. Its solution gives the first order correction of the equilibrium state of the full Hamiltonian, instead of the expected non-equilibrium stationary state. The derived Drude weight formula is applicable only for infinite-size systems; applying

it directly to finite-size systems involves dealing with unphysical  $\delta$ -function peaks. In order to fix these difficulties, we now discuss how to calculate the non-equilibrium stationary states from the Redfield equation, which takes the connection between system and baths explicitly into consideration.

### 3.4 Open Kubo formula: linear response theory for open finite-size systems

For concreteness, let us assume that the central system is coupled to thermal baths kept at temperatures  $T_{L/R} = T \pm \frac{\Delta T}{2}$  and investigate the thermal transport in the resulting steady state. If  $\Delta T \ll T$ , this will lead to a Kubo-like formula which replaces Eq. (3.15). This approach can be generalized straightforwardly to derive a Kubo-like formula for charge transport.

The general Redfield equation can be written as:

$$\frac{\partial \rho(t)}{\partial t} = [L_H + L_L(T_L) + L_R(T_R)] \rho(t), \quad (3.29)$$

where  $L_H \rho = -i[H, \rho]$ , just like for an isolated system, while  $L_{L/R}$  are additional terms that describe the effects of the left/right thermal baths (assumed to be in equilibrium at their corresponding temperatures  $T_{L/R}$ ) on the evolution of the system. We have seen from Eq. (2.48) how the expressions for  $L_{L/R}$  depend on the Hamiltonian  $H$  of the system and on its coupling to the baths. Generally speaking,  $H$  could also contain an external potential due to coupling to the external field,  $V_{ext}$ , such that  $H = H_S + V_{ext}$ . Such a term is expected to appear for charge transport, but not for thermal transport, therefore in the following we set  $V_{ext} = 0$ .

As we have seen in Eq. (2.48), the temperature and chemical potential of the left (right) baths enter the Redfield equation only via average particle numbers  $n(\epsilon, T_L, \mu_L)$  ( $n(\epsilon, T_R, \mu_R)$ ). Therefore, if  $\Delta T \ll T$ , we can Taylor expand the particle number into a large part and a small part. Thus we also expand the  $L_{L/R}$  and re-arrange the Redfield equation to read:

$$\frac{\partial \rho(t)}{\partial t} = [L_{H_S} + L_B(T) + L_P(\Delta T)] \rho(t) = L \rho(t), \quad (3.30)$$

where  $L_B(T) = L_R(T) + L_L(T)$  is the contribution from the thermal baths if both are kept at the same temperature, while  $L_P(\Delta T)$  collects the terms proportional to  $\Delta T$ .

### 3.4. OKF: the Kubo formula for open finite-size systems

---

We are interested in the  $t \rightarrow \infty$ , stationary state solution  $\rho(\infty)$  of the above equation, satisfying both Eq. (2.88) and Eq. (2.89), which are rewritten in the following form for convenience,

$$L\rho(\infty) = 0, \quad (3.31)$$

and

$$\bar{L}\rho(\infty) = \nu. \quad (3.32)$$

As we have shown in examples in the previous chapter,  $L$  has one non-degenerate zero eigenvalue and all its other (transient) eigenvalues have a negative real part, so  $\rho(\infty)$  is unique for any value of  $\Delta T$ . We have also shown that for small systems, Eq. (3.31) and Eq. (3.32) can be solved numerically. We call this solution  $\rho_{ex}$  and we use it to validate the solutions of various approximation schemes.

A Kubo-like formula, which is potentially more efficient, can be obtained using linear response theory. The first step is to separate the Liouvillian  $L$  of Eq. (3.30) into a “large” plus a “small” part. There are two possible choices:

$$\begin{cases} L_0^{(1)} = L_{H_S} + L_B(T) \\ \Delta L^{(1)} = L_P(\Delta T) \end{cases} \quad (3.33)$$

or

$$\begin{cases} L_0^{(2)} = L_{H_S} \\ \Delta L^{(2)} = L_B(T) + L_P(\Delta T) \end{cases} \quad (3.34)$$

We begin with the first choice. Assume that  $L_0^{(1)}$  has eigenvalues  $\{L_{0,\mu}^{(1)}\}$  and left/right eigenvectors  $\{|\mathcal{L}_\mu\rangle\}$ ,  $\{|\mathcal{R}_\mu\rangle\}$ . As discussed, the unique (zero order in perturbation theory) steady-state solution of  $L_0^{(1)}\rho_0 = 0$  is  $\rho_0 = \rho_{eq}(H_S)$ . The deviation  $\delta\rho_K^{(1)}$  due to the perturbation  $\Delta L^{(1)}$  is obtained like in Eq. (3.13):

$$\begin{aligned} \delta\rho^{(1)}(\infty) &= \sum_{\mu} \int_0^{\infty} dt e^{L_{0,\mu}^{(1)}t - \eta t} |\mathcal{R}_\mu\rangle \langle \mathcal{L}_\mu| \Delta L^{(1)} \rho_0 \\ &= - \sum_{\mu} \frac{|\mathcal{R}_\mu\rangle \langle \mathcal{L}_\mu|}{L_{0,\mu}^{(1)} - \eta} \Delta L^{(1)} \rho_0 = - \sum_{\mu > 0} \frac{|\mathcal{R}_\mu\rangle \langle \mathcal{L}_\mu|}{L_{0,\mu}^{(1)}} \Delta L^{(1)} \rho_0. \end{aligned} \quad (3.35)$$

Note that the only divergent term, due to  $L_{0,0}^{(1)} = 0$ , disappears because  $\langle \mathcal{L}_0| \Delta L^{(1)} \rho_0 = (\rho_0| \Delta L^{(1)} \rho_0 = 0$ . To see why, we start from Eq. (3.31),

### 3.4. OKF: the Kubo formula for open finite-size systems

---

$L(\rho_0 + \delta\rho) = 0$ , project it on  $(\rho_0|$  and keep terms only to the first order, to find  $0 = (\rho_0| \left( L_0^{(1)} + \Delta L^{(1)} \right) (\rho_0 + \delta\rho) = (\rho_0| \Delta L^{(1)} \rho_0$  since  $L_0^{(1)} \rho_0 = 0$ . As a result, Eq. (3.35) has only regular contributions. A similar approach has been suggested in Ref. [88], but for the local-operator Lindblad equation [90] instead of the Redfield equation.

Eq. (3.35) is difficult to use in practice: finding all eigenstates of  $L_0^{(1)}$  is a hard task unless the system has an extremely small Hilbert space. A computationally simpler solution is obtained from Eq. (3.32), where, in matrix terms,  $\bar{L}$  is defined by replacing the first row of the equation  $L\rho(\infty) = 0$  by  $Tr(\rho(\infty)) = 1$ , so that  $\nu$  is a vector whose first element is 1, all remaining ones being 0. As a result  $\det(\bar{L}) \neq 0$  while  $\det(L) = 0$ .

We can also solve it to obtain a Kubo-like formula by dividing  $\bar{L} = \bar{L}_0^{(1)} + \Delta\bar{L}^{(1)}$ . Again, the overbar shows that in matrix terms,  $\bar{L}_0^{(1)}$  is obtained from  $L_0^{(1)}$  by replacing its first row with  $Tr(\rho(\infty)) = 1$ , while  $\Delta\bar{L}^{(1)}$  is obtained from  $\Delta L^{(1)}$  by replacing its first row with zeros. We find

$$\delta\bar{\rho}^{(1)}(\infty) = -[\bar{L}_0^{(1)}]^{-1} \Delta\bar{L}^{(1)} \rho_0. \quad (3.36)$$

This is much more convenient because inverting the non-singular matrix  $\bar{L}_0^{(1)}$  is a much simpler task than finding all the eigenvalues and eigenvectors of  $L_0^{(1)}$ . We have verified that both schemes produce identical results on systems on which both of them can be performed. We denote  $\rho_0 + \delta\bar{\rho}^{(1)}(\infty) = \rho^{(1)}(\infty)$ .

The second option is to take  $L_0^{(2)} = L_{H_S}$  and  $\Delta L^{(2)} = L_B(T) + L_P(\Delta T)$ . In this case, we can still *choose* the stationary solution associated with  $L_0^{(2)}$  to be the thermal equilibrium state at  $T$ ,  $\rho_0 = \rho_{eq}(H_S)$ . However, this solution is no longer unique, since any matrix  $\rho_0$  that is diagonal in the eigenbasis of  $H_S$  satisfies  $L_0^{(2)} \rho_0 = 0$ . Expanding the corresponding analogue of Eq. (3.14) in the eigenbasis of  $H_S$ , we now find:

$$\delta\rho^{(2)}(\infty) = -i \sum_{n,m} \frac{\langle m | \Delta L^{(2)} \rho_0 | n \rangle}{\epsilon_m - \epsilon_n - i\eta} |m\rangle \langle n|. \quad (3.37)$$

We call  $\rho_0 + \delta\rho^{(2)}(\infty) = \rho^{(2)}(\infty)$ . Note that unlike  $\rho^{(1)}(\infty)$  of Eq. (3.36), this solution has divergent contributions from states with  $\epsilon_n = \epsilon_m$ . As such, it is analogous to the standard Kubo formula for infinite systems. This is not an accident. As discussed, the standard Kubo formula for infinite systems always ignores the coupling to the leads. It also takes  $L_0 = L_{H_S}$  and assumes that  $\rho_0 = \rho_{eq}(H_S)$ . Moreover, the driving force for transport

is only the potential  $V_{ext}$  added to  $H_S$ , so that  $\Delta L \rightarrow L_{V_{ext}}$ . With these assumptions, Eq. (3.37) maps straightforwardly into the standard Kubo formula of Eq. (3.17).

### 3.5 Comparison of the two open Kubo formulae

To see which of these two solutions – the regular solution  $\rho^{(1)}(\infty)$  or the singular solution  $\rho^{(2)}(\infty)$  – gives a proper density matrix, we compare them against the exact numerical solution  $\rho_{ex}$  of Eq. (3.31) in the limit  $\Delta T \ll T$ .

We do this for an  $N$ -site chain of spinless fermions

$$H_S = -t \sum_{l=1}^{N-1} \left( c_l^\dagger c_{l+1} + c_{l+1}^\dagger c_l \right) + V_0 \sum_{l=1}^{N-1} c_{l+1}^\dagger c_{l+1} c_l^\dagger c_l. \quad (3.38)$$

coupled to two heat baths, modeled as collections of fermions:

$$H_B = \sum_{k,\alpha=L,R} \omega_{k,\alpha} b_{k,\alpha}^\dagger b_{k,\alpha}, \quad (3.39)$$

where  $\alpha$  indexes the left and right-side baths and we set  $\hbar = 1$ ,  $k_B = 1$ , the lattice constant  $a = 1$ , and hopping  $t = 1$ . The system-baths coupling is chosen as:

$$V_{SB} = \lambda \sum_{k,\alpha} V_k^\alpha \left( c_\alpha^\dagger b_{k,\alpha} + c_\alpha b_{k,\alpha}^\dagger \right), \quad (3.40)$$

where the left (right) bath is coupled to the first (last) site:  $c_L = c_1$  and  $c_R = c_N$ . Bath parameters, i.e. the temperature and chemical potential, are chosen to be  $(T_L, \mu)$  and  $(T_R, \mu)$  with  $T_{L/R} = T \pm \frac{\Delta T}{2}$ .

The corresponding Redfield equation reads from Eq. (2.48),

$$\begin{aligned} \frac{\partial \rho(t)}{\partial t} &= -i[H_S, \rho(t)] \\ -\lambda^2 \sum_{\alpha=L,R} &\left\{ [c_\alpha^\dagger, \hat{m}_\alpha \rho(t)] + [c_\alpha, \hat{\hat{m}}_\alpha \rho(t)] + h.c. \right\}, \end{aligned} \quad (3.41)$$

where operators  $\hat{m}_\alpha$  and  $\hat{\hat{m}}_\alpha$  are defined by Eq. (2.49), which is rewritten here for convenience:

$$\hat{m}_\alpha = \pi \sum_{m,n} |m\rangle \langle n| \langle m| c_\alpha |n\rangle (1 - n_\alpha(\Omega_{nm})), \quad (3.42a)$$

$$\hat{\hat{m}}_\alpha = \pi \sum_{m,n} |m\rangle \langle n| \langle m| c_\alpha^\dagger |n\rangle n_\alpha(\Omega_{mn}). \quad (3.42b)$$

### 3.5. Comparison of the two OKFs

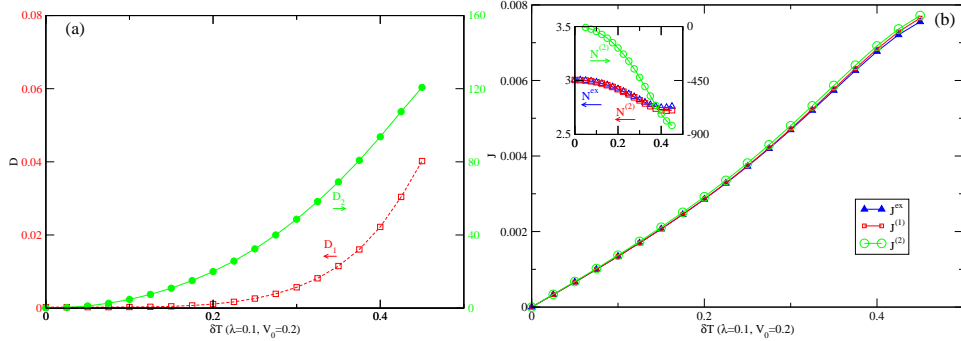


Figure 3.1: (a)  $D_1$  (squares) and  $D_2$  (circles) of Eq. (3.43) vs.  $\delta = \Delta T / 2T$ , for  $N = 8, t = 1.0, V_0 = 0.2, T = 2.0, \mu = -1.0, \lambda = 0.1, \eta = 0.00001$ . (b) the steady-state electric current calculated with  $\rho_{ex}$  (triangles) and  $\rho^{(1,2)}(\infty)$  (squares, circles and stars). The inset shows the corresponding particle numbers.

Eq. (3.41) is an example of the general Eq. (3.29). Since  $T_{L/R}$  enters only in the Fermi-Dirac distributions, it is easy to expand when  $T_{L/R} = T \pm \frac{\Delta T}{2}, \Delta T \ll T$  to identify  $L_B(T)$  and  $L_P(\Delta T)$ .

We characterize the distance between the exact numerical solution  $\rho_{ex}$  and the two possible Kubo solutions  $\rho^{(i)}(\infty), i = 1, 2$  using the norm:

$$D_i = \sqrt{\sum_{n,m} |\langle n | \rho_{ex} - \rho^{(i)}(\infty) | m \rangle|^2}. \quad (3.43)$$

For the proper solution, this difference should be small but still finite, because of higher-order perturbation terms.

Results typical of those found in all the cases we investigated are shown for  $N = 8, V_0 = 0.2, \lambda = 0.1, \eta = 10^{-5}$  in Fig. 3.1(a), where we plot  $D_{1,2}$  vs.  $\delta = \Delta T / 2T$ . We see that  $D_2$  (circles, axis on the right) is very large. In fact, because of the singular contributions from  $\epsilon_n = \epsilon_m$  states,  $D_2$  is divergent, with a magnitude controlled by the cutoff  $\eta$ . In contrast,  $D_1$  (squares, left axis) is small and independent of  $\eta$ . Fig. 3.1(b) shows the electric current ( $J$ ) and the total number of particles ( $N$ ) calculated with  $\rho_{ex}$ , and  $\rho(\infty)^{(1,2)}$  (triangles, squares, respectively circles). Both  $N^{(1)}$  and  $J^{(1)}$  are very close to the exact values  $N^{ex}, J^{ex}$ . However,  $N^{(2)}$  is very different from  $N^{ex}$  while  $J^{(2)}$  is close to  $J^{ex}$ . These results confirm that  $\rho^{(1)}(\infty)$  of Eq. (3.36) is the proper Kubo solution. They also show that  $\rho^{(2)}(\infty)$  can also be used, but only for quantities  $A$  for which  $\langle m | A | n \rangle = 0$

### 3.5. Comparison of the two OKFs

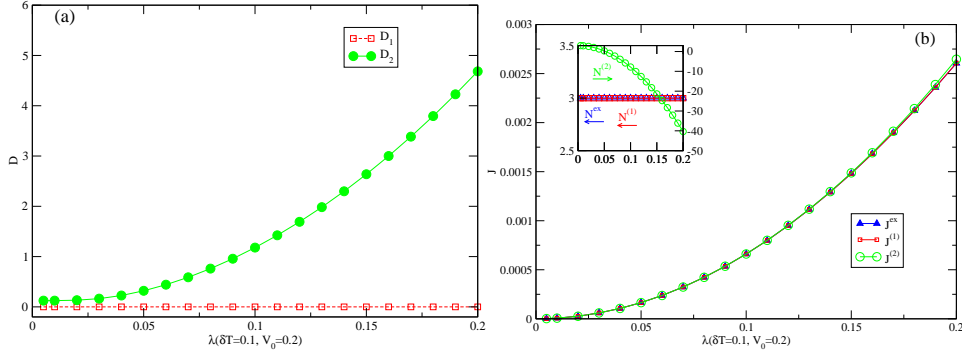


Figure 3.2: (a)  $D_1$  (squares) and  $D_2$  (circles) of Eq. (3.43) vs.  $\lambda$ , for  $N = 8, t = 1.0, V_0 = 0.2, T = 2.0, \mu = -1.0, \delta = 0.1, \eta = 0.00001$ . (b) the steady-state electric current calculated with  $\rho_{ex}$  (triangles) and  $\rho^{(1,2)}(\infty)$  (squares and circles). The inset shows the corresponding particle numbers.

whenever  $\epsilon_m = \epsilon_n$ , so that the divergences in Eq. (3.37) disappear. This explains the previous success of this formula to be somewhat of an accident.

Fig. 3.2 shows the same quantities as Fig. 3.1, at a fixed bias  $\Delta T$  as a function of the strength of the system-bath coupling  $\lambda$ . It confirms again that  $\rho^{(1)}(\infty)$  is the proper approximation of  $\rho_{ex}$ , but that for the charge current  $\rho^{(2)}(\infty)$  works well too. This also shows that the non-equilibrium stationary states depend on the coupling strength  $\lambda$ . This is not surprising for a finite-size system: the intrinsic conductance of the system is added to comparable “contact” contributions from the interfaces between the system and the baths, and experiments measure the total conductance. It follows that quantitative modeling of transport in finite systems will require a careful consideration of the entire experimental set-up.

Fig. 3.3 shows again the same quantities as Fig. 3.1, at a fixed bias  $\Delta T$  as a function of the strength of the interaction  $V_0$ . It confirms again that  $\rho^{(1)}(\infty)$  is the proper approximation of  $\rho_{ex}$ . We also find that values of currents  $J^{ex}$  are quite different between  $V_0 = 0$  and  $V_0 = 1$  for example. The charge currents calculated from both  $\rho^{(1,2)}(\infty)$  indeed capture the major part of such difference. One may note a discontinuity in the data around  $V_0 = 0.6$ . We think this is due to numerical reasons. The calculation depends very strongly on the values of energy differences among all energy levels. For different values of  $V_0$ , such energy differences may either shift continuously or change qualitatively.

### 3.6. Summary and discussion

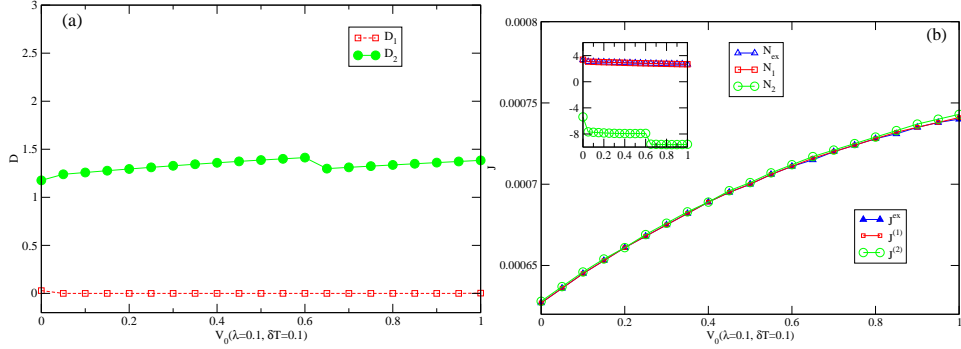


Figure 3.3:  $D_1$  (squares) and  $D_2$  (circles) of Eq. (3.43) vs.  $V_0$ , for  $N = 8, t = 1.0, T = 2.0, \mu = -1.0, \lambda = 0.1, \delta = 0.1, \eta = 0.00001$ . (b) the steady-state electric current calculated with  $\rho_{ex}$  (triangles) and  $\rho^{(1,2)}$  (squares and circles). The inset shows the corresponding particle numbers.

### 3.6 Summary and discussion

To conclude, we first showed that the standard Kubo formula fails to provide an approximation for non-equilibrium stationary states, instead approximating the equilibrium state of the whole Hamiltonian. Secondly, applying the standard Kubo formula to finite systems generically leads to divergences, which are unphysical. We then showed that taking into consideration the coupling to baths explicitly solves both problems and leads to a well-behaved Kubo-like formula. Finally, we showed that the improper solution similar to those used in literature can give correct average values but only for certain physical quantities. Although we only considered small systems so as to be able to calculate  $\rho_{ex}$ , Eqs. (3.36) and (3.37) can be used for larger systems, with the latter being more efficient but not always valid.

In fact, the above results give us enough grounds to question the validity of the standard Kubo formula, where the effect of the baths are taken care of only via an additional potential. We believe that this is not enough. There are two different types of “driving forces” responsible for a steady-state current flow. The first force is the applied electric field, which gives rise to an additional interaction term  $V_{ext}$  to be included in the total Hamiltonian  $H = H_S + V_{ext}$  of the system. The second one is the imbalance in the chemical potentials and/or temperatures of the two baths, which results in a non-equilibrium distribution function  $\rho(\infty)$ . As we have shown above, the standard Kubo formula calculates the current from  $\rho_{eq}(H)$ , the thermal equilibrium state of the full Hamiltonian, so it takes into account only the

### 3.6. Summary and discussion

---

effect of  $V_{ext}$ , but not the full non-equilibrium distribution function. We believe that this approach is problematic when calculating charge currents.

This approach is even less reliable for thermal currents, where there is only one driving force: the non-equilibrium distribution. There is no thermal equivalent for the electric potential. Some additional assumptions such as local equilibrium [39] or use of gravitational potentials [40] have been used to make the situation similar to that of charge transport. Either way, an artificial thermal potential term  $V_{ext}$  is constructed and added to  $H_S$  and then one uses  $\rho_{eq}(H)$  instead of the proper non-equilibrium stationary state, in direct analogy with the usual approach for charge currents.

The work presented in this chapter points to a solution for these conceptual problems, if the baths are explicitly taken into consideration. However, the resulting open Kubo formula can still only be used for system of up to  $N \sim 20$ , which may be too small for transport in solid state systems.

In the next two chapters, we present two efficient ways to solve the Redfield equation for larger systems. Furthermore, unlike the open Kubo formula based on linear response theory, the new methods are applicable even when the baths' bias is not small.

## Chapter 4

# BBGKY-like hierarchy for the Redfield equation

### 4.1 Introduction

In this chapter we introduce a much more efficient way to solve the Redfield equation, based on a BBGKY-like hierarchy. Its efficiency depends on the level at which the hierarchy is truncated. At first order, where only single-particle Green's functions are involved, it leads to a linear system with  $N^2$  unknowns for a  $N$ -site spinless fermionic system. This makes it possible to analyze systems larger than those that can be treated with the non-equilibrium Green's function method.

Like the diagrammatic perturbation theory [18], the BBGKY equation hierarchy for systems in equilibrium also provides an equivalent systematic approach to calculate many-particle correlation functions [68, 69]. For non-interacting systems, the hierarchy is decoupled, meaning that the equation of a single-particle Green's function is only related to other single-particle Green's functions, forming a closed system of equations. The same holds for general  $n$ -particle Green's functions denoted as  $G_n$ . However, when there are interactions in the system, equations of all orders of Green's functions are coupled together. Generically, equations for  $n$ -particle Green's functions,  $G_n$ , also involve  $G_{n+1}$ , so that the system of BBGKY equations becomes infinite. In this case, approximations such as the cluster expansions can be used to truncate and then solve the truncated hierarchy [69, 94].

Here we use exactly the same idea but now for the Redfield equation. Not surprisingly, for non-interacting central systems we find that the hierarchy is decoupled, just like for systems in equilibrium. In fact, in Ref. [36], the Redfield equation with  $N \sim 100$  has been solved in terms of single-particle Green's functions. However, they did not regard this as a special case of the more general BBGKY-like equation hierarchy. From this point of view, our idea is basically to extend this Green's function based solution of the Redfield equation from Ref. [36] to interacting systems, where equations for

Green's functions of various orders become coupled.

Two systematic approximations are proposed to truncate and solve the hierarchy. As a test of reliability of the proposed methods, we apply them to small systems which can also be solved with exact direct methods. Consistent results are found. Just as the usual Wick's theorem of non-interacting systems provides a basis for the usual diagrammatic perturbation theory of interacting systems, one of the approximations requires a non-equilibrium Wick's theorem. Such a theorem is proved starting from the Redfield equation of non-interacting systems.

This chapter is organized as follow. In Section §4.2, using a specific example, a BBGKY-like equation hierarchy is derived from the Redfield equation. In Section §4.3, non-interacting systems are discussed and a non-equilibrium Wick's theorem is proved. In Section §4.4, we introduce the two methods to truncate and solve the coupled hierarchy for interacting systems, and compare them against exact results. We find that both methods are significantly more efficient than the direct methods. The first is capable of dealing with relatively small systems but with strong interactions, while the second can deal with much larger systems but with relatively weaker interactions. For the latter case, we demonstrate that a systematic increase in the level at which the truncation is performed leads to a systematic improvement of the results, as well as an increase in the range of interactions for which good accuracy is obtained.

## 4.2 Derivation of the BBGKY-like hierarchy

For concreteness in presenting our general formulation, let us start from the same Redfield equation describing an  $N$ -site chain of spinless fermions coupled with two fermionic baths. Our system of interest is described by:

$$H_S = -t \sum_{l=1}^{N-1} \left( c_l^\dagger c_{l+1} + c_{l+1}^\dagger c_l \right) + V_0 \sum_{l=1}^{N-1} c_{l+1}^\dagger c_{l+1} c_l^\dagger c_l = H_0 + V_S, \quad (4.1)$$

and its Redfield equation, given by Eq. (3.41), is rewritten here for convenience:

$$\frac{\partial \rho(t)}{\partial t} = -i[H_S, \rho(t)] - \lambda^2 \sum_{\alpha=L,R} \left\{ \left[ c_\alpha^\dagger, \hat{m}_\alpha \rho(t) \right] + \left[ c_\alpha, \hat{m}_\alpha \rho(t) \right] + h.c. \right\}, \quad (4.2)$$

## 4.2. Derivation of the BBGKY-like hierarchy

---

where the operators  $\hat{m}$  and  $\hat{\hat{m}}$  are defined as follows:

$$\hat{m}_\alpha = \sum_k |V_k^\alpha|^2 \int_0^\infty d\tau c_\alpha(-\tau) e^{-i\omega_{k,\alpha}\tau} \langle 1 - n(\omega_{k,\alpha}) \rangle, \quad (4.3a)$$

$$\hat{\hat{m}}_\alpha = \sum_k |V_k^\alpha|^2 \int_0^\infty d\tau c_\alpha^\dagger(-\tau) e^{i\omega_{k,\alpha}\tau} \langle n(\omega_{k,\alpha}) \rangle. \quad (4.3b)$$

Here,  $\alpha = L, R$  refer to the two baths,  $c_\alpha$  correspond to the two sites at the boundaries coupled each to its corresponding bath,  $\omega_{k,\alpha}$  are the energies of the modes in bath  $\alpha$ , and  $\langle n(\omega_{k,\alpha}) \rangle$  are their average occupation numbers.

If  $U(t) = e^{-iH_S t}$  is known, then so are  $c_\alpha(t) = U^\dagger(t) c_\alpha U(t)$  and therefore the operators  $\hat{m}$ . Finding explicit forms for  $\hat{m}$  and  $\hat{\hat{m}}$  thus requires a full diagonalization of  $H_S$ . Using its eigenvectors, one can perform the above integrals to get these operators. More details are included in Appendix A.

Again we are only interested in the long-time steady-state solution  $\rho(\infty)$  and we want to calculate the values of various correlation functions. For a physical quantity of the central system, denoted by the operator  $A$ , from Eq. (4.2) we find:

$$0 = i \langle [A, H_0] \rangle + i \langle [A, V_S] \rangle + \lambda^2 \sum_\alpha \left\{ \left\langle [A, c_\alpha^\dagger] \hat{m}_\alpha \right\rangle + \langle [A, c_\alpha] \hat{\hat{m}}_\alpha \rangle - \left\langle \hat{m}_\alpha^\dagger [A, c_\alpha] \right\rangle - \left\langle \hat{\hat{m}}_\alpha^\dagger [A, c_\alpha^\dagger] \right\rangle \right\}, \quad (4.4)$$

where  $\langle A \rangle = \text{tr}(A\rho(\infty))$  and  $\hat{m}_\alpha^\dagger$  ( $\hat{\hat{m}}_\alpha^\dagger$ ) is the hermitian conjugate of  $\hat{m}_\alpha$  ( $\hat{\hat{m}}_\alpha$ ). Here we have used the cyclic property of the trace operator. All equations of Green's functions in the rest of this paper will be derived from this equation. For example, the first and the second equation of the hierarchy for respectively single-particle Greens functions:

$$G_1(m^\dagger, n) = \langle c_m^\dagger c_n \rangle \quad (4.5)$$

and two-particle Greens functions:

$$G_2(m^\dagger, n^\dagger, m', n') = \langle c_m^\dagger c_n^\dagger c_{m'} c_{n'} \rangle \quad (4.6)$$

can be derived by using  $A = c_m^\dagger c_n$ , respectively  $A = c_m^\dagger c_n^\dagger c_{m'} c_{n'}$  in Eq(4.4):

## 4.2. Derivation of the BBGKY-like hierarchy

---

$$0 = it \langle c_{m-1}^\dagger c_n \rangle + it \langle c_{m+1}^\dagger c_n \rangle - it \langle c_m^\dagger c_{n+1} \rangle - it \langle c_m^\dagger c_{n-1} \rangle \quad (4.7a)$$

$$\begin{aligned} & -iV_0 \langle c_m^\dagger c_{n-1}^\dagger c_n c_{n-1} \rangle + iV_0 \langle c_{m+1}^\dagger c_m^\dagger c_{m+1} c_n \rangle \\ & -iV_0 \langle c_{n+1}^\dagger c_m^\dagger c_{n+1} c_n \rangle + iV_0 \langle c_m^\dagger c_{m-1}^\dagger c_n c_{m-1} \rangle \end{aligned} \quad (4.7b)$$

$$-\lambda^2 \sum_{\alpha} \langle \delta_{m\alpha} c_n \hat{m}_{\alpha} + \delta_{n\alpha} \hat{m}_{\alpha}^\dagger c_m^\dagger - \delta_{n\alpha} c_m^\dagger \hat{m}_{\alpha} - \delta_{m\alpha} \hat{m}_{\alpha}^\dagger c_n \rangle, \quad (4.7c)$$

and

$$\begin{aligned} 0 = & it \langle c_{m-1}^\dagger c_n^\dagger c_{m'} c_{n'} \rangle + it \langle c_{m+1}^\dagger c_n^\dagger c_{m'} c_{n'} \rangle + it \langle c_m^\dagger c_{n-1}^\dagger c_{m'} c_{n'} \rangle \\ & + it \langle c_m^\dagger c_{n+1}^\dagger c_{m'} c_{n'} \rangle - it \langle c_m^\dagger c_n^\dagger c_{m'} c_{n'+1} \rangle - it \langle c_m^\dagger c_n^\dagger c_{m'} c_{n'-1} \rangle \\ & - it \langle c_m^\dagger c_n^\dagger c_{m'+1} c_{n'} \rangle - it \langle c_m^\dagger c_n^\dagger c_{m'-1} c_{n'} \rangle \\ & + iV_0 \langle c_m^\dagger c_n^\dagger c_{m'} c_{n'} \rangle \left( \delta_{m'+1, n'} + \delta_{m'-1, n'} - \delta_{m+1, n} - \delta_{m-1, n} \right) \end{aligned} \quad (4.8a)$$

$$\begin{aligned} & -iV_0 \sum_{l=m\pm 1, n\pm 1} \langle c_l^\dagger c_m^\dagger c_n^\dagger c_l c_{m'} c_{n'} \rangle \\ & + iV_0 \sum_{l=m'\pm 1, n'\pm 1} \langle c_l^\dagger c_m^\dagger c_n^\dagger c_l c_{m'} c_{n'} \rangle \end{aligned} \quad (4.8b)$$

$$\begin{aligned} & -\lambda^2 \sum_{\alpha} \left\{ \delta_{m'\alpha} \langle c_m^\dagger c_n^\dagger c_{n'} \hat{m}_{\alpha} \rangle - \delta_{n'\alpha} \langle c_m^\dagger c_n^\dagger c_{m'} \hat{m}_{\alpha} \rangle \right. \\ & + \delta_{m\alpha} \langle c_n^\dagger c_{m'} c_{n'} \hat{m}_{\alpha} \rangle - \delta_{n\alpha} \langle c_m^\dagger c_{m'} c_{n'} \hat{m}_{\alpha} \rangle + \delta_{n'\alpha} \langle \hat{m}_{\alpha}^\dagger c_m^\dagger c_n^\dagger c_{m'} \rangle \\ & \left. - \delta_{m'\alpha} \langle \hat{m}_{\alpha}^\dagger c_m^\dagger c_n^\dagger c_{n'} \rangle + \delta_{n\alpha} \langle \hat{m}_{\alpha}^\dagger c_m^\dagger c_{m'} c_{n'} \rangle - \delta_{m\alpha} \langle \hat{m}_{\alpha}^\dagger c_n^\dagger c_{m'} c_{n'} \rangle \right\}. \end{aligned} \quad (4.8c)$$

Note that since the set of all polynomials of  $\{c_l, c_l^\dagger\}$  form a complete basis of the operator space, operators  $\hat{m}$  are certainly functions of polynomials of  $\{c_l, c_l^\dagger\}$ . Therefore, we expected  $G_1$  to depend on  $G_2$  from Eq(4.7b), and possibly also  $G_3$  or higher Green's functions from Eq(4.7c); while  $G_2$  is coupled to  $G_3$  from Eq(4.8b), and possibly also  $G_4$  or higher Green's functions from Eq(4.8c). Solving this full hierarchy is no easier than directly solving the Redfield equation, unless  $V_S = 0$  so that the set of equations for  $G_1$  is closed, i.e. not coupled to  $G_2$ .

We may, however, solve these equations by truncating the hierarchy at a certain level using further approximations, such as the molecular-chaos

assumption in the classical Boltzmann equation [51], or replacing higher order Green's functions by a cluster expansion of lower order ones [69, 94, 95]. We use the following two approximate methods: (1) substitution of certain higher-order Green's functions by their values at equilibrium; (2) expressing higher-order Green's functions as combinations of lower-order ones plus a correlation part via cluster expansion, and then ignoring the correlation part at a certain order. A rough estimate of the accuracy of these substitutions at different orders can be found in Appendix C. Here we focus on the potential of this BBGKY-like formulation and discuss briefly the performance of the two approximations.

### 4.3 Non-interacting systems: proof for a non-equilibrium Wick's theorem

In this section, we will prove that when  $V_0 = 0$ ,

$$G_2(k_1^\dagger, k_2^\dagger, k_3, k_4) = G_1(k_1^\dagger, k_4) G_1(k_2^\dagger, k_3) - G_1(k_1^\dagger, k_3) G_1(k_2^\dagger, k_4), \quad (4.9)$$

where  $G_1$  and  $G_2$  are defined as

$$G_1(k_1^\dagger, k_2) = \langle c_{k_1}^\dagger c_{k_2} \rangle, \quad (4.10)$$

respectively

$$G_2(k_1^\dagger, k_2^\dagger, k_3, k_4) = \langle c_{k_1}^\dagger c_{k_2}^\dagger c_{k_3} c_{k_4} \rangle. \quad (4.11)$$

In a general non-equilibrium state, one may have  $\langle c_{k_3} c_{k_4} \rangle \neq 0$ . In that case, the above Wick's theorem should have a more general form. In all of our examples, our choice of the specific system-baths coupling makes such Green's functions vanish. If there are terms involving two creation or two annihilation operators in the coupling between the central system and the baths, the situation is different.

Here it is more convenient to work in the momentum representation than the position representation, therefore we define:

$$c_k = \frac{1}{\sqrt{N}} \sum_{l=1}^N \sin \frac{kl\pi}{N+1} c_l. \quad (4.12)$$

### 4.3. Non-equilibrium Wick's theorem

---

For a tight-binding chain with  $N$  sites and free ends ( $c_0 = 0 = c_{N+1}$ ), the usual plane-waves of infinite-size systems  $e^{ikl}$  are replaced by the eigenstates  $\sin \frac{kl\pi}{N+1}$ , hence this transformation. In this representation,

$$H_0 = \sum_{k=1}^N \epsilon_k c_k^\dagger c_k, \quad (4.13)$$

where

$$\epsilon_k = -2t \cos \frac{\pi k}{N+1}. \quad (4.14)$$

Starting from Eq(4.4) with the above  $H_0$  in momentum space and using  $A = c_{k_1}^\dagger c_{k_2}$  and  $A = c_{k_1}^\dagger c_{k_2}^\dagger c_{k_3} c_{k_4}$ , we find the equations for  $G_1(k_1^\dagger, k_2)$  and respectively  $G_2(k_1^\dagger, k_2^\dagger, k_3, k_4)$  as follows:

$$\begin{aligned} 0 &= i(\epsilon_{k_2} - \epsilon_{k_1}) G_1(k_1^\dagger, k_2) \\ &- \lambda^2 \frac{2\pi}{N+1} \sum_{\alpha} \sin \frac{k_1 \pi l_{\alpha}}{N+1} \sin \frac{k_2 \pi l_{\alpha}}{N+1} (n(k_1) + n(k_2)) \\ &+ \lambda^2 \frac{2\pi}{N+1} \sum_{\alpha, k} \left[ \sin \frac{k_2 \pi l_{\alpha}}{N+1} \sin \frac{k \pi l_{\alpha}}{N+1} G_1(k_1^\dagger, k) \right. \\ &\quad \left. + \sin \frac{k_1 \pi l_{\alpha}}{N+1} \sin \frac{k \pi l_{\alpha}}{N+1} G_1(k^\dagger, k_2) \right] \end{aligned} \quad (4.15)$$

### 4.3. Non-equilibrium Wick's theorem

---

and

$$\begin{aligned}
0 &= i(\epsilon_{k_4} + \epsilon_{k_3} - \epsilon_{k_2} - \epsilon_{k_1}) G_2(k_1^\dagger, k_2^\dagger, k_3, k_4) \\
&+ \lambda^2 \frac{2\pi}{N+1} \sum_{\alpha, k} \sin \frac{k_1 \pi l_\alpha}{N+1} \sin \frac{k \pi l_\alpha}{N+1} G_2(k_1^\dagger, k_2^\dagger, k_3, k_4) \\
&+ \lambda^2 \frac{2\pi}{N+1} \sum_{\alpha, k} \sin \frac{k_2 \pi l_\alpha}{N+1} \sin \frac{k \pi l_\alpha}{N+1} G_2(k_1^\dagger, k_2^\dagger, k_3, k_4) \\
&+ \lambda^2 \frac{2\pi}{N+1} \sum_{\alpha, k} \sin \frac{k_3 \pi l_\alpha}{N+1} \sin \frac{k \pi l_\alpha}{N+1} G_2(k_1^\dagger, k_2^\dagger, k, k_4) \\
&+ \lambda^2 \frac{2\pi}{N+1} \sum_{\alpha, k} \sin \frac{k_4 \pi l_\alpha}{N+1} \sin \frac{k \pi l_\alpha}{N+1} G_2(k_1^\dagger, k_2^\dagger, k_3, k) \\
&+ \lambda^2 \frac{2\pi}{N+1} \sum_{\alpha} \sin \frac{k_2 \pi l_\alpha}{N+1} \sin \frac{k_4 \pi l_\alpha}{N+1} G_1(k_1^\dagger, k_3) (n(k_2) + n(k_4)) \\
&- \lambda^2 \frac{2\pi}{N+1} \sum_{\alpha} \sin \frac{k_2 \pi l_\alpha}{N+1} \sin \frac{k_3 \pi l_\alpha}{N+1} G_1(k_1^\dagger, k_4) (n(k_2) + n(k_3)) \\
&- \lambda^2 \frac{2\pi}{N+1} \sum_{\alpha} \sin \frac{k_1 \pi l_\alpha}{N+1} \sin \frac{k_4 \pi l_\alpha}{N+1} G_1(k_2^\dagger, k_3) (n(k_1) + n(k_4)) \\
&+ \lambda^2 \frac{2\pi}{N+1} \sum_{\alpha} \sin \frac{k_1 \pi l_\alpha}{N+1} \sin \frac{k_3 \pi l_\alpha}{N+1} G_1(k_2^\dagger, k_4) (n(k_1) + n(k_3)) \quad (4.16)
\end{aligned}$$

Each of these forms a closed linear system of equations and has a unique solution. Therefore, we only need to find one solution and that must be the unique solution. We first apply Eq(4.9) to Eq(4.16) to expand  $G_2$  into products of  $G_1$ . It is then easy to prove that the resulting equation is equivalent with Eq(4.15), meaning that a solution of Eq(4.15) is also a solution of Eq(4.16). For example, if we collect terms with  $G_1(k_2^\dagger, k_4)$  together, we will have

$$\begin{aligned}
&G_1(k_2^\dagger, k_4) \left\{ i(\epsilon(k_3) - \epsilon(k_1)) G_1(k_1^\dagger, k_3) \right. \\
&- \lambda^2 \frac{2\pi}{N+1} \sum_{\alpha} \sin \frac{k_1 \pi l_\alpha}{N+1} \sin \frac{k_3 \pi l_\alpha}{N+1} (n(k_1) + n(k_3)) \\
&+ \lambda^2 \frac{2\pi}{N+1} \sum_{\alpha, k} \left[ \sin \frac{k_3 \pi l_\alpha}{N+1} \sin \frac{k \pi l_\alpha}{N+1} G_1(k_1^\dagger, k) \right. \\
&\quad \left. \left. + \sin \frac{k_1 \pi l_\alpha}{N+1} \sin \frac{k \pi l_\alpha}{N+1} G_1(k^\dagger, k_3) \right] \right\}, \quad (4.17)
\end{aligned}$$

where the term in curly brackets is zero according to Eq(4.15). Therefore, the solutions of Eq(4.15) satisfy Eq(4.16) as well, as long as Eq(4.9), the non-equilibrium Wick Theorem, holds. Since the combined equation has a unique solution, the solution with Eq(4.9) valid is the only possible solution. Therefore, Eq(4.9) is proved.

From this, we also know that for non-interacting systems, it is enough to solve only for the single-particle Green's functions, which form a linear system of equations with  $N^2$  unknowns. All higher order Green's functions can be factorized in products of various  $G_1$ .

## 4.4 Truncation of the hierarchy

As already shown, for interacting systems the equations for all Green's functions are coupled to one another. In order to solve Eq(4.7) explicitly, we first have to find explicit forms of the operators  $\hat{m}$  in terms of the operators  $\{c_l, c_l^\dagger\}$ . In Appendix A, we present an exact numerical calculation and a perturbational calculation for these operators. Correspondingly, based on these two methods of finding the operators  $\hat{m}$ , we discuss in this section two ways of turning Eq(4.7) into a closed equation by approximating the  $G_2$  terms. This is the lowest meaningful level of truncation.

We will first discuss a more accurate method, which works for larger interactions  $V_0$ , but which is computationally costly: perturbation based on two-particle Green's functions at equilibrium. Then we present a relatively less accurate but computationally much more efficient method, the non-equilibrium cluster expansion. The latter works only for relatively smaller  $V_0$  but can be applied to much larger systems. The values  $G_1(m^\dagger, n)$  obtained from both methods will be compared against  $G_1^{Ex}(m^\dagger, n)$ , the exact solution of Eq(4.2) via the linear system Eq. (2.89). Finally, we generalize the latter method by truncating it at the next level. This improves its accuracy and range of applicability, without sacrificing its efficiency.

### 4.4.1 Method 1: using equilibrium Green's functions

As explicitly worked out in Eq(A.2) of Appendix A, the operators  $\hat{m}$  can be written in terms of eigenmodes of  $H_S$ , which can be found from an exact diagonalization of  $H_S$ . This is a  $2^N$ -dimensional eigenvalue problem. Then, in the language of a super-operator space [88], where operators are treated like vectors – so called super-vectors –  $\hat{m}$  can be expanded under the basis

#### 4.4. Truncation of the hierarchy

---

of all polynomials of  $\{c_l, c_l^\dagger\}$  as:

$$\hat{m}_\alpha = \sum_l d_{\alpha;l} c_l + V_0 D_\alpha \quad (4.18a)$$

$$\hat{\bar{m}}_\alpha = \sum_l \bar{d}_{\alpha;l} c_l^\dagger + V_0 \bar{D}_\alpha, \quad (4.18b)$$

where using the definition of inner product between super-vectors  $\langle\langle A|B\rangle\rangle = \text{tr}(A^\dagger B)$ , we have

$$d_{\alpha;l} = \frac{1}{2^{(N-1)}} \text{tr}(c_l^\dagger \hat{m}_\alpha), \quad (4.19a)$$

$$\bar{d}_{\alpha;l} = \frac{1}{2^{(N-1)}} \text{tr}(c_l \hat{\bar{m}}_\alpha). \quad (4.19b)$$

Here  $2^{N-1}$  is a normalization constant to make  $d_{\alpha,l} = 1$  when  $\hat{m}_\alpha = c_l$ . Also,  $d_{\alpha;l}$  and  $\bar{d}_{\alpha;l}$  are the expansion coefficients at the linear order in  $c_l$  and  $c_l^\dagger$ ; operators  $V_0 D$  and  $V_0 \bar{D}$  are the remaining terms in the expansion of the operators  $\hat{m}$  and  $\hat{\bar{m}}$ , respectively.  $V_0$  is explicitly factorized out because of the fact that when  $V_0 = 0$ , this remaining part vanishes.

With these expressions for  $\hat{m}$ , Eq(4.7) becomes,

$$0 = it \langle c_{m-1}^\dagger c_n \rangle + it \langle c_{m+1}^\dagger c_n \rangle - it \langle c_m^\dagger c_{n+1} \rangle - it \langle c_m^\dagger c_{n-1} \rangle + \lambda^2 \sum_{l,\alpha} \langle \delta_{n\alpha} (d_{\alpha;l} + \bar{d}_{\alpha;l}^*) c_m^\dagger c_l + \delta_{m\alpha} (\bar{d}_{\alpha;l} + d_{\alpha;l}^*) c_l^\dagger c_n \rangle \quad (4.20a)$$

$$- \lambda^2 \sum_\alpha [\delta_{m\alpha} \bar{d}_{\alpha;n} + \delta_{n\alpha} \bar{d}_{\alpha;m}^*] \quad (4.20b)$$

$$- iV_0 \langle c_m^\dagger c_{n-1}^\dagger c_n c_{n-1} \rangle + iV_0 \langle c_{m+1}^\dagger c_m^\dagger c_{m+1} c_n \rangle - iV_0 \langle c_{n+1}^\dagger c_m^\dagger c_{n+1} c_n \rangle + iV_0 \langle c_m^\dagger c_{m-1}^\dagger c_n c_{m-1} \rangle \quad (4.20c)$$

$$- \lambda^2 V_0 \sum_\alpha \langle \delta_{m\alpha} c_n \bar{D}_\alpha + \delta_{n\alpha} \bar{D}_\alpha^\dagger c_m^\dagger - \delta_{n\alpha} c_m^\dagger D_\alpha - \delta_{m\alpha} D_\alpha^\dagger c_n \rangle. \quad (4.20d)$$

Note that every  $c_0, c_0^\dagger, c_{N+1}$  and  $c_{N+1}^\dagger$  that appears in the equation should be set to 0. First let us replace all  $G_2$ s in Eq(4.20c) by their values at equilibrium, denoted here as  $G_2^{E,(0)}$  where the superscripts indicate the use of thermal equilibrium (denoted by superscript  $E$ ) as the zeroth order approximation (denoted by  $(0)$ ) of the non-equilibrium  $G_2$ . Using the first term as an example,

$$G_2^{E,(0)}(m^\dagger, n) = \text{tr}(c_m^\dagger c_{n-1}^\dagger c_n c_{n-1} \rho_{eq}(H_S)), \quad (4.21)$$

#### 4.4. Truncation of the hierarchy

---

where  $\rho_{eq}(H_S) = \frac{1}{Z} e^{-\frac{H_S}{k_B T}}$ . This requires knowing the eigenstates of  $H_S$ . Similarly one can define  $G_D^{E,(0)}$  from Eq(4.20d), using the first term as an example,

$$G_D^{E,(0)}(m^\dagger, n) = \delta_{m\alpha} \text{tr}(c_n \bar{D}_\alpha \rho_{eq}(H_S)). \quad (4.22)$$

Next let us calculate  $G_1^{E,(1)}$  from Eq(4.20), where the superscript (1) means that the approximate calculation takes care of the first equation of the hierarchy, Eq(4.20). We organize all  $G_1^{E,(1)}(m^\dagger, n)$  as a vector,

$$g_1^{E,(1)} = \left[ G_1(1^\dagger, 1), G_1(1^\dagger, 2), \dots, G_1(N^\dagger, N) \right]^T, \quad (4.23)$$

and then Eq(4.20) for given values of  $m, n$  is the equation occupying the  $(mN + n)$ th row and in total there are  $N^2$  such equations. After substituting  $G_2^{E,(0)}$  and  $G_D^{E,(0)}$  for the exact but unknown  $G_2$  and  $G_D$ , the whole set of Eq(4.20) for all  $m, n$  becomes a linear system for  $g_1^{E,(1)}$  with dimension  $N^2$ ,

$$\Gamma^{(1)} g_1^{E,(1)} = iV_0 g_2^{E,(0)} + \lambda^2 \nu + \lambda^2 V_0 g_D^{E,(0)}, \quad (4.24)$$

where the vector  $\nu$  comes from ordering Eq(4.20b) in the same way as  $g_1^{E,(1)}$ . The same holds for  $g_2^{E,(0)}$  and  $g_D^{E,(0)}$  correspondingly from ordering Eq(4.20c) and Eq(4.20d). The matrix  $\Gamma^{(1)}$  is extracted from Eq(4.20a). For example, assuming  $m$  and  $n$  are not at the boundaries, one may read from Eq(4.20),

$$\nu_{mN+n} = \sum_\alpha [\delta_{m\alpha} \bar{d}_{\alpha;n} + \delta_{n\alpha} \bar{d}_{\alpha;m}^*], \quad (4.25a)$$

$$\Gamma_{mN+n, (m-1)N+n}^{(1)} = it. \quad (4.25b)$$

We can calculate single-particle equilibrium Green's functions,  $G_1^{E,(0)}$ , and organize them in the same way into a vector denoted as  $g_1^{E,(0)}$ .

We define the distance between two vectors  $A$  and  $B$  as,

$$d_B^A = \frac{\sqrt{\sum_i |A_i - B_i|^2}}{\sqrt{\sum_i |B_i|^2}}. \quad (4.26)$$

In order to gauge the accuracy, we compare  $d^{E,(0)}$ , the difference between the zeroth order  $g_1^{E,(0)}$  and the exact solution  $g_1^{Ex}$ , and  $d^{E,(1)}$ , the difference between the first order solution above,  $g_1^{E,(1)}$  and the exact solution  $g_1^{Ex}$ . Here  $G^{Ex}(m^\dagger, n) = \text{tr}(c_m^\dagger c_n \rho_{ex})$ , where  $\rho_{ex}$  is the exact solution from Eq(4.2).

## Results

First, we keep  $V_0 = 0.2$  as a constant, and check the accuracy of  $g_1^{E,(1)}$  for different values of  $\Delta T$ . From Fig.4.1(a) we can see that the worst is  $d^{(1)} \approx 1\%$ . Secondly, we set  $\Delta T = 0.4T$  as a constant, and check the accuracy of  $g_1^{E,(1)}$  for different values of  $V_0$ . The worst case is  $d^{(1)} \approx 0.3\%$  as shown in Fig.4.1(b). Overall, the distance  $d^{E,(1)}$  is always much smaller than  $d^{E,(0)}$ . We also compared the particle current calculated from this Green's functions, defined as:

$$J = \frac{ie}{N-1} \sum_{l=1}^{N-1} (G(l+1, l) - G(l, l+1)). \quad (4.27)$$

$J^{E,(0)}$ ,  $J^{E,(1)}$ ,  $J^{Ex}$  are calculated respectively from  $g_1^{E,(0)}$ ,  $g_1^{E,(1)}$  and  $g_1^{Ex}$ . From Fig.4.1(c) and (d) we see that in both cases,  $J^{E,(1)}$  is very close to the exact value,  $J^{Ex}$ , while  $J^{E,(0)}$ , the current in the equilibrium state, is always zero. Very high accuracy is found especially for small  $\Delta T$ . This indicates that the approximation captures the essential part of the non-equilibrium stationary states. It is also worth mentioning that this method generates reasonable results for very large  $V_0$ . Furthermore, it is likely that the approximation could be further improved, by expansions to higher order polynomials of  $c_l, c_l^\dagger$  and substitution of their values at equilibrium for the higher order unknown Green's functions in the higher-order equations of the hierarchy. Stopping the expansion of operators  $\hat{m}$  at linear order of  $V_0$  is compatible with solving only the first equation of the hierarchy. If further equations of the hierarchy are used then one should also expand operators  $\hat{m}$  to higher orders of  $V_0$ .

In order to estimate the accuracy of this level of approximation and also get a rough estimate of the accuracy of higher levels of truncation, we study the leading order of residues in terms of  $\lambda^2$  and  $\frac{\Delta T}{T}$ , both of which are assumed to be small in the following. Thus  $\lambda^2 V_0 \ll V_0$ , therefore we know that  $g_D$  is smaller than the  $g_2$  term so we drop it. Similarly, since  $\lambda^2 \Delta T \ll \Delta T$ , we drop the  $\lambda^2 \Delta T$  term in  $\lambda^2 \nu$  in Eq(4.24),

$$\lambda^2 \nu = \lambda^2 \nu_0(T) + \lambda^2 \Delta T \nu_{,T}, \quad (4.28)$$

and keep only the large term,  $\lambda^2 \nu_0(T)$ , which is independent of  $\Delta T$ . Here  $\nu_{,T}$  denotes formally a derivative of  $T$  on  $\nu - \frac{d}{dT} \nu$ . The general idea is then to write down equations for  $g_1^{Ex}$  and  $g_1^{E,(1)}$  (as shown in Eq. (C.2) of Appendix C), and then compare them to get an estimate for  $\Delta_1^{E,(1)} = g_1^{E,(1)} - g_1^{Ex}$ . In

#### 4.4. Truncation of the hierarchy

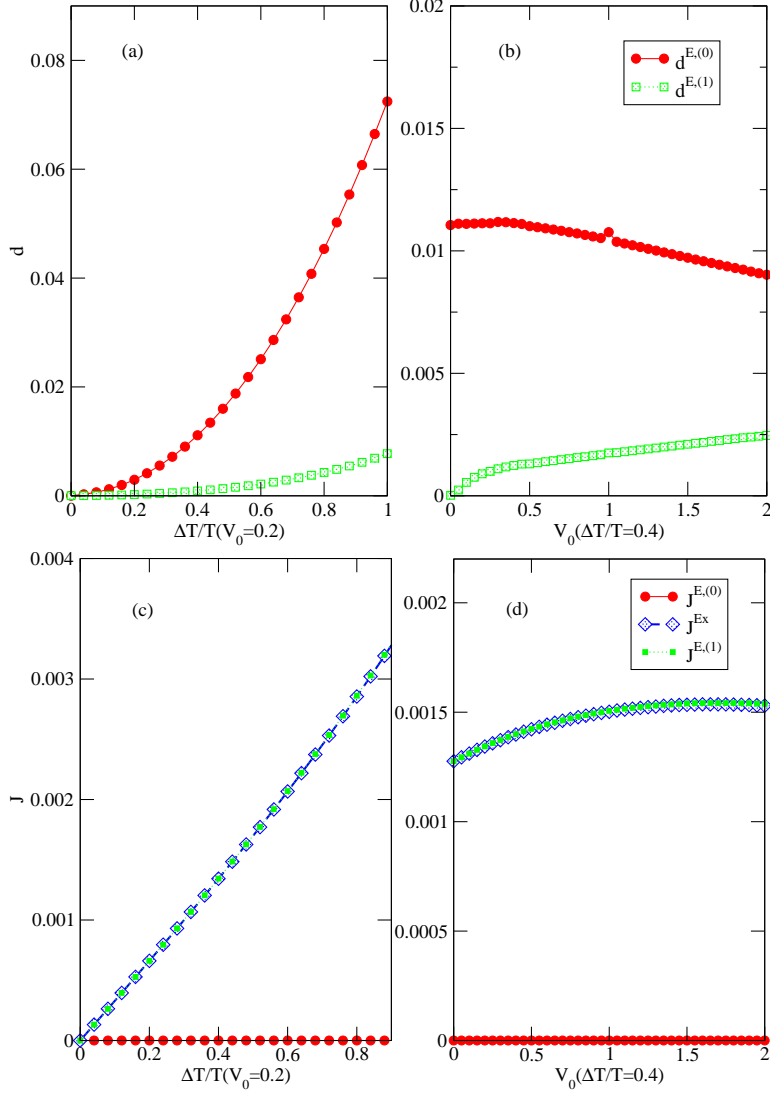


Figure 4.1:  $g_1^{E,(1)}$  is compared with  $g_1^{Ex}$  for interacting systems at non-equilibrium.  $d^{E,(1)}$  ( $d^{E,(0)}$ ) is the difference between  $g_1^{E,(1)}$  ( $g_1^{E,(0)}$ ) and  $g_1^{Ex}$  defined using Eq. (4.26). Both  $d^{E,(1)}$  and  $d^{E,(0)}$  are plotted vs. respectively  $\Delta T$  in (a) and  $V_0$  in (b). In both cases,  $d^{E,(1)}$  is much smaller than  $d^{E,(0)}$ . In (c) and (d)  $J^{E,(0)}$  and  $J^{E,(1)}$ , plotted vs. respectively  $\Delta T$  and  $V_0$ , are compared against  $J^{Ex}$ . We see that  $J^{E,(0)}$  is zero while  $J^{E,(1)}$  is close to  $J^{Ex}$  even for relatively large  $V_0$ . In all these sample calculations,  $t = 1.0$ ,  $\lambda = 0.1$ ,  $\mu = -1.0$ .

#### 4.4. Truncation of the hierarchy

---

order to understand how an approximation to the next order improves the accuracy, we also want to compare  $\Delta_1^{E,(1)}$  to  $\Delta_1^{E,(0)} = g_1^{E,(0)} - g_1^{Ex}$ , which is estimated in the same way from the difference between the equations respectively for  $g_1^{Ex}$  and  $g_1^{E,(0)}$ , see Appendix C for further details. Here we summarize the results, namely

$$\Delta_1^{E,(0)} = \Delta T \left( \Gamma_0^{(1)} \right)^{-1} \Gamma_{,T}^{(1)} g_1^{Ex} + iV_0 \left( \Gamma_0^{(1)} \right)^{-1} \Delta_2^{E,(0)} \quad (4.29)$$

and

$$\begin{aligned} \Delta_1^{E,(1)} = & \left( \Gamma_0^{(1)} \right)^{-1} \left[ -V_0^2 \left( \Gamma_0^{(2)} \right)^{-1} \Delta_3^{E,(0)} \right. \\ & \left. + iV_0 \Delta T \left( \Gamma_0^{(2)} \right)^{-1} \Gamma_{,T}^{(2)} g_2^{Ex} + iV_0 \lambda^2 \left( \Gamma_0^{(2)} \right)^{-1} \Delta_1^{E,(0)} \right]. \end{aligned} \quad (4.30)$$

Here  $\Delta_n^{E,(0)} = g_n^{E,(0)} - g_n^{Ex}$  and  $\Delta_n^{E,(1)} = g_n^{E,(1)} - g_n^{Ex}$  for general  $n$ -particle Green's functions  $g_n$ . We refer readers to Appendix C for definitions of all  $\Gamma$  matrices. Most importantly here we see that (from the last term in Eq. (4.30))  $\Delta_1^{E,(0)}$  is multiplied by a small number  $\lambda^2 V_0$  and then is included into  $\Delta_1^{E,(1)}$ . Furthermore, this relation holds generally for higher-order levels of this approximation. Judging from this it follows that, as long as  $\lambda^2 V_0 \ll t$  the method is very reasonable. As for the other two terms, they can be regarded as  $(V_0^2 g_3^{Ex} + V_0 g_2^{Ex}) \Delta T$ . Therefore, the maximum value of  $V_0$  where this method is still accurate is determined by  $|g_2^{Ex}|^{-1}$  or  $|g_3^{Ex}|^{-\frac{1}{2}}$ . Such limit could be much larger than 1 since roughly  $|g_n^{Ex}| = |g^{Ex}|^n$  — smaller for larger  $n$ . This explains why this method is applicable even for  $V_0$  larger than  $t$ , as we see from Fig.4.1.

Here, we note that since this approximation requires a full diagonalization of  $H_S$ , it is necessarily not efficient for large systems. As a result, we now discuss another approach, that can be used for much larger systems.

#### 4.4.2 Method 2: the non-equilibrium cluster expansion — first level

A different way to turn Eq(4.7) into a closed equation is to use the cluster expansion. Taking  $G_2$  as an example, this leads to:

$$\begin{aligned} G_2 \left( m^\dagger, n^\dagger, m', n' \right) = & -G_1 \left( m^\dagger, m' \right) G_1 \left( n^\dagger, n' \right) \\ & + G_1 \left( m^\dagger, n' \right) G_1 \left( n^\dagger, m' \right) + \mathfrak{G}_2 \left( m^\dagger, n^\dagger, m', n' \right). \end{aligned} \quad (4.31)$$

#### 4.4. Truncation of the hierarchy

---

If we set the part that describes correlations,

$$\mathfrak{G}_2 \rightarrow 0 \tag{4.32}$$

we have an approximative expression of  $G_2$  in terms of  $G_1$ , which allows us to obtain a close set of equations for  $G_1$  (for more details, see below). This approach can be applied to higher-order Green's functions, for example using a similar expansion for  $G_3$  in terms of  $G_1$  and  $G_2$  and setting  $\mathfrak{G}_3 = 0$ . In fact the non-equilibrium Wick's Theorem proved in Section §4.3 shows that indeed  $\mathfrak{G}_2 = 0$  when  $V_0 = 0$ . This makes such expansions plausible for non-equilibrium Green's functions. Setting  $\mathfrak{G}_2 = 0$  with  $V_0 \neq 0$  is similar to using the Hartree-Fock approximation. Depending on the system and the physical problem under investigation, one may need to go to the next level of approximation, i.e. keeping  $\mathfrak{G}_2$  but ignoring  $\mathfrak{G}_3$  to truncate the equation hierarchy at the level instead of the first one. Here, we will study both levels, beginning first with the lowest level approximation, i.e. setting  $\mathfrak{G}_2 \rightarrow 0$ .

However, the cluster expansion cannot be applied to the operators  $D$  defined in the previous section. Instead, we have to expand the operators  $\hat{m}$  in higher-order polynomials of  $\{c_l, c_l^\dagger\}$ . This can be done as follows. In order to avoid the costly exact diagonalization, the operators  $\hat{m}$  can also be found analytically using perturbation theory (see Appendix A for full details). The basic idea is to start by assuming

$$c_l(t) = c_l^{(0)}(t) + V_0 c_l^{(1)}(t) + O(V_0^2), \tag{4.33}$$

and then derive and solve the equations of motion of  $c_l^{(0)}, c_l^{(1)}$  from Heisenberg's equation. In this way, one avoids the direct diagonalization of  $H_S$ . This simplifies the calculation but its accuracy depends on the order of  $V_0$  at which the expansion stops. Stopping at the linear order of  $V_0$  is compatible with the cluster expansion for  $G_2$  (first level of approximation). If the cluster expansion in a higher-order Green's functions is applied, then the operators  $\hat{m}$  should also be expanded to higher orders of  $V_0$ . Keeping only the first order, the operators  $\hat{m}$  become

$$\hat{m}_\alpha = \sum_m \mathfrak{D}_{\alpha;m} c_m + V_0 \sum_{m_1 m_2 m_3} \mathfrak{D}_{\alpha;m_1 m_2 m_3} c_{m_1} c_{m_2}^\dagger c_{m_3} + O(V_0^2) \tag{4.34a}$$

$$\hat{\bar{m}}_\alpha = \sum_m \bar{\mathfrak{D}}_{\alpha;m} c_m^\dagger - V_0 \sum_{m_1 m_2 m_3} \mathfrak{D}_{\alpha;m_1 m_2 m_3} c_{m_3}^\dagger c_{m_2} c_{m_1}^\dagger + O(V_0^2), \tag{4.34b}$$

where the definitions of  $\mathfrak{D}_{\alpha;m}$  and  $\mathfrak{D}_{\alpha;m_1 m_2 m_3}$  are given in Appendix A.

#### 4.4. Truncation of the hierarchy

---

With the first-order cluster expansion and the above expansion of operators  $\hat{m}$  plugged into Eq(4.7), we have

$$\begin{aligned}
0 = & itG_1 \left( (m-1)^\dagger, n \right) + itG_1 \left( (m+1)^\dagger, n \right) \\
& - itG_1 \left( m^\dagger, n+1 \right) - itG_1 \left( m^\dagger, n-1 \right) \\
& + \lambda^2 \sum_{l,\alpha} \left[ \delta_{n\alpha} \left( \mathfrak{D}_{\alpha;l} + \bar{\mathfrak{D}}_{\alpha;l}^* \right) G_1 \left( m^\dagger, l \right) \right. \\
& \left. + \delta_{m\alpha} \left( \bar{\mathfrak{D}}_{\alpha;l} + \mathfrak{D}_{\alpha;l}^* \right) G_1 \left( l^\dagger, n \right) \right] \quad (4.35a)
\end{aligned}$$

$$\begin{aligned}
& + \lambda^2 V_0 \sum_{\alpha, m_1, m_2} \left( \mathfrak{D}_{\alpha;nm_2m_1} - \mathfrak{D}_{\alpha;m_1m_2n} \right) G_1 \left( m_1^\dagger, m_2 \right) \delta_{m\alpha} \\
& + \lambda^2 V_0 \sum_{\alpha, m_1, m_2} \left( \mathfrak{D}_{\alpha;mm_2m_1} - \mathfrak{D}_{\alpha;m_1m_2m} \right) G_1 \left( m_2^\dagger, m_1 \right) \delta_{n\alpha} \quad (4.35b)
\end{aligned}$$

$$- \lambda^2 \sum_{\alpha} \left( \delta_{m\alpha} \bar{\mathfrak{D}}_{\alpha;n} + \delta_{n\alpha} \bar{\mathfrak{D}}_{\alpha;m}^* \right) \quad (4.35c)$$

$$+ \lambda^2 V_0 \sum_{\alpha, m_1} \left( \mathfrak{D}_{\alpha;m_1m_1n} \delta_{m\alpha} + \mathfrak{D}_{\alpha;m_1m_1m} \delta_{n\alpha} \right) \quad (4.35d)$$

$$\begin{aligned}
& - iV_0 G \left( m^\dagger, (n-1)^\dagger, n, n-1 \right) \\
& + iV_0 G \left( (m+1)^\dagger, m^\dagger, (m+1), n \right) \\
& - iV_0 G \left( (n+1)^\dagger, m^\dagger, n+1, n \right) \\
& + iV_0 G \left( m^\dagger, (m-1)^\dagger, n, m-1 \right). \quad (4.35e)
\end{aligned}$$

Here  $G_2$  should be interpreted according to Eq. (4.31) with  $\mathfrak{G}_2 \rightarrow 0$ . This is the closed system of equations for the unknowns  $G_1$ . Next we define a vector  $g_1^{C,(1)}$ , where as before superscript  $C$  means cluster expansion and (1) symbolizes keeping only the first equation in the hierarchy. For simplicity we order Eq(4.35e) in the same way and denote it as  $g_2^{C,(1)} = \Pi \left( g_1^{C,(1)} \right)$ , where  $\Pi$  refers to the nonlinear function — summation of products — of  $g_1^{C,(1)}$  in Eq(4.35e). Then the above equation can be written in matrix form as:

$$\left( \Gamma_0^{(1)} + \lambda^2 V_0 \Gamma_D^{(1)} \right) g_1^{C,(1)} = \lambda^2 \nu_0 + \lambda^2 V_0 \nu_1 + iV_0 g_2^{C,(1)}, \quad (4.36)$$

where the five terms are respectively the five sub equations in Eq(4.35), for

#### 4.4. Truncation of the hierarchy

---

example,

$$(\nu_0)_{mN+n} = \sum_{\alpha} (\delta_{m\alpha} \bar{\mathcal{D}}_{\alpha;n} + \delta_{n\alpha} \bar{\mathcal{D}}_{\alpha;m}^*). \quad (4.37)$$

This equation can be solved iteratively

$$g_1^{[n+1]} = \left( \Gamma_0^{(1)} + \lambda^2 V_0 \Gamma_D^{(1)} \right)^{-1} \left( \lambda^2 \nu_0 + \lambda^2 V_0 \nu_1 + i V_0 \Pi \left( g_1^{[n]} \right) \right), \quad (4.38)$$

starting from the initial value

$$g_1^{[0]} = \left( \Gamma_0^{(1)} \right)^{-1} \lambda^2 \nu_0. \quad (4.39)$$

Here we start from  $g_1^{[0]} = g_1^{C,(0)}$ , which is the exact solution of Eq(4.36) when  $V_0 = 0$ . Through the iteration defined above we get the solution  $g_1^{C,(1)} = \lim_{n \rightarrow \infty} g_1^{[n]}$ . In practice we stop at large enough  $n$  such that  $g_1^{[n]} - g_1^{[n-1]}$  is small enough.

### Results

Using again Eq. (4.26), we define  $d^{C,(0)}$  as the relative distance between  $g_1^{C,(0)}$  and  $g_1^{Ex}$ , and  $d^{C,(1)}$  as the relative distance between  $g_1^{C,(1)}$  and  $g_1^{Ex}$ . First, we keep  $V_0 = 0.2$  as a constant, and check the accuracy of  $g_1^{C,(1)}$  for different values of  $\Delta T$ . From Fig.4.2(a) we see that the worst case is  $d^{(1)} \approx 1\%$ . Secondly, we set  $\Delta T = 0.4T$  as a constant, and check the accuracy of  $g_1^{C,(1)}$  for different values of  $V_0$ . The worst case is  $d^{(1)} \approx 2\%$  as shown in Fig.4.2(b). Overall, the difference  $d^{C,(1)}$  is always much smaller than  $d^{C,(0)}$ . From Fig.4.2(c) we see that for a small  $V_0$ ,  $J^{C,(0)}$  already provides most of the total current. However, Fig.4.2(d) shows that as  $V_0$  increases, the difference between  $J^{C,(1)}$  and  $J^{C,(0)}$  grows. We should also note that for larger  $V_0$ ,  $J^{C,(1)}$  starts to deviate from  $J^{Ex}$ . This indicates that the approximation captures the essential part of the interaction but it is quantitatively accurate only for small  $V_0$ . Of course, this can be improved by going to the next level in the truncation, as shown in section 4.4.3.

In order to estimate the accuracy of this approximation, let us assume that  $\lambda^2$  and  $V_0$  are small. We define  $\Delta_n^{C,(0)} = g_n^{C,(0)} - g_n^{Ex}$  and  $\Delta_n^{C,(1)} = g_n^{C,(1)} - g_n^{Ex}$ . Again we start from the equations of the three:  $g_1^{C,(0)}$ ,  $g_1^{C,(1)}$  and  $g_1^{Ex}$  (as we have done in Eq. (C.14) of Appendix C), and then compare them while ignoring certain higher-order, smaller terms such as those which

#### 4.4. Truncation of the hierarchy

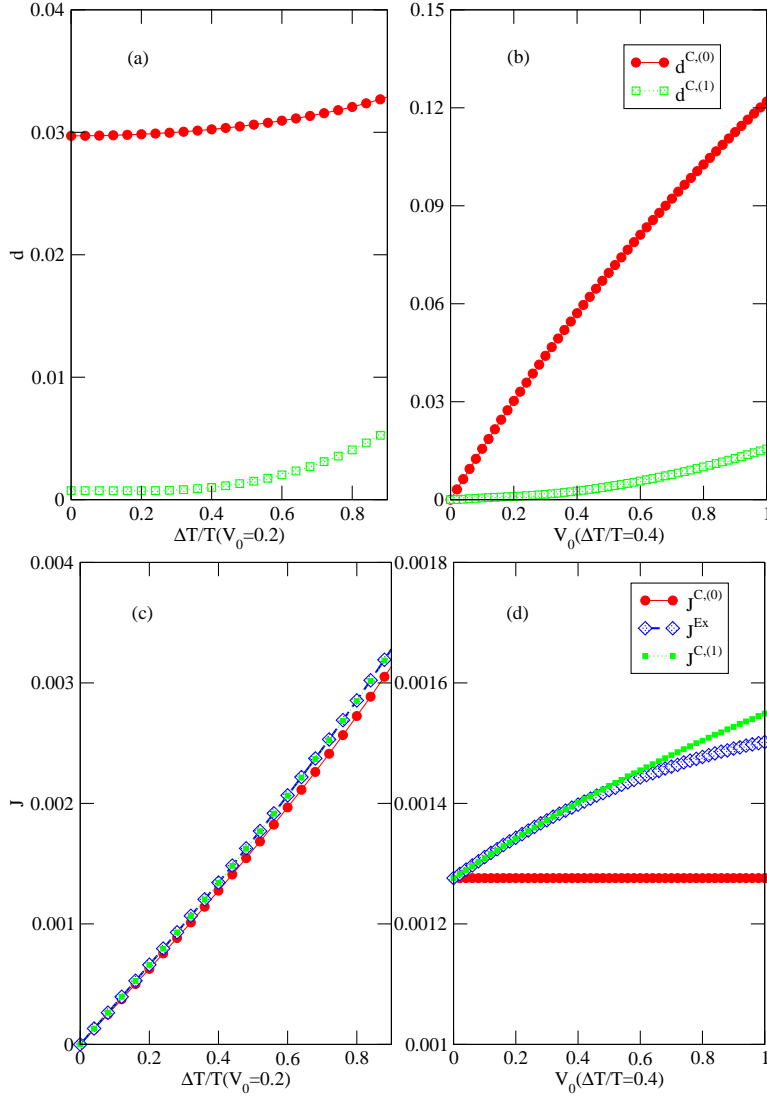


Figure 4.2:  $g_1^{C,(1)}$  is compared with  $g_1^{Ex}$  for non-equilibrium interacting systems. Both  $d^{C,(1)}$  and  $d^{C,(0)}$  are plotted vs. respectively  $\Delta T$  in (a) and  $V_0$  in (b). In both cases,  $d^{C,(1)}$  is always much smaller than  $d^{C,(0)}$ . In (c) and (d)  $J^{C,(0)}$  and  $J^{C,(1)}$ , plotted vs. respectively  $\Delta T$  and  $V_0$ , are compared against  $J^{Ex}$ . From (c), where  $V_0 = 0.2$  and it is relatively small, we see that for a given value of  $V_0$ , both  $J^{C,(0)}$  and  $J^{C,(1)}$  are consistent with  $J^{Ex}$ . From (d) we find that for relatively larger  $V_0$ ,  $J^{C,(1)}$  agrees much better with  $J^{Ex}$  than  $J^{C,(0)}$ .

#### 4.4. Truncation of the hierarchy

---

are proportional to  $\lambda^2 V_0$ , see Appendix C for more details. We arrive at:

$$\Delta_1^{C,(0)} = -iV_0 \left( \Gamma_0^{(1)} \right)^{-1} g_2^{Ex} \sim V_0 |g_1^{Ex}|^2, \quad (4.40)$$

and

$$\begin{aligned} \Delta_1^{C,(1)} &= \left( \Gamma_0^{(1)} \right)^{-1} \left[ iV_0^2 \left( \Gamma_0^{(2)} \right)^{-1} g_3^{Ex} \right. \\ &\left. + \lambda^2 V_0 \left( \Gamma_0^{(2)} \right)^{-1} \Delta_1^{C,(0)} \right] \sim V_0^2 |g_1^{Ex}|^3 + \lambda^2 V_0^2 |g_1^{Ex}|^2. \end{aligned} \quad (4.41)$$

We refer the readers to Appendix C for definitions of all  $\Gamma$  matrices.

This estimate agrees with the numerical results that  $\Delta_1^{C,(0)}$  is proportional to  $V_0$  while  $\Delta_1^{C,(1)}$  is proportional to  $V_0^2$ . Most importantly, we see again that  $\Delta_1^{C,(0)}$  is multiplied by a small number  $\lambda^2 V_0$  and then becomes a part of  $\Delta_1^{C,(1)}$ . Since roughly  $|g_n^{Ex}| = |g^{Ex}|^n$ , the other term,  $V_0^2 g_3^{Ex} \sim V_0^2 |g_1^{Ex}|^3$ , is also much smaller than  $\Delta_1^{C,(0)} \sim V_0 |g_1^{Ex}|^2$ . However, for large enough  $V_0$  the other approximation used in this method, the perturbational expansion of the operators  $\hat{m}$ , becomes invalid. Therefore, as long as  $V_0 \ll t$  this level of approximation is expected to be very reasonable. It should be noted that this method is capable of dealing with large systems since it does not require a direct diagonalization of a  $2^N$ -dimension matrix, like the previous method. Instead, it deals with vectors of dimension  $N^2$ .

#### 4.4.3 Method 2: second-level cluster expansion

In the previous section, we showed that even truncation at first level leads to quite accurate results, and a very efficient method. Here, we discuss the truncation at the second level of the BBGKY hierarchy. This requires us to keep  $\mathfrak{G}_2$  as unknowns in the equations which now include the equations for  $G_2$ , while letting  $\mathfrak{G}_3 = 0$  in order to truncate the resulting larger system. While the first-level approximation is equivalent to the Hartree-Fock approximation, this second-level form goes beyond that. The cluster expansion of  $G_3$  [94] expresses it in terms of  $G_1$ ,  $\mathfrak{G}_2$  and  $\mathfrak{G}_3$  (see Appendix B for the explicit expression):

$$\begin{aligned} G \left( m_1^\dagger, m_2^\dagger, m_3^\dagger, m_4, m_5, m_6 \right) &= \sum_P (-1)^P G_1 G_1 G_1 + \sum_P (-1)^P G_1 \mathfrak{G}_2 \\ &+ \mathfrak{G}_3 \left( m_1^\dagger, m_2^\dagger, m_3^\dagger, m_4, m_5, m_6 \right). \end{aligned} \quad (4.42)$$

#### 4.4. Truncation of the hierarchy

---

Here  $\sum_P (-1)^P G_1 G_1 G_1$  is a short-hand notation for the various ways of pairing  $\{m_1^\dagger, m_2^\dagger, m_3^\dagger, m_4, m_5, m_6\}$  into three groups using  $G_1$  and taking care of the anti-commutation relations, for example

$$G_1 \left( m_1^\dagger, m_6 \right) G_1 \left( m_2^\dagger, m_5 \right) G_1 \left( m_3^\dagger, m_4 \right). \quad (4.43)$$

Similarly  $\sum_P (-1)^P G_1 \mathfrak{G}_2$  denotes all different ways of pairing these into two groups using  $G_1$  and  $\mathfrak{G}_2$ , for example

$$G_1 \left( m_1^\dagger, m_6 \right) \mathfrak{G} \left( m_2^\dagger, m_3^\dagger, m_4, m_5 \right). \quad (4.44)$$

Setting  $\mathfrak{G}_3 \rightarrow 0$ , we aim to derive a close system of equations for  $G_1$  and  $\mathfrak{G}_2$  from Eq. (4.7) and Eq. (4.8). In order to be consistent, i.e. so that all terms lower than  $G_3$  should be included in both equations, bath operators  $\hat{m}_\alpha$  should be truncated to second order, i.e. at terms proportional to  $V_0^2$ . However, including the  $V_0^2$  terms greatly complicates both equations (see Appendix B for details). Therefore, here we use only the expression of operators  $\hat{m}_\alpha$  truncated at the first order of  $V_0$ . In this case, Eq. (4.7) becomes an equation very similar to Eq. (4.35) but with a different meaning for  $G_2$ :  $G_2$  should be interpreted according to Eq. (4.31) with explicit  $\mathfrak{G}_2$  included. We denote this, using compressed notations similar to the ones in Eq. (4.24) and Eq. (4.36), as

$$\Gamma^{(1)} g_1 = \lambda^2 \nu_0 + \lambda^2 V_0 \nu_1 + i V_0 \pi (g_1 g_1) + i V_0 \mathfrak{g}_2. \quad (4.45)$$

Note that now we have an additional term  $i V_0 \mathfrak{g}_2$ , so this is not a closed equation by itself. Here  $\pi (g_1 g_1)$  is the short-hand notation for the combinations of products between  $g_1$  and  $g_1$  the cluster expansions in Eq. (4.31). Meanwhile, Eq. (4.8) becomes,

$$\begin{aligned} \Gamma^{(2)} \mathfrak{g}_2 = & -\Gamma^{(2)} \pi (g_1 g_1) + \lambda^2 g_1 + \lambda^2 V_0 g_1 \\ & + i V_0 \pi (g_1 g_1 g_1) + i V_0 \pi (g_1 \mathfrak{g}_2), \end{aligned} \quad (4.46)$$

such that we get a closed system of equations when we combine the two sets. The explicit form of this latter equation can be found in Appendix B. Here  $\pi (g_1 \mathfrak{g}_2)$  is the short-hand notation for the combinations of products between  $g_1$  and  $\mathfrak{g}_2$  from Eq. (4.42). Same holds for  $\pi (g_1 g_1 g_1)$ . The matrices  $\Gamma^{(1)}$  and  $\Gamma^{(2)}$  come from the following terms

$$\Gamma^{(1)} = \Gamma_{H_0}^{(1)} + \lambda^2 \Gamma_{B_0}^{(1)} + \lambda^2 V_0 \Gamma_{B_1}^{(1)}, \quad (4.47a)$$

$$\Gamma^{(2)} = \Gamma_{H_0}^{(2)} + i V_0 \Gamma_V^{(2)} + \lambda^2 \Gamma_{B_0}^{(2)} + \lambda^2 V_0 \Gamma_{B_1}^{(2)}. \quad (4.47b)$$

#### 4.4. Truncation of the hierarchy

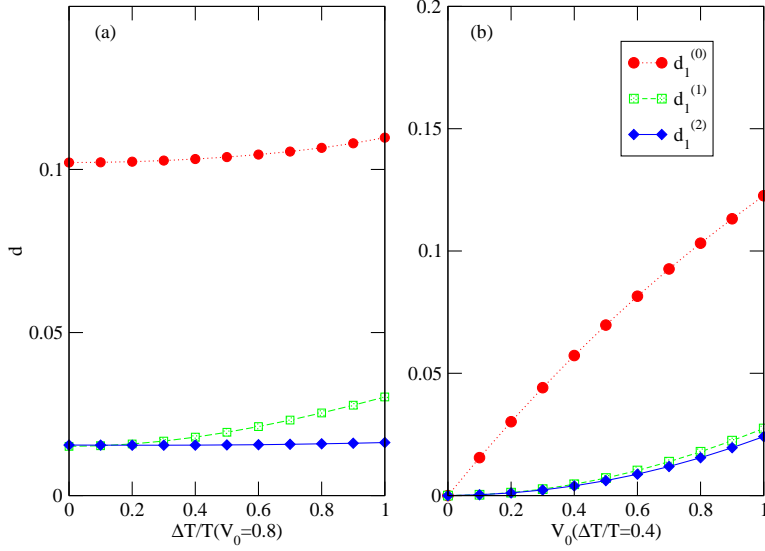


Figure 4.3:  $G_1$  calculated with different levels of the approximations are compared.  $d_1^{(2)}$  is plotted in addition to the previous shown  $d_1^{(1)}$  and  $d_1^{(0)}$ . We see that the distance  $d_1^{(2)}$  is smaller than, but rather close to  $d_1^{(1)}$ , while both are much smaller than  $d_1^{(0)}$ .

The various  $\Gamma$ 's are obtained by considering only the term indicated by their subscripts. For example,  $\Gamma_{H_0}^{(1)}$  is the one derived from  $H_0$  only, without using the potential  $V$  and bath operators  $\hat{m}_\alpha$ , while  $\lambda^2\Gamma_{B_0}^{(1)}$  ( $\lambda^2\Gamma_{B_1}^{(1)}$ ) is related to the component of the bath operators that is of the zeroth (first) order in  $V_0$ . The combination of Eq. (4.45) and Eq. (4.46) is a closed system for  $g_1$  and  $\mathfrak{g}_2$ . Solving it gives us results of the second-level cluster expansion, and provides finite values for  $\mathfrak{G}_2$ . In other words, explicit correlations are built in, and thus this method goes well beyond the Hartree-Fock approximation.

In the following we are investigate how large are these  $\mathfrak{G}_2$  and also what is the gain in accuracy when compared against exact numerical solutions, and against the first-level truncation.

First, we define  $d_1^{(2)}$  to be the difference between the  $G_1$  calculated from this second-order cluster expansion and the exact  $G_1$ , similarly as  $d^{C,(1)}$ , which is now denoted as  $d_1^{(1)}$ . In Fig.4.3 we find that  $d_1^{(2)}$  is smaller than but very close to  $d_1^{(1)}$ . This means that the second-order cluster expansion has better accuracy, but quantitatively does not lead to a significant improvement of  $G_1$ .

#### 4.4. Truncation of the hierarchy

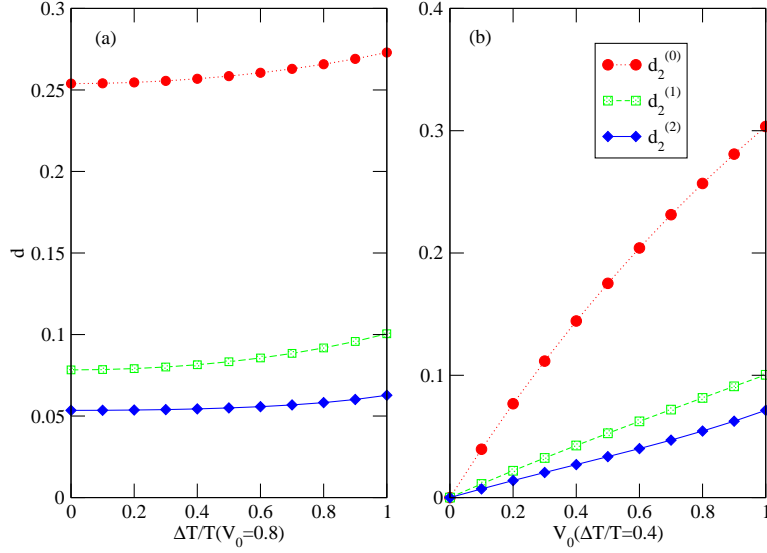


Figure 4.4:  $G_2$  calculated with different levels of the approximations are compared.  $d_2^{(2)}$  is plotted v.s.  $\Delta T$  and  $V_0$ . We see that  $d_2^{(2)}$  is significantly smaller than  $d_2^{(1)}$ .

Second, in the same way, we define  $d_2^{(2)}$  and compare the differences between  $G_2$ s calculated from the various truncations to the exact  $G_2$ . From Fig.4.4 we find that the second order truncation leads to a sizable improvement in  $G_2$ .

To find how significant is this difference for physical quantities, we compare the currents calculated from the approximations and exact calculation. In order to enhance these differences, we increase the coupling constant to  $\lambda = 0.5$  in the following figures. This is because the absolute value of the particle current depends very strongly on the value of  $\lambda$  ( $J \propto \lambda^2$ ). For the same purpose we have also set  $V = 0.8$  instead of  $V = 0.4$  when checking the  $\Delta T$  dependence.

Figure 4.5 shows that the agreement between  $J^{(2)}$  and  $J^{Ex}$  is much better than the one between  $J^{(1)}$  and  $J^{Ex}$ , especially for larger  $V_0$ . This proves that the correlations kept at the second-level truncation are important for an accurate description of the transport properties.

Since the second-level approximation allows us to calculate  $\mathfrak{G}_2$  — the correlated part of  $G_2$  — we also consider the heat current, a physical quantity

#### 4.4. Truncation of the hierarchy

---

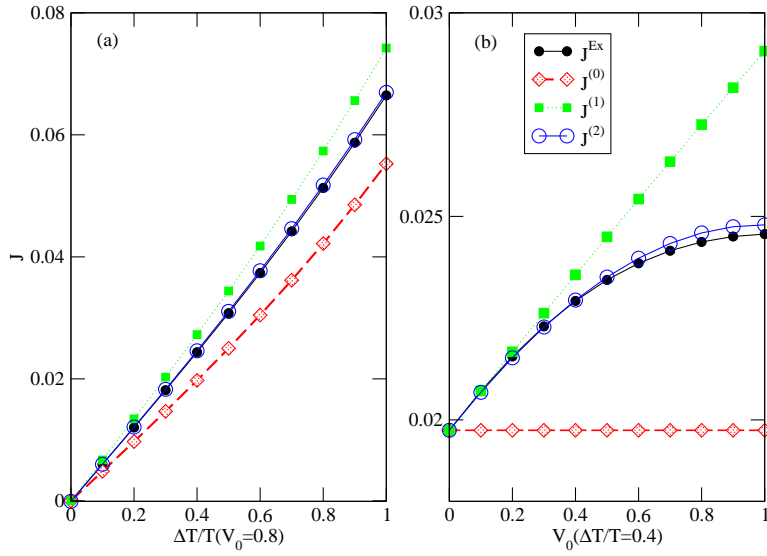


Figure 4.5: Particle currents,  $J^{(2)}$ ,  $J^{(1)}$ ,  $J^{(0)}$ , calculated respectively from the second-, first- and the zeroth-order truncations are compared against  $J^{Ex}$ , which is found from the exact diagonalization method. For all the range of  $V_0$  shown in this figure,  $J^{(2)}$  is very close to  $J^{Ex}$ , while  $J^{(1)}$  is accurate only for small  $V_0$ .

#### 4.4. Truncation of the hierarchy

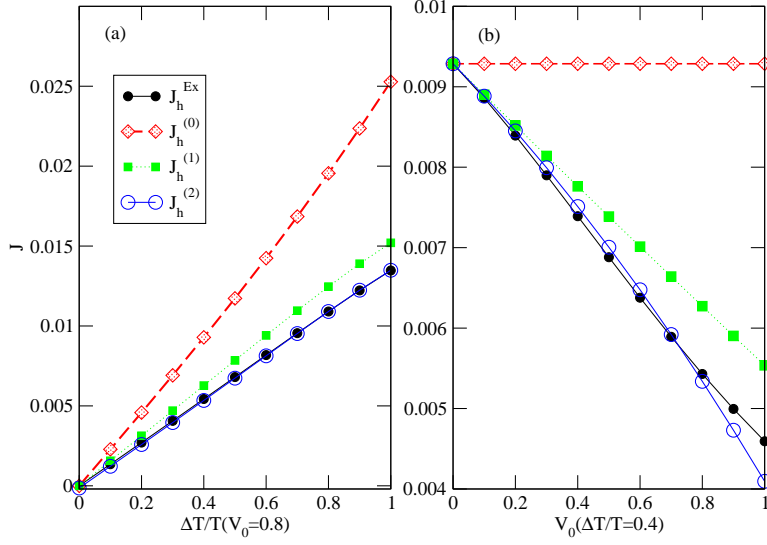


Figure 4.6: Heat currents,  $J_h^{(2)}$ ,  $J_h^{(1)}$ ,  $J_h^{(0)}$  are compared against  $J_h^{Ex}$ . For all range of  $V_0$  shown in this figure,  $J_h^{(2)}$  is close to  $J_h^{Ex}$ .  $J_h$  depends strongly on  $G_2$  while particle current  $J$  in the previous figure relies on  $G_1$ .

making explicit use of  $G_2$ :

$$\begin{aligned} \langle J_h \rangle = & \frac{-2}{N-2} \sum_{l=2}^{N-2} \text{Im} [t^2 G_1(l-1, l+1) \\ & + Vt G_2(l-1, l+1; l, l+1) + Vt G_2(l-1, l+1; l, l-1)], \end{aligned} \quad (4.48)$$

which is derived from

$$J_h = \sum_{l=2}^{N-2} i [h_{l-1}^B, h_l^B] \quad (4.49)$$

and

$$h_l^B = -tc_l^\dagger c_{l+1} - tc_{l+1}^\dagger c_l + Vc_l^\dagger c_l c_{l+1}^\dagger c_{l+1}. \quad (4.50)$$

Again, we find from Fig.4.6 that the agreement between  $J_h^{(2)}$  and  $J_h^{Ex}$  is much better than the one between  $J_h^{(1)}$  and  $J_h^{Ex}$ , especially for larger  $V_0$ . This indicates that the finite  $\mathfrak{G}_2$  are essential for getting proper values of heat currents.

Keeping orders of  $V_0^2$  in the bath operators  $\hat{m}_\alpha$  is consistent with truncation at  $\mathfrak{G}_3 = 0$  and may improve accuracy for the second-level truncation even further. However, including these terms greatly complicates the linear equation for  $G_2$ , so that it has about 200 different terms (see Appendix A for more details). An investigation of their effect on the overall results is left as future work.

## 4.5 Conclusion and discussion

To conclude, a BBGKY-like equation hierarchy is derived from the Redfield equation and two systematic approximations are suggested to truncate and solve the hierarchy. Using the first-level of the first method and both the first- and the second-levels of the second method, non-equilibrium stationary states of interacting systems are calculated. It is found [these](#) are in good agreement with exact results, for small systems where the latter are available. We also estimated the accuracy of the two approximations.

We find that the first method works for strong interaction  $V_0$ . However, because it requires an explicit diagonalization of the Hamiltonian, it is less computationally efficient. We imagine this method being used to study, for example, systems of a few strongly coupled quantum dots which have large charging energies.

The second method is much more efficient and therefore it can be applied to much larger systems, but its accuracy decreases with increasing interaction strength  $V_0$ . However, truncation at a higher level is shown to significantly improve both its accuracy, and its range of validity. Even at the second level, good accuracy for physical quantities is seen up to rather high values of  $V_0$  and  $\Delta T$ , and the results have the correct trends even when they become quantitatively less accurate. It is likely that going to even higher levels of truncation further improves accuracy, although, of course, this also leads to significantly more involved computations.

In future work, one can investigate the generalization to higher level truncations. Even more interesting, however, is the application of this method to physical problems.

## Chapter 5

# Solving the Redfield equation using coherent-state representations

### 5.1 Introduction

In quantum optics, a common technique to solve quantum master equations for density matrices is to use the coherent-state representation [70]. Quite often a quantum master equation for a single photon (boson) mode is solved in the coherent-state representation, where the operator-form quantum master equation becomes a differential equation of  $c$ -numbers and a density operator becomes a “distribution” function. The problem of the Hilbert space’s infinite dimension is bypassed. For example, a distribution function over  $N$  complex numbers is sufficient to describe a  $N$ -site Bose-Hubbard model [96, 97]. The equations for these distribution functions can be solved analytically or through numerical simulations of certain equivalent stochastic differential equations such as Langevin equations (see Refs. [70, 98] and also Appendix E for the relation between generalized Fokker-Planck equations and Langevin equations).

A common coherent-state representation is the  $P$ -representation (see Ref [70] and also the Appendix D for details on various forms of coherent-state representations). In the  $P$ -representation coherent eigenvalues  $\xi$  and  $\xi^*$  are treated as conjugate complex numbers, thus one solves only the equations for  $\xi$ . Sometimes it is also useful to work with generalizations of the  $P$ -representation [70]. In fact, the generalized  $P$ -representation, where coherent eigenvalues  $\xi$  and  $\xi^*$  are treated independently, has been used in simulations of both thermal equilibrium and dynamical evolution of quantum systems (see for example [72] and references therein). It has been shown that this approach is capable of dealing with the pure dynamical evolution of an interacting quantum system with 150000 atoms and  $10^6$  momentum modes [75]. The work presented in this chapter can be regarded as an ex-

tension of this method from simulations of equilibrium and pure dynamical states to simulations of non-equilibrium stationary states.

Thus, in this chapter we introduce another efficient method to solve the Redfield equation: using the coherent-state representation, the Redfield equation is mapped onto a generalized Fokker-Planck equation. For non-interacting systems, analytical results are obtained for the non-equilibrium stationary states. For interacting systems, we find that the resulting equations can be solved efficiently via classical simulations.

The existence of a general distribution function for systems in thermal equilibrium, which depends only on the Hamiltonian and the temperature, greatly simplifies the calculation of equilibrium properties. However, there is no known general distribution for non-equilibrium stationary states. For each problem, therefore, one has to calculate the distribution from a quantum master equation, such as the Redfield equation, which is capable of taking into account the role of the baths, besides the central system.

However, we have seen in the previous chapters that it is very hard to solve the Redfield equation efficiently. The fact that there is no analytical expression for non-equilibrium stationary states may simply be due to the technical difficulty in solving the quantum master equation. A more efficient way of solving this equation might lead to different results, or maybe to a proof that there is no general expression describing non-equilibrium stationary states. In this chapter, using the coherent-state representation, we derive an analytical expression for non-equilibrium stationary states of non-interacting systems. The question of finding such non-equilibrium stationary states for non-interacting systems has been numerically investigated via the time-dependent density matrix renormalization [99, 100], however for the local-operator Lindblad equation instead of the Redfield equation.

The focus of this chapter, however, is to study the efficiency of this approach when applied to interacting systems.

The chapter is organized as follows. In section 5.2, we introduce the model system, define its Redfield equation and then convert the operator-form Redfield equation into a differential equation in the coherent-state representation. We find the mapped equation to be in the form of a generalized Fokker-Planck equation. We then proceed to find analytical solutions of the generalized Fokker-Planck equation for non-interacting systems in Section 5.3. In Section 5.4, we show that the same BBGKY-like hierarchy can be derived from the generalized Fokker-Planck equation as from the original Redfield equation. This provides further support for the work presented in the previous chapter. In section 5.5, we solve the generalized Fokker-Planck equation via numerical simulations for interacting bosonic systems.

The method is also applicable to other quantum master equations such as the local-operator Lindblad equation, as we demonstrate in section 5.6. In section 5.7, we conclude that this new method based on the coherent-state representation leads to analytical solutions for non-interacting systems and comment on its possible further development and applications.

## 5.2 The model and its effective equation of motion

For concreteness, the system of interest in this chapter is a 1-D Bose-Hubbard chain [96, 97] coupled to a bath at each of its ends. The left (right) bath is maintained at temperature  $T_L = T + \frac{\Delta T}{2}$  ( $T_R = T - \frac{\Delta T}{2}$ ). We are interested in the stationary state of the central system. The Hamiltonian of the central system ( $H_S$ ), the baths ( $H_{B\alpha}$ ) and the couplings ( $H_{SB}$ ) are, respectively:

$$H_S = H_0 + V_S = \sum_{l=1}^{N-1} \left( a_l^\dagger a_{l+1} + a_{l+1}^\dagger a_l \right) + \frac{U}{2} \sum_{l=1}^N n_l (n_l - 1), \quad (5.1a)$$

$$H_B = \sum_{k,\alpha} \omega_{k,\alpha} \left( b_{k,\alpha}^\dagger b_{k,\alpha} + 1 \right), \quad (5.1b)$$

$$H_{SB} = \lambda \sum_{k,\alpha=L,R} \left( V_k^\alpha a_\alpha^\dagger b_{k,\alpha} + h.c. \right). \quad (5.1c)$$

Note that only the ends are coupled to baths ( $\alpha = L, R$ ):  $a_L = a_1, a_R = a_N$  etc. The system of interest, the Bose-Hubbard chain, has been realized experimentally [97].

Neglecting the shift of the spectrum of the central system due to the coupling to the baths, the Redfield equation reads, from Eq. (2.48):

$$\begin{aligned} \frac{\partial \rho(t)}{\partial t} &= -i[\mathcal{H}_S, \rho(t)] \\ -\lambda^2 \sum_{\alpha=L,R} &\left\{ \left[ a_\alpha^\dagger, \hat{m}_\alpha \rho(t) \right] + \left[ a_\alpha, \hat{\hat{m}}_\alpha \rho(t) \right] + h.c. \right\}, \end{aligned} \quad (5.2)$$

## 5.2. The model and its effective equation of motion

---

where  $\hat{m}_L(\hat{m}_R)$  is related to  $a_1(a_N)$  while  $\hat{\tilde{m}}_L(\hat{\tilde{m}}_R)$  is related to  $a_1^\dagger(a_N^\dagger)$ ,

$$\hat{m}_\alpha = \sum_k |V_k^\alpha|^2 \int_0^\infty d\tau a_\alpha(-\tau) e^{-i\omega_{k,\alpha}\tau} \langle 1 + n(\omega_{k,\alpha}) \rangle, \quad (5.3a)$$

$$\hat{\tilde{m}}_\alpha = \sum_k |V_k^\alpha|^2 \int_0^\infty d\tau a_\alpha^\dagger(-\tau) e^{i\omega_{k,\alpha}\tau} \langle n(\omega_{k,\alpha}) \rangle. \quad (5.3b)$$

Here  $\langle n(\omega_{k,\alpha}) \rangle = \left( e^{\frac{\omega_{k,\alpha} - \mu_\alpha}{T_\alpha}} + 1 \right)^{-1}$  is the Bose-Einstein distribution for the bath modes. Note that later we will switch the summation over momentum  $k$  into an integral over energy  $\epsilon$ , which involves a density of states  $D(\epsilon)$ . Generally both  $D(\epsilon)$  and  $|V_k^\alpha|^2$  may depend on  $\epsilon$ . However, for simplicity we set the density of state and also  $|V_k^\alpha|^2$  to constants and absorb them into the coupling constant  $\lambda$ .

Next we map the Redfield equation into a differential equation in the coherent-state representation. A similar approach has been used in earlier works mentioned in Ref. [72]. However, they are based on different equations of motion, such as the pure dynamical equation or the local-operator Lindblad equation [90] with bath temperature set at zero, while we use the Redfield equation for finite bath temperatures. From a technical point of view, in the coherent-state representation it is easier to deal with the local-operator Lindblad equation than the Redfield equation. However, we have shown in section 2.5 of chapter 2 that in order to get proper non-equilibrium stationary states, it is necessary to use the more complicated Redfield equation.

As we demonstrated in Appendix A, for fermions the operators  $\hat{m}$  and  $\hat{\tilde{m}}$  can be derived perturbationally to avoid direct diagonalization of  $H_S$ . Here we apply the same procedure for bosons. Assuming that the Hubbard  $U$  is small, we may solve the Heisenberg equation order by order to get

$$a_l(t) = \sum_n U^n a_l^{(n)}(t), \quad a_l^\dagger(t) = \sum_n U^n a_l^{\dagger,(n)}(t), \quad (5.4)$$

and then carry out the integrals to get the operators  $\hat{m}$  and  $\hat{\tilde{m}}$ .

An important observation is that when  $U = 0$  the problem is exactly solvable and  $a_l(t)$  ( $a_l^\dagger(t)$ ) is a linear combination of all  $a_m$  ( $a_m^\dagger$ ),

$$a_l(t) = a_l^{(0)}(t) = \frac{2}{N+1} \sum_{km} \sin \frac{\pi kl}{N+1} \sin \frac{\pi km}{N+1} e^{-i\epsilon_k t} a_m, \quad (5.5)$$

## 5.2. The model and its effective equation of motion

---

where  $\epsilon_k = 2 \cos \frac{k\pi}{N+1}$ . This is because for finite-size systems with free ends, the Fourier transform is discrete and  $e^{ikl}$  is replaced by the  $\sin \frac{\pi kl}{N+1}$  wavefunction, see for example Eq. (A.4).

For interacting systems, in principle it is possible to perform this perturbational calculation up to a large  $n$ , however here we will stop at the first order,  $a_l^{(1)}(t)$ ,

$$a_l^{(1)}(t) = i \int_0^t d\tau \left( a_l^{\dagger,(0)}(\tau) a_l^{(0)}(\tau) a_l^{(0)}(\tau) \right). \quad (5.6)$$

After some tedious but straightforward algebra( see Ref. [101] and also Appendix A for details), we find, to the linear order in  $U$ , that:

$$\hat{m}_\alpha = \sum_m \mathfrak{D}_{\alpha;m} a_m + U \sum_{m_1 m_2 m_3} \mathfrak{D}_{\alpha;m_1 m_2 m_3} a_{m_1}^\dagger a_{m_2} a_{m_3} + O(U^2) \quad (5.7a)$$

$$\hat{m}_\alpha = \sum_m \bar{\mathfrak{D}}_{\alpha;m} a_m^\dagger + U \sum_{m_1 m_2 m_3} \mathfrak{D}_{\alpha;m_1 m_2 m_3} a_{m_3}^\dagger a_{m_2}^\dagger a_{m_1} + O(U^2), \quad (5.7b)$$

where

$$D_{\alpha;m} = \pi \frac{2}{N+1} \sum_k \sin \frac{\pi k l_\alpha}{N+1} \sin \frac{\pi k m}{N+1} [1 + n(\epsilon_k, T_\alpha, \mu_\alpha)], \quad (5.8a)$$

$$\bar{D}_{\alpha;m} = \pi \frac{2}{N+1} \sum_k \sin \frac{\pi k l_\alpha}{N+1} \sin \frac{\pi k m}{N+1} n(\epsilon_k, T_\alpha, \mu_\alpha), \quad (5.8b)$$

$$\begin{aligned} D_{\alpha;m_1 m_2 m_3} &= \pi \left( \frac{2}{N+1} \right)^4 \\ &\cdot \sum_{k, m, k_1, k_2, k_3} \frac{n(\epsilon(k_2) + \epsilon(k_3) - \epsilon(k_1), T_\alpha, \mu_\alpha) - n(\epsilon(k), T_\alpha, \mu_\alpha)}{\epsilon(k_2) + \epsilon(k_3) - \epsilon(k_1) - \epsilon(k)} \\ &\cdot \sin \frac{\pi k l_\alpha}{N+1} \sin \frac{\pi k m}{N+1} \sin \frac{\pi k_1 m_1}{N+1} \sin \frac{\pi k_2 m_2}{N+1} \\ &\cdot \sin \frac{\pi k_3 m_3}{N+1} \sin \frac{\pi k_1 m}{N+1} \sin \frac{\pi k_2 m}{N+1} \sin \frac{\pi k_3 m}{N+1}. \end{aligned} \quad (5.8c)$$

Here  $n(\epsilon, T, \mu)$  is the average Bose-Einstein occupation number of a state with energy  $\epsilon$ , temperature  $T$  and chemical potential  $\mu$ .

Next, as summarized in Appendix D, the creation and annihilation operators  $a_l^\dagger$  and  $a_l$  become differential operators in the coherent representation, for example:

$$a_l^\dagger \rho \leftrightarrow \left( \xi_l^* - \frac{\partial}{\partial \xi_l} \right) P(\vec{\xi}). \quad (5.9)$$

## 5.2. The model and its effective equation of motion

---

Using the above approximation for the operators  $\hat{m}_\alpha$  and the transformation from creation/annihilation operators to differential operators, Eq.(5.2) becomes, in the coherent  $P$ -representation, a generalized Fokker-Planck equation,

$$\frac{\partial P}{\partial t} = \left( \mathcal{L}_{H_0} + U \mathcal{L}_V + \lambda^2 \mathcal{L}_B^{(0)} + \lambda^2 U \mathcal{L}_B^{(1)} \right) P. \quad (5.10)$$

where

$$\mathcal{L}_{H_0} = \sum_{l=1}^{N-1} \left[ i \frac{\partial}{\partial \xi_{l+1}} \xi_l + i \frac{\partial}{\partial \xi_l} \xi_{l+1} + c.c. \right], \quad (5.11a)$$

$$\mathcal{L}_V = \sum_{l=1}^N \left[ -i \frac{\partial^2}{\partial \xi_l^2} \frac{\xi_l^2}{2} + i \frac{\partial}{\partial \xi_l} (\xi_l^* \xi_l^2) + c.c. \right], \quad (5.11b)$$

$$\mathcal{L}_B^{(0)} = \sum_{\alpha, m} \left[ (D_{\alpha, m} - \bar{D}_{\alpha, m}) \frac{\partial}{\partial \xi_\alpha} \xi_m + \bar{D}_{\alpha, m} \frac{\partial^2}{\partial \xi_\alpha \partial \xi_m^*} + c.c. \right], \quad (5.11c)$$

$$\begin{aligned} \mathcal{L}_B^{(1)} = & \sum_{\alpha, m_i} D_{\alpha, m_1 m_2 m_3} \left[ \frac{\partial^2}{\partial \xi_\alpha \partial \xi_{m_2}^*} \xi_{m_1}^* \xi_{m_3} \right. \\ & + \frac{\partial^2}{\partial \xi_\alpha \partial \xi_{m_3}^*} \xi_{m_1}^* \xi_{m_2} - \frac{\partial^2}{\partial \xi_\alpha \partial \xi_{m_1}} \xi_{m_2} \xi_{m_3} + c.c. \end{aligned} \quad (5.11d)$$

$$\left. - \frac{\partial^3}{\partial \xi_\alpha^* \partial \xi_{m_2} \partial \xi_{m_3}} \xi_{m_1} + c.c. \right]. \quad (5.11e)$$

Here  $c.c.$  refers to the complex conjugate and it is performed formally, *e.g.*  $-i \frac{\partial}{\partial \xi_{l+1}^*} \xi_l^*$  is the  $c.c.$  of  $i \frac{\partial}{\partial \xi_{l+1}} \xi_l$ . The last term, Eq. (5.11e), of  $\mathcal{L}_B^{(1)}$  is separated from the other terms intentionally for reasons that will become apparent soon.

If only equilibrium states are of interest, then the first and second term can be discarded since equilibrium states commute with  $H_S$ . However, for non-equilibrium stationary states those terms are important. Setting  $\frac{\partial}{\partial t} P = 0$ , we get the stationary state  $P(\vec{\xi}, \infty)$ , which in the following is denoted simply as  $P(\vec{\xi})$ . Next, we will calculate the stationary of Eq. (5.10). We first discuss non-interacting systems and then turn to interacting ones.

### 5.3 Exact solution for non-interacting systems

For  $U = 0$  only the terms  $\mathcal{L}_{H_0}$  and  $\mathcal{L}_B^{(0)}$  contribute, and the stochastic equation is a Fokker-Plank equation [98], in terms of complex variables:

$$\frac{\partial}{\partial t} P = \sum_{i,j} \left[ -\frac{\partial}{\partial \xi_i} \Gamma_{ij} \xi_j + \frac{\partial^2}{\partial \xi_i \partial \xi_j^*} \mathcal{D}_{ij^*} + c.c. \right] P. \quad (5.12)$$

For our specific case of a non-interacting system we have:

$$\Gamma_{lm} = -i(\delta_{l,m-1} + \delta_{l,m+1}) - \sum_{\alpha,m} \lambda^2 \pi \delta_{l\alpha} \delta_{\alpha m}, \quad (5.13)$$

and

$$\mathcal{D}_{lm^*} = \frac{1}{2} \lambda^2 \sum_{\alpha} (\bar{D}_{\alpha,l} \delta_{m\alpha} + \bar{D}_{\alpha,m} \delta_{l\alpha}). \quad (5.14)$$

Note that we have verified that  $\mathcal{D}^\dagger = \mathcal{D}$ .

This is in fact a standard Fokker-Planck equation (FPE) for the Ornstein-Uhlenbeck process. Such a FPE can be solved analytically [70, 98]. Its stationary solution is found to be a Gaussian function:

$$P(\vec{\xi}) = \frac{1}{Z} e^{-\frac{1}{2} \xi^\dagger \sigma^{-1} \xi}, \quad (5.15)$$

where  $Z$  is a normalization constant and

$$\Gamma \sigma + \sigma \Gamma^\dagger + \mathcal{D} = 0, \quad (5.16)$$

which has the solution,

$$\sigma = - \sum_{l,m} \frac{1}{\kappa_l + \kappa_m^*} \langle \nu^l | \mathcal{D} | \nu^m \rangle |\mu_l\rangle \langle \mu_m|. \quad (5.17)$$

Here  $\kappa, |\mu\rangle, \langle \nu|$  are respectively the eigenvalues, right eigenvectors and left eigenvectors of  $\Gamma$  and  $\langle \mu|, |\nu\rangle$  are the complex conjugate of the two corresponding vectors. This expression is correct for both equilibrium and non-equilibrium states. The only difference is in the matrix  $D$ , in whether  $T_L$  is the same as, or is different from  $T_R$ . The only needed numerical task is to find an eigenvector decomposition of  $\Gamma$ , an  $N$ -dimensional matrix. Once  $\sigma$  is known, all correlation functions can be calculated, in particular the single-particle Green's function is  $G(l^\dagger, m) = \langle \xi_l^* \xi_m \rangle = 2\sigma_{lm}$ .

### 5.3. Exact solution for non-interacting systems

---

Next we work out explicitly the distribution function for a two-site ( $N = 2$ ) sample system to firstly confirm that it leads to the proper thermal equilibrium, and secondly to show the general procedure to find such a distribution function. It should be emphasized that the dimension of the space grows linearly with system size, so we chose to work with  $N = 2$  just because it is easier to get some intuitive picture, not because of algorithm complexity issues. In principle, for two-site systems we need to work with 4-dimensional matrices, but for non-interacting systems they reduce to 2-dimensional matrices. We have for this specific case,

$$\Gamma = \begin{bmatrix} -\lambda^2\pi & -i \\ -i & -\lambda^2\pi \end{bmatrix}, \mathcal{D} = \begin{bmatrix} \mathcal{D}_{11} & \mathcal{D}_{12} \\ \mathcal{D}_{12} & \mathcal{D}_{22} \end{bmatrix}, \quad (5.18)$$

where

$$\begin{aligned} \mathcal{D}_{11} &= \lambda^2\pi \frac{n(1, T_L, \mu_L) + n(-1, T_L, \mu_L)}{2}, \\ \mathcal{D}_{12} &= \lambda^2\pi \frac{n(1, T_L, \mu_L) - n(-1, T_L, \mu_L) + n(1, T_R, \mu_R) - n(-1, T_R, \mu_R)}{4}, \\ \mathcal{D}_{22} &= \lambda^2\pi \frac{n(1, T_R, \mu_R) + n(-1, T_R, \mu_R)}{2}. \end{aligned} \quad (5.19)$$

From this we get the stationary distribution,

$$\sigma = \frac{1}{4\lambda^2\pi} \begin{bmatrix} \mathcal{D}_{11} + \mathcal{D}_{22} & 2\mathcal{D}_{12} \\ 2\mathcal{D}_{12} & \mathcal{D}_{11} + \mathcal{D}_{22} \end{bmatrix} + \frac{\mathcal{D}_{11} - \mathcal{D}_{22}}{4(\lambda^4\pi^2 + 1)} \begin{bmatrix} \lambda^2\pi & -i \\ i & -\lambda^2\pi \end{bmatrix}. \quad (5.20)$$

For equilibrium states  $T_L = T_R = T$ ,  $\mu_L = \mu_R = \mu$  and therefore  $\mathcal{D}_{11} = \mathcal{D}_{22}$ , so that

$$P(\vec{\xi}) \propto e^{-\frac{1}{n(1, T, \mu)} \frac{\xi_1^* + \xi_2^*}{\sqrt{2}} \frac{\xi_1 + \xi_2}{\sqrt{2}} - \frac{1}{n(-1, T, \mu)} \frac{\xi_1^* - \xi_2^*}{\sqrt{2}} \frac{\xi_1 - \xi_2}{\sqrt{2}}}, \quad (5.21)$$

which is exactly the  $P$ -representation form of the Boltzmann distribution in terms of the eigenmodes  $\frac{a_1 \pm a_2}{\sqrt{2}}$  with eigenenergies  $\pm 1$ . Note that this is independent of the coupling constant  $\lambda$  since the second term in  $\sigma$  vanishes and the  $\lambda^2$  in the first term cancel out. This confirms that the equilibrium state of the central system does not depend on the details of the coupling between the system and the baths. However, this is unique for equilibrium states. A general NESS does depend on  $\lambda$ . In fact, the non-equilibrium part  $\mathcal{D}_{1,1} - \mathcal{D}_{2,2} \propto \lambda^2$ . In the following calculation, a relatively large  $\lambda$  is used in order to enhance this non-equilibrium part.

Next we compare correlations from the non-equilibrium distribution with correlations calculated with the BBGKY-like method discussed in the previous chapter [101]. Numerical exact solution for non-interacting systems have been reported in Refs. for the Redfield equation. For non-interacting systems, the BBGKY method can be solved exactly. Here we use it as a reference to check the analytical solution for non-interacting systems. We denote the single-particle correlation functions calculated from the above analytical solution of generalized Fokker-Planck equation, respectively from the numerical solution of the BBGKY-like method as  $G_1^{re,An}$  and  $G_1^{re,B}$ . Similar notations are used for particle currents  $J^{re,An}$  and  $J^{re,B}$ . We measure the difference between the two correlations, for example the analytical solution and the BBGKY solution, through,

$$d_B^{re,An} = \frac{\sqrt{\sum_{l,m} \left| G_1^{re,An}(l^\dagger, m) - G_1^{re,B}(l^\dagger, m) \right|^2}}{\sqrt{\sum_{l,m} \left| G_1^{re,B}(l^\dagger, m) \right|^2}}. \quad (5.22)$$

In Fig.5.1, we compare this analytical solution and the BBGKY-like numerical results for the Redfield equation. Since  $d^{re} \approx 0$ , the two methods are indeed equivalent. The inset shows that currents calculated from both methods also agree. This validates the fact that the generalized Fokker-Planck equation approach produces accurate results at least for non-interacting systems. In the same figure, we also plot  $d_B^{re,nu}$  and  $J^{re,nu}$ , which are obtained from a numerical solution that will be discussed in detail in section 5.4. There is a small but finite distance between the two correlation functions, however this has no contribution to the current, which is found to be in good agreement with the exact solution.

## 5.4 Interacting systems: BBGKY-like hierarchy derived from the generalized Fokker-Planck equation

For central systems with interactions, Eq.(5.10) is a generalized Fokker-Planck equation which has additional triple derivative terms added to the standard Fokker-Planck equation. It is still possible to solve directly this generalized Fokker-Planck equation via a set of equivalent stochastic difference equations, which are generalizations of the Langevin equation [98, 102]. We will discuss this technique in the next section §5.5. Before doing that,

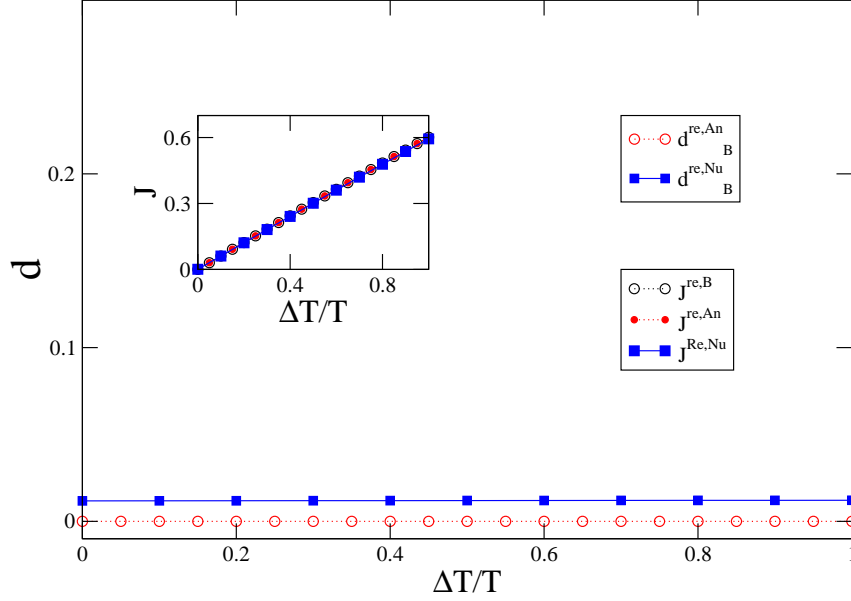


Figure 5.1: Analytical solution of the generalized Fokker-Planck equation is compared against the BBGKY numerical solution for non-interacting systems. The red (circles) curve in the main plot shows the comparison between the above analytical solution and the BBGKY-like numerical solution of the Redfield equation. Both Green's functions ( $d_B^{re,An}$ , main panel) and particle currents ( $J^{re,An}$  and  $J^{re,B}$ , inset) exactly agree with each other. The blue (square) curve is a comparison between a numerical simulation, to be discussed in §5.4, and the BBGKY solution. Here we find that the numerical simulation agrees with analytical solution quite well. Other parameters are  $\lambda = 0.5, T = 2.0, \mu = -2.0$ .

#### 5.4. Interacting systems: BBGKY-like hierarchy derived from the GFPE

we verify here that the same equation hierarchy as the one presented in the previous chapter can also be derived from this generalized Fokker-Planck equation. The derivation of the BBGKY equations for bosonic systems mirrors that of the previous chapter, and can be found in Appendix F.

We focus again only on the single-particle stationary state Green's functions  $G(l^\dagger; n)$ , defined as  $\langle \xi_l^* \xi_n \rangle = \int d\vec{\xi} \xi_l^* \xi_n P(\vec{\xi})$ . Let us then derive a set of equations for them from the generalized Fokker-Planck equation, Eq. (5.10). For example, consider a first-order derivative term in Eq. (5.11b). After performing a partial integration, we have,

$$\begin{aligned}
& \sum_m \int d\vec{\xi} \xi_l^* \xi_n i \frac{\partial}{\partial \xi_m} (\xi_m^* \xi_m^2 P(\vec{\xi}, \infty)) \\
&= -i \sum_m \int d\vec{\xi} P(\vec{\xi}, \infty) \xi_m^* \xi_m^2 \frac{\partial}{\partial \xi_m} (\xi_l^* \xi_n) \\
&= -i \int d\vec{\xi} P(\vec{\xi}, \infty) \xi_l^* \xi_n^* \xi_n^2 \\
&= -i \langle \xi_l^* \xi_n^* \xi_n^2 \rangle.
\end{aligned} \tag{5.23}$$

Therefore, setting  $\frac{\partial}{\partial t} \langle \xi_l^* \xi_n \rangle$  to zero, we have

$$0 = -i \langle \xi_l^* \xi_{n+1} \rangle - i \langle \xi_l^* \xi_{n-1} \rangle + i \langle \xi_{l+1}^* \xi_n \rangle + i \langle \xi_{l-1}^* \xi_n \rangle \tag{5.24a}$$

$$+ \lambda^2 \sum_{\alpha, m} (\bar{D}_{\alpha, m} - D_{\alpha, m}) [\delta_{n\alpha} \langle \xi_l^* \xi_m \rangle + \delta_{l\alpha} \langle \xi_m^* \xi_n \rangle] \tag{5.24b}$$

$$+ \lambda^2 \sum_{\alpha} (\bar{D}_{\alpha, n} \delta_{l\alpha} + \bar{D}_{\alpha, l} \delta_{n\alpha}) \tag{5.24c}$$

$$+ iU \langle \xi_l^* \xi_l^* \xi_l \xi_n \rangle - iU \langle \xi_l^* \xi_n^* \xi_n \xi_n \rangle \tag{5.24d}$$

$$\begin{aligned}
& + \lambda^2 U \sum_{\alpha, m_i} D_{\alpha, m_1 m_2 m_3} [\delta_{n\alpha} (\langle \xi_{m_1}^* \xi_{m_2} \rangle \delta_{l m_3} + \langle \xi_{m_1}^* \xi_{m_3} \rangle \delta_{l m_2}) \\
& + \delta_{l\alpha} (\langle \xi_{m_2}^* \xi_{m_1} \rangle \delta_{n m_3} + \langle \xi_{m_3}^* \xi_{m_1} \rangle \delta_{n m_2})].
\end{aligned} \tag{5.24e}$$

This is exactly the same with Eq. (4.7). This confirms that the BBGKY-like hierarchy method and the generalized Fokker-Planck equation in the coherent-state representation are equivalent, as expected. Next, we discuss how to solve numerically the generalized Fokker-Planck equation. Results from the BBGKY-like method will be used as a reference.

## 5.5 Approximate numerical solution for interacting systems

The generalized Fokker-Planck equation, Eq.(5.10), has triple derivative terms. The Pawula theorem [98] states that a distribution function with negative values will arise from a generalized Fokker-Planck equation with a finite series of derivatives beyond the second order. This does not, however, rule out the possibility that a generalized Fokker-Planck equation with an infinite series of derivatives may lead to a positively valued distribution function. Our Redfield equation is, in principle, such a generalized Fokker-Planck equation with infinite derivatives, if all terms in the expansion of the  $\hat{m}$  operators are kept. A truncation at a certain finite order might provide a more accurate result than a truncation at the second order, but the resulting distribution function will have negative values in some small regions. Ref. [98] presented such an example. Of course, new techniques are required to solve such generalized Fokker-Planck equation. Besides the example from Ref. [98], Ref. [102] proposed a set of equivalent stochastic difference equations for a generalized Fokker-Planck equation with triple derivative terms. The authors showed that a better distribution function than the one obtained after truncating at second derivatives, is given by their technique, which is based on a specific kind of stochastic difference equation [102]. However, this technique is still under development and discussion.

One may totally avoid such triple derivative terms by using generalized Gaussian phase-space method [72] or applying the phase-space method to the whole composite system [103]. Especially with the latter approach, one can simulate the dynamics of the whole system instead of that of the central system only. Of course, in this case, the baths will be treated as large but finite systems. Another benefit of this approach is that one could also go beyond Markov approximation.

On the other hand, one should also note the possibility that dropping such triple derivative terms may be appropriate in certain circumstances [104]. For example, in Eq. (5.24) — the first-order BBGKY equation derived above for two-variable (corresponding to single-particle) correlations, we see that these third-order terms are not in the equation explicitly. They appear only in equations of three-or-more-variable correlations, for example in the equation of four-variable correlations, which itself appears in the equation of two-variable correlation. Therefore such third order terms affect two-variable correlations, but indirectly via four-variable correlations. Following this line of logic we have assumed that odd-number-variable cor-

## 5.5. Approximate numerical solution for interacting systems

---

relations vanish.

Since the hierarchical cluster expansion method [101] generally relates higher order correlations to lower ones, if one truncates it at a certain order as we do here, one captures certain aspects of the interaction although not its whole effects. This is better than not taking the interaction in consideration at all. In this sense, neglecting the third order terms is equivalent to the first order of the cluster expansion, where the four-variable correlations are approximated by products of two-variable ones such that effects of the third order derivatives are neglected.

To summarize, in the rest of this chapter we will neglect all third order derivatives in the generalized Fokker-Planck equation, Eq.(5.10). The effects of their inclusion will be the topic of further investigations.

For our specific two-site interacting system, a classical simulation of the generalized Fokker-Planck equation without the third order derivatives can be casted into the following form,

$$\begin{aligned} \frac{\partial}{\partial t} P = \sum_{i,j} \left[ -\frac{\partial}{\partial \xi_i} \Gamma_{ij}^{(2)} \xi_j - \frac{\partial}{\partial \eta_i} \Gamma_{i^*j^*}^{(2)} \eta_j \right. \\ \left. + \frac{\partial^2}{\partial \xi_i \partial \xi_j} \mathcal{D}_{ij}^{(2)} + \frac{\partial^2}{\partial \eta_i \partial \eta_j} \mathcal{D}_{i^*j^*}^{(2)} \right. \end{aligned} \quad (5.25)$$

$$\left. + \frac{\partial^2}{\partial \xi_i \partial \eta_j} \mathcal{D}_{ij^*}^{(2)} + \frac{\partial^2}{\partial \eta_i \partial \xi_j} \mathcal{D}_{i^*j}^{(2)} \right] P, \quad (5.26)$$

where we have replaced  $\xi_i^*$  with  $\eta_i$  and treat them as independent variables. This treatment in fact means that we are now working in the positive-P representation [70, 73]. For non-interacting systems, the diffusion matrix  $\mathcal{D}$  is always positive definite so that we can work with the P representation. For interacting systems, however,  $\mathcal{D}$  is not positive definite therefore we have to use the more general representation. Here we use the the positive-P representation. We denote the coefficients as  $\Gamma_{ij}^{(2)}$ ,  $\Gamma_{i^*j^*}^{(2)}$  and  $\mathcal{D}_{ij}^{(2)}$ ,  $\mathcal{D}_{i^*j^*}^{(2)}$ ,  $\mathcal{D}_{ij^*}^{(2)}$ ,  $\mathcal{D}_{i^*j}^{(2)}$ . In principle, there could also be terms such as  $-\frac{\partial}{\partial \xi_i} \Gamma_{ij^*}^{(2)} \eta_j$ , but for this specific problem such terms do not appear. The explicit definitions of those coefficients are,

$$\Gamma_{ij}^{(2)} = \Gamma_{ij} + iU\xi_i\eta_i\delta_{ij}, \Gamma_{i^*j^*}^{(2)} = (\Gamma_{ij})^* - iU\xi_i\eta_i\delta_{ij}, \quad (5.27)$$

and

$$\mathcal{D}_{ij}^{(2)} = -i\frac{U}{2}\xi_i^2\delta_{ij} - \frac{\lambda^2 U}{2} \sum_{\alpha, m_1, m_2} (D_{\alpha, j, m_1, m_2} \delta_{\alpha, i} + D_{\alpha, i, m_1, m_2} \delta_{\alpha, j}) \xi_{m_1} \xi_{m_2}, \quad (5.28a)$$

### 5.5. Approximate numerical solution for interacting systems

---

$$\mathcal{D}_{i^*j^*}^{(2)} = i\frac{U}{2}\eta_i^2\delta_{ij} - \frac{\lambda^2 U}{2} \sum_{\alpha, m_1, m_2} (D_{\alpha, j, m_1, m_2}\delta_{\alpha, i} + D_{\alpha, i, m_1, m_2}\delta_{\alpha, j}) \eta_{m_1}\eta_{m_2}, \quad (5.28b)$$

$$\begin{aligned} \mathcal{D}_{ij^*}^{(2)} = \mathcal{D}_{j^*i}^{(2)} = \mathcal{D}_{ij^*} + \frac{\lambda^2 U}{2} \sum_{\alpha, m_1, m_2} [(D_{\alpha, m_1, j, m_2} + D_{\alpha, m_1, m_2, j})\delta_{\alpha, i} \\ + (D_{\alpha, m_2, i, m_1} + D_{\alpha, m_2, m_1, i})\delta_{\alpha, j}] \eta_{m_1}\xi_{m_2}. \end{aligned} \quad (5.28c)$$

Eq. (5.26) can be solved through the following Langevin equation [98] in positive-P representation [70, 72],

$$d\xi_i = \sum_j \Gamma_{ij}^{(2)} \xi_j dt + \sqrt{2} dw_i(t), \quad (5.29a)$$

$$d\eta_i = \sum_j \Gamma_{i^*j^*}^{(2)} \eta_j dt + \sqrt{2} d\bar{w}_i(t), \quad (5.29b)$$

where  $dw(t)$  and  $d\bar{w}(t)$  are stochastic processes satisfying,

$$\langle dw_i(t) dw_j(t') \rangle = \mathcal{D}_{ij}^{(2)} \delta_{tt'} dt, \quad (5.30a)$$

$$\langle dw_i(t) d\bar{w}_j(t') \rangle = \mathcal{D}_{ij^*}^{(2)} \delta_{tt'} dt, \quad (5.30b)$$

$$\langle d\bar{w}_i(t) dw_j(t') \rangle = \mathcal{D}_{i^*j}^{(2)} \delta_{tt'} dt, \quad (5.30c)$$

$$\langle d\bar{w}_i(t) d\bar{w}_j(t') \rangle = \mathcal{D}_{i^*j^*}^{(2)} \delta_{tt'} dt. \quad (5.30d)$$

We can define a  $2N$ -dimensional symmetric matrix  $D$ ,

$$D = \begin{bmatrix} \left( \mathcal{D}_{ij}^{(2)} \right)_{N \times N} & \left( \mathcal{D}_{ij^*}^{(2)} \right)_{N \times N} \\ \left( \mathcal{D}_{i^*j}^{(2)} \right)_{N \times N} & \left( \mathcal{D}_{i^*j^*}^{(2)} \right)_{N \times N} \end{bmatrix}. \quad (5.31)$$

Then these random variables can be simplified further and organized as a linear transformations of  $2N$  independent Wiener noises  $d\vec{w}$  [70],

$$d\vec{w} = B d\vec{\omega}, \quad (5.32)$$

where

$$D = BB^T. \quad (5.33)$$

This requires a diagonalization of the  $2N \times 2N$  matrix  $D$  at every time step, which is the most time consuming part. However, it is still much simpler

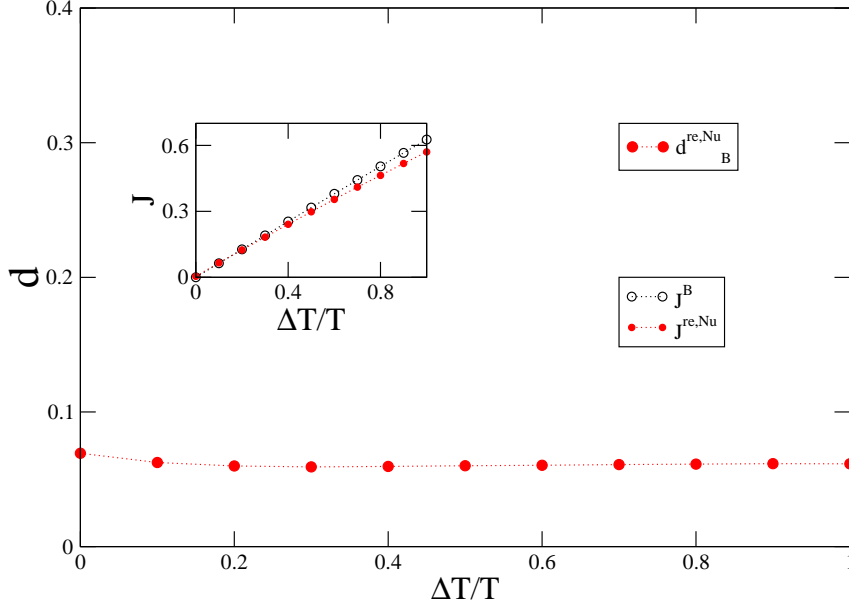


Figure 5.2: The numerical simulation of the generalized Fokker-Planck equation approach is compared against the BBGKY-like numerical solution of the Redfield equation, for interacting systems. The calculated current  $J^{re,Nu}$  is very close to  $J^{re,B}$  while  $d_B^{re,Nu}$  in the main panel is relatively large. Other parameters are set to be  $\lambda = 0.5, U = 0.1, T = 2.0, \mu = -2.0$ .

than solving directly the  $d^2$ -dimension linear system for the central system with a  $d$ -dimensional Hilbert space, since  $d$  increases exponentially with  $N$ .

We have seen in Fig.5.1 that the numerical simulation leads to accurate results for non-interacting systems, where analytical solutions are possible. Next, we compare this numerical simulation against the BBGKY-like method for interacting systems, in Fig.5.2. The currents  $J_{re,Nu}$  and  $J^{re,B}$  are in agreement with each other up to high temperature biases. However,  $d_B^{re,Nu}$  — the difference between the two Green's functions — is relatively large. This indicates that a reasonable result can be obtained using this numerical simulation, but there is space its improvement.

In the numerical simulation of the generalized Fokker-Planck equations we used the Euler method for the Itô form of the stochastic differential equation. The Euler method is not always stable, especially for large  $U$ . In fact, more stable and efficient methods such as the semi-implicit method for the Stratonovich form have been developed to solve Fokker-Planck equa-

tions [105]. Using such methods might improve stability and accuracy of the results. However, currently there is an additional technical difficulty in implementing such methods for the Redfield equation: matrices  $B$  are found numerically so it is hard to derive the corresponding Stratonovich form. The relatively large  $d_B^{re, Nu}$  could also be due to the truncation of the true generalized Fokker-Planck equation to the standard Fokker-Planck equation. This calls for new methods to solve the generalized Fokker-Planck equation.

## 5.6 Solving the local-operator Lindblad equation via the generalized Fokker-Planck equation method

Instead of the Redfield equation, some authors prefer to use the local-operator Lindblad equation in the study of transport [58, 59, 99]. In this section, we demonstrate how to find NESSs from the local-operator Lindblad equation using the coherent-state representation. The Redfield equation finds that the operators  $\hat{m}_\alpha$  for the sites coupled to baths typically involve more than just the operator at the coupling sites. The local-operator Lindblad equation, on the other hand, chooses  $\hat{m}_\alpha \propto \langle 1 + n(\omega_{k,\alpha}) \rangle a_\alpha$ , which results in the much simpler form of the coupling to baths:

$$\begin{aligned} \frac{\partial \rho(t)}{\partial t} = & -i[\mathcal{H}_S, \rho(t)] \\ & -\lambda^2 \pi \left\{ \langle 1 + n(\epsilon_1, T_L, \mu_L) \rangle \left[ a_1^\dagger, a_1 \rho(t) \right] + \langle n(\epsilon_1, T_L, \mu_L) \rangle \left[ a_1, a_1^\dagger \rho(t) \right] + h.c. \right. \\ & \left. + \langle 1 + n(\epsilon_N, T_R, \mu_R) \rangle \left[ a_N^\dagger, a_N \rho(t) \right] + \langle n(\epsilon_N, T_R, \mu_R) \rangle \left[ a_N, a_N^\dagger \rho(t) \right] + h.c. \right\}. \end{aligned} \quad (5.34)$$

In the case of this specific two-site systems, we have chosen that  $N = 2$  and  $\epsilon_{1,2} = 0$ . Note that we get Eq. (5.34) from the Redfield equation Eq. (5.2) by letting

$$\begin{aligned} D_{\alpha;m} &= \pi \delta_{\alpha m} [1 + n(\epsilon_\alpha, T_\alpha, \mu_\alpha)], \\ \bar{D}_{\alpha;m} &= \pi \delta_{\alpha m} n(\epsilon_\alpha, T_\alpha, \mu_\alpha), \\ D_{\alpha;m_1 m_2 m_3} &= 0. \end{aligned} \quad (5.35)$$

These relations greatly simplify the resulting generalized Fokker-Planck equation. Following the same procedure as for the Redfield equation, we

derive a similar Langevin equation for Eq. (5.34),

$$d\xi_n = \left[ -i(\xi_{n-1} + \xi_{n+1}) - iU\xi_n^2\eta_n - \lambda^2\pi \sum_{\alpha} (\delta_{\alpha n}\xi_{\alpha}) \right] dt + B_{1\nu}^{(n)} dw_{\nu}^{(n)}, \quad (5.36a)$$

$$d\eta_n = \left[ i(\eta_{n-1} + \eta_{n+1}) + iU\xi_n\eta_n^2 - \lambda^2\pi \sum_{\alpha} (\delta_{\alpha n}\eta_{\alpha}) \right] dt + B_{2\nu}^{(n)} dw_{\nu}^{(n)}, \quad (5.36b)$$

where the matrix  $B^{(n)} = (B_{\mu\nu}^{(n)})_{2 \times 2}$  satisfies,

$$B^{(n)} (B^{(n)})^T = \begin{bmatrix} -iU\xi_n^2 & 2\lambda^2\pi \sum_{\alpha} n(\epsilon_{\alpha}, T_{\alpha}, \mu_{\alpha}) \delta_{n\alpha} \\ 2\lambda^2\pi \sum_{\alpha} n(\epsilon_{\alpha}, T_{\alpha}, \mu_{\alpha}) \delta_{n\alpha} & iU\eta_n^2 \end{bmatrix}, \quad (5.37)$$

and  $\{dw_{\nu}^{(n)}\}$  is a set of  $2N$  independent Wiener noises. Note that similar equations have been used to describe pure isolated dynamics [75] or  $T = 0$  systems driven by the local-operator Lindblad equation [73], for interacting bosonic systems. The  $2N$ -dimensional matrices  $B$  are decoupled into  $N$  2-dimensional matrices  $B^{(n)}$ , which can be diagonalized analytically. Therefore, it is technically easier to solve the local-operator Lindblad equation than the Redfield equation and the Stratonovich form is readily supplied into the xmds software [105]. Results from this local-operator Lindblad equation have been plotted in Fig.5.3. For non-interacting systems, analytical expressions can be derived, and one finds that the NESSs from the local-operator Lindblad equation follows the general Gaussian distribution in Eq. (5.15) and that the correlation matrix  $\sigma^{lole}$  becomes,

$$\begin{aligned} \sigma^{lole} &= \frac{n(0, T_L, \mu_L) + n(0, T_R, \mu_R)}{4} \begin{bmatrix} 1 & 0 \\ 0 & 1 \end{bmatrix} \\ &+ \frac{\lambda^2\pi [n(0, T_L, \mu_L) - n(0, T_R, \mu_R)]}{4(\lambda^4\pi^2 + 1)} \begin{bmatrix} \lambda^2\pi & i \\ -i & -\lambda^2\pi \end{bmatrix}. \end{aligned} \quad (5.38)$$

In Fig.5.3, we have compared these analytical and numerical results against the BBGKY results. Results for both currents and Green's functions are found to be consistent for the two approaches. This confirms that our generalized Fokker-Planck equation method works for both the Redfield equation and the local-operator Lindblad equation.

## 5.7. Conclusions

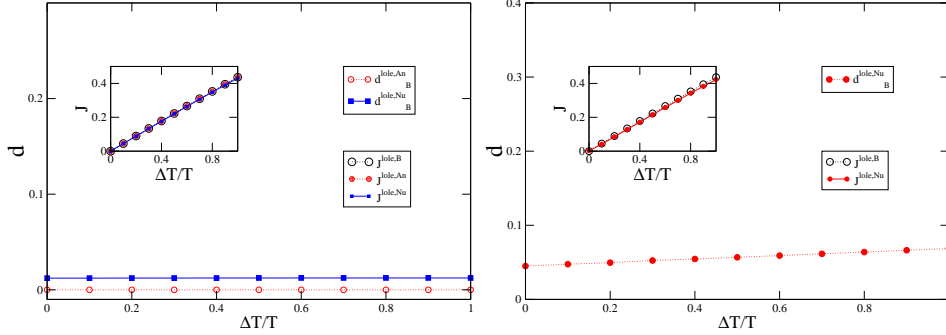


Figure 5.3: Results from the generalized Fokker-Planck equation approach are compared against the BBGKY solution of the local-operator Lindblad equation for non-interacting(a) and interacting systems(b). Results for both calculated currents and the Green’s functions are consistent.

## 5.7 Conclusions

To summarize, in this section we map the Redfield equation into a generalized Fokker-Planck equation, using the coherent-state representation. For non-interacting systems, the resulting generalized Fokker-Planck equation can be solved analytically and an expression of non-equilibrium stationary states is obtained. This avoids working with the quantum master equation in a space with an exponentially growing (fermions and spins) or infinite (bosons) dimension. For interacting systems, firstly this approach is found to be consistent with the BBGKY-like method. Secondly, a preliminary classical simulation via the Langevin equation with  $2N$  continuous complex numbers is discussed. It is found to work well for weakly interacting systems, although more work is needed. The advantage of this method, if it can be made to be accurate at stronger interactions, is that the total number of variables ( $2N$ ) grows linearly with the system size.

The same method is applied to solve the local-operator Lindblad equation. Here the method is even more efficient, since at every time step one needs to solve  $N$  2-dimensional eigenvalue problems instead of a  $2N$ -dimensional one, like for the Redfield equation. Results are found to be consistent with those from the BBGKY-like method.

Further development of the techniques for solving the generalized Fokker-Planck equation is required to make full use of the potential of this approach based on the coherent-state representation.

## Chapter 6

# Application: heat transport in spin chains

### 6.1 Introduction

The physical question addressed in this chapter is the validity of the phenomenological Fourier’s law of thermal transport. A system which obeys (disobeys) Fourier’s law is said to have normal (anomalous) transport, so this question is equivalent with identifying the conditions for normal transport. Even for classical systems this issue is not completely settled (see Ref. [76] for a review), although it was found that normal transport is closely related to the onset of chaos. For quantum systems a similar relation has also been proposed [106], where the quantum chaos is characterized by features of level spacing statistics [37, 107–113].

A widely believed conjecture is that anomalous heat transport occurs in systems described by integrable Hamiltonians (see Ref. [34] for a review). In this context, integrability is usually taken to mean the existence of a Bethe ansatz solution [114]. The validity of this conjecture is still not clear for heat transport in quantum spin chains, despite considerable effort [19, 35, 36, 42–44, 56, 59, 60, 82, 83, 106, 115]. Most of this work [35, 42–44, 60, 82, 115] studied infinite and/or periodic chains, and used the standard Kubo formula [6, 40] where finite/zero Drude weight signals anomalous/normal transport. For integrable systems, the standard Kubo formula always predicts anomalous heat transport. In fact, full integrability is not even necessary, all that is needed is commutation of the heat current operator with the total Hamiltonian [115]. However, in Chapter 3, we have shown that the validity of the standard Kubo formula is questionable in the study of thermal transport, and that one needs to consider explicitly a system connected to baths. We note that the “integrability” of the chain connected to baths may be lost even if the isolated chain is integrable, since the terms describing the coupling to the baths lead to a non-vanishing commutator between the heat current operator and the total Hamiltonian [116–118]. Both these facts

might invalidate the main argument for anomalous transport of integrable systems, based on the standard Kubo formula. For simplicity of terminology, here we call a system integrable if it is so when isolated, since the term is used in this sense in the above conjecture.

Studies which explicitly consider the effects of the baths, while fewer, also give contradictory results. Using the local-operator Lindblad equation, Prosen et al. showed that an integrable gaped ( $J_z > J_{xy}$ ) XXZ chain has normal spin conductivity while its energy transport is anomalous [59, 119], while using the same approach, Michel et al. claimed that when  $J_z > 1.6J_{xy}$ , spin chains have normal energy transport [56]. Particularly, a recent work in Ref. [119] shows that results from the local-operator Lindblad equation and from the standard Kubo formula are consistent. Such conflicting results exist not only in theoretical studies, but also in experiments. Anomalous heat transport observed experimentally in systems described by integrable models, such as  $(\text{Sr,Ca})_{14}\text{Cu}_{24}\text{O}_{41}$ ,  $\text{Sr}_2\text{CuO}_3$  and  $\text{CuGeO}_3$ , [79, 120, 121] seems to validate this conjecture, but Ref. [81] finds normal transport in  $\text{Sr}_2\text{CuO}_3$  at high temperatures.

Even if there was no conflict between results based on the local-operator Lindblad equation [56, 59], as discussed in Chapter 2 this approach is less reliable than the Redfield equation. For example, only the latter leads to the proper Boltzmann distribution if the baths are not biased. This is why here we investigate heat transport in finite spin chains coupled to thermal baths, using the Redfield equation. There are already several other such studies [36, 83]. However, these are for spin systems that are either non-interacting (thus trivially integrable), or are non-integrable. (We call a spin chain “non-interacting” if it can be mapped, for example through a Jordan-Wigner transformation, to a Hamiltonian for non-interacting spinless fermions). Anomalous transport is found for the former and normal transport is found for the latter. Disordered spin systems have also been found to have normal transport [37]. There are no examples of clean, interacting but integrable systems investigated via the Redfield equation.

We study such systems here. We find no direct relation between integrability and anomalous transport. Instead, based on our systematic investigations, we propose a new conjecture: anomalous conductivity is observed in systems that can be mapped to non-interacting fermions. Those that map to interacting fermion models, whether integrable or not, show normal transport. This is in qualitative agreement with the demonstration by Sirker et al. that diffusion is universally present in interacting 1D systems [42].

It is important to note that, chronologically, this was the first project undertaken once the formalism of the Redfield equation was adopted. This

explains why the results shown below are derived using (inefficient) direct methods to solve the Redfield equation, and therefore are restricted to rather small systems. This is also why our conjecture needs to be further examined, for larger systems. It was this computational inefficiency that drove the subsequent research on more efficient methods, presented in the previous chapters. In future, we plan to use these efficient methods to extend this study to larger systems.

The chapter is organized as follows. Section 6.2 defines the system and its Redfield equation. In Sections 6.3 we discuss the numerical methods and in Section 6.4 we define the thermal current and local temperatures. We then proceed to present numerical results in Section 6.5, and then conclude.

## 6.2 The model and its Redfield equation

We consider an  $N$ -site chain of spins- $\frac{1}{2}$  described by the Hamiltonian:

$$\mathcal{H}_S = \sum_{i=1}^{N-1} [J_x s_i^x s_{i+1}^x + J_y s_i^y s_{i+1}^y + J_z s_i^z s_{i+1}^z] - \vec{B} \cdot \sum_{i=1}^N \vec{s}_i \quad (6.1)$$

while the heat baths are collections of bosonic modes:

$$\mathcal{H}_B = \sum_{k,\alpha} \omega_{k,\alpha} b_{k,\alpha}^\dagger b_{k,\alpha} \quad (6.2)$$

where  $\alpha = R/L$  indexes the right/left-side baths. The system-baths coupling is taken as:

$$V = \lambda \sum_{k,\alpha} V_k^{(\alpha)} s_\alpha^y \otimes (b_{k,\alpha}^\dagger + b_{k,\alpha}) \quad (6.3)$$

where  $s_L^y = s_1^y$  and  $s_R^y = s_N^y$ , i.e. the left (right) thermal bath is only coupled to the first (last) spin and can induce its spin-flipping. This is because we choose  $\vec{B} \cdot \vec{e}_y = 0$  while  $|\vec{B}|$  is finite, meaning that spins primarily lie in the  $x0z$  plane so that  $s^y$  acts as a spin-flip operator.

From Eq. (2.29), the resulting Redfield equation for  $\rho(t)$  is:

$$\frac{\partial \rho(t)}{\partial t} = -i[H_S, \rho(t)] - \lambda^2 \sum_{\alpha=L,R} ([s_\alpha^y, \hat{m}_\alpha \rho(t)] + h.c.) \quad (6.4)$$

where  $\hat{m}_\alpha = s_\alpha^y \cdot \Sigma_\alpha$ . Here,  $(\cdot)$  refers to the element-wise product of two matrices,  $\langle n|a \cdot b|m \rangle = \langle n|a|m \rangle \langle n|b|m \rangle$ . The bath matrices  $\Sigma_{L,R}$  are defined

in terms of the eigenstates of the system's Hamiltonian  $H_S|n\rangle = E_n|n\rangle$  as:

$$\begin{aligned} \Sigma_\alpha = \pi \sum_{m,n} |m\rangle\langle n| & \left[ \Theta(\Omega_{mn}) n_\alpha(\Omega_{mn}) D_\alpha(\Omega_{mn}) |V_{k_{mn}}^{(\alpha)}|^2 \right. \\ & \left. + \Theta(\Omega_{nm}) (1 + n_\alpha(\Omega_{nm})) D_\alpha(\Omega_{nm}) |V_{k_{nm}}^{(\alpha)}|^2 \right] \end{aligned}$$

where  $\Omega_{mn} = E_m - E_n = -\Omega_{nm}$  and  $k_{mn}$  is defined by  $\omega_{k_{mn},\alpha} = \Omega_{mn}$ , *i.e.* a bath mode resonant with this transition. Furthermore,  $\Theta(x)$  is the Heaviside function,  $n_\alpha(\Omega) = [e^{\beta_\alpha \Omega} - 1]^{-1}$  is the Bose-Einstein equilibrium distribution for the bosonic modes of energy  $\Omega$  at the bath temperature  $T_\alpha = 1/\beta_\alpha$ , and  $D_\alpha(\Omega)$  is the bath's density of states. The product  $D_\alpha(\Omega_{mn}) |V_{k_{mn}}^{(\alpha)}|^2$  is the bath's spectral density function. For simplicity, we take it to be a constant independent of  $\alpha$ ,  $m$  and  $n$ .

### 6.3 Numerical methods

It is straightforward to use the Runge-Kutta method to integrate the Redfield equation, Eq. (6.4), starting from some initial states. The memory cost is proportional to  $2^{2N}$  for an  $N$ -spin chain, but it takes a very long time for the integration to converge to the stationary state. This is not surprising since, in principle, the stationary state is reached only as  $t \rightarrow \infty$ .

As already discussed, another approach [58] is to solve directly for the stationary state from:

$$L\rho(\infty) = 0, \tag{6.5}$$

*i.e.* to find the eigenstate for the zero eigenvalue of the  $2^N$ -dimensional matrix  $L$ . However, in this case, the memory cost is proportional to  $4^{2N}$ , which is much worse than for the Runge-Kutta method.

The method which has better memory efficiency than this eigenvalue problem and also better time efficiency than the Runge-Kutta method, is to convert the equation into a linear system and solve it via matrix-free methods like the Krylov space methods, which requires only matrix-vector multiplication but not explicitly the matrix. The eigenvalue problem can be rewritten as a linear system of equations after explicitly using the normalization condition  $tr(\rho) = 1$  such that

$$\bar{L}\rho(\infty) = \nu, \tag{6.6}$$

where  $\nu = [1, 0, \dots]^T$  and  $\bar{L}$  is found from  $L$  by replacing the first row by  $tr(\rho)$ . Then we use for example the generalized minimal residual method

(GMRES) [122], which requires only the matrix-vector multiplication rule. This new way of solving the Redfield equation has memory cost of  $\sim 2^{2N}$  and time efficiency of a linear system with dimension  $2^{2N}$ . It is still a direct method so its efficiency is not comparable with methods such as the BBGKY-like approach and the coherent-state representation method that we discussed previously, however, unlike them it gives an exact result. This is important until one can understand whether the further approximations made in the more efficient methods can, for example, destroy the integrability of the system. Also, because the commutation relations between spin operators are quite different from those of fermions and bosons, the more efficient methods are not readily generalizable. Developing and applying them to this problem will be the topic of future work.

## 6.4 Definitions of the thermal current and local temperatures

We rewrite  $H_S = \sum_{i=1}^{N-1} h_{i,i+1} + \sum_{i=1}^N h_i$ , where  $h_{i,i+1}$  is the exchange between nearest-neighbor spins and  $h_i$  is the on-site coupling to the magnetic field. We can then define a local site Hamiltonian

$$h_i^{(S)} = \frac{1}{2}h_{i-1,i} + h_i + \frac{1}{2}h_{i,i+1} \quad (6.7)$$

with  $h_{0,1} = h_{N,N+1} = 0$ , and a local bond Hamiltonian

$$h_i^{(B)} = \frac{1}{2}h_i + h_{i,i+1} + \frac{1}{2}h_{i+1} \quad (6.8)$$

such that

$$H_S = \sum_{i=1}^N h_i^{(S)} = \sum_{i=1}^{N-1} h_i^{(B)}. \quad (6.9)$$

The local bond Hamiltonians can be used to derive the heat current operator from the continuity equation

$$\hat{j}_{i \rightarrow i+1} - \hat{j}_{i-1 \rightarrow i} = \nabla \hat{j} = -\frac{\partial h_i^{(B)}}{\partial t} = -i \left[ H_S, h_i^{(B)} \right]. \quad (6.10)$$

This results in

$$\hat{j}_{i \rightarrow i+1} = i \left[ h_i^{(B)}, h_{i+1}^{(B)} \right] \quad (6.11)$$

#### 6.4. Definitions of the thermal current and local temperatures

---

for  $i = 1, \dots, N - 2$ . As expected, in the steady state we find  $\langle \hat{j}_{i \rightarrow i+1} \rangle = \text{tr} \left( \hat{j}_{i \rightarrow i+1} \rho(\infty) \right) = J$  to be independent of  $i$ . Similarly, we define the spin polarization  $\langle s_i^z \rangle$  and the spin current for XXZ model,

$$J_s = J_{xy} \langle s_i^y s_{i+1}^x - s_i^x s_{i+1}^y \rangle. \quad (6.12)$$

Knowledge of the steady state heat current  $J$ , as such, is not enough to decide whether the transport is normal or not. Consider an analogy with charge transport in a metal connected to two biased leads. What shows whether the transport is anomalous or not is the profile of the electric potential, not the value of the electric current. In anomalous transport (for clean, non-interacting metals) all the voltage drop occurs at the ends of the sample, near the contacts. Away from these contact regions, electrons move ballistically and the electric potential is constant, implying zero intrinsic resistance. For a dirty metal, scattering takes place everywhere inside the sample and the electric potential decreases monotonically in between the contact regions, *i.e.* the sample has finite intrinsic resistivity.

In principle, the scaling of the current with the sample size, for a fixed effective bias, also reveals the type of transport: for anomalous transport, the current is independent of the sample size once its length exceeds the sum of the two contact regions, while for normal transport it decreases like inverse length. The problem with this approach is that one needs to keep constant the effective bias, *i.e.* the difference between the applied bias and that in the contact regions. Furthermore, since we can only study relatively short chains, the results of such scaling may be questionable.

It is therefore desirable to use the equivalent of the electric potential for heat transport and to calculate its profile along the chain, in order to determine the type of transport. This, of course, is the “local temperature”, which is a difficult quantity to define properly. One consistency condition for any definition is that if  $T_L = T_R = T$ , *i.e.* the system is in thermal equilibrium at  $T$ , then all local temperatures should equal  $T$ . We define local site temperatures  $T_i$  which fulfill this condition in the following way. Since we know all eigenstates of  $\mathcal{H}_S$ , it is straightforward to calculate its equilibrium density matrix at a given  $T$ ,  $\rho_{eq}(T) = \frac{1}{Z} \sum_n e^{-\beta E_n} |n\rangle\langle n|$ , where  $Z = \sum_n e^{-\beta E_n}$ . Let then  $\langle h_i^{(S)} \rangle_{eq}(T) = \text{tr}[\rho_{eq}(T) h_i^{(S)}]$ . We define  $T_i$  to be the solution of the equation:

$$\langle h_i^{(S)} \rangle_{eq}(T_i) = \text{tr}[\rho(\infty) h_i^{(S)}]. \quad (6.13)$$

In other words, the steady-state value of the energy at that site equals the energy the site would have if the whole system was in equilibrium at  $T_i$ .

Of course, we can also use other “local” operators such as  $h_i^{(B)}$  to calculate a local bond temperature  $T_{i+\frac{1}{2}}$ . We find that when these definitions are meaningful, the results are in very good agreement no matter what “local” operator is used.

This type of definition of  $T_i$  is meaningful only if a large magnetic field  $B$  is applied. For small  $B$ , the expectation values  $\langle h_i^{(S)} \rangle_{eq}(T)$  are very weakly  $T$ -dependent, so that tiny numerical errors in the steady-state value can lead to huge variations in  $T_i$ . Addition of a large  $B$  is needed to obtain  $\langle h_i^{(S)} \rangle_{eq}(T)$  which varies fast enough with  $T$  for values of interest, so that a meaningful  $T_i$  can be extracted. Since we could not find a meaningful definition for  $T_i$  when  $|\vec{B}| \rightarrow 0$ , we cannot investigate such cases. Note, however, that most integrable models remain integrable under addition of an external field  $\vec{B} = B\hat{e}_z$ .

## 6.5 Results

In all our calculations, we take  $B_z = 1$  and the exchange  $J \sim 0.1$ . Temperatures  $T_{L/R} = T(1 \pm \delta/2)$  should not be so large that the steady state is insensitive to the model, or so small that only the ground-state is activated. Reasonable choices lie between  $\min(J_x, J_y, J_z)$  and  $NB$ , which are roughly the smallest, respectively the largest energy scales for the  $N$ -site spin chain.

In Fig. 6.1 we show typical results for (a) local temperature profiles  $T_i, T_{i+\frac{1}{2}}$  and (b) local spin polarization profiles  $S_i^z$ . We apply a large bias  $\delta = (T_L - T_R)/T = 0.4$  for clarity, but we find similar results for smaller  $\delta$ . For these values, it seems that the “contact regions” include only the end spins. The profile of the central part of the chain is consistent with anomalous transport (flat profile) for the  $XX$  chain ( $J_x = J_y, J_z = 0$ ) and shows normal transport (roughly linear profile) in all the other cases.  $XY$  chains with  $J_x \neq J_y$  behave similarly with the  $XX$  chain. We find similar results for ferromagnetic couplings. We also find that the ratio between the effective temperature difference,  $T_2 - T_{N-1}$ , and the applied temperature difference  $T_L - T_R$ , is not a constant for different system sizes  $N$ . Therefore, in our numerical calculation, it is not possible to keep the effective temperature difference as a constant by applying the same temperature difference on the ends while changing the system size  $N$ . This implies that the dependence of  $J$  v.s.  $N$  can not be used as an indicator of normal or anomalous transport. At most, it can provide a very rough qualitative picture. We have plotted several of the  $J$  vs.  $N$  in Fig.6.2. We see that  $J$  is independent of  $N$  for  $XX$

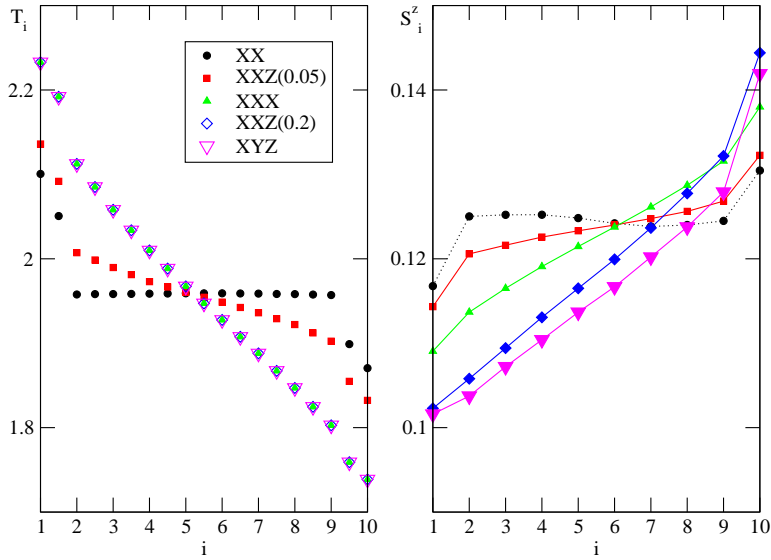


Figure 6.1: Plot of (a) local temperature profile and (b) local spin polarization profile for chains with  $N = 10$ . In all cases  $T_L = 2.4, T_R = 1.6, \lambda = 0.1, J_x = 0.1, B_z = 1.0$ . Other parameters are  $J_y = 0.1, J_z = 0.0$  (XX);  $J_y = 0.1, J_z = 0.05$  (XXZ0.05);  $J_y = J_z = 0.1$  (XXX);  $J_y = 0.1, J_z = 0.2$  (XXZ0.2) and  $J_y = 0.2, J_z = 0.3$  (XYZ). Only the  $XX$  chain shows flat  $T_i$  and  $S_i^z$  profiles. All other models have almost linearly decreasing profiles of both temperature and  $S^z$ .

## 6.5. Results

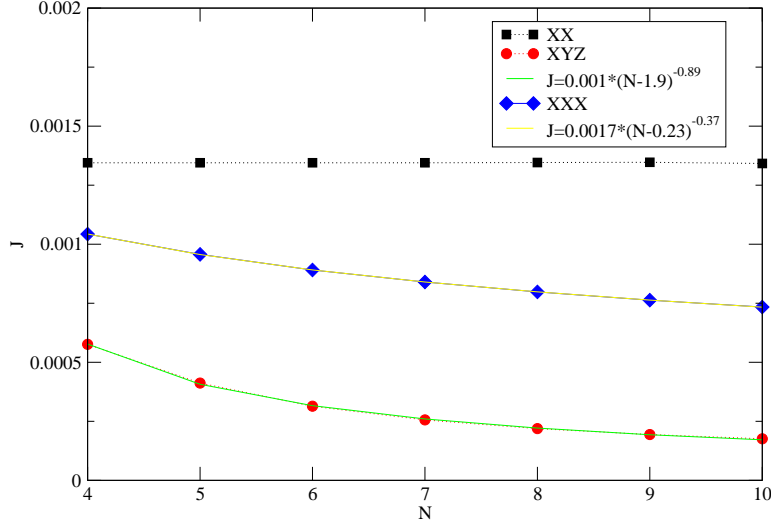


Figure 6.2: Heat currents are plotted as a function of system size for three models:  $XX$ ,  $XYZ$  and  $XXX$ .  $J$  is independent of  $N$  for  $XX$  chains, and it decreases with  $N$  for the other two cases. Due to the uncertainty about the effective applied temperature difference, the fitting curves should only be regarded as a guide for eyes. The same parameters as those in Fig.6.1 are used.

chains while it decreases with increasing  $N$  for  $XYZ$  and  $XXX$  chains.

Another way to examine size-dependence is to compare the temperature and  $S^z$  profiles for all available sizes. We normalize all the profiles for various models with different sizes by harvesting only the data in the central regions and converting them into dimensionless values in  $[0, 1]$ , for example, from  $(i, T_i)$  to  $(\frac{i-2}{N-3}, \frac{T_i - T_{N-1}}{T_2 - T_{N-1}})$ ,  $i = 2, 3, \dots, N - 1$ . In Fig.6.3, we plot such normalized temperature and  $S^z$  profiles. We see that curves for all values of  $N$  collapse onto one single straight line and furthermore, there is no difference between  $XYZ$  and  $XXX$  chains. Currently we can only study small systems, but from these normalized profiles, no qualitative difference has been found for different sizes.

All these are integrable models. The  $XX$  model is special because it can be mapped to non-interacting spinless fermions with the Jordan-Wigner transformation [84]. A finite  $J_z$  leads to nearest-neighbor interactions between fermions. Eigenmodes for models with  $J_z \neq 0$  can be found using Bethe's ansatz, but they cannot be mapped to non-interacting fermions.

In order to investigate where this transition between anomalous and

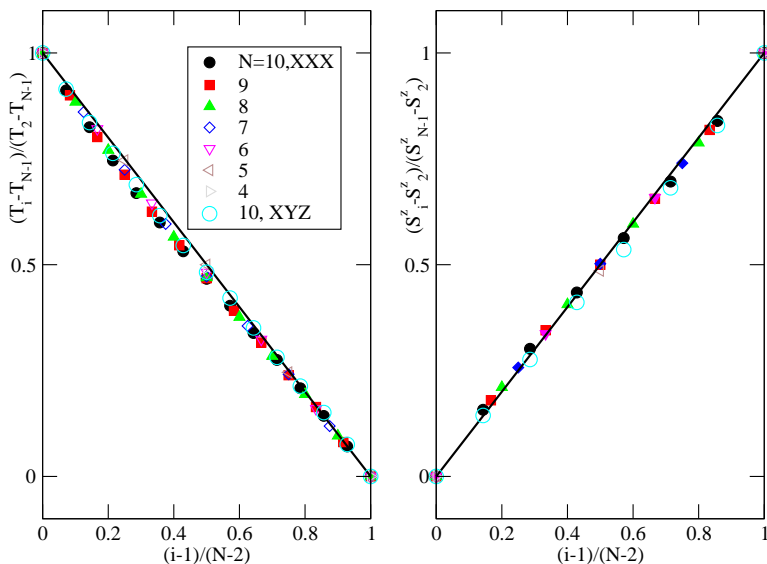


Figure 6.3: Normalized temperature and  $S^z$  profiles are plotted. Curves for different values of  $N$  collapse onto a single straight line and we see no difference between  $XYZ$  and  $XXX$  chains.

normal transport occurs, we plot temperature profiles for systems with small  $J_z$  in Fig.6.4(a).

We see that even for very small  $J_z$  the above observation still holds. For  $J_z = 0.01$  there is a slight qualitative difference, namely that the contact regions seem larger than just the end spins, as can be seen from the normalized profiles. We think this may be due merely to limitations of the numerical accuracy. In Fig.6.4(b), we investigate what is the minimum value of  $B_z$  that we can use with confidence. As we pointed out before, our definition of local temperature and also the idea of local a spin polarization  $S_i^z$  are only meaningful for sufficiently large  $B_z$ . We find that roughly this implies  $B_z > 0.3$ . This is reasonable, since for this limiting value the energy scale due to coupling to the local  $B_z$  field ( $0.3/2$ ) is comparable with the energy related to exchange ( $3 \times 0.1/4$ ).

We found this generic behavior for a wide range of parameters. When  $\lambda \in [0.03, 0.2]$ ,  $T \in [0.3, 30.0]$  and  $\delta \geq 0.01$ , the spin chain has normal conductivity when  $J_z \in [0.02, 0.5]$  and anomalous conductivity when  $J_z = 0$ . These results lead us to conjecture that it is the presence or absence of interactions, rather than integrability, that determines whether or not the heat transport is normal. We find no difference between thermal transport

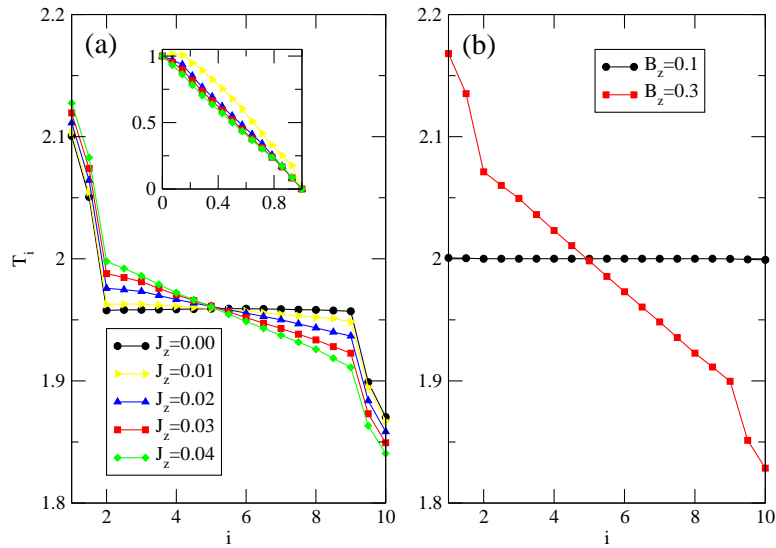


Figure 6.4: (a) Temperature profiles for small  $J_z$  values are plotted. Here  $J_x = J_y = 0.1$ ,  $B_z = 1.0$ . The effective temperature drop becomes smaller for smaller  $J_z$ , but the slope is still finite if  $J_z \geq 0.02$ . The inset plots normalized profiles, and shows no obvious differences for models with  $J_z \geq 0.02$ . The case of  $J_z = 0.01$  shows a finite slope but the normalized profile indicates a slight difference: the contact regions seem to be more extended than in the other cases. (b) Temperature profiles of  $XXX$  chains with  $J = 0.1$  and small values of  $B_z$ . A linear temperature drop is observed for  $B_z = 0.3$ , but a flat profile for  $B_z = 0.1$ . Other parameters are the same as in Fig.6.1.

## 6.5. Results

---

and spin transport, unlike the results of Prosen et al. [59], based on the local-operator Lindblad equation.

The conjecture may be tested further on various systems. One candidate is the Ising model in a transverse field  $B_x$ . It maps to non-interacting spinless fermions [123] and if we add a  $B_z$  field, it becomes interacting. Another closely related model is a system of spinless fermions on a tight-binding chain, with the nearest-neighbor interaction:

$$H_S = \epsilon \sum_{l=1}^N c_l^\dagger c_l - t \sum_{l=1}^{N-1} \left( c_l^\dagger c_{l+1} + c_{l+1}^\dagger c_l \right) + V_0 \sum_{l=1}^{N-1} c_{l+1}^\dagger c_{l+1} c_l^\dagger c_l, \quad (6.14)$$

$$H_B = \sum_{k,\alpha=L,R} \omega_{k,\alpha} b_{k,\alpha}^\dagger b_{k,\alpha}, \quad (6.15)$$

$$V_{SB} = \lambda \sum_{k,\alpha} \left( c_\alpha^\dagger b_{k,\alpha} + c_\alpha b_{k,\alpha}^\dagger \right). \quad (6.16)$$

The XXZ chains map exactly into this  $H_S$  model, after using the Jordan-Wigner transformation. However, the coupling to the baths in this fermionic system is different from that in the spin systems. For a spin system, the Jordan-Wigner transformation maps the  $\sigma^y$  operator into an operator much more complicated than the  $c^\dagger$  or  $c$  used in this fermionic model. Therefore, although the two models are closely related, they are not identical. Results on this model can be interpreted as another test of our conjecture or at least a check of whether the observations reported above are influenced by the specific model for the system-bath coupling.

In Fig.6.5, we plot local temperature profiles along the Ising spin chains in panel (a) and for fermionic chains in panel (b). The results support our conjecture: interactions lead to normal transport. Note that  $\epsilon$  is set to be much larger than  $t$ , to mirror the condition  $B_z \gg J$ . When  $\epsilon$  is comparable to  $t$ , both non-interacting and interacting systems show almost flat temperature profiles.

In summary, the first conclusion we draw from these results is that integrability is not sufficient to guarantee anomalous transport: several integrable models show normal heat transport, in agreement with other studies [42, 58, 59]. The second conclusion is that only models that map onto Hamiltonians of non-interacting fermions exhibit anomalous heat transport. This is a reasonable sufficient condition, since once inside the sample (past the contact regions) such fermions propagate ballistically. However, we cannot, at this stage, demonstrate that this is a necessary condition as well. We therefore can only conjecture that this is the criterion determining whether

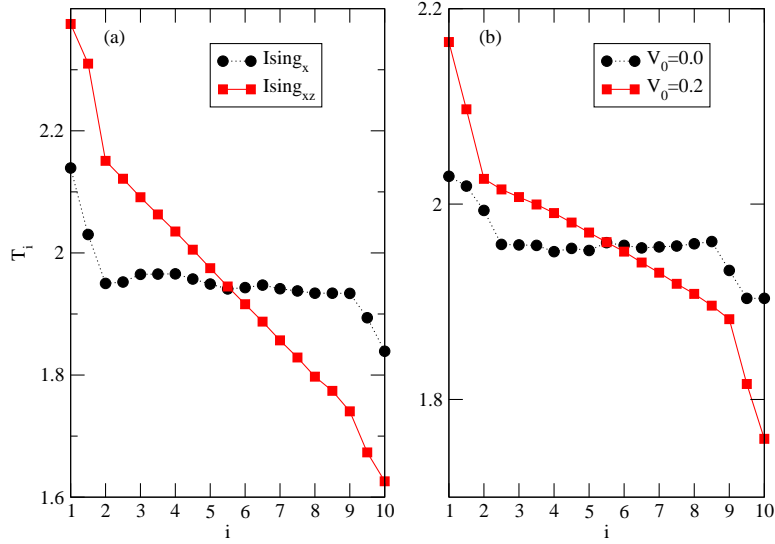


Figure 6.5: Temperature profiles of (a) Ising spin chains and (b) the  $V-t$  model of fermionic chains. The Ising spin chains have anomalous transport when  $B_z = 0$  ( $Ising_x$ , circles) and normal transport when  $B_z = 1.0$  ( $Ising_{xz}$ , squares). The fermionic chains show a flat temperature profile when  $V_0 = 0$  (circles) but a linear temperature drop when  $V_0 = 0.2$  (squares). Other parameters are  $J_z = 0.1$ ,  $B_x = 1.0$ ,  $\epsilon = 1.0$ ,  $t = 0.1$ ,  $T_L = 2.4$ ,  $T_R = 1.6$ ,  $\mu = -1.0$ ,  $\lambda = 0.1$ ,  $N = 10$ .

the heat transport is anomalous. If we believe that our results are not artifacts due to mainly the boundary effects of the limited system sizes, then this conjecture is the only consistent qualitative conclusion that we may draw from all above results.

In this context, it is important to emphasize again the essential role played by the connection to the baths. In its absence, an isolated integrable model is described by Bethe ansatz type wavefunctions. Diffusion is impossible since the conservation of momentum and energy guarantees that, upon scattering, pairs of fermions either keep or interchange their momenta. For a system connected to baths, however, fermions are continuously exchanged with the baths, and the survival of a Bethe ansatz type of wavefunction becomes impossible. In fact, even the total momentum is no longer a good quantum number. We believe that this explains why normal transport in systems mapping to interacting fermions is plausible.

Normal transport is also possible for non-interacting fermions, if they are subject to elastic scattering on disorder. This can be realized, for example, by adding to the  $XY$  model a random field  $B_z$  at various sites. In that case, as expected, normal conductance has been found in disordered systems [37].

On the other hand, anomalous transport can also occur in models which map to homogeneous interacting fermions if the bath temperatures are very low. Specifically, consider the  $XXZ$  models. Because of the large  $B_z$  we use, the ground-state of the isolated chain is ferromagnetic with all spins up. The first manifold of low-energy eigenstates have one spin flipped (single magnon states), followed by states with two spins flipped (two magnon states), etc. The separation between these manifolds is roughly  $B_z$ , although because of the exchange terms each manifold has a fairly considerable spread in energies and usually overlaps partially with other manifolds.

If both  $T_L, T_R \ll B_z$ , only single-magnon states participate in the transport. We can then study numerically very long chains by assuming that the steady-state matrix elements  $\rho_{nm}$  vanish for all other eigenstates ( $S_{z,tot}$  is a good quantum number for these models). In this case we find anomalous transport for all models, whether integrable or not. This is reasonable, since the lone magnon (fermion) injected on the chain has nothing else to interact with, so it must propagate ballistically.

We can repeat this restricted calculation by including the two-magnon, three-magnon, etc. manifolds in the computation. As expected, the results agree at low  $T_L, T_R$ , but differences appear for higher  $T_L, T_R$ , when these higher-energy manifolds become thermally activated. In such cases, the transport becomes normal for the models mapping to interacting fermions as soon as the probability to be in the two (or more) magnon sector be-

comes finite. In other words, as soon as multiple excitations (fermions) are simultaneously on the chain, and inelastic scattering between them becomes possible. These results may explain the heat transport observed experimentally in compounds such as  $\text{Sr}_2\text{CuO}_3$  [81], where at low temperature anomalous transport was found while at high temperature normal transport was reported.

## 6.6 Conclusions

Based on an extensive study of quantum spin chains using the Redfield equation, we propose a new conjecture for what determines the appearance of anomalous heat transport at all temperatures in spin chains. Unlike previous suggestions linking it to the integrability of the Hamiltonian or the existence of energy gaps, we propose that, for clean systems, the criterion is the mapping of the Hamiltonian onto a model of non-interacting fermions. Our results showing normal energy and spin transport in systems with finite  $J_z$  contradict the major conclusions of Ref. [56] and Ref. [59], which, however, are based on the less trustworthy local-operator Lindblad equation.

This conjecture should be checked for larger systems, where more reliable information on the relation between  $J$  and  $N$  can be extracted. The more efficient methods presented in the previous two chapters might allow us to undertake such a study. For discussion of the thermal conductance, which is related to higher order Green's functions —  $G_2$  and  $G_3$ , not only  $G_1$  — extension of the methods to higher orders may be needed.

## Chapter 7

# Conclusions and discussions

We began this project with a study of the thermal transport of spin chains in the framework of theories of open quantum systems. At that time, similar questions had been investigated using either the standard Kubo formula, the non-equilibrium Green's functions method or the local-operator Lindblad equation. However, the idea of using the Redfield equation for these questions had just been proposed and it had been applied only to non-interacting systems or very small interacting but non-integrable systems. We first developed and applied the direct methods to the Redfield equation for spin systems. From the preliminary results for short chains we found a new conjecture, linking anomalous transport to existence of mapping onto non-interacting fermions. This is the main result of Chapter 6.

It then became necessary to study larger interacting systems to either confirm or reject this observation. However, at the time there were no available methods capable of solving the Redfield equation for large interacting systems. Thus, we turned to investigate such methods. We first tried to make direct use of the standard Kubo formula. However, we found that the standard Kubo formula is not applicable to open systems explicitly coupled to baths and instead we had to derive a similar Kubo formula from the Redfield equation using linear response theory. We call the result the open Kubo formula. This is the content of Chapter 3. Several forms of such OKFs were proposed and tested. The proper approach was shown to not suffer from singularities, like the the standard Kubo formula, however it is not very efficient. A more efficient OKF was also identified, however only for certain types of quantities. Neither approach is efficient enough to allow the study of systems of the same size as permitted by the non-equilibrium Green's functions method.

Next, inspired by the non-equilibrium Green's function method[13–15] and also by Saito's work on non-interacting systems[36], we focused on Green's functions instead of the reduced density matrices and developed the BBGKY-like hierarchical method presented in Chapter 4. Further approximations are needed to truncate this hierarchy, if there are interactions. We identified two possible approaches. The first replaces, at a certain level of

the hierarchy, all higher-order Green's functions by their equilibrium values. This method is computationally less efficient but accurate up to large values of the interaction. The second method uses a cluster expansion, basically factorizing the higher-order Green's functions in terms of lower-order ones. This approach is applicable to much larger systems. While the simplest version (truncation at first level of the hierarchy) is accurate only for rather small interactions, we showed that systematic increase of the truncation level leads to both a systematic improvement of its accuracy, and a larger range of interactions where this holds. Also, truncation at second level generates correlated two-particle Green's functions, beyond the Hartree-Fock approximation.

In Chapter 5 we proposed another method: solving the Redfield equation in the coherent-state representation. The resulting differential equation has the form of the generalized Fokker-Planck equation, so we call this method the generalized Fokker-Planck equation method. Similar methods have been applied to pure dynamical evolution or equilibrium states, where studies of large interacting systems with roughly  $10^{5000000}$ -dimensional Hilbert spaces have been performed[72–74]. We extend the method to apply it to the Redfield equation and study also non-equilibrium stationary states. We have confirmed that for non-interacting systems exact results can be found analytically with this new approach, even for non-equilibrium stationary states. Other advantages are that, from a numerical point of view, in this approach interacting systems are handled similarly like non-interacting systems. Also, Green's functions of all orders can be calculated all at once. The challenge, still not fully settled, is to find efficient and stable ways to solve these differential equations. We showed some preliminary results, based on classical simulations, that are promising yet require more work.

The next step will naturally be to apply these methods to the studies of transport properties of various systems, this time for large systems. The question of validity of Fourier's Law is not yet answered definitely. The second-order form of the BBGKY-like method seems to have a good potential there. However, the study of spin systems requires different kinds of BBGKY-like equations, and also to understand whether the cluster approximation interferes with the integrability of a model. Therefore, although the methods we proposed are in principle applicable to this problem, specific forms of hierarchical equations need to be re-derived. Future possible projects, thus, are to develop the BBGKY-like method for spin systems, or to use the current BBGKY-like method to discuss thermal transport of bosonic or fermionic systems, instead of spin systems. Alternatively, we can also use the generalized Fokker-Planck equation method. Currently the simulation

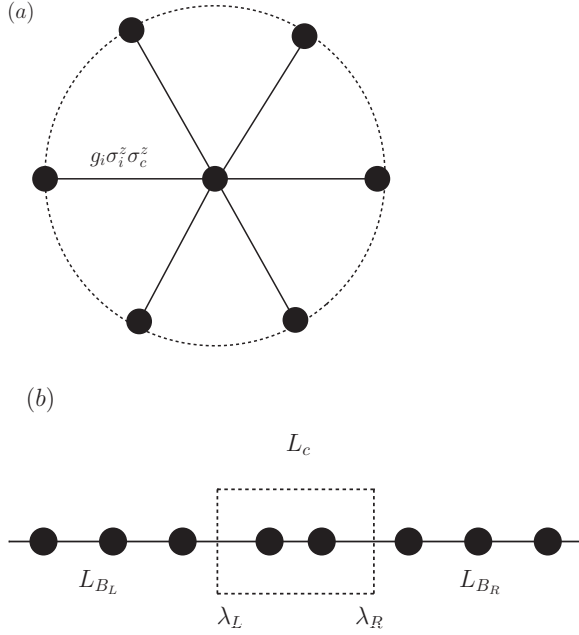


Figure 7.1: (a) A sketch of exactly solvable decoherence model: a single spin ( $\vec{\sigma}_c$ ) is coupled to a bath of  $N$  spins  $\{\vec{\sigma}_i\}$ . (b) A variation of (a) in that the central system is coupled to the baths only via the ends.

is not stable enough and it works only for bosonic systems. Improving this, and also developing similar methods for fermionic systems could be another future project.

There are also many small systems showing rich physics, such as systems of a few coupled quantum dots or molecular devices coupled to reservoirs. Application of the proposed methods to such systems should be very straightforward.

The methods can also be applied to more general physical systems, not only to study transport but also other physical questions, such as decoherence control and classical simulations of quantum computations. In all models studied in this thesis, the baths are assumed to be collections of eigenmodes  $|\omega^\nu(k)\rangle$ , connected to the central systems via  $\lambda V_k^\nu$  (see for example Eq. (2.44)). We then assume  $V_k^\nu$  to have certain properties. A more realistic and specific setup is to connect the baths locally to the central system, as sketched in Fig.7.1(b). In that case,  $V_k^\nu$  is implicitly defined.

The system sketched in Fig.7.1(a) is in fact a famous exactly solvable model of quantum decoherence [85, 124]: a single spin- $\frac{1}{2}$  is connected to a

bath of  $N$  spins- $\frac{1}{2}$  via Ising coupling with strength  $g_i$  to bath  $i$  [125]. The dynamics of the whole composite system is exactly solvable and Zurek et al. showed that the off-diagonal elements (in  $\sigma_z$  basis), thus the coherent part, die out very quickly. A related but rather ambitious question is to study a counterpart with a thermal bath and to ask the following questions: whether or not the reduced density matrix of the central system converges to the expected thermal equilibrium state; whether or not the off-diagonal elements disappear and if so, which “diagonal” and “off-diagonal” parts are relevant, and how that depends on the specific forms of interaction? In fact, such a natural selection of the basis is called, in theories of quantum measurement, eiselection of the pointer states [85, 124]. Furthermore, how do the answers to the above questions depend on various parameters of the composite systems, such as size of the bath, coupling strength between the central system and the bath, and temperature of the bath and so on. We can ask all the questions for a similar setup but now with two baths, biased or not, connected to the systems locally, as sketched in Fig.7.1(b).

These questions can be investigated using different approaches: starting from the pure dynamics of the whole composite system, which usually however is only applicable to non-interacting systems (both the central system and the baths); through the Redfield equation, which assumes the Markovian approximation, weak coupling and idealized infinite-size baths; and finally by the non-equilibrium Green’s function method, which is typically applied for configurations similar to the variation in Fig.7.1(b). In fact, there is another approach — the exact master equation or the influence functional method, which relaxes the assumption of the Markovian approximation and the weak coupling limit, but still takes the baths to be infinitely large. However, it currently works only for non-interacting systems since it is hard to solve such an exact master equation for interacting systems. So let us focus on the above three methods.

The generalized Fokker-Planck equation method makes it possible to implement the first approach even for large interacting systems. The second approach can be realized through either the BBGKY-like method or the generalized Fokker-Planck equation method. Implementations of the third method are already well developed. Note, however, that if we set the temperatures of the baths to be equal then the non-equilibrium Green’s function arrives at the corresponding equilibrium state of the whole composite system, which does not guarantee that the reduced density matrix of the central system follows the proper equilibrium distribution. On the other hand, the reduced density matrix generally converges to an equilibrium distribution in the theories of open quantum systems approach. Therefore, it will not

be much of a surprise if the non-equilibrium Green's function leads to qualitatively different results. If we want to compare them, a proper model, on which the non-equilibrium Green's function method and the Redfield equation ideally should produce the same result, is required. Comparison between the first two might shed some light on differences between the Markovian and the non-Markovian approximation, the validity of the infinite-size bath assumption, etc. Comparison between the latter two might help us understand them better or even improve both.

Lastly, our efficient methods for the Redfield equation can be applied as well to solving the local-operator Lindblad equation. This should make the local-operator Lindblad equation a more powerful tool in those cases where it is applicable. As we mentioned earlier, there are still many groups that use the local-operator Lindblad equation instead of the Redfield equation. It should be very straightforward to implement the methods for the local-operator Lindblad equation.

# Bibliography

- [1] G. Mahler and V.A. Weberruß. *Quantum Networks: Dynamics of Open Nanostructures*. Springer-Verlag, 1998.
- [2] H.-P. Breuer and F. Petruccione. *The theory of open quantum systems*. Oxford, 2002.
- [3] U. Weiss. *Quantum Dissipative Systems*. World Scientific, 1999.
- [4] S. Datta. *Quantum Transport: Atom to Transistor*. Cambridge University Press, 2005.
- [5] D.K. Ferry and S. M. Goodnick. *Transport in Nanostructures*. Cambridge Univ. Press, 1997.
- [6] R. Kubo. Statistical-mechanical theory of irreversible processes 1. general theory and simple applications to magnetic and conduction problems. *Journal of the Physical Society of Japan*, 12(6):570–586, 1957.
- [7] R. Kubo, M. Yokota, and S. Nakajima. Statistical-mechanical theory of irreversible processes 2. response to thermal disturbance. *Journal of the Physical Society of Japan*, 12(11):1203–1211, 1957.
- [8] R. Landauer. Electrical resistance of disordered one-dimensional lattices. *Philosophical Magazine*, 21(172):863–867, 1970.
- [9] R. Landauer. Spatial variation of currents and fields due to localized scatterers in metallic conduction. *IBM Journal of Research and Development*, 1(3):223–231, 1957.
- [10] M. Buttiker. 4-terminal phase-coherent conductance. *Physical Review Letters*, 57(14):1761–1764, 1986.
- [11] M. Buttiker, Y. Imry, R. Landauer, and S. Pinhas. Generalized many-channel conductance formula with application to small rings. *Physical Review B*, 31(10):6207–6215, 1985.

- [12] H. Haug and A. P. Jauho. *Quantum Kinetics in Transport and Optics of Semiconductors*. Springer-Verlag, 1996.
- [13] M. Koentopp, C. Chang, K. Burke, and R. Car. Density functional calculations of nanoscale conductance. *Journal of Physics-Condensed Matter*, 20(8):083203, 2008.
- [14] C. Caroli, R. Combescio, P. Norzieses, and D. Saintjam. Direct calculation of tunneling current. *Journal of Physics C-Solid State Physics*, 4(8):916–929, 1971.
- [15] R. Combescio. Direct calculation of tunneling current 3: Effect of localized impurity states in barrier. *Journal of Physics C-Solid State Physics*, 4(16):2611–2622, 1971.
- [16] J. Taylor, H. Guo, and J. Wang. Ab initio modeling of quantum transport properties of molecular electronic devices. *Physical Review B*, 63(24):245407, 2001.
- [17] A. G. Redfield. Relaxation theory: density matrix formulation. In D. M. Grant and R. K. Harris, editors, *Encyclopedia Nuclear Magnetic Resonance*, pages 4085–4092. Wiley, 1996.
- [18] G. D. Mahan. *Many-Particle Physics*. Plenum Press, 1990.
- [19] A. V. Sologubenko and H. R. Ott. Energy transport in one-dimensional spin systems. In D. Baeriswyl and L. Degiorgi, editors, *Strong Interactions in Low Dimensions*, chapter 12, pages 383–417. Springer, 2005.
- [20] A. Yacoby. Transport in quantum wire. In D. Baeriswyl and L. Degiorgi, editors, *Strong Interactions in Low Dimensions*, chapter 10, pages 321–346. Springer, 2005.
- [21] A. Nitzan and M. A. Ratner. Electron transport in molecular wire junctions. *SCIENCE*, 300(5624):1384–1389, 2003.
- [22] A Salomon, D Cahen, S Lindsay, J Tomfohr, VB Engelkes, and CD Frisbie. Comparison of electronic transport measurements on organic molecules. *Advanced Materials*, 15(22):1881–1890, 2003.
- [23] N. J. Tao. Electron transport in molecular junctions. *Nature Nanotechnology*, 1(3):173–181, 2006.
- [24] W. Goepel and C. Ziegler. *Nanostructures Based on Molecular Materials*. Wiley-VCH, 1992.

- [25] L. P. Kouwenhoven, C. M. Marcus, P. L. Mceuen, S. Tarucha, R. M. Westervelt, and N. S. Wingreen. Electron transport in quantum dots. In L. L. Sohn, L. P. Kouwenhoven, and G. Schon, editors, *Mesoscopic Electron Transport*, volume 345 of *NATO ADVANCED SCIENCE INSTITUTES SERIES, SERIES E, APPLIED SCIENCES*, pages 105–214, 1997.
- [26] D. Natelson. *Handbook of Organic Electronics and Photonics*. American Scientific Publishers, 2006.
- [27] A. V. Sologubenko, T. Lorenz, H. R. Ott, and A. Freimuth. Thermal conductivity via magnetic excitations in spin-chain materials. *Journal of Low Temperature Physics*, 147(3-4):387–403, 2007.
- [28] A. V. Sologubenko, K. Berggold, T. Lorenz, A. Rosch, E. Shimshoni, M. D. Phillips, and M. M. Turnbull. Magnetothermal transport in the spin- $\frac{1}{2}$  chains of copper pyrazine dinitrate. *Phys. Rev. Lett.*, 98(10):107201, Mar 2007.
- [29] A. V. Sologubenko, T. Lorenz, J. A. Mydosh, A. Rosch, K. C. Short-sleeves, and M. M. Turnbull. Field-dependent thermal transport in the haldane chain compound nenp. *Phys. Rev. Lett.*, 100(13):137202, Apr 2008.
- [30] C. W. Chang, D. Okawa, H. Garcia, A. Majumdar, and A. Zettl. Breakdown of fourier’s law in nanotube thermal conductors. *Phys. Rev. Lett.*, 101(7):075903, Aug 2008.
- [31] B. Soree, W. Magnus, and W. Schoenmaker. Energy and momentum balance equations: An approach to quantum transport in closed circuits. *Physical Review B*, 66(3):035318, 2002.
- [32] T. H. Stoof and Y. V. Nazarov. Time-dependent resonant tunneling via two discrete states. *Physical Review B*, 53(3):1050–1053, 1996.
- [33] O. N. Jouravlev and Y. V. Nazarov. Electron transport in a double quantum dot governed by a nuclear magnetic field. *Physical Review Letters*, 96(17):176804, 2006.
- [34] X. Zotos and P. Prelovsek. Transport in one dimensional quantum systems. In D. Baeriswyl and L. Degiorgi, editors, *Strong Interactions in Low Dimensions*, chapter 11, pages 347–382. Springer, 2005.

## Bibliography

---

- [35] X. Zotos, F. Naef, and P. Prelovsek. Transport and conservation laws. *Physical Review B*, 55(17):11029–11032, 1997.
- [36] K. Saito, S. Takesue, and S. Miyashita. Energy transport in the integrable system in contact with various types of phonon reservoirs. *Physical Review E*, 61(3):2397–2409, 2000.
- [37] Y. Yan, C.-Q. Wu, G. Casati, T. Prosen, and B. Li. Nonballistic heat conduction in an integrable random-exchange ising chain studied with quantum master equations. *Physical Review B*, 77(17):172411, 2008.
- [38] J. Wu and M. Berciu. Heat transport in quantum spin chains: the relevance of integrability. *arXiv:1003.1559, submitted to PRB*, 2010.
- [39] H. Mori. Statistical-mechanical theory of transport in fluids. *Physical Review*, 112(6):1829–1842, 1958.
- [40] J. M. Luttinger. Theory of thermal transport coefficients. *Physical Review*, 135(6):A1505–A1514, 1964.
- [41] D. S. Fisher and P. A. Lee. Relation between conductivity and transmission matrix. *Physical Review B*, 23(12):6851–6854, 1981.
- [42] J. Sirker, R. G. Pereira, and I. Affleck. Diffusion and ballistic transport in one-dimensional quantum systems. *Physical Review Letters*, 103(21):216602, 2009.
- [43] F. Heidrich-Meisner, A. Honecker, and W. Brenig. Thermal transport of the xxz chain in a magnetic field. *Physical Review B*, 71(18):184415, 2005.
- [44] M. Rigol and B. S. Shastry. Drude weight in systems with open boundary conditions. *Physical Review B*, 77(16):161101, 2008.
- [45] C. Toher, A. Filippetti, S. Sanvito, and K. Burke. Self-interaction errors in density-functional calculations of electronic transport. *Physical Review Letters*, 95(14), 2005.
- [46] F Evers, F Weigend, and M Koentopp. Conductance of molecular wires and transport calculations based on density-functional theory. *Physical Review B*, 69(23), 2004.
- [47] R. P. Feynman and F. L. Vernon. the theory of a general quantum system interacting with a linear dissipative system. *Annals of Physics*, 24(1):118–173, 1963.

## Bibliography

---

- [48] A. J. Leggett, S. Chakravarty, A. T. Dorsey, M. P. A. Fisher, A. Garg, and W. Zwerger. Dynamics of the dissipative 2-state system. *Reviews of Modern Physics*, 59(1):1–85, 1987.
- [49] B. L. Hu, J. P. Paz, and Y. H. Zhang. Quantum brownian-motion in a general environment - exact master equation with nonlocal dissipation and colored noise. *Physical Review D*, 45(8):2843–2861, 1992.
- [50] C.-H. Chou, T. Yu, and B. L. Hu. Exact master equation and quantum decoherence of two coupled harmonic oscillators in a general environment. *Physical Review E*, 77(1):011112, 2008.
- [51] R. Kubo, M. Toda, and N. Hashitsume. *Statistical physics II: nonequilibrium statistical mechanics*. Springer, 2nd edition, 1991.
- [52] A. G. Redfield. On the theory of relaxation processes. *IBM Journal of Research and Development*, 1(1):19–31, 1957.
- [53] A. G. Redfield. The theory of relaxation processes. *Adv. Magn. Reson.*, 1:1–32, 1965.
- [54] W. T. Pollard, A. K. Felts, and R. A. Friesner. The redfield equation in condensed-phase quantum dynamics. *Advances in Chemical Physics*, 93:77–134, 1996.
- [55] J. M. Jean, R. A. Friesner, and G. R. Fleming. Application of a multi-level redfield theory to electron-transfer in condensed phases. *Journal of Chemical Physics*, 96(8):5827–5842, 1992.
- [56] M. Michel, O. Hess, H. Wichterich, and J. Gemmer. Transport in open spin chains: A monte carlo wave-function approach. *Physical Review B*, 77(10):104303, 2008.
- [57] S. Andergassen, V. Meden, J. Splettstoesser, H. Schoeller, and M. R. Wegewijs. Charge transport through single molecules, quantum dots and quantum wires. *Nanotechnology*, 21(27), 2010.
- [58] M. Michel, M. Hartmann, J. Gemmer, and G. Mahler. Fourier’s law confirmed for a class of small quantum systems. *European Physical Journal B*, 34(3):325–330, 2003.
- [59] T. Prosen and M. Znidaric. Matrix product simulations of non-equilibrium steady states of quantum spin chains. *Journal of Statistical Mechanics-Theory and Experiment*, page P02035, 2009.

## Bibliography

---

- [60] K. Saito. Strong evidence of normal heat conduction in a one-dimensional quantum system. *Europhysics Letters*, 61(1):34–40, 2003.
- [61] W. Huisinga, L. Pesce, R. Kosloff, and P. Saalfrank. Faber and newton polynomial integrators for open-system density matrix propagation. *Journal of Chemical Physics*, 110(12):5538–5547, 1999.
- [62] W. T. Pollard and R. A. Friesner. Solution of the redfield equation for the dissipative quantum dynamics of multilevel systems. *Journal of Chemical Physics*, 100(7):5054–5065, 1994.
- [63] H. Guo and R. Q. Chen. Short-time chebyshev propagator for the Liouville-Von Neumann equation. *Journal of Chemical Physics*, 110(14):6626–6634, 1999.
- [64] I. Kondov, U. Kleinekathofer, and M. Schreiber. Efficiency of different numerical methods for solving redfield equations. *Journal of Chemical Physics*, 114(4):1497–1504, 2001.
- [65] H. Wichterich, M. J. Henrich, H.-P. Breuer, J. Gemmer, and M. Michel. Modeling heat transport through completely positive maps. *Physical Review E*, 76(3):031115, 2007.
- [66] H.-P. Breuer and F. Petruccione. Stochastic dynamics of quantum jumps. *Physical Review E*, 52(1):428–441, 1995.
- [67] P Saalfrank. Stochastic wave packet vs direct density matrix solution of liouville-von neumann equations for photodesorption problems. *Chemical Physics*, 211(1-3):265–276, 1996.
- [68] D. Y. Petrina. *Mathematical foundations of quantum statistical mechanics*. Kluwer Acad. Publ., 1995.
- [69] L. P. Kadanoff and P. C. Martin. Theory of many-particle systems II: superconductivity. *Physical Review*, 124(3):670–697, 1961.
- [70] C. W. Gardiner and P. Zoller. *Quantum Noise*. Springer, 2000.
- [71] K. E. Cahill and R. J. Glauber. Density operators for fermions. *Physical Review A*, 59(2):1538–1555, 1999.
- [72] P. D. Drummond, P. Deuar, and J. F. Corney. Quantum many-body simulations using gaussian phase-space representations. *Optics and Spectroscopy*, 103(1):7–16, 2007.

- [73] P. Deuar and P. D. Drummond. First-principles quantum dynamics in interacting bose gases: I. the positive p representation. *Journal of Physics A-Mathematical and General*, 39(5):1163–1181, 2006.
- [74] P. Deuar and P. D. Drummond. First-principles quantum dynamics in interacting bose gases ii: stochastic gauges. *Journal of Physics A-Mathematical and General*, 39(11):2723–2755, 2006.
- [75] P. Deuar and P. D. Drummond. Correlations in a bec collision: First-principles quantum dynamics with 150 000 atoms. *Physical Review Letters*, 98(12):120402, 2007.
- [76] S. Lepri, R. Livi, and A. Politi. Thermal conduction in classical low-dimensional lattices. *Physics Reports-Review Section of Physics Letters*, 377(1):1–80, 2003.
- [77] K. Damle and S. Sachdev. Spin dynamics and transport in gapped one-dimensional heisenberg antiferromagnets at nonzero temperatures. *Physical Review B*, 57(14):8307–8339, 1998.
- [78] A. V. Sologubenko, S. M. Kazakov, H. R. Ott, T. Asano, and Y. Ajiro. Diffusive energy transport in the s=1 haldane-gap spin chain compound agvp2s6. *Journal of Magnetism and Magnetic Materials*, 272(Suppl. 1):E689–E690, 2004.
- [79] A. V. Sologubenko, K. Gianno, H. R. Ott, A. Vietkine, and A. Revcolevschi. Heat transport by lattice and spin excitations in the spin-chain compounds srcuo2 and sr2cuo3. *Physical Review B*, 64(5):054412, 2001.
- [80] N. Hlubek, P. Ribeiro, R. Saint-Martin, A. Revcolevschi, G. Roth, G. Behr, B. Buechner, and C. Hess. Ballistic heat transport of quantum spin excitations as seen in srcuo2. *Physical Review B*, 81(2):020405, 2010.
- [81] K. R. Thurber, A. W. Hunt, T. Imai, and F. C. Chou. O-17 nmr study of q=0 spin excitations in a nearly ideal s=1/2 1d heisenberg antiferromagnet, sr2cuo3, up to 800 k. *Physical Review Letters*, 87(24):247202, 2001.
- [82] F. Heidrich-Meisner, A. Honecker, D. C. Cabra, and W. Brenig. Zero-frequency transport properties of one-dimensional spin-1/2 systems. *Physical Review B*, 68(13):134436, 2003.

## Bibliography

---

- [83] K. Saito, S. Takesue, and S. Miyashita. Thermal conduction in a quantum system. *Physical Review E*, 54(3):2404–2408, 1996.
- [84] P. Jordan and E. Wigner. über das paulische Äquivalenzverbot. *Zeitschrift für Physik A Hadrons and Nuclei*, 47(9-10):631, 1928.
- [85] M. A. Schlosshauer. *Decoherence and the Quantum-To-Classical Transition*. Springer, 2007.
- [86] J.-H. An and W.-M. Zhang. Non-markovian entanglement dynamics of noisy continuous-variable quantum channels. *Physical Review A*, 76(4):042127, 2007.
- [87] K. Blum. *Density Matrix Theory and Applications: Physics of Atoms and Molecules*. Springer, 2nd edition, 1996.
- [88] M. Michel, J. Gemmer, and G. Mahler. Heat conductivity in small quantum systems: Kubo formula in liouville space. *European Physical Journal B*, 42(4):555–559, 2004.
- [89] M. Michel, G. Mahler, and J. Gemmer. Fourier’s law from schrodinger dynamics. *Physical Review Letters*, 95(18):180602, 2005.
- [90] G. Lindblad. Generators of quantum dynamical semigroups. *communications in mathematical physics*, 48(2):119–130, 1976.
- [91] V. Gorini, A. Kossakowski, and E. C. G. Sudarshan. Completely positive dynamical semigroups of N-level systems. *Journal of Mathematical Physics*, 17(5):821–825, 1976.
- [92] U. Brandt and M. Moraweck. Rigorous results on the dc kubo-greenwood conductivity of disordered-systems. *Journal of Physics C-Solid State Physics*, 15(25):5255–5268, 1982.
- [93] D. J. Thouless and S. Kirkpatrick. Conductivity of the disordered linear-chain. *Journal of Physics C-Solid State Physics*, 14(3):235–245, 1981.
- [94] M. Kira and S. W. Koch. Many-body correlations and excitonic effects in semiconductor spectroscopy. *Progress in quantum electronics*, 30(5):155–296, 2006.
- [95] P. C. Martin and J. Schwinger. Theory of many-particle systems i. *Physical Review*, 115(6):1342–1373, 1959.

- [96] D. Jaksch, C. Bruder, J. I. Cirac, C. W. Gardiner, and P. Zoller. Cold bosonic atoms in optical lattices. *Physical Review Letters*, 81(15):3108–3111, 1998.
- [97] M. Greiner, O. Mandel, T. Esslinger, T. W. Hansch, and I. Bloch. Quantum phase transition from a superfluid to a mott insulator in a gas of ultracold atoms. *NATURE*, 415(6867):39–44, 2002.
- [98] H. Risken. *The Fokker-Planck Equation: Methods of Solutions and Applications*. Springer, 1989.
- [99] T. Prosen and B. Zunkovic. Exact solution of markovian master equations for quadratic fermi systems: thermal baths, open xy spin chains and non-equilibrium phase transition. *New Journal of Physics*, 12:025016, 2010.
- [100] S. R. Clark, J. Prior, M. J. Hartmann, D. Jaksch, and M. B. Plenio. Exact matrix product solutions in the heisenberg picture of an open quantum spin chain. *New Journal of Physics*, 12:025005, 2010.
- [101] J. Wu. Non-equilibrium stationary states from the equation of motion of open systems. *New Journal of Physics*, 12:083042, 2010.
- [102] L. I. Plimak, M. K. Olsen, M. Fleischhauer, and M. J. Collett. Beyond the fokker-planck equation: Stochastic simulation of complete wigner representation for the optical parametric oscillator. *Europhysics Letters*, 56(3):372–378, 2001.
- [103] Benoit Palmieri, Yuki Nagata, and Shaul Mukamel. Phase-space algorithm for simulating quantum nonlinear response functions of bosons using stochastic classical trajectories. *Physical Review E*, 82:046706, 2010.
- [104] S.E. Hoffmann, J.F. Corney, and P. D. Drummond. Hybrid phase-space simulation method for interacting bose fields. *Physical Review A*, 78:013622, 2008.
- [105] J. et al. Hope. Xmds: extensible multi-dimensional simulator, <http://xmds.sourceforge.net>.
- [106] C. Mejia-Monasterio, T. Prosen, and G. Casati. Fourier’s law in a quantum spin chain and the onset of quantum chaos. *Europhysics Letters*, 72(4):520–526, 2005.

## Bibliography

---

- [107] M. Distasio and X. Zotos. Connection between low-energy effective-hamiltonians and energy-level statistics. *Physical Review Letters*, 74(11):2050–2053, 1995.
- [108] Y. Avishai, J. Richert, and R. Berkovits. Level statistics in a heisenberg chain with random magnetic field. *Physical Review B*, 66(5):052416, 2002.
- [109] T. A. Brody, J. Flores, J. B. French, P. A. Mello, A. Pandey, and S. S. M. Wong. Random-matrix physics - spectrum and strength fluctuations. *Reviews of Modern Physics*, 53(3):385–479, 1981.
- [110] T. C. Hsu and J. C. A. Dauriac. Level repulsion in integrable and almost-integrable quantum spin models. *Physical Review B*, 47(21):14291–14296, 1993.
- [111] K. Kudo and T. Deguchi. Unexpected non-wigner behavior in level-spacing distributions of next-nearest-neighbor coupled xxz spin chains. *Physical Review B*, 68(5):052510, 2003.
- [112] K. Kudo and T. Deguchi. Level statistics of xxz spin chains with discrete symmetries: Analysis through finite-size effects. *Journal of the Physical Society of Japan*, 74(7):1992–2000, 2005.
- [113] K. Kudo and T. Deguchi. Level statistics of xxz spin chains with a random magnetic field. *Physical Review B*, 69(13):132404, 2004.
- [114] V. E. Korepin, N. M. Bogoliubov, and A. G. Izergin. *Quantum Inverse Scattering Method and Correlation Functions*. Cambridge University Press, 1993.
- [115] A. Klumper and K. Sakai. The thermal conductivity of the spin-1/2 xxz chain at arbitrary temperature. *Journal of Physics A-Mathematical and General*, 35(9):2173–2182, 2002.
- [116] V. E. Korepin, N. M. Bogoliubov, and A. G. Izergin. *Quantum Inverse Scattering Method and Correlation Functions*. Cambridge University Press, 1993.
- [117] M. Shiroishi and M. Wadati. Integrable boundary conditions for the one-dimensional hubbard model. *Journal of the Physical Society of Japan*, 66(8):2288–2301, 1997.

- [118] E. K. Sklyanin. Boundary-conditions for integrable quantum-systems. *Journal of Physics A-Mathematical and General*, 21(10):2375–2389, 1988.
- [119] T. Prosen. Open xxz spin chain: Nonequilibrium steady state and strict bound on ballistic transport. *arXiv:1103.1350v2*, 2011.
- [120] A. V. Sologubenko, E. Felder, K. Gianno, H. R. Ott, A. Vietkine, and A. Revcolevschi. Thermal conductivity and specific heat of the linear chain cuprate sr2cuo3: Evidence for thermal transport via spinons. *Physical Review B*, 62(10):R6108–R6111, 2000.
- [121] Y. Ando, J. Takeya, D. L. Sisson, S. G. Doettinger, I. Tanaka, R. S. Feigelson, and A. Kapitulnik. Thermal conductivity of the spin-peierls compound cugeo3. *Physical Review B*, 58(6):R2913–R2916, 1998.
- [122] Y. Saad and M.H. Schultz. Gmres - a generalized minimal residual algorithm for solving nonsymmetric linear systems. *SIAM Journal on Scientific and Statistical Computing*, 7(3):856–869, 1986.
- [123] R. V. Jensen and R. Shankar. Statistical behavior in deterministic quantum-systems with few degrees of freedom. *Physical Review Letters*, 54(17):1879–1882, 1985.
- [124] M. Schlosshauer. Decoherence, the measurement problem, and interpretations of quantum mechanics. *Review of Modern Physics*, 76(4):1267–1305, 2004.
- [125] F. M. Cucchietti, J. P. Paz, and W. H. Zurek. Decoherence from spin environments. *Physical Review A*, 72(5):052113, 2005.
- [126] G. Hu. *Non-equilibrium Statistical Physics*. unpublished, 2002.

# Appendix A

## Perturbational decomposition of the operators $\hat{m}$

In this appendix we will derive expressions of operators  $\hat{m}$  and  $\hat{m}$  in two ways: using the eigenvectors of  $H_S = H_0 + V_S$  and expanding the operators perturbationally in orders of  $V_0$  based on expressions of the operators for the corresponding non-interaction  $H_0$ .

### A.1 Expanded in eigenbasis of $H_S$

From its definition in Eq(4.3), in the representation of eigenvalues  $\{E_m\}$  and eigenstates  $\{|m\rangle\}$  of  $H_S$ , the operator  $\hat{m}$  can be written as

$$\begin{aligned}
 \langle m | \hat{m}_\alpha | n \rangle &= (\hat{m}_\alpha)_{mn} \\
 &= (c_\alpha)_{mn} \sum_k |V_k^\alpha|^2 \int_0^\infty d\tau e^{i(E_n - E_m - \omega_{k,\alpha})\tau} \langle 1 - n_\alpha(\omega_{k,\alpha}) \rangle \\
 &= (c_\alpha)_{mn} \pi \int d\omega D^\alpha(\omega) |V^\alpha(\omega)|^2 \langle 1 - n_\alpha(\omega) \rangle \delta(\Omega_{mn} - \omega) \\
 &= (c_\alpha)_{mn} \pi D^\alpha(E_n - E_m) |V^\alpha(E_n - E_m)|^2 \langle 1 - n_\alpha(E_n - E_m) \rangle, \quad (\text{A.1})
 \end{aligned}$$

where we have used  $\int_0^\infty d\tau e^{i\omega\tau} = \pi\delta(\omega) + iP(\frac{1}{\omega})$  and neglected the principal value part. We have also assumed that it is possible to perform a change of variable on  $V_k^\alpha$  such that it becomes  $V^\alpha(k_{nm})$ , where  $k_{nm}$  is defined by  $\omega_{k_{nm},\alpha} = \Omega_{mn} = E_m - E_n = -\Omega_{nm}$ , i.e. a bath mode resonant with this transition. This limits the possible forms of  $V_k^\alpha$  and  $\omega_{k,\alpha}$ . For example, for each given energy  $\Omega_{mn}$ , there should be a unique value of  $V_{k_{nm}}^\alpha$ . In all the work in this thesis, we take  $V_k^\alpha$  as a constant so this condition is satisfied.

## A.2. Perturbational expansion starting from non-interacting systems

---

$D_\alpha(\omega)$  is the bath's density of states. We arrive at

$$\hat{m}_\alpha = \pi \sum_{m,n} |m\rangle \langle n| \langle m|c_\alpha|n\rangle (1 - n_\alpha(\Omega_{nm})) D_\alpha(\Omega_{nm}) |V_{k_{nm}}^\alpha|^2, \quad (\text{A.2a})$$

$$\hat{m}_\alpha = \pi \sum_{m,n} |m\rangle \langle n| \langle m|c_\alpha^\dagger|n\rangle n_\alpha(\Omega_{mn}) D_\alpha(\Omega_{mn}) |V_{k_{mn}}^\alpha|^2. \quad (\text{A.2b})$$

We furthermore set  $V_{k_{nm}}^\alpha D_\alpha(\omega)$  as a constant and absorb it into  $\lambda^2$ . Similar expressions can be derived for bosonic systems with the Fermi-Dirac distribution replaced by the Bose-Einstein distribution and  $(1 - n_\alpha(\Omega_{nm}))$  replaced by  $(1 + n_\alpha(\Omega_{nm}))$ . This approach involves a direct diagonalization of the isolated system  $H_S$ . One can avoid the diagonalization by finding such operators  $\hat{m}$  perturbationally.

## A.2 Perturbational expansion starting from non-interacting systems

To present the general idea concretely, let us work on a specific system, the Hamiltonian  $H_S = H_0 + V_S$  defined in Eq. (4.1), which we rewrite here for convenience,

$$H_S = -t \sum_{l=1}^{N-1} (c_l^\dagger c_{l+1} + c_{l+1}^\dagger c_l) + V_0 \sum_{l=1}^{N-1} c_{l+1}^\dagger c_{l+1} c_l^\dagger c_l = H_0 + V_S. \quad (\text{A.3})$$

Next assuming  $V_0$  is small and treating it perturbationally, we want to express the operator  $\hat{m}_\alpha$  in terms of polynomials of  $\{c_m\}$  operators and in various orders of  $V_0$ . When  $V_0 = 0$  the system is a tight-binding open chain. The following basis transformation — discrete Fourier transform for open chains

$$c_k = \frac{1}{\sqrt{N}} \sum_{l=1}^N \sin \frac{kl\pi}{N+1} c_l, \quad (\text{A.4})$$

diagonalizes  $H_0$ ,

$$H_0 = \sum_{k=1}^N \epsilon_k c_k^\dagger c_k, \quad (\text{A.5})$$

where

$$\epsilon_k = -2t \cos \frac{\pi k}{N+1}. \quad (\text{A.6})$$

## A.2. Perturbational expansion starting from non-interacting systems

---

Therefore,  $c_\alpha(t)$  is a linear function of all  $c_m$ ,

$$c_l(t) \equiv c_l^{(0)}(t) = \frac{2}{N+1} \sum_{km} \sin \frac{\pi kl}{N+1} \sin \frac{\pi km}{N+1} e^{-i\epsilon_k t} c_m. \quad (\text{A.7})$$

Hence,  $\hat{m}_\alpha$  is also a linear combination of all  $c_m$  operators. One can imagine that for small  $V_0$ ,  $\hat{m}_L$  should not be too far from such a linear combination. Let us call  $c_l(t)$  when  $V_0 = 0$  as  $c_l^{(0)}(t)$ . Treating this as the zeroth order form for the full dynamical  $c_l(t)$ , and expanding

$$c_l(t) = \sum_n V_0^n c_l^{(n)}(t), \quad (\text{A.8})$$

we derive a perturbation equation of  $c_l^{(n)}(t)$ :

$$\dot{c}_l^{(n)} = it \left( c_{l-1}^{(n)} + c_{l+1}^{(n)} \right) - i d_l^{(n-1)}, \quad (\text{A.9})$$

where we define, for non-negative integers  $n, n_1, n_2, n_3$ ,

$$d_l^{(n)} = \sum_{\substack{n_1, n_2, n_3 \\ \sum_i n_i = n}} \left\{ c_l^{(n_1)} c_{l-1}^{\dagger, (n_2)} c_{l-1}^{(n_3)} + c_l^{(n_1)} c_{l+1}^{\dagger, (n_2)} c_{l+1}^{(n_3)} \right\}. \quad (\text{A.10})$$

The solution of the above equation can be written as

$$c_l^{(n)}(t) = -i \int_0^t d\tau \frac{2}{N+1} \sum_{km} \sin \frac{\pi kl}{N+1} \sin \frac{\pi km}{N+1} e^{-i\epsilon_k(t-\tau)} d_m^{(n-1)}(\tau). \quad (\text{A.11})$$

Here the initial condition  $c^{(n)}(0) = 0 (\forall n \geq 1)$  is used. As the expression of  $c_l^{(0)}$  is given in Eq. (A.7), explicitly the expression of  $c_l^{(1)}$  is

$$\begin{aligned} c_l^{(1)}(t) &= \left( \frac{2}{N+1} \right)^4 \sum_{\substack{km \\ k, m_i}} \frac{e^{i(\epsilon(k_2) - \epsilon(k_1) - \epsilon(k_3))t} - e^{i\epsilon(k)t}}{\epsilon(k_1) + \epsilon(k_3) - \epsilon(k_2) - \epsilon(k)} \\ &\cdot \sin \frac{\pi kl}{N+1} \sin \frac{\pi k_1 l}{N+1} \sin \frac{\pi km}{N+1} \sin \frac{\pi k_1 m_1}{N+1} \sin \frac{\pi k_2 m_2}{N+1} \sin \frac{\pi k_3 m_3}{N+1} \\ &\cdot \left[ \sin \frac{\pi k_2(l-1)}{N+1} \sin \frac{\pi k_3(l-1)}{N+1} + \sin \frac{\pi k_2(l+1)}{N+1} \sin \frac{\pi k_3(l+1)}{N+1} \right] \\ &\cdot c_{m_1} c_{m_2}^\dagger c_{m_3}. \end{aligned} \quad (\text{A.12})$$

A.2. *Perturbational expansion starting from non-interacting systems*

---

Similarly we can derive  $c_l^{(2)}$ , which will be shown explicitly later when we discuss terms proportional to  $V_0^2$  in bath operators  $\hat{m}$ . Plugging this general solution into Eq(4.3), and after straightforward but tedious algebra, we arrive at the decomposition of  $\hat{m}_\alpha$  and  $\hat{\bar{m}}_\alpha$  in Eq(4.34) with expansion coefficients defined as follows,

$$\mathfrak{D}_{\alpha;m} = \pi \frac{2}{N+1} \sum_k \sin \frac{\pi k l_\alpha}{N+1} \sin \frac{\pi k m}{N+1} [1 - n(\epsilon_k, T_\alpha)], \quad (\text{A.13a})$$

$$\bar{\mathfrak{D}}_{\alpha;m} = \pi \frac{2}{N+1} \sum_k \sin \frac{\pi k l_\alpha}{N+1} \sin \frac{\pi k m}{N+1} n(\epsilon_k, T_\alpha), \quad (\text{A.13b})$$

for the zeroth order expansion,

$$\begin{aligned} \mathfrak{D}_{\alpha;m_1 m_2 m_3} &= \pi \left( \frac{2}{N+1} \right)^4 \sum_{k,m,k_1,k_2,k_3} \\ &\cdot \frac{n(\epsilon(k), T_\alpha) - n(\epsilon(k_1) + \epsilon(k_3) - \epsilon(k_2), T_\alpha)}{\epsilon(k_1) + \epsilon(k_3) - \epsilon(k_2) - \epsilon(k)} \\ &\cdot \sin \frac{k\pi l_\alpha}{N+1} \sin \frac{k_1\pi m_1}{N+1} \sin \frac{k_2\pi m_2}{N+1} \sin \frac{k_3\pi m_3}{N+1} \sin \frac{k\pi m}{N+1} \sin \frac{k_1\pi m}{N+1} \\ &\cdot \left( \sin \frac{k_2\pi(m+1)}{N+1} \sin \frac{k_3\pi(m+1)}{N+1} + \sin \frac{k_2\pi(m-1)}{N+1} \sin \frac{k_3\pi(m-1)}{N+1} \right), \end{aligned} \quad (\text{A.14})$$

A.2. *Perturbational expansion starting from non-interacting systems*

---

for the first order expansion. For the second order expansion we make use of  $c_l^{(2)}$  and we have

$$\begin{aligned}
\mathfrak{D}_{\alpha; m_1 m_2 m_3 m_4 m_5} &= \pi \left( \frac{2}{N+1} \right)^7 \sum_{k, m, k_0, m_0, k_1, k_2, k_3, k_4, k_5} \\
&\cdot \sin \frac{\pi k m}{N+1} \left( \prod_{i=0}^5 \sin \frac{\pi k_i m_i}{N+1} \right) \sin \frac{\pi k l_\alpha}{N+1} \sin \frac{\pi k_1 l_\alpha}{N+1} \\
&\left\{ \frac{1}{\epsilon(k_1) + \epsilon(k_3) - \epsilon(k_2) - \epsilon(k_0)} \left[ \frac{n(\epsilon(k)) - n(\epsilon(k_5) - \epsilon(k_0) - \epsilon(k_4))}{\epsilon(k_0) + \epsilon(k_4) - \epsilon(k_5) + \epsilon(k)} \right. \right. \\
&\quad \left. \left. - \frac{n(\epsilon(k)) - n(\epsilon(k_1) + \epsilon(k_3) + \epsilon(k_5) - \epsilon(k_2) - \epsilon(k_4))}{\epsilon(k_2) + \epsilon(k_4) - \epsilon(k_1) - \epsilon(k_3) - \epsilon(k_5) + \epsilon(k)} \right] \right. \\
&\quad \cdot \sin \frac{\pi k_0 l_\alpha}{N+1} \sum_{\delta=\pm 1} \left( \sin \frac{\pi k_2(l_\alpha + \delta)}{N+1} \sin \frac{\pi k_3(l_\alpha + \delta)}{N+1} \right) \\
&\quad \cdot \sum_{\delta=\pm 1} \left( \sin \frac{\pi k_4(l_\alpha + \delta)}{N+1} \sin \frac{\pi k_5(l_\alpha + \delta)}{N+1} \right) \\
&+ \frac{1}{\epsilon(k_2) + \epsilon(k_4) - \epsilon(k_3) - \epsilon(k_0)} \left[ \frac{n(\epsilon(k)) - n(\epsilon(k_0) + \epsilon(k_1) + \epsilon(k_5))}{\epsilon(k) - \epsilon(k_0) - \epsilon(k_1) - \epsilon(k_5)} \right. \\
&\quad \left. - \frac{n(\epsilon(k)) - n(\epsilon(k_1) + \epsilon(k_3) + \epsilon(k_5) - \epsilon(k_2) - \epsilon(k_4))}{\epsilon(k_2) + \epsilon(k_4) - \epsilon(k_1) - \epsilon(k_3) - \epsilon(k_5) + \epsilon(k)} \right] \\
&\quad \cdot \sum_{\delta=\pm 1} \left( \sin \frac{\pi k_0(l_\alpha + \delta)}{N+1} \sin \frac{\pi k_4(l_\alpha + \delta)}{N+1} \frac{\pi k_5(l_\alpha + \delta)}{N+1} \right. \\
&\quad \cdot \left[ \sin \frac{\pi k_2 l_\alpha}{N+1} \sin \frac{\pi k_3 l_\alpha}{N+1} + \sin \frac{\pi k_2(l_\alpha + 2\delta)}{N+1} \sin \frac{\pi k_3(l_\alpha + 2\delta)}{N+1} \right] \Big) \\
&+ \frac{1}{\epsilon(k_3) + \epsilon(k_5) - \epsilon(k_4) - \epsilon(k_0)} \left[ \frac{n(\epsilon(k)) - n(\epsilon(k_1) - \epsilon(k_0) - \epsilon(k_2))}{\epsilon(k) + \epsilon(k_0) - \epsilon(k_1) + \epsilon(k_2)} \right. \\
&\quad \left. - \frac{n(\epsilon(k)) - n(\epsilon(k_1) + \epsilon(k_3) + \epsilon(k_5) - \epsilon(k_2) - \epsilon(k_4))}{\epsilon(k_2) + \epsilon(k_4) - \epsilon(k_1) - \epsilon(k_3) - \epsilon(k_5) + \epsilon(k)} \right] \\
&\quad \cdot \sum_{\delta=\pm 1} \left( \sin \frac{\pi k_0(l_\alpha + \delta)}{N+1} \sin \frac{\pi k_2(l_\alpha + \delta)}{N+1} \sin \frac{\pi k_3(l_\alpha + \delta)}{N+1} \right. \\
&\quad \cdot \left. \left[ \sin \frac{\pi k_4 l_\alpha}{N+1} \sin \frac{\pi k_5 l_\alpha}{N+1} + \sin \frac{\pi k_4(l_\alpha + 2\delta)}{N+1} \sin \frac{\pi k_5(l_\alpha + 2\delta)}{N+1} \right] \right) \Big\}. \tag{A.15}
\end{aligned}$$

Here we introduce a short-hand notation  $\delta = \pm 1$  in  $(l_\alpha + \delta)$  to stand for the neighbor sites of  $l_\alpha$ . In the last expression we have denoted  $n(\epsilon(k), T_\alpha)$  as

A.2. *Perturbational expansion starting from non-interacting systems*

---

$n(\epsilon(k))$  to make it fit into the page width. Therefore up to the order of  $V_0^2$ , the bath operators can be written down as

$$\begin{aligned} \hat{m}_\alpha &= \sum_m \mathfrak{D}_{\alpha;m} c_m + V_0 \sum_{m_1 m_2 m_3} \mathfrak{D}_{\alpha;m_1 m_2 m_3} c_{m_1} c_{m_2}^\dagger c_{m_3} \\ + V_0^2 \sum_{m_1 m_2 m_3 m_4 m_5} \mathfrak{D}_{\alpha;m_1 m_2 m_3 m_4 m_5} c_{m_1} c_{m_2}^\dagger c_{m_3} c_{m_4}^\dagger c_{m_5} + O(V_0^3) \end{aligned} \quad (\text{A.16a})$$

$$\begin{aligned} \hat{\bar{m}}_\alpha &= \sum_m \bar{\mathfrak{D}}_{\alpha;m} c_m^\dagger - V_0 \sum_{m_1 m_2 m_3} \mathfrak{D}_{\alpha;m_1 m_2 m_3} c_{m_3}^\dagger c_{m_2} c_{m_1}^\dagger \\ - V_0^2 \sum_{m_1 m_2 m_3 m_4 m_5} \mathfrak{D}_{\alpha;m_1 m_2 m_3 m_4 m_5} c_{m_5}^\dagger c_{m_4} c_{m_3}^\dagger c_{m_2} c_{m_1}^\dagger + O(V_0^3). \end{aligned} \quad (\text{A.16b})$$

The same procedure is applicable for bosonic systems and similar expressions can be derived. This has been used in Chapter 5 to calculate the operators  $\hat{m}_\alpha$  and  $\hat{\bar{m}}_\alpha$ , and find non-equilibrium stationary states for bosonic systems using the BBGKY-like method.

## Appendix B

# Second-order cluster expansion and second-order equations of $G_1$ , $\mathfrak{G}_2$

In this chapter we present explicitly forms of the second-order cluster expansion and the second-order equations for  $G_1$ ,  $\mathfrak{G}_2$ .

### B.1 Second-order cluster expansion

First-order cluster expansion as in Eq. (4.31) expresses  $G_2$  in terms of  $G_1$  and neglecting  $\mathfrak{G}_2$ . For convenience, we rewrite it here,

$$\begin{aligned} G_2(m^\dagger, n^\dagger, m', n') &= -G_1(m^\dagger, m') G_1(n^\dagger, n') \\ &+ G_1(m^\dagger, n') G_1(n^\dagger, m') + \mathfrak{G}_2(m^\dagger, n^\dagger, m', n'). \end{aligned} \quad (\text{B.1})$$

## B.2. Second-order equations of $G_1$ and $\mathfrak{G}_2$

---

A second-order cluster expansion similarly writes  $G_3$  in terms of  $G_1, G_2$  and neglecting  $\mathfrak{G}_3$ [94],

$$\begin{aligned}
 G\left(m_1^\dagger, m_2^\dagger, m_3^\dagger, m_4, m_5, m_6\right) &= G\left(m_1^\dagger, m_6\right) G\left(m_2^\dagger, m_5\right) G\left(m_3^\dagger, m_4\right) \\
 &+ G\left(m_1^\dagger, m_5\right) G\left(m_2^\dagger, m_4\right) G\left(m_3^\dagger, m_6\right) \\
 &+ G\left(m_1^\dagger, m_4\right) G\left(m_2^\dagger, m_6\right) G\left(m_3^\dagger, m_5\right) \\
 &- G\left(m_1^\dagger, m_6\right) G\left(m_2^\dagger, m_4\right) G\left(m_3^\dagger, m_5\right) \\
 &- G\left(m_1^\dagger, m_5\right) G\left(m_2^\dagger, m_6\right) G\left(m_3^\dagger, m_4\right) \\
 &- G\left(m_1^\dagger, m_4\right) G\left(m_2^\dagger, m_5\right) G\left(m_3^\dagger, m_6\right) \tag{B.2a}
 \end{aligned}$$

$$\begin{aligned}
 &+ G\left(m_1^\dagger, m_6\right) \mathfrak{G}\left(m_2^\dagger, m_3^\dagger, m_4, m_5\right) \\
 &- G\left(m_1^\dagger, m_5\right) \mathfrak{G}\left(m_2^\dagger, m_3^\dagger, m_4, m_6\right) \\
 &+ G\left(m_1^\dagger, m_4\right) \mathfrak{G}\left(m_2^\dagger, m_3^\dagger, m_5, m_6\right) \\
 &+ G\left(m_2^\dagger, m_5\right) \mathfrak{G}\left(m_1^\dagger, m_3^\dagger, m_4, m_6\right) \\
 &- G\left(m_2^\dagger, m_4\right) \mathfrak{G}\left(m_1^\dagger, m_3^\dagger, m_5, m_6\right) \\
 &- G\left(m_2^\dagger, m_6\right) \mathfrak{G}\left(m_1^\dagger, m_3^\dagger, m_4, m_5\right) \\
 &+ G\left(m_3^\dagger, m_4\right) \mathfrak{G}\left(m_1^\dagger, m_2^\dagger, m_5, m_6\right) \\
 &- G\left(m_3^\dagger, m_5\right) \mathfrak{G}\left(m_1^\dagger, m_2^\dagger, m_4, m_6\right) \\
 &+ G\left(m_3^\dagger, m_6\right) \mathfrak{G}\left(m_1^\dagger, m_2^\dagger, m_4, m_5\right) \tag{B.2b}
 \end{aligned}$$

$$+ \mathfrak{G}\left(m_1^\dagger, m_2^\dagger, m_3^\dagger, m_4, m_5, m_6\right). \tag{B.2c}$$

The same equation has been written down in short-hand notation in Eq. (4.42).

## B.2 Second-order equations of $G_1$ and $\mathfrak{G}_2$

Using the perturbational expansion of bath operators Eq. (A.13), Eq. (A.14) and Eq. (A.15) together with cluster expansions Eq. (B.1) and Eq. (B.2),

B.2. Second-order equations of  $G_1$  and  $\mathfrak{G}_2$

---

Eq. (4.7) of  $G_1$  — the first equation of the equation hierarchy becomes

$$\begin{aligned}
0 = & itG\left((m-1)^\dagger, n\right) + itG\left((m+1)^\dagger, n\right) \\
& - itG\left(m^\dagger, n+1\right) - itG\left(m^\dagger, n-1\right) \\
& + \lambda^2 \sum_{l,\alpha} \left[ \delta_{n\alpha} (\mathfrak{D}_{\alpha;l} + \bar{\mathfrak{D}}_{\alpha;l}^*) G\left(m^\dagger, l\right) \right. \\
& \quad \left. + \delta_{m\alpha} (\bar{\mathfrak{D}}_{\alpha;l} + \mathfrak{D}_{\alpha;l}^*) G\left(l^\dagger, n\right) \right] \\
& + \lambda^2 V_0 \sum_{\alpha, m_1, m_2} (\mathfrak{D}_{\alpha;nm_2m_1} - \mathfrak{D}_{\alpha;m_1m_2n}) G\left(m_1^\dagger, m_2\right) \delta_{m\alpha} \\
& + \lambda^2 V_0 \sum_{\alpha, m_1, m_2} (\mathfrak{D}_{\alpha;mm_1m_2} - \mathfrak{D}_{\alpha;m_2m_1m}) G\left(m_1^\dagger, m_2\right) \delta_{n\alpha} \\
& + \lambda^2 V_0^2 \sum_{\alpha, m_1, m_2, m_3} [\mathfrak{D}_{\alpha;m_3m_2m_1m_3n} + \mathfrak{D}_{\alpha;m_3m_3nm_2m_1} \\
& \quad + \mathfrak{D}_{\alpha;nm_2m_3m_3m_1} - \mathfrak{D}_{\alpha;m_1m_2m_3m_3n} \\
& \quad - \mathfrak{D}_{\alpha;m_3m_3m_1m_2n} - \mathfrak{D}_{\alpha;m_3m_2nm_3m_1}] G\left(m_1^\dagger, m_2\right) \delta_{m\alpha} \\
& + \lambda^2 V_0^2 \sum_{\alpha, m_1, m_2, m_3} [\mathfrak{D}_{\alpha;mm_1m_3m_3m_2} + \mathfrak{D}_{\alpha;m_3m_3mm_1m_2} \\
& \quad + \mathfrak{D}_{\alpha;m_3m_1m_2m_3m} - \mathfrak{D}_{\alpha;m_3m_1mm_3m_2} \\
& \quad - \mathfrak{D}_{\alpha;m_3m_3m_2m_1m} - \mathfrak{D}_{\alpha;m_2m_1m_3m_3m}] G\left(m_1^\dagger, m_2\right) \delta_{n\alpha} \quad (\text{B.3a}) \\
& - \lambda^2 \sum_{\alpha} (\delta_{m\alpha} \bar{\mathfrak{D}}_{\alpha;n} + \delta_{n\alpha} \bar{\mathfrak{D}}_{\alpha;m}^*)
\end{aligned}$$

$$\begin{aligned}
& + \lambda^2 V_0 \sum_{\alpha, m_1} (\mathfrak{D}_{\alpha;m_1m_1n} \delta_{m\alpha} + \mathfrak{D}_{\alpha;m_1m_1m} \delta_{n\alpha}) \\
& + \lambda^2 V_0^2 \sum_{\alpha, m_1, m_2} (\mathfrak{D}_{\alpha;m_1m_1m_2m_2n} \delta_{m\alpha} + \mathfrak{D}_{\alpha;m_1m_1m_2m_2m} \delta_{n\alpha}) \quad (\text{B.3b})
\end{aligned}$$

$$\begin{aligned}
& - iV_0 G\left(m^\dagger, (n-1)^\dagger, n, n-1\right) + iV_0 G\left((m+1)^\dagger, m^\dagger, (m+1), n\right) \\
& - iV_0 G\left((n+1)^\dagger, m^\dagger, n+1, n\right) + iV_0 G\left(m^\dagger, (m-1)^\dagger, n, m-1\right) \\
& + \lambda^2 V_0^2 \sum_{\alpha, m_1, m_2, m_3, m_4} \left\{ G\left(m_1^\dagger, m_2^\dagger, m_3, m_4\right) \right. \\
& \quad \cdot [\delta_{m\alpha} (\mathfrak{D}_{\alpha;m_1m_3nm_4m_2} + \mathfrak{D}_{\alpha;nm_3m_2m_4m_1} - \mathfrak{D}_{\alpha;m_2m_4m_1m_3n}) \\
& \quad \left. + \delta_{n\alpha} (\mathfrak{D}_{\alpha;m_3m_1mm_2m_4} - \mathfrak{D}_{\alpha;mm_1m_3m_2m_4} - \mathfrak{D}_{\alpha;m_4m_2m_3m_1m}) \right\} \quad (\text{B.3c})
\end{aligned}$$

*B.2. Second-order equations of  $G_1$  and  $\mathfrak{G}_2$*

---

Using the condensed  $\Gamma$  matrices notation introduced in Chapter 4, we can denote this equation as

$$\begin{aligned} & \left( \Gamma_{H_0}^{(1)} + \lambda^2 \Gamma_{B_0}^{(1)} + \lambda^2 V_0 \Gamma_{B_1}^{(1)} + \lambda^2 V_0 \Gamma_{B_2}^{(1)} \right) g_1 = \\ & \lambda^2 \nu_0 + \lambda^2 V_0 \nu_1 + \lambda^2 V_0^2 \nu_2 + (iV_0 + \lambda^2 V_0^2) \pi(g_1 g_1) + (iV_0 + \lambda^2 V_0^2) \mathfrak{g}_2. \end{aligned} \quad (\text{B.4})$$

Similarly we can derive an equation for  $\mathfrak{g}_2$  truncated at the order of  $V_0^2$  using these bath operators. It is a 10-pages long tedious equation so we here just write down its formal form in condensed matrices notation,

$$\begin{aligned} & \left( \Gamma_{H_0}^{(2)} + \lambda^2 \Gamma_{B_0}^{(2)} + \lambda^2 V_0 \Gamma_{B_1}^{(2)} + \lambda^2 V_0 \Gamma_{B_2}^{(2)} \right) (\mathfrak{g}_2 + \pi(g_1 g_1)) = \\ & \lambda^2 g_1 + \lambda^2 V_0 g_1 + \lambda^2 V_0^2 g_1 + (iV_0 + \lambda^2 V_0^2) \pi(g_1 g_1 g_1) + (iV_0 + \lambda^2 V_0^2) \pi(g_1 \mathfrak{g}_2). \end{aligned} \quad (\text{B.5})$$

In the calculation illustrated in the main text, we truncated the bath operators at the order of  $V_0$  instead of  $V_0^2$ . In this case, the second equation of

the hierarchy becomes,

$$\begin{aligned}
 0 = & itG\left(m^\dagger, (n-1)^\dagger, m', n'\right) + itG\left(m^\dagger, (n+1)^\dagger, m', n'\right) \\
 & + itG\left((m-1)^\dagger, n^\dagger, m', n'\right) + itG\left((m+1)^\dagger, n^\dagger, m', n'\right) \\
 & - itG\left(m^\dagger, n^\dagger, m', (n'+1)\right) - itG\left(m^\dagger, n^\dagger, m', (n'-1)\right) \\
 & - itG\left(m^\dagger, n^\dagger, (m'+1), n'\right) - itG\left(m^\dagger, n^\dagger, (m'-1), n'\right) \\
 & + iV_0G\left(m^\dagger, n^\dagger, m', n'\right) \left(\delta_{m'+1, n'} + \delta_{m'-1, n'}\right) \\
 & - iV_0G\left(m^\dagger, n^\dagger, m', n'\right) \left(\delta_{m+1, n} + \delta_{m-1, n}\right) \tag{B.6a}
 \end{aligned}$$

$$\begin{aligned}
 & - iV_0 \sum_{l=m\pm 1, n\pm 1} G\left(l^\dagger, m^\dagger, n^\dagger, l, m', n'\right) \\
 & + iV_0 \sum_{l=m'\pm 1, n'\pm 1} G\left(l^\dagger, m^\dagger, n^\dagger, l, m', n'\right) \tag{B.6b}
 \end{aligned}$$

$$\begin{aligned}
 -\lambda^2 \sum_{\alpha} \{ & \delta_{m\alpha} \left[ G\left(n^\dagger, m'\right) \bar{\mathfrak{D}}_{\alpha, n'} - G\left(n^\dagger, n'\right) \bar{\mathfrak{D}}_{\alpha, m'} \right] \\
 & - \delta_{n\alpha} \left[ G\left(m^\dagger, m'\right) \bar{\mathfrak{D}}_{\alpha, n'} - G\left(m^\dagger, n'\right) \bar{\mathfrak{D}}_{\alpha, m'} \right] \\
 & + \delta_{m'\alpha} \left[ G\left(m^\dagger, n'\right) \bar{\mathfrak{D}}_{\alpha, n} - G\left(n^\dagger, n'\right) \bar{\mathfrak{D}}_{\alpha, m} \right] \\
 & - \delta_{n'\alpha} \left[ G\left(m^\dagger, m'\right) \bar{\mathfrak{D}}_{\alpha, n} - G\left(n^\dagger, m'\right) \bar{\mathfrak{D}}_{\alpha, m} \right] \} \tag{B.6c} \\
 & + \lambda^2 \sum_{\alpha, l} (\mathfrak{D}_{\alpha, l} + \bar{\mathfrak{D}}_{\alpha, l})
 \end{aligned}$$

$$\begin{aligned}
 & \cdot \left[ \delta_{m\alpha} G\left(l^\dagger, n^\dagger, m', n'\right) + \delta_{n\alpha} G\left(m^\dagger, l^\dagger, m', n'\right) \right. \\
 & \left. + \delta_{m'\alpha} G\left(m^\dagger, n^\dagger, l, n'\right) + \delta_{n'\alpha} G\left(m^\dagger, n^\dagger, m', l\right) \right] \tag{B.6d}
 \end{aligned}$$

... to be continued

continued

$$\begin{aligned}
 & +V_0\lambda^2 \sum_{\alpha, m_1} \left\{ \delta_{m'_\alpha} \left[ G(m^\dagger, n') \mathfrak{D}_{\alpha, m_1 m_1 n} - G(n^\dagger, n') \mathfrak{D}_{\alpha, m_1 m_1 m} \right. \right. \\
 & \qquad \qquad \qquad \left. \left. + G(m_1^\dagger, n') (\mathfrak{D}_{\alpha, n m_1 m} - \mathfrak{D}_{\alpha, m m_1 n}) \right] \right. \\
 & - \delta_{n'_\alpha} \left[ G(m^\dagger, m') \mathfrak{D}_{\alpha, m_1 m_1 n} - G(n^\dagger, m') \mathfrak{D}_{\alpha, m_1 m_1 m} \right. \\
 & \qquad \qquad \qquad \left. \left. + G(m_1^\dagger, m') (\mathfrak{D}_{\alpha, n m_1 m} - \mathfrak{D}_{\alpha, m m_1 n}) \right] \right. \\
 & + \delta_{m_\alpha} \left[ G(n^\dagger, m') \mathfrak{D}_{\alpha, m_1 m_1 n'} - G(n^\dagger, n') \mathfrak{D}_{\alpha, m_1 m_1 m'} \right. \\
 & \qquad \qquad \qquad \left. \left. + G(n^\dagger, m_1) (\mathfrak{D}_{\alpha, n' m_1 m'} - \mathfrak{D}_{\alpha, m' m_1 n'}) \right] \right. \\
 & - \delta_{n_\alpha} \left[ G(m^\dagger, m') \mathfrak{D}_{\alpha, m_1 m_1 n'} - G(m^\dagger, n') \mathfrak{D}_{\alpha, m_1 m_1 m'} \right. \\
 & \qquad \qquad \qquad \left. \left. + G(m^\dagger, m_1) (\mathfrak{D}_{\alpha, n' m_1 m'} - \mathfrak{D}_{\alpha, m' m_1 n'}) \right] \right\} \quad (\text{B.6e}) \\
 & +V_0\lambda^2 \sum_{\alpha, m_1, m_2} \left\{ \delta_{m'_\alpha} \left[ \mathfrak{D}_{\alpha, m_1 n' m_2} G(m^\dagger, n^\dagger, m_1, m_2) \right. \right. \\
 & \qquad - (\mathfrak{D}_{\alpha, m_1 m_2 m} - \mathfrak{D}_{\alpha, m m_2 m_1}) G(m_2^\dagger, n^\dagger, m_1, n') \\
 & \qquad + (\mathfrak{D}_{\alpha, m_1 m_2 n} - \mathfrak{D}_{\alpha, n m_2 m_1}) G(m_2^\dagger, m^\dagger, m_1, n') \\
 & \qquad \qquad - \delta_{n'_\alpha} \left[ \mathfrak{D}_{\alpha, m_1 m' m_2} G(m^\dagger, n^\dagger, m_1, m_2) \right. \\
 & \qquad - (\mathfrak{D}_{\alpha, m_1 m_2 m} - \mathfrak{D}_{\alpha, m m_2 m_1}) G(m_2^\dagger, n^\dagger, m_1, m') \\
 & \qquad \left. \left. + (\mathfrak{D}_{\alpha, m_1 m_2 n} - \mathfrak{D}_{\alpha, n m_2 m_1}) G(m_2^\dagger, m^\dagger, m_1, m') \right] \right. \\
 & \qquad \qquad + \delta_{m_\alpha} \left[ \mathfrak{D}_{\alpha, m_1 n m_2} G(m_1^\dagger, m_2^\dagger, m', n') \right. \\
 & \qquad + (\mathfrak{D}_{\alpha, m_1 m_2 n'} - \mathfrak{D}_{\alpha, n' m_2 m_1}) G(n^\dagger, m_1^\dagger, m', m_2) \\
 & \qquad - (\mathfrak{D}_{\alpha, m_1 m_2 m'} - \mathfrak{D}_{\alpha, m' m_2 m_1}) G(n^\dagger, m_1^\dagger, n', m_2) \\
 & \qquad \qquad - \delta_{n_\alpha} \left[ \mathfrak{D}_{\alpha, m_1 m m_2} G(m_1^\dagger, m_2^\dagger, m', n') \right. \\
 & \qquad \left. \left. + (\mathfrak{D}_{\alpha, m_1 m_2 n'} - \mathfrak{D}_{\alpha, n' m_2 m_1}) G(m^\dagger, m_1^\dagger, m', m_2) \right. \right. \\
 & \qquad \left. \left. - (\mathfrak{D}_{\alpha, m_1 m_2 m'} - \mathfrak{D}_{\alpha, m' m_2 m_1}) G(m^\dagger, m_1^\dagger, n', m_2) \right] \right\} \quad (\text{B.6f})
 \end{aligned}$$

 Here  $G_3$  should be interpreted according to Eq. (4.42) but neglecting  $\mathfrak{G}_3$ .

*B.2. Second-order equations of  $G_1$  and  $\mathfrak{G}_2$*

---

However, for certain systems with relatively stronger interaction, it might be necessary to use these new equations at the order of  $V_0^2$ .

## Appendix C

# Estimation of convergence of the two methods of truncating the BBGKY-like hierarchy

In this chapter we present our estimation of the leading order of  $G_1$  such as  $\Delta_1^{E,(1)}$  and  $\Delta_1^{C,(1)}$ , defined in Chapter 4. We will see that  $\Delta_1^{E,(1)}$  in fact involves  $\Delta_2^{E,(0)}$ , which in turn needs Eq. (4.8) — the equation of  $G_2$ . A similar equation is needed for estimation of  $\Delta_1^{C,(1)}$ .

### C.1 $\Delta_1^{E,(1)}$ from method 1

In order to estimate the accuracy of the first-order form of this approximation and also to get an estimate of accuracy for higher orders, we study the leading order of residues in terms of  $\lambda^2$  and  $\frac{\Delta T}{T}$ , both of which are assumed to be small in the following. Thus  $\lambda^2 V_0 \ll V_0$ , therefore we know that in Eq. (4.24) the  $g_D$  term is smaller than the other  $g_2$  term so we drop it. Similarly since  $\lambda^2 \Delta T \ll \Delta T$ , we drop the  $\lambda^2 \Delta T$  term in  $\lambda^2 \nu$  in Eq(4.24),

$$\lambda^2 \nu = \lambda^2 \nu_0(T) + \lambda^2 \Delta T \nu_{,T}, \quad (\text{C.1})$$

and keep only the large term,  $\lambda^2 \nu_0(T)$ , which is independent of  $\Delta T$ . Here  $\nu_{,T}$  denotes formally a derivative of  $T$  on  $\nu$  —  $\frac{d}{dT} \nu$ . The general idea is then to write down respectively equations for  $g_1^{Ex}$  and  $g_1^{E,(1)}$ , and then compare the two to estimate  $\Delta_1^{E,(1)} = g_1^{E,(1)} - g_1^{Ex}$ . In order to understand how an approximation to the next order improves the accuracy, we also want to compare  $\Delta_1^{E,(1)}$  to  $\Delta_1^{E,(0)} = g_1^{E,(0)} - g_1^{Ex}$ , which is estimated in the same way from the difference between the equations respectively for  $g_1^{Ex}$  and  $g_1^{E,(0)}$ . More generally we define  $\Delta_n^{E,(0)} = g_n^{E,(0)} - g_n^{Ex}$  and  $\Delta_n^{E,(1)} = g_n^{E,(1)} - g_n^{Ex}$  for  $n$ -particle Green's functions  $g_n$ .

C.1.  $\Delta_1^{E,(1)}$  from method 1

---

After dropping the  $g_D$  term and the term which is proportional to  $\lambda^2 \Delta T$ , and keeping only up to the linear order of  $\Delta T$ ,  $g_1^{Ex}$ ,  $g_1^{E,(0)}$  and  $g_1^{E,(1)}$  respectively satisfy

$$\left(\Gamma_0^{(1)} + \Gamma_{,T}^{(1)} \Delta T\right) g_1^{Ex} = iV_0 g_2^{Ex} + \lambda^2 \nu_0, \quad (\text{C.2a})$$

$$\Gamma_0^{(1)} g_1^{E,(0)} = iV_0 g_2^{E,(0)} + \lambda^2 \nu_0, \quad (\text{C.2b})$$

$$\left(\Gamma_0^{(1)} + \Gamma_{,T}^{(1)} \Delta T\right) g_1^{E,(1)} = iV_0 g_2^{E,(0)} + \lambda^2 \nu_0, \quad (\text{C.2c})$$

where  $\Gamma_0^{(1)} + \Gamma_{,T}^{(1)} \Delta T$  is the zeroth and first order in  $\Delta T$  from  $\Gamma^{(1)}$  of Eq(4.24).  $\Gamma_{,T}^{(1)}$  denotes formally a derivative of  $T$  on  $\Gamma^{(1)}$  —  $\frac{d}{dT} \Gamma^{(1)}$ . To consider  $\Delta_1^{E,(0)}$ , one may use Eq(C.2a) and Eq(C.2b),

$$\Delta_1^{E,(0)} = \Delta T \left(\Gamma_0^{(1)}\right)^{-1} \Gamma_{,T}^{(1)} g_1^{Ex} + iV_0 \left(\Gamma_0^{(1)}\right)^{-1} \Delta_2^{E,(0)}. \quad (\text{C.3})$$

$\Delta_1^{E,(1)}$  can be estimated from Eq(C.2a) and Eq(C.2c),

$$\Delta_1^{E,(1)} = iV_0 \left(\Gamma_0^{(1)} + \Gamma_{,T}^{(1)} \Delta T\right)^{-1} \Delta_2^{E,(0)}, \quad (\text{C.4})$$

where  $\Delta_2^{E,(0)}$  is required. We find that roughly speaking  $\Delta_1^{E,(1)}$  takes the second term of  $\Delta_1^{E,(0)}$  but drops the first term. Therefore, next we only need to show that the second term,  $iV_0 \left(\Gamma_0^{(1)}\right)^{-1} \Delta_2^{E,(0)}$ , is much smaller than the first term, or equivalently, smaller than the whole  $\Delta_1^{E,(0)}$ .

Estimation of  $\Delta_2^{E,(0)}$  involves the second equation of the hierarchy, i.e. equation of  $G_2$ , which can be derived from substituting Eq(4.18) into Eq(4.8):

$$\begin{aligned}
0 = & it \langle c_m^\dagger c_n^\dagger c_{m'} c_{n'+1} \rangle + it \langle c_m^\dagger c_n^\dagger c_{m'} c_{n'-1} \rangle \\
& + it \langle c_m^\dagger c_n^\dagger c_{m'+1} c_{n'} \rangle + it \langle c_m^\dagger c_n^\dagger c_{m'-1} c_{n'} \rangle \\
& - it \langle c_m^\dagger c_{n-1}^\dagger c_{m'} c_{n'} \rangle - it \langle c_m^\dagger c_{n+1}^\dagger c_{m'} c_{n'} \rangle \\
& - it \langle c_{m-1}^\dagger c_n^\dagger c_{m'} c_{n'} \rangle - it \langle c_{m+1}^\dagger c_n^\dagger c_{m'} c_{n'} \rangle \\
& + \lambda^2 \sum_{l,\alpha} \left\{ \delta_{n'\alpha} d_{\alpha;l} \langle c_m^\dagger c_n^\dagger c_{m'} c_l \rangle + \delta_{m'\alpha} d_{\alpha;l} \langle c_m^\dagger c_n^\dagger c_l c_{n'} \rangle \right. \\
& + \delta_{n\alpha} \bar{d}_{\alpha;l} \langle c_m^\dagger c_l^\dagger c_{m'} c_{n'} \rangle + \delta_{m\alpha} \bar{d}_{\alpha;l} \langle c_l^\dagger c_n^\dagger c_{m'} c_{n'} \rangle \\
& + \delta_{n\alpha} d_{\alpha;l}^* \langle c_m^\dagger c_l^\dagger c_{m'} c_{n'} \rangle + \delta_{m\alpha} d_{\alpha;l}^* \langle c_l^\dagger c_n^\dagger c_{m'} c_{n'} \rangle \\
& \left. + \delta_{n'\alpha} \bar{d}_{\alpha;l}^* \langle c_m^\dagger c_n^\dagger c_{m'} c_l \rangle + \delta_{m'\alpha} \bar{d}_{\alpha;l}^* \langle c_m^\dagger c_n^\dagger c_l c_{n'} \rangle \right\} \\
& + iV_0 \langle c_m^\dagger c_n^\dagger c_{m'} c_{n'} \rangle \left( \delta_{m'+1,n'} + \delta_{m'-1,n'} - \delta_{m+1,n} - \delta_{m-1,n} \right) \quad (C.5a)
\end{aligned}$$

$$\begin{aligned}
& - iV_0 \sum_{l=m\pm 1, n\pm 1} \langle c_l^\dagger c_m^\dagger c_n^\dagger c_l c_{m'} c_{n'} \rangle \\
& + iV_0 \sum_{l=m'\pm 1, n'\pm 1} \langle c_l^\dagger c_m^\dagger c_n^\dagger c_l c_{m'} c_{n'} \rangle \quad (C.5b)
\end{aligned}$$

$$\begin{aligned}
& - \lambda^2 \sum_{\alpha} \left[ \delta_{n\alpha} \bar{d}_{\alpha;m'} \langle c_m^\dagger c_{n'} \rangle + \delta_{m\alpha} \bar{d}_{\alpha;n'} \langle c_n^\dagger c_{m'} \rangle \right. \\
& + \delta_{m'\alpha} \bar{d}_{\alpha;n} \langle c_m^\dagger c_{n'} \rangle + \delta_{n'\alpha} \bar{d}_{\alpha;m} \langle c_n^\dagger c_{m'} \rangle \\
& - \delta_{n\alpha} \bar{d}_{\alpha;n'} \langle c_m^\dagger c_{m'} \rangle - \delta_{m\alpha} \bar{d}_{\alpha;m'} \langle c_n^\dagger c_{n'} \rangle \\
& \left. - \delta_{n'\alpha} \bar{d}_{\alpha;n}^* \langle c_m^\dagger c_{m'} \rangle - \delta_{m'\alpha} \bar{d}_{\alpha;m}^* \langle c_n^\dagger c_{n'} \rangle \right] \quad (C.5c)
\end{aligned}$$

$$\begin{aligned}
& - \lambda^2 V_0 \sum_{\alpha} \left\{ \delta_{m'\alpha} \langle c_m^\dagger c_n^\dagger c_{n'} D_{\alpha} \rangle - \delta_{n'\alpha} \langle c_m^\dagger c_n^\dagger c_{m'} D_{\alpha} \rangle \right. \\
& + \delta_{m\alpha} \langle c_n^\dagger c_{m'} c_{n'} \bar{D}_{\alpha} \rangle - \delta_{n\alpha} \langle c_m^\dagger c_{m'} c_{n'} \bar{D}_{\alpha} \rangle + \delta_{n'\alpha} \langle \bar{D}_{\alpha}^\dagger c_m^\dagger c_n^\dagger c_{m'} \rangle \\
& \left. - \delta_{m'\alpha} \langle \bar{D}_{\alpha}^\dagger c_m^\dagger c_n^\dagger c_{n'} \rangle + \delta_{n\alpha} \langle D_{\alpha}^\dagger c_m^\dagger c_{m'} c_{n'} \rangle - \delta_{m\alpha} \langle D_{\alpha}^\dagger c_n^\dagger c_{m'} c_{n'} \rangle \right\}. \quad (C.5d)
\end{aligned}$$

This can be written in a compact matrix form as

$$\Gamma^{(2)} g_2^{Ex} = iV_0 g_3^{Ex} + \lambda^2 g_1^{Ex} + \lambda^2 V_0 g_{D3}^{Ex}, \quad (C.6)$$

C.1.  $\Delta_1^{E,(1)}$  from method 1

---

where vector  $g_2^{Ex}$  is defined as follows,

$$g_2^{Ex} = \left[ G_2 \left( 1^\dagger, 1^\dagger, 1, 1 \right), G_2 \left( 1^\dagger, 1^\dagger, 1, 2 \right), \dots, G_2 \left( N^\dagger, N^\dagger, N, N \right) \right]^T. \quad (\text{C.7})$$

Note that some of the elements of  $g_2^{Ex}$  are naturally zero but we still keep them in this vector.  $g_3^{Ex}$ ,  $g_1^{Ex}$  and  $g_{D3}^{Ex}$  come from ordering respectively Eq(C.5b), Eq(C.5c) and Eq(C.5d) in the same way as  $g_2^{Ex}$ . The matrix  $\Gamma^{(2)}$  can be read off from Eq(C.5a), for example assuming  $m, n, m', n'$  are all different and not equal to 1 or  $N$ , we have

$$\Gamma_{mN^3+nN^2+m'N+n', mN^3+nN^2+m'N+n'+1}^{(2)} = it. \quad (\text{C.8})$$

Since  $\lambda^2 V_0 \ll V_0$  we drop the  $g_{D3}^{Ex}$  term in the following estimation of the accuracy. Therefore, the exact solution and the equilibrium solution satisfy respectively,

$$\left( \Gamma_0^{(2)} + \Gamma_{,T}^{(2)} \Delta T \right) g_2^{Ex} = iV_0 g_3^{Ex} + \lambda^2 g_1^{Ex}, \quad (\text{C.9a})$$

$$\Gamma_0^{(2)} g_2^{E,(0)} = iV_0 g_3^{E,(0)} + \lambda^2 g_1^{E,(0)}, \quad (\text{C.9b})$$

where  $\Gamma_0^{(2)}$  and  $\Gamma_{,T}^{(2)} \Delta T$  stand for the zeroth and first order in  $\Delta T$  in  $\Gamma^{(2)}$ . Now  $\Delta_2^{E,(0)}$  can be analyzed:

$$\Delta_2^{E,(0)} = iV_0 \left( \Gamma_0^{(2)} \right)^{-1} \Delta_3^{E,(0)} + \left( \Gamma_0^{(2)} \right)^{-1} \Gamma_{,T}^{(2)} \Delta T g_2^{Ex} + \left( \Gamma_0^{(2)} \right)^{-1} \lambda^2 \Delta_1^{E,(0)}. \quad (\text{C.10})$$

Here, in fact  $\Gamma^{(1)}$  and  $\Gamma^{(2)}$  have different dimensions. However, in this estimation of order of magnitudes, we ignore this difference and furthermore the matrices are regarded as constants with order 1. For the moment, let us focus on the last term of  $\Delta_2^{E,(0)}$ . Recall that we want to compare  $iV_0 \left( \Gamma_0^{(1)} \right)^{-1} \Delta_2^{E,(0)}$  against  $\Delta_1^{E,(0)}$ . Focusing only on the last term, we have

$$iV_0 \Delta_2^{E,(0)} \approx iV_0 \lambda^2 \Delta_1^{E,(0)}, \quad (\text{C.11})$$

which is much smaller than  $\Delta_1^{E,(0)}$  as long as  $V_0 \lambda^2 \ll 1$ .

All together we have arrived at:

$$\Delta_1^{E,(0)} = \Delta T \left( \Gamma_0^{(1)} \right)^{-1} \Gamma_{,T}^{(1)} g_1^{Ex} + iV_0 \left( \Gamma_0^{(1)} \right)^{-1} \Delta_2^{E,(0)} \quad (\text{C.12})$$

C.2.  $\Delta_1^{C,(1)}$  from method 2

---

while

$$\Delta_1^{E,(1)} = \left(\Gamma_0^{(1)}\right)^{-1} \left[ -V_0^2 \left(\Gamma_0^{(2)}\right)^{-1} \Delta_3^{E,(0)} + iV_0 \Delta T \left(\Gamma_0^{(2)}\right)^{-1} \Gamma_{,T}^{(2)} g_2^{Ex} + iV_0 \lambda^2 \left(\Gamma_0^{(2)}\right)^{-1} \Delta_1^{E,(0)} \right]. \quad (\text{C.13})$$

Most importantly here we see that  $\Delta_1^{E,(0)}$  is multiplied by a small number  $\lambda^2 V_0$  and then becomes a part of  $\Delta_1^{E,(1)}$ . Judging from this it follows that, as long as  $\lambda^2 V_0$  is a small number compared with  $t$  the method is very reasonable. As for the other two additional terms, they can be regarded as  $(V_0^2 g_3^{Ex} + V_0 g_2^{Ex}) \Delta T$ . Therefore, the limit of maximum value of  $V_0$ , where this method is still applicable, is determined by  $|g_2^{Ex}|^{-1}$  or  $|g_3^{Ex}|^{-\frac{1}{2}}$ . Such limit could be much larger than 1 since roughly  $|g_n^{Ex}| = |g^{Ex}|^n$  — smaller for larger  $n$ . This explains why this method is applicable even for  $V_0$  larger than  $t$ , as confirmed from Fig.4.1.

## C.2 $\Delta_1^{C,(1)}$ from method 2

In order to estimate the accuracy of this approximation, let us assume that  $\lambda^2$  and  $V_0$  are small. We define  $\Delta_n^{C,(0)} = g_n^{C,(0)} - g_n^{Ex}$  and  $\Delta_n^{C,(1)} = g_n^{C,(1)} - g_n^{Ex}$ . Again we start from the equations of the three:  $g_1^{C,(0)}$ ,  $g_1^{C,(1)}$  and  $g_1^{Ex}$ , and then compare the three equations while ignoring certain higher-order terms such as terms which are proportional to  $\lambda^2 V_0$ .

In this case, after dropping the  $\Gamma_D^{(1)}$  term and terms which are proportional to  $\lambda^2 V_0$ , we find that  $g_1^{Ex}$ ,  $g_1^{C,0}$  and respectively  $g_1^{C,(1)}$  satisfy the following equations:

$$\Gamma_0^{(1)} g_1^{Ex} = iV_0 g_2^{Ex} + \lambda^2 \nu_0, \quad (\text{C.14a})$$

$$\Gamma_0^{(1)} g_1^{C,(0)} = \lambda^2 \nu_0, \quad (\text{C.14b})$$

$$\Gamma_0^{(1)} g_1^{C,(1)} = iV_0 g_2^{C,(1)} + \lambda^2 \nu_0. \quad (\text{C.14c})$$

From Eq(C.14b) and Eq(C.14a) we find

$$\Delta_1^{C,(0)} = -iV_0 \left(\Gamma_0^{(1)}\right)^{-1} g_2^{Ex}. \quad (\text{C.15})$$

C.2.  $\Delta_1^{C,(1)}$  from method 2

---

Comparing Eq(C.14c) and Eq(C.14a), we get

$$\Delta_1^{C,(1)} = iV_0 \left( \Gamma_0^{(1)} \right)^{-1} \left( g_2^{C,(1)} - g_2^{Ex} \right). \quad (\text{C.16})$$

Note that the magnitude of  $\Delta_2^{C,(1)} = \left( g_2^{C,(1)} - g_2^{Ex} \right)$  is in fact smaller than the magnitude of  $\Delta_2^{C,(0)} = \left( g_2^{C,(0)} - g_2^{Ex} \right)$ . Both involve the second equation of the hierarchy, i.e. the equation for  $G_2$ . So we may analyze the latter to get an upper bound of the former. In this case, we substitute Eq(4.34) into Eq(4.8). The resulting equation will have the same structure as Eq(C.5) but every  $d_{\alpha;l}$  and  $\bar{d}_{\alpha;l}$  are replaced respectively by  $\mathfrak{D}_{\alpha;m}$  and  $\bar{\mathfrak{D}}_{\alpha;m}$ , and a similar substitution for  $D_\alpha$  and  $\bar{D}_\alpha$ . Ignoring terms which are proportional to  $\lambda^2 V_0$ , it follows that  $g_2^{Ex}$  and  $g_2^{C,(0)}$  are respectively the solutions of

$$\Gamma_0^{(2)} g_2^{Ex} = iV_0 g_3^{Ex} + \lambda^2 g_1^{Ex}, \quad (\text{C.17a})$$

$$\Gamma_0^{(2)} g_2^{C,(0)} = \lambda^2 g_1^{C,(0)}. \quad (\text{C.17b})$$

Comparing these two equations, we find that

$$\Delta_2^{C,(0)} = -iV_0 \left( \Gamma_0^{(2)} \right)^{-1} g_3^{Ex} - \lambda^2 \left( \Gamma_0^{(2)} \right)^{-1} \Delta_1^{C,(0)}. \quad (\text{C.18})$$

Focusing only on the last term, we have

$$iV_0 \Delta_2^{C,(0)} \approx -iV_0 \lambda^2 \Delta_1^{C,(0)}, \quad (\text{C.19})$$

which is much smaller than  $\Delta_1^{C,(0)}$  as long as  $V_0 \lambda^2 \ll 1$ .

We arrived at:

$$\Delta_1^{C,(0)} = -iV_0 \left( \Gamma_0^{(1)} \right)^{-1} g_2^{Ex} \sim V_0 |g_1^{Ex}|^2, \quad (\text{C.20})$$

and

$$\begin{aligned} \Delta_1^{C,(1)} &= \left( \Gamma_0^{(1)} \right)^{-1} \left[ iV_0^2 \left( \Gamma_0^{(2)} \right)^{-1} g_3^{Ex} + \lambda^2 V_0 \left( \Gamma_0^{(2)} \right)^{-1} \Delta_1^{C,(0)} \right] \\ &\sim V_0^2 |g_1^{Ex}|^3 + \lambda^2 V_0^2 |g_1^{Ex}|^2. \end{aligned} \quad (\text{C.21})$$

This agrees with the numerical results that  $\Delta_1^{C,(0)}$  is proportional to  $V_0$  while  $\Delta_1^{C,(1)}$  is proportional to  $V_0^2$ . Most importantly, we see again that  $\Delta_1^{C,(0)}$  is multiplied by a small number  $\lambda^2 V_0$  and then becomes a part of  $\Delta_1^{C,(1)}$ . Since

### C.2. $\Delta_1^{C,(1)}$ from method 2

---

roughly  $|g_n^{Ex}| = |g^{Ex}|^n$ , the other term,  $V_0^2 g_3^{Ex} \sim V_0^2 |g_1^{Ex}|^3$ , is also much smaller than  $\Delta_1^{C,(0)} \sim V_0 |g_1^{Ex}|^2$ . However, for large enough  $V_0$  the other approximation used in this method, the perturbational expansion of the operators  $\hat{m}$ , becomes invalid. Therefore, as long as  $V_0$  is a small number compared to  $t$  the method is very reasonable. It should be noted that this method is capable of dealing with large systems since it does not require a direct diagonalization of a  $2^N$ -dimension matrix.

## Appendix D

# Coherent states and coherent-state representation

To provide a convenient reference, in this appendix, we briefly describe the general idea of coherent-state representation. More details can be found in for example Ref. [70, 71]. Here we will only discuss bosonic coherent states. Fermionic ones can be defined similarly with the usual complex numbers replaced by Grassman numbers[71].

In the §D.1, coherent states for single-mode bosonic systems is introduced and the simplest  $P$ -representation is discussed. In the §D.2, we discuss correspondingly the coherent-state representations for multi-mode bosonic systems. We also briefly review the more general positive  $P$ -representation.

### D.1 Coherent states for systems with a single mode

A single-mode bosonic system is defined by a Hamiltonian  $H(a, a^\dagger)$ , where  $a, a^\dagger$  are respectively annihilation and creation operators of a particle with the particular mode. Its Hilbert space, expanded in occupation-number representation, is  $\{|n\rangle\}$ , where  $n = 0, 1, 2, \dots$ .

A coherent state  $|\xi\rangle$  is defined to be an eigenstate of annihilation operator,

$$a |\xi\rangle = \xi |\xi\rangle \quad (\text{D.1})$$

with eigenvalue  $\xi$ . Operator  $a$  is not a hermitian operator so  $\xi$  is not a real but a complex number ( $c$ -number). Let us define a displacement operator

$$D(\xi) = e^{\xi a^\dagger - \xi^* a}, \quad (\text{D.2})$$

which equals to

$$D(\xi) = e^{-\frac{|\xi|^2}{2}} e^{\xi a^\dagger} e^{-\xi^* a}, \quad (\text{D.3})$$

### D.1. Coherent states for systems with a single mode

---

utilizing the Baker-Campbell-Hausdorff formula[70]. From there one can verify that

$$|\xi\rangle = D(\xi) |0\rangle, \quad (\text{D.4})$$

where  $|0\rangle$  is the vacuum state.

This can be seen in the following. Let us express  $D(\xi) |0\rangle$  in terms of occupation-number states  $|n\rangle$  and note  $|n\rangle = \frac{(a^\dagger)^n}{\sqrt{n!}} |0\rangle$ ,

$$\begin{aligned} D(\xi) |0\rangle &= e^{-\frac{|\xi|^2}{2}} e^{\xi a^\dagger} |0\rangle \\ &= e^{-\frac{|\xi|^2}{2}} \sum_{n=0}^{\infty} \frac{\xi^n}{n!} (a^\dagger)^n |0\rangle \\ &= e^{-\frac{|\xi|^2}{2}} \sum_{n=0}^{\infty} \frac{\xi^n}{\sqrt{n!}} |n\rangle. \end{aligned} \quad (\text{D.5})$$

Therefore

$$\begin{aligned} aD(\xi) |0\rangle &= e^{-\frac{|\xi|^2}{2}} \sum_{n=0}^{\infty} \frac{\xi^n}{\sqrt{(n-1)!}} |n-1\rangle \\ &= \xi e^{-\frac{|\xi|^2}{2}} \sum_{m=0}^{\infty} \frac{\xi^m}{\sqrt{(m)!}} |m\rangle = \xi D(\xi) |0\rangle. \end{aligned} \quad (\text{D.6})$$

Inner product between two coherent states  $|\xi\rangle$  and  $|\eta\rangle$  is,

$$\langle \xi | \eta \rangle = e^{\xi^* \eta - \frac{|\xi|^2}{2} - \frac{|\eta|^2}{2}}, \quad (\text{D.7})$$

so

$$|\langle \xi | \eta \rangle|^2 = e^{-|\xi - \eta|^2}, \quad (\text{D.8})$$

which is close to zero when  $\xi$  is very different from  $\eta$ . This implies that although no pair of the coherent states are orthogonal to each other but the overlap tends to be small if their corresponding eigenvalues are very different.

This suggests that maybe the set of coherent states can be used as a basis to expand operators and vectors. Due to the non-orthogonal relation, such forms of basis are not unique. One particular convenient and important choice is

$$I = \frac{1}{\pi} \int d^2\xi |\xi\rangle \langle \xi|. \quad (\text{D.9})$$

This can be verified by considering arbitrary  $|n\rangle$  such that

$$|n\rangle = \frac{1}{\pi} \int d^2\xi |\xi\rangle \langle \xi | n \rangle, \quad (\text{D.10})$$

which becomes

$$\begin{aligned} |n\rangle &= \sum_m \frac{1}{\pi} \int d^2\xi |m\rangle \langle m | \xi \rangle \langle \xi | n \rangle \\ &= \sum_m |m\rangle \frac{1}{\pi} \int d^2\xi e^{-|\xi|^2} \frac{\xi^m}{\sqrt{(m)!}} \frac{(\xi^*)^n}{\sqrt{(n)!}} \\ &= \sum_m |m\rangle \delta_{mn} = |n\rangle. \end{aligned} \quad (\text{D.11})$$

Here we have used

$$\frac{1}{\pi} \int d^2\xi e^{-|\xi|^2} \frac{\xi^m}{\sqrt{(m)!}} \frac{(\xi^*)^n}{\sqrt{(n)!}} = \delta_{mn}, \quad (\text{D.12})$$

which is 1 only when  $m = n$  and zero otherwise.

With this basis, a density matrix  $\rho$  (or a more general physical observable operator  $A$ ) can always be expanded as[126]

$$\rho = \frac{1}{\pi^2} \iint d^2\xi d^2\eta e^{-\frac{|\xi|^2}{2} - \frac{|\eta|^2}{2}} R(\xi^*, \eta) |\xi\rangle \langle \eta|. \quad (\text{D.13})$$

where

$$R(\xi^*, \eta) = e^{\frac{|\xi|^2}{2} + \frac{|\eta|^2}{2}} \langle \xi | \rho | \eta \rangle. \quad (\text{D.14})$$

This distribution function  $R(\xi^*, \eta)$  holds generally for all  $\rho$  and it is called the  $R$  representation. However, since the overcompleteness and the non-uniqueness of the coherent-state representation, there are other expansions, which hold not for all but a large class of density matrices[70]. For example, the  $P$  representation and the Positive  $P$  representation are respectively defined as

$$\rho = \int d^2\xi P(\xi^*, \xi) |\xi\rangle \langle \xi|, \quad (\text{D.15})$$

and

$$\rho = \iint d^2\xi d^2\eta P(\xi, \eta) e^{\frac{|\xi|^2}{2} + \frac{|\eta|^2}{2} - \xi\eta} |\xi\rangle \langle \eta^*|. \quad (\text{D.16})$$

## D.2. Coherent states for multi-mode systems

---

Next we convert operator  $a$  and  $a^\dagger$  to be operators acting on such distribution function  $P$ , in for example, the  $P$  representation. For  $a\rho$ ,

$$\begin{aligned} a\rho &= \int d^2\xi P(\xi^*, \xi) a|\xi\rangle \langle\xi| \\ &= \int d^2\xi \xi P(\xi^*, \xi) |\xi\rangle \langle\xi|, \end{aligned} \quad (\text{D.17})$$

so  $a \rightarrow \xi$ . For  $a^\dagger\rho$ , noticing  $a^\dagger|\xi\rangle = \frac{d}{d\xi}|\xi\rangle$

$$\begin{aligned} a^\dagger\rho &= \int d^2\xi P(\xi^*, \xi) \left(\frac{d}{d\xi}|\xi\rangle\right) \langle\xi| \\ &= \int d^2\xi \left(\xi^* - \frac{d}{d\xi}\right) P(\xi^*, \xi) |\xi\rangle \langle\xi|, \end{aligned} \quad (\text{D.18})$$

so  $a^\dagger \rightarrow \xi^* - \frac{d}{d\xi}$ . Similarly we need to consider also  $\rho a$  and  $\rho a^\dagger$ . Summarize all those operators, we have

$$\begin{aligned} a\rho &\leftrightarrow \xi P(\xi^*, \xi), \\ \rho a^\dagger &\leftrightarrow \xi^* P(\xi^*, \xi), \\ a^\dagger\rho &\leftrightarrow \left(\xi^* - \frac{\partial}{\partial\xi}\right) P(\xi^*, \xi), \\ \rho a &\leftrightarrow \left(\xi - \frac{\partial}{\partial\xi^*}\right) P(\xi^*, \xi). \end{aligned} \quad (\text{D.19})$$

## D.2 Coherent states for multi-mode systems

For a multi-mode (countably many, denoted as  $N$ ) system, a coherent basis can be defined similarly as

$$|\vec{\xi}\rangle = D(\vec{\xi})|0\rangle = e^{\vec{\xi}\cdot\vec{a}^\dagger - \vec{\xi}^*\cdot\vec{a}}|0\rangle = e^{-\frac{|\vec{\xi}|^2}{2}} e^{\vec{\xi}\cdot\vec{a}^\dagger}|0\rangle, \quad (\text{D.20})$$

where  $\vec{\xi} = (\xi_1, \xi_2, \dots, \xi_N)^T$  and  $\vec{a}^\dagger = (a_1^\dagger, a_2^\dagger, \dots, a_N^\dagger)^T$ .  $a_l^\dagger$  is the creation operator at site  $l$ ,  $\xi_l$  is a  $c$  number and  $|0\rangle$  is the vacuum state. Coherent states are over complete. One convenient choice of representation is the  $P$ -representation[70], which decomposes the identity as

$$I = \frac{1}{\pi} \int d^2\xi |\vec{\xi}\rangle \langle\vec{\xi}|, \quad (\text{D.21})$$

*D.2. Coherent states for multi-mode systems*

---

and it maps a density matrix  $\rho$  (a physical quantity  $A$ ) to a function  $P(\vec{\xi}^*, \vec{\xi})$  ( $A(\vec{\xi}^*, \vec{\xi})$ ) such that

$$\rho = \int d^2\vec{\xi} P(\vec{\xi}^*, \vec{\xi}) |\vec{\xi}\rangle \langle \vec{\xi}|, \quad (\text{D.22})$$

$$\langle A \rangle = \int d^2\vec{\xi} P(\vec{\xi}^*, \vec{\xi}) A(\vec{\xi}^*, \vec{\xi}). \quad (\text{D.23})$$

If  $A$  is in normal order of  $a_l, a_l^\dagger$ .

In this representation, operators  $a, a^\dagger$  become differential operators on  $P(\vec{\xi}^*, \vec{\xi})$ ,

$$\begin{aligned} a_l \rho &\leftrightarrow \xi_l P(\vec{\xi}^*, \vec{\xi}), \\ \rho a_l^\dagger &\leftrightarrow \xi_l^* P(\vec{\xi}^*, \vec{\xi}), \\ a_l^\dagger \rho &\leftrightarrow \left( \xi_l^* - \frac{\partial}{\partial \xi_l} \right) P(\vec{\xi}^*, \vec{\xi}), \\ \rho a_l &\leftrightarrow \left( \xi_l - \frac{\partial}{\partial \xi_l^*} \right) P(\vec{\xi}^*, \vec{\xi}). \end{aligned} \quad (\text{D.24})$$

In this way, the operator-form QME can be mapped to a differential equation.

## Appendix E

# Fokker-Planck equation and Langevin equation

A standard Fokker-Planck equation with time-independent coefficients reads,

$$\frac{\partial}{\partial t} P(\vec{\xi}, t) = \left[ - \sum_j \frac{\partial}{\partial \xi_j} \mathcal{A}_j(\vec{\xi}) + \frac{1}{2} \sum_{i,j} \frac{\partial^2}{\partial \xi_i \partial \xi_j} \mathcal{D}_{ij}(\vec{\xi}) \right] P(\vec{\xi}, t). \quad (\text{E.1})$$

When there are higher-order derivative terms besides the above first two terms, it is called a generalized Fokker-Planck equation. The Pawula theorem[98] states that in order to keep the distribution function ( $P(\vec{\xi}, t)$ ) non-negative, there has to be either only 2 terms or infinity terms. In the later case, unless the equation is exactly solvable usually the generalized Fokker-Planck equation is truncated first and then solved. However, while truncation at the second order keeps the positiveness, a further truncation beyond the second order which destroys such positiveness in small regions, could result a more accurate distribution function[98].

In this appendix we discuss solutions of the Fokker-Planck equation and the generalized Fokker-Planck equation. Note here  $\vec{\xi}$  is a vector of real random variables. It is not directly applicable for the generalized Fokker-Planck equation in  $c$ -numbers we derived in the previous chapters.

### E.1 Langevin equation for standard Fokker-Planck equations

There are several approaches to solve the standard Fokker-Planck equation besides brute-force numerical solution in the whole space of  $\{\vec{\xi}\}$ . Converting it to a set of equivalent Langevin equation[98] with white noise and then numerically simulate the Langevin equation is a common and general method. A standard Langevin equation states,

$$\dot{\xi}_i = h_i(\vec{\xi}) + g_{ij}(\vec{\xi}) w_j(t), \quad (\text{E.2})$$

*E.1. Langevin equation for standard FPEs*

---

where we only consider the time-independent coefficients  $\mathcal{A}_j(\vec{\xi})$  and  $\mathcal{D}_{ij}(\vec{\xi})$ , and  $\vec{w}(t)$  is a white noise,

$$\langle w_i(t) \rangle = 0, \langle w_i(t) w_j(t') \rangle = \delta_{ij} \delta(t - t'). \quad (\text{E.3})$$

Using Itô calculus[98], one can define a correspondence between the standard Fokker-Planck equation and the Langevin equation. Assuming  $\mathcal{D}_{ij}(\vec{\xi})$  is positive semidefinite such that there is a matrix  $G$  satisfying

$$\mathcal{D}(\vec{\xi}) = G(\vec{\xi}) G^\dagger(\vec{\xi}), \quad (\text{E.4})$$

then

$$g_{ij}(\vec{\xi}) = G_{ij}(\vec{\xi}), \quad (\text{E.5})$$

$$h_i(\vec{\xi}) = \mathcal{A}_i(\vec{\xi}). \quad (\text{E.6})$$

In numerical simulation, one works with directly

$$d\xi_i = h_i(\vec{\xi}) dt + g_{ij}(\vec{\xi}) dW_j(t), \quad (\text{E.7})$$

where

$$\langle dW_i(t) \rangle = 0, \langle dW_i(t) dW_j(t') \rangle = \delta_{ij} dt \delta_{t,t'}. \quad (\text{E.8})$$

Here  $\delta_{t,t'}$  is the Kronecker  $\delta$  not the Dirac  $\delta$ .

Another way to solve the Fokker-Planck equation is to convert it into equations of correlations by considering for example,  $\langle x_l \rangle$  and  $\langle x_l x_m \rangle$  etc.. Let us work out the first derivative term for the above one-variable average,

$$\begin{aligned} \frac{d}{dt} \langle \xi_l \rangle &= - \langle \xi_l \sum_j \frac{\partial}{\partial \xi_j} \mathcal{A}_j \rangle \\ &= - \langle \sum_j \frac{\partial}{\partial \xi_j} \xi_l \mathcal{A}_j \rangle + \langle \mathcal{A}_l \sum_j \frac{\partial}{\partial \xi_j} \xi_l \rangle = \langle \mathcal{A}_l \rangle. \end{aligned} \quad (\text{E.9})$$

Here we have used the following property: for arbitrary  $F(\vec{\xi})$ , as long as  $\lim_{\xi_j \rightarrow \infty} F(\vec{\xi})$  does not diverge, we have

$$\left\langle \frac{\partial}{\partial \xi_j} F(\vec{\xi}) \right\rangle = \int d^2 \vec{\xi} \frac{\partial}{\partial \xi_j} [F(\vec{\xi}) P(\vec{\xi})] = 0. \quad (\text{E.10})$$

In this way, one can derive equations for correlations of any number of variables. However, then one has to solve such possibly coupled equations if many-variable correlations are of interest.

## E.2 Analytical solution for the Ornstein-Uhlenbeck process

For a special case – the Ornstein-Uhlenbeck process, there is an analytical solution. An Ornstein-Uhlenbeck process has a constant diffusion matrix  $\mathcal{D}$  and a linear drift term  $\vec{A} = \Gamma \vec{\xi}$ . We further require  $\Gamma$  is positive definite in order to have a non-divergent distribution function. Although time-dependent solution is also possible, here we focus on stationary solution,

$$P = (2\pi)^{-\frac{N}{2}} (\text{Det}\sigma)^{-\frac{1}{2}} e^{-\frac{1}{2}\vec{\xi}^T \sigma^{-1} \vec{\xi}}, \quad (\text{E.11})$$

where

$$\sigma = \sum_{l,m} \frac{1}{\kappa_l + \kappa_m^*} \langle v^l | \mathcal{D} | v^m \rangle |u_l\rangle \langle u_m|, \quad (\text{E.12})$$

and

$$\Gamma = \sum_l \kappa_l |u_l\rangle \langle v^l|. \quad (\text{E.13})$$

The last expression defines  $\langle v^l |$  ( $|u_l\rangle$ ) as the left (right) eigenvector of  $\Gamma$  with eigenvalue  $\kappa_l$ . Out of all above approaches, only the simulation via Langevin equation is generally applicable, even for generalized Fokker-Planck equations.

## E.3 Stochastic difference equation for truncated generalized Fokker-Planck equations

A generalized Fokker-Planck equation with time-independent coefficients truncated at the third-order derivatives reads,

$$\begin{aligned} \frac{\partial}{\partial t} P(\vec{\xi}) = & \left[ - \sum_j \frac{\partial}{\partial \xi_j} \mathcal{A}_j(\vec{\xi}) + \frac{1}{2} \sum_{i,j} \frac{\partial^2}{\partial \xi_i \partial \xi_j} \mathcal{D}_{ij}(\vec{\xi}) \right. \\ & \left. + \frac{1}{6} \sum_{i,j,k} \frac{\partial^3}{\partial \xi_i \partial \xi_j \partial \xi_k} \mathcal{D}_{ijk}(\vec{\xi}) \right] P(\vec{\xi}). \end{aligned} \quad (\text{E.14})$$

Now let us solutions of this generalized Fokker-Planck equation. For such generalized Fokker-Planck equation an equivalent stochastic difference equation[102] for numerical molecular dynamical simulations can be found. In that case, usually the positive  $P$ -representation[72] or the gauge  $P$ -representation is

### E.3. Stochastic difference equation for truncated GFPEs

---

used. The basic idea is to use proper random variables to mimic the effect of the third order term just like what was done for the second derivative terms. For example,

$$\frac{\partial}{\partial \xi_i} \mathcal{A}_i \rightarrow \langle \Delta \xi_i \rangle = \mathcal{A}_i \Delta T, \quad (\text{E.15})$$

$$\frac{\partial^2}{\partial \xi_i \partial \xi_j} \mathcal{D}_{ij} \rightarrow \langle \Delta \xi_i \Delta \xi_j \rangle = \mathcal{D}_{ij} \Delta T, \quad (\text{E.16})$$

$$\frac{\partial^3}{\partial \xi_i \partial \xi_j \partial \xi_k} \mathcal{D}_{ijk} \rightarrow \langle \Delta \xi_i \Delta \xi_j \Delta \xi_k \rangle = \mathcal{D}_{ijk} \Delta T. \quad (\text{E.17})$$

Therefore, there will be terms like  $\eta_{ijk} (\Delta T)^{\frac{1}{3}}$  appearing in the stochastic difference equation to make sure the above average holds,

$$\Delta \xi_i = h_i \Delta t + g_i (\Delta t)^{\frac{1}{2}} + k_i (\Delta T)^{\frac{1}{3}}. \quad (\text{E.18})$$

just like  $g_i$  happens to be  $g_{ij} w_j$  such that Eq. (E.16) is satisfied,  $k_i$  has to be defined properly to obey Eq. (E.17). Generally relation between  $k_i$  and  $\mathcal{D}_{ijk}$  is still missing, but specific forms for example equations can be found in Ref.[102].

## Appendix F

# Solving the Redfield equation and the local-operator Lindblad equation of bosonic systems with BBGKY-like hierarchy

The BBGKY-like method is based on the equation of motion of the Green's functions. The method starts from turning the Redfield equation, Eq. (4.2) into equation of motion of Green's functions, which is defined by single-particle Green's function  $G(l^\dagger; n) = \langle a_l^\dagger a_n \rho(\infty) \rangle$  ( $G_1$  for short), two-article Green's function  $G(i^\dagger, j^\dagger; l, n) = \langle a_i^\dagger a_j^\dagger a_l a_n \rho(\infty) \rangle$  ( $G_2$  for short) and so on. Here again the density matrix  $\rho(\infty)$  refers to a stationary state and it is defined by  $L\rho(\infty) = 0$ . Then generally for interacting systems the stationary equation becomes an equation hierarchy, in the first order of which are equations for  $G_1$ . But such  $G_1$  is coupled to  $G_2$ . The next order in the hierarchy are equations for  $G_2$  and such  $G_2$  is coupled to  $G_1$  and  $G_3$ , and so on. The hierarchy can be truncated and solved if one takes certain further approximations such as cluster expansion[101]. Since the difference between the Redfield equation and the local-operator Lindblad equation is only at the bath operators, the following calculation is in fact valid for both equations. Of course, all those coefficients  $D_{\gamma,m}$  should then be substituted properly for the local-operator Lindblad equation.

The operator-form Redfield equation reads

$$\frac{\partial \rho}{\partial t} = \mathcal{L}_{H_0} \rho + U \mathcal{L}_V \rho + \lambda^2 \mathcal{L}_B^0 \rho + \lambda^2 U \mathcal{L}_B^1 \rho, \quad (\text{F.1})$$

where

$$\mathcal{L}_{H_0}\rho = -i \sum_{l=1}^{N-1} \left[ a_l^\dagger a_{l+1} + a_{l+1}^\dagger a_l, \rho \right] \quad (\text{F.2a})$$

$$\mathcal{L}_V\rho = \frac{-i}{2} \sum_{l=1}^N \left[ a_l^\dagger a_l (a_l^\dagger a_l - 1), \rho \right] \quad (\text{F.2b})$$

$$\mathcal{L}_B^{(0)}\rho = - \sum_{\gamma=L,R} \left\{ D_{\gamma,m} \left[ a_\gamma^\dagger, a_m \rho \right] + \bar{D}_{\gamma,m} \left[ a_\gamma, a_m^\dagger \rho \right] + h.c. \right\} \quad (\text{F.2c})$$

$$\begin{aligned} \mathcal{L}_B^{(1)}\rho = - \sum_{\gamma,m_1,m_2,m_3} D_{\gamma,m_1 m_2 m_3} \left\{ \left[ a_\gamma^\dagger, a_{m_1}^\dagger a_{m_2} a_{m_3} \rho \right] \right. \\ \left. + \left[ a_\gamma, a_{m_3}^\dagger a_{m_2}^\dagger a_{m_1} \rho \right] + h.c. \right\}. \end{aligned} \quad (\text{F.2d})$$

Let us now transform the above Redfield equation in the operator form into equations of Green's functions by multiplying  $a_l^\dagger a_n$  at the RHS of Eq.(3.30) and then performing a trace,

$$0 = -i\langle a_l^\dagger a_{n+1} \rangle - i\langle a_l^\dagger a_{n-1} \rangle + i\langle a_{l+1}^\dagger a_n \rangle + i\langle a_{l-1}^\dagger a_n \rangle \quad (\text{F.3a})$$

$$+ \lambda^2 \sum_{\gamma,m} (\bar{D}_{\gamma,m} - D_{\gamma,m}) \left[ \delta_{n\gamma} \langle a_l^\dagger a_m \rangle + \delta_{l\gamma} \langle a_m^\dagger a_n \rangle \right] \quad (\text{F.3b})$$

$$+ \lambda^2 \sum_{\gamma} (\bar{D}_{\gamma,n} \delta_{l\gamma} + \bar{D}_{\gamma,l} \delta_{n\gamma}) \quad (\text{F.3c})$$

$$+ iU \langle a_l^\dagger a_l^\dagger a_l a_n \rangle - iU \langle a_l^\dagger a_n^\dagger a_n a_n \rangle \quad (\text{F.3d})$$

$$\begin{aligned} + \lambda^2 U \sum_{\gamma,m_i} D_{\gamma,m_1 m_2 m_3} \left[ \delta_{n\gamma} \left( \langle a_{m_1}^\dagger a_{m_2} \rangle \delta_{lm_3} + \langle a_{m_1}^\dagger a_{m_3} \rangle \delta_{lm_2} \right) \right. \\ \left. + \delta_{l\gamma} \left( \langle a_{m_2}^\dagger a_{m_1} \rangle \delta_{nm_3} + \langle a_{m_3}^\dagger a_{m_1} \rangle \delta_{nm_2} \right) \right]. \end{aligned} \quad (\text{F.3e})$$

## F.1 Exact solution on non-interacting systems

Note that when  $U = 0$  only Eq. (F.3a), Eq. (F.3b) and Eq. (F.3c) are there so that this equation is closed. In this section we consider only the  $U = 0$  case. This is an  $N^2$ -dimension linear system for unknown  $G_1^{(0)}$ , where (0) refers to  $U = 0$ ,

$$\Gamma_{H_0} g_1^{(0)} + \lambda^2 \Gamma_{B_0} g_1^{(0)} = \lambda^2 \nu^{(0)}. \quad (\text{F.4})$$

Here we arrange all unknown  $G_1$  into a vector  $g_1 = (G_1(1,1), G_1(1,2), \dots)^T$ . Elements of the two matrices and the vector can be read off from Eq. (4.7).

For example,

$$(\Gamma_{H_0})_{l*N+n, l*N+n+1} = -i, \quad (\text{F.5})$$

and when  $l = 1$  (or  $l = N$ , or  $n = 1, N$ ),

$$\nu_{1*N+n}^{(0)} = \lambda^2 \bar{D}_{1,n}, \quad (\text{F.6})$$

otherwise, it is zero. Solving this  $N^2$ -dimension linear system we find all  $G_1$ .

## F.2 Approximate solution on interacting systems

Note that when  $U \neq 0$  this equation is not closed. This means that one need to consider the next order equation in terms of  $G_2$  together to solve the whole Eq.(3.30). One can derive such equation by multiplying  $a_i^\dagger a_j^\dagger a_l a_n$  and then performing a trace. In fact, if one do so, one will find that equations of  $G_2$  is coupled to  $G_3$  and so on[101]. Therefore, one has to solve the whole hierarchy to solve Eq.(3.30) exactly, which is as hard as dealing with directly Eq. (3.30). So we have to come up with some further approximation to truncate the hierarchy and then solve it. In the present work, we will truncate the hierarchy at the first order by using the cluster expansion[101],

$$\langle a_i^\dagger a_l^\dagger a_l a_n \rangle = 2 \langle a_l^\dagger a_l \rangle \langle a_i^\dagger a_n \rangle + o(U). \quad (\text{F.7})$$

So we will do not need explicitly the second order equations here.

After taking the approximation of the cluster expansion, Eq. (F.3d) becomes,

$$iU2 \langle a_l^\dagger a_l \rangle \langle a_i^\dagger a_n \rangle - iU2 \langle a_i^\dagger a_n \rangle \langle a_n^\dagger a_n \rangle. \quad (\text{F.8})$$

Therefore, Eq. (F.3) becomes a closed equation,

$$\Gamma_{H_0} g_1^{(1)} + \lambda^2 \Gamma_{B_0} g_1^{(1)} + \lambda^2 U \Gamma_{B_1} g_1^{(1)} = \lambda^2 \nu^{(0)} + iU \pi \left( g_1^{(1)} \right), \quad (\text{F.9})$$

where

$$\begin{aligned} \pi \left( g_1^{(1)} \right)_{l*N+n} &= 2 \left( g_1^{(1)} \right)_{l*N+n} \left( g_1^{(1)} \right)_{n*N+n} \\ &\quad - 2 \left( g_1^{(1)} \right)_{l*N+l} \left( g_1^{(1)} \right)_{l*N+n}. \end{aligned} \quad (\text{F.10})$$

*F.2. Approximate solution on interacting systems*

---

This equation can be solved iteratively,

$$g_1^{[n+1]} = \left( \Gamma_{H_0} + \lambda^2 \Gamma_D^{(0)} + \lambda^2 U \Gamma_D^{(1)} \right)^{-1} \left[ \lambda^2 \nu^{(0)} + iU \Pi \left( g_1^{[n]} \right) \right], \quad (\text{F.11})$$

with initial solution  $g^{[0]} = g_1^{(0)}$  for the corresponding non-interacting system. Then the solution is

$$g_1^{(1)} = \lim_{n \rightarrow \infty} g_1^{[n]}, \quad (\text{F.12})$$

which in practice stops at large enough  $n$  such that  $g_1^{[n]} - g_1^{[n-1]}$  is small enough.